

# **Modulation of *Plasmodium falciparum* chaperones PfHsp70-1 and PfHsp70-x by small molecules**

**A thesis submitted in fulfillment of the requirements for the degree**

**of**

**DOCTOR OF PHILOSOPHY  
in Biochemistry**

**of**

**Rhodes University, South Africa  
Department of Biochemistry, Microbiology and Biotechnology, Faculty of Science**

**By**

**Ingrid Louise Cockburn  
December 2012**

## ABSTRACT

---

The heat shock proteins of ~ 70 kDa (Hsp70s) are a conserved group of molecular chaperones important in maintaining the protein homeostasis in cells, carrying out functions including refolding of misfolded or unfolded proteins. Hsp70s function in conjunction with a number of other proteins including Hsp40 co-chaperones. Central to the regulation Hsp70 activity is the Hsp70 ATPase cycle, involving ATP hydrolysis by Hsp70, and stimulation of this ATP hydrolysis by Hsp40. PfHsp70-1, the major cytosolic Hsp70 in the malaria parasite, *Plasmodium falciparum*, and PfHsp70-x, a novel malarial Hsp70 recently found to be exported to the host cell cytosol during the erythrocytic stages of the *P. falciparum* lifecycle, are both thought to play important roles in the malaria parasite's survival and virulence, and thus represent novel antimalarial targets. Modulation of the function of these proteins by small molecules could thus lead to the development of antimalarials with novel targets and mechanisms. In the present study, malarial Hsp70s (PfHsp70-1 and PfHsp70-x), human Hsp70 (HSPA1A), malarial Hsp40 (PfHsp40) and human Hsp40 (Hsj1a) were recombinantly produced in *Escherichia coli*. In a characterisation of the chaperone activity of recombinant PfHsp70-x, the protein was found to have a basal ATPase activity (15.7 nmol ATP/min/mg protein) comparable to that previously described for PfHsp70-1, and an aggregation suppression activity significantly higher than that of PfHsp70-1. *In vitro* assays were used to screen five compounds of interest (lapachol, bromo- $\beta$ -lapachona and malonganenones A, B and C) belonging to two compound classes (1,4 naphthoquinones and prenylated alkaloids) for modulatory effects on PfHsp70-1, PfHsp70-x and HsHsp70. A wide range of effects by compounds on the chaperone activities of Hsp70s was observed, including differential effects by compounds on different Hsp70s despite high conservation ( $\geq 70$  % sequence identity) between the Hsp70s. The five compounds were shown to interact with all three Hsp70s in *in vitro* binding studies. Differential modulation by compounds was observed between the Hsj1a-stimulated ATPase activities of different Hsp70s, suggestive of not only a high degree of specificity of compounds to chaperone systems, but also distinct interactions between different Hsp70s and Hsj1a. The effects of compounds on the survival of *P. falciparum* parasites as well as mammalian cells was assessed. Bromo- $\beta$ -lapachona was found to have broad effects across all systems, modulating the chaperone activities of all three Hsp70s, and showing significant toxicity toward both *P. falciparum* parasites and mammalian cells in culture. Malonganenone A was found to modulate only the malarial Hsp70s, not human Hsp70, showing significant toxicity toward malarial parasites ( $IC_{50} \sim 0.8 \mu M$ ), and comparatively low toxicity toward mammalian cells, representing therefore a novel starting point for a new class of antimalarials potentially targeting a new antimalarial drug target, Hsp70.

## DECLARATION

---

I, Ingrid Louise Cockburn, declare that this thesis is my own, unaided work. It is being submitted for the degree of Doctor of Philosophy at Rhodes University. It has not been submitted before for any degree or examination in any other university.

.....  
INGRID LOUISE COCKBURN

Signed on the ..... at .....

## ACKNOWLEDGEMENTS

---

*I gratefully acknowledge the following individuals for their contributions to this project:*

My project supervisors, Professor Gregory Blatch and Dr. Aileen Boshoff for the knowledge and expertise they've shared with me, and for the guidance and encouragement they've offered. I am especially grateful to Professor Gregory Blatch for not only for making the amazing opportunities and experiences I've had in the last few years possible, but for sharing his enthusiasm and passion for this work with me.

Dr. Eva-Rachele Pesce for not only the constant encouragement, interest and input into in my work, but also for the friendship we've shared.

The many willing contributors of time and expertise to my work: Professor Mike Davies-Coleman, Dr. Earl Prinsloo, Dr. Adrienne Edkins, Dr. Jo-Anne de la Mare, Dr. Linda Stephens: thank you all for your contributions.

Dr. Jude Przyborski and Professor Klaus Lingelbach and their research group at Phillips Universität Marburg (Germany) for hosting me and for the significant contributions you made toward my project. Many thanks in particular also to Dr. Stefan Baumeister and Nadja Braun for technical training and assistance with LDH parasite growth inhibition assays.

I gratefully acknowledge the funders of this research (DFG: Deutsche Forschungsgemeinschaft; NRF: National Research Foundation) as well as the funders of my studies (DAAD: Deutscher Akademischer Austauschdienst, the Henderson and Andrew Mellon Funds, NRF).

*Personal acknowledgements:*

To my wonderful family, Kevin, Stella and Jessica Cockburn: your encouragement, support and interest mean so much to me!

Buhle Moyo and Jo-Anne de la Mare: thank you for the special friendship and encouragement.

To Chesney Long: I am so grateful for your love, your patience and your unwavering support.

## TABLE OF CONTENTS

---

ABSTRACT.....	I
DECLARATION.....	II
ACKNOWLEDGEMENTS .....	III
TABLE OF CONTENTS.....	IV
LIST OF FIGURES.....	VIII
LIST OF TABLES .....	X
LIST OF OUTPUTS .....	XI
LIST OF SYMBOLS AND ABBREVIATIONS .....	XII

### CHAPTER 1: INTRODUCTION

<b>1.1. LITERATURE REVIEW .....</b>	<b>2</b>
1.1.1. Malaria and <i>Plasmodium falciparum</i> .....	2
1.1.1.1. The Global burden of malaria .....	2
1.1.1.2. <i>Plasmodium falciparum</i> biology.....	2
1.1.1.3. Current antimalarials, drug resistance and vaccine research.....	7
1.1.2. Molecular chaperones and heat shock proteins.....	9
1.1.3. <i>P. falciparum</i> heat shock proteins .....	16
1.1.3.1. <i>P. falciparum</i> Hsp70s .....	17
1.1.3.2. <i>P. falciparum</i> Hsp40s .....	19
1.1.4. Hsp70 as a drug target.....	20
1.1.4.1. Hsp70 modulation.....	22
<b>1.2. RESEARCH MOTIVATION .....</b>	<b>26</b>
<b>1.3. HYPOTHESIS.....</b>	<b>26</b>
<b>1.4. OBJECTIVES.....</b>	<b>27</b>
<b>2.1. INTRODUCTION .....</b>	<b>29</b>
<b>2.2. MATERIALS AND METHODS.....</b>	<b>34</b>
2.2.1. Materials .....	34
2.2.2. Expression of recombinant proteins in <i>E. coli</i> : induction and solubility studies .....	35
2.2.2.1. Induction studies for the assessment of target protein expression in <i>E. coli</i> .....	35

2.2.2.2.	Solubility studies for the assessment of the solubility of target protein expressed in <i>E. coli</i>	36
2.2.3.	Purification of recombinant proteins from <i>E. coli</i> .....	36
<b>2.3.</b>	<b>RESULTS .....</b>	<b>39</b>
2.3.1.	Expression and purification.....	39
2.3.1.1.	PfHsp70- 1 wild type .....	39
2.3.1.2.	PfHsp70-1 (codon optimized) .....	41
2.3.1.3.	PfHsp70-x .....	43
2.3.1.4.	HsHsp70 .....	45
2.3.1.5.	PfHsp40 .....	47
2.3.1.6.	Hsj1a.....	50
<b>2.4.</b>	<b>DISCUSSION .....</b>	<b>53</b>
<b>3.1.</b>	<b>INTRODUCTION .....</b>	<b>60</b>
<b>3.2.</b>	<b>MATERIALS AND METHODS.....</b>	<b>63</b>
3.2.1.	Materials .....	63
3.2.2.	Preparation of test compounds .....	63
3.2.3.	MDH aggregation suppression assays .....	65
3.2.4.	ATPase assays.....	66
3.2.5.	Sequence alignments of Hsp70s .....	67
<b>3.3.</b>	<b>RESULTS .....</b>	<b>68</b>
3.3.1.	Inhibition of the aggregation suppression activity of PfHsp70-1 and PfHsp70-x .....	68
3.3.2.	Characterisation of the steady-state ATPase activity of PfHsp70-x.....	72
3.3.3.	Modulation of the basal and Hsp40-stimulated ATPase activity of PfHsp70-1, PfHsp70-x and HsHsp70 by small molecules.....	73
3.3.4.	Sequence alignments of PfHsp70-1, PfHsp70-x and HsHsp70.....	80
<b>3.4.</b>	<b>DISCUSSION .....</b>	<b>84</b>
<b>4.1.</b>	<b>INTRODUCTION .....</b>	<b>90</b>
<b>4.2.</b>	<b>MATERIALS AND METHODS.....</b>	<b>94</b>
4.2.1.	Materials .....	94
4.2.2.	Surface Plasmon resonance spectroscopy: BIAcore® X system .....	94

4.2.2.1.	Protein preparation.....	95
4.2.2.2.	Docking, priming and preconditioning of sensor chips.....	95
4.2.2.3.	Protein pre-concentration .....	95
4.2.2.4.	Protein immobilisation.....	96
4.2.3.	Surface Plasmon resonance spectroscopy: ProteOn™ XPR36 system .....	97
4.2.3.1.	Protein preparation.....	98
4.2.3.2.	Docking, preconditioning and stabilisation of sensor chip .....	98
4.2.3.3.	Protein immobilisation.....	99
4.2.3.4.	Assessment of Hsp70-compound interactions .....	99
4.3.3.1.	Effects of malonganenone A on Hsp70-Hsj1a interactions .....	112
<b>4.4.</b>	<b>DISCUSSION .....</b>	<b>113</b>
<b>5.1.</b>	<b>INTRODUCTION .....</b>	<b>122</b>
<b>5.2.</b>	<b>METHODS AND MATERIALS.....</b>	<b>123</b>
5.2.1.	Materials .....	123
5.2.2.	Assessment of the potential permeability and solubility of test compounds .....	123
5.2.3.	Growth and maintenance of <i>P. falciparum</i> cultures.....	125
5.2.4.	LDH growth inhibition assay .....	125
5.2.5.	Growth and maintenance of human cell lines.....	127
5.2.6.	MTT cell proliferation assay .....	127
<b>5.3.</b>	<b>RESULTS .....</b>	<b>128</b>
5.3.1.	The predicted permeability and solubility of test compounds.....	128
5.3.2.	Effects of compounds on the growth of <i>P. falciparum</i> parasites in vitro .....	129
5.3.3.	Effects of compounds on the growth of human cell lines .....	131
<b>5.4.</b>	<b>DISCUSSION .....</b>	<b>133</b>
<b>6.1.</b>	<b>SUMMARY OF EXPERIMENTS AND KEY FINDINGS .....</b>	<b>137</b>
<b>6.2.</b>	<b>CONCLUSIONS AND DISCUSSION .....</b>	<b>140</b>
<b>6.3.</b>	<b>FUTURE WORK.....</b>	<b>148</b>
6.3.1.	Validation of biophysical findings .....	148
6.3.2.	Elucidating mechanisms of Hsp70(-Hsp40) modulation by small molecules .....	148
6.3.3.	Development of novel antimalarials targeting PfHsp70s based on malonganenone A .....	149

6.3.4.	Identification of PfHsp70s as targets .....	150
<b>REFERENCES</b>		<b>152</b>
<b>APPENDIX</b>		<b>177</b>
7.1.	<b>APPENDIX A: GENERAL BIOCHEMICAL AND MOLECULAR BIOLOGY TECHNIQUES.....</b>	<b>177</b>
7.2.	<b>APPENDIX B: SUPPLEMENTARY DATA .....</b>	<b>182</b>



## LIST OF FIGURES

---

<b>Figure 1.1:</b> Life cycle of <i>P. falciparum</i> .	5
<b>Figure 1.2:</b> The classification of Hsp40s according to the presence and organization of conserved domains.	12
<b>Figure 1.3:</b> The ATPase cycle associated with Hsp70-mediated protein folding.	14
<b>Figure 1.4:</b> Structures of previously identified Hsp70 modulators 15-deoxyspergualin (A), MAL-3-39 (B) DMT002264 (C), 116-5c (D) and 115-7c (E).	25
<b>Figure 2.1:</b> Expression and purification of PfHsp70-1 (wild type) from <i>E. coli</i> XL1 Blue.	40
<b>Figure 2.2:</b> Expression, solubility and purification of PfHsp70-1 (optimized) from <i>E. coli</i> XL1 Blue.	42
<b>Figure 2.3:</b> Expression, solubility and purification of PfHsp70-x from <i>E. coli</i> M15[pRep4].	44
<b>Figure 2.4:</b> Expression and purification of HsHsp70 from <i>E. coli</i> BL21.	46
<b>Figure 2.5:</b> Expression, solubility and purification of PfHsp40.	49
<b>Figure 2.6:</b> Expression and purification of Hsj1a from <i>E. coli</i> XL1 Blue.	51
<b>Figure 3.1:</b> MDH aggregation assays – control reactions and compound screening.	69
<b>Figure 3.2:</b> Concentration-dependent effects of compounds on the aggregation suppression activity of PfHsp70-1.	70
<b>Figure 3.3:</b> Concentration dependent effects of compounds on the aggregation suppression activity of PfHsp70-x.	71
<b>Figure 3.4:</b> Kinetic characterisation of the steady-state ATPase activity of PfHsp70-x.	72
<b>Figure 3.5:</b> Effects of compounds on the basal steady-state activities of PfHsp70-1, PfHsp70-x and HsHsp70.	74
<b>Figure 3.6:</b> Effects of compounds on the Hsj1a-stimulated steady-state ATPase activities of PfHsp70-1, PfHsp70-x and HsHsp70.	75
<b>Figure 3.7:</b> Effects of compounds on the PfHsp40-stimulated steady-state ATPase activity of PfHsp70-1.	76
<b>Figure 3.8:</b> Concentration-dependent effects of compounds on the basal ATPase activity of PfHsp70-x.	77
<b>Figure 3.9:</b> Effects of malonganenone A on the stimulation of PfHsp70-x ATPase activity by Hsj1a.	79
<b>Figure 3.10:</b> Alignment of DnaK with corresponding regions of PfHsp70-1, PfHsp70-x, HsHsp70.	83
<b>Figure 4.1:</b> Example of an SPR sensorgram.	91
<b>Figure 4.2:</b> Schematic representation of the configuration of ProteOn™ XPR36 sensor chips.	98
<b>Figure 4.3:</b> SPR analysis of the interaction between lapachol and PfHsp70-1.	105

<b>Figure 4.4:</b> SPR analysis of the interaction between malonganenone A and PfHsp70-1.	107
<b>Figure 4.5:</b> SPR analysis of the interaction between malonganenone A and PfHsp70-x.	108
<b>Figure 4.6:</b> SPR sensorgrams of the analysis Hsp70-Hsj1a interactions.	111
<b>Figure 4.7:</b> The effects of malonganenone A on the interaction between Hsj1a and Hsp70s determined by surface plasmon resonance.	112
<b>Figure 5.1:</b> The effects of two positive control compounds (A: blasticidin and B: WR99210) and a vehicle control (C: DMSO) on the survival of <i>P. falciparum</i> 3D7 parasites after 72 hour treatment.	129
<b>Figure 5.2:</b> The effect lapachol, bromo- $\beta$ -lapachona, malonganenone A and malonganenone C on the survival of two human cell lines.	132
<b>Figure 7.1:</b> Plasmid maps of each expression vector used to express and purify proteins of interest in this study.	182
<b>Figure 7.2:</b> Confirmation of the identities of expression plasmids by diagnostic restriction enzyme digests and 0.8 % agarose gel electrophoresis.	183
<b>Figure 7.3:</b> Effect of DMSO on the basal and Hsp40-stimulated ATPase activities of Hsp70s.	184
<b>Figure 7.4:</b> The effect of selected compounds on the aggregation of MDH.	185
<b>Figure 7.5:</b> Pre-concentration and immobilisation procedures carried out toward the immobilisation of recombinant proteins on CM5 sensor chips.	186
<b>Figure 7.6:</b> Sensorgram of the procedure carried out toward the immobilisation of recombinant proteins onto a GLH sensor chip.	187
<b>Figure 7.7:</b> SPR analysis of the potential interaction between lapachol and PfHsp70-x.	188
<b>Figure 7.8:</b> SPR analysis of the potential interaction between bromo- $\beta$ -lapachona and PfHsp70-1.	189
<b>Figure 7.9:</b> SPR analysis of the potential interaction between bromo- $\beta$ -lapachona and PfHsp70-x.	190
<b>Figure 7.10:</b> SPR analysis of the potential interaction between malonganenone B and PfHsp70-1.	191
<b>Figure 7.11:</b> SPR analysis of the potential interaction between malonganenone C and PfHsp70-1.	192
<b>Figure 7.12:</b> SPR analysis of the interactions between lapachol and Hsp70s.	195
<b>Figure 7.13:</b> SPR analysis of the interactions between bromo- $\beta$ -lapachona and Hsp70s.	196
<b>Figure 7.14:</b> SPR analysis of the interactions between malonganenone A and Hsp70s.	198
<b>Figure 7.15:</b> SPR analysis of the interactions between malonganenone B and Hsp70s.	200
<b>Figure 7.16:</b> SPR analysis of the interactions between malonganenone C and Hsp70s.	202

## LIST OF TABLES

---

<b>Table 1.1:</b> <i>Plasmodium falciparum</i> Hsp70s.	18
<b>Table 2.1:</b> Recently produced recombinant <i>P. falciparum</i> proteins of therapeutic interest.	31
<b>Table 2.2:</b> Yields of recombinant proteins isolated from transformed <i>E. coli</i> cells.	52
<b>Table 3.1:</b> Names and structures of compounds of interest.	63
<b>Table 3.2:</b> Summary of the effects of test compounds (100 $\mu$ M) on the basal and Hsp40-stimulated ATPase activities of PfHsp70-1, PfHsp70-x and HsHsp70.	76
<b>Table 3.3:</b> Pairwise homologies between PfHsp70-1, PfHsp70-x and HsHsp70.	80
<b>Table 4.1:</b> Summary of the preliminary results of the assessment of the potential interactions between small molecules and Hsp70s.	110
<b>Table 5.1:</b> Assessment of the potential permeability and solubility of test compounds according to Lipinski's Rule of Five, based on chemical structure.	128
<b>Table 5.2:</b> The toxicity of compounds of interest toward <i>P. falciparum</i> parasites cultured <i>in vitro</i> .	130
<b>Table 6.1:</b> Summary of the results of the assessment of compounds in terms of Hsp70 modulation, biophysical interactions with Hsp70s, toxicities toward <i>P. falciparum</i> and mammalian cells <i>in vitro</i> , and predicted oral bioavailability.	139
<b>Table 7.1:</b> Plasmids used in the expression of target proteins.	181
<b>Table 7.2:</b> Levels of immobilisation of recombinant proteins on SPR sensor chips.	187

## LIST OF OUTPUTS

---

### Publications in peer-reviewed journals:

- **Review article:**

Pesce, E.-R. , Cockburn, I.L., Goble, J.L., Stephens, L.L., and Blatch, G.L. (2010). **Malaria heat shock proteins: Drug targets that chaperone other drug targets.** *Infectious Disorders - Drug Targets*, 10, 147-157.

- **Research article:**

Cockburn, I.L., Pesce, E.-R., Przyborski, J.M., Davies-Coleman, M.T., Clark, P.G.K., Keyzers, R.A., Stephens, L.L. and Blatch, G.L. (2011). **Screening for small molecule modulators of Hsp70 chaperone activity using protein aggregation suppression assays: inhibition of the plasmodial chaperone PfHsp70-1.** *Biological Chemistry*, 392, 431-438.

### Posters presented at conferences:

- Cockburn, I.L., Pesce, E.-R., Stephens, L.L. and Blatch, G.L. (2010). **Recombinant expression & purification of PfHsp70, Pfj4 and human Hsp70 for the screening of potential anti-malarial drugs using MDH assays.** 22<sup>nd</sup> South African Society of Biochemistry and Molecular Biology (SASBMB) congress, Bloemfontein, South Africa.
- Cockburn, I.L., Pesce, E.-R., Boshoff, A., Edkins, A.L., Prinsloo, E., Davies-Coleman, M.T. and Blatch, G.L. (2012). **Effects and specificities of natural small molecules with antiplasmodial activity on the chaperone activities of PfHsp70-1, PfHsp70-x and human Hsp70.** 4<sup>th</sup> Molecular Applications to Malaria (MAM) meeting, Lorne, Australia.
- Pesce, E.-R., Cockburn, I.L., Prinsloo, E. and Blatch, G.L. (2012). **Plasmodium falciparum Hsp70-1 and Hsp70-x: Interactions with different co-chaperones?** 4<sup>th</sup> Molecular Applications to Malaria (MAM) meeting, Lorne, Australia.

## LIST OF SYMBOLS AND ABBREVIATIONS

---

(List is ordered alphabetically according to the full name / explanation column.)

<b>SYMBOL / ABBREVIATION</b>	<b>FULL NAME / EXPLANATION</b>
DSG	15-deoxyspergualin
EDC	1-ethyl-3-(3-dimethylaminopropyl)carbodiimide hydrochloride
MTT	3-[4,5-dimethylthiazol-2-yl]-2,5-diphenyl tetrazolium bromide
APAD	3-acetylpyridine dinucleotide
A <sub>600</sub>	Absorbance at 600 nm
AMP-PNP	Adenosine 5'-( $\beta,\gamma$ -imido)triphosphate lithium salt hydrate
ADP	Adenosine diphosphate
ATP	Adenosine triphosphate
K <sub>A</sub>	Affinity constant
$\alpha$	Alpha
k <sub>a</sub>	Association rate constant
bp	Base pairs
$\beta$	Beta
BSA	Bovine serum albumin
$\chi^2$	Chi <sup>2</sup>
CSP	Circumsporozoite protein
° C	Degrees Celcius
DNA	Deoxyribonucleic acid
DHFR	Dihydrofolate reductase
DHPS	Dihydropteroate synthase
DMSO	Dimethyl sulfoxide
k <sub>d</sub>	Dissociation rate constant
DTT	Dithiothreitol
DMEM	Dulbecco's Modified Eagle Medium
ER	Endoplasmic reticulum
ERAD	Endoplasmic reticulum-associated degradation
EGF	Epidermal growth factor
K <sub>D</sub>	Equilibrium association constant
<i>E. coli</i>	<i>Escherichia coli</i>
EDTA	Ethylene diamine tetra-acetic acid
FPLC	Fast Protein Liquid Chromatography
FCS	Fetal calf serum
FTIR	Fourier Transform Infrared Resonance
GPARC	Global Plan for Artemisinin Resistance Containment
GST	Glutathione S-transferase
GF domain	Glycine-phenylalanine rich domain
g/mol	Grams per mole
<i>g</i>	Gravitational force
IC <sub>50</sub>	Half maximal inhibitory concentration
Hsc	Heat shock cognate protein
Hsp	Heat shock protein
HPD motif	Histidine-proline-aspartic acid motif
HRP	Horse radish peroxidase

HT	Host targeting sequence
Hop	Hsp70-Hsp90 organising protein
HCl	Hydrochloric acid
ICAM-1	Intercellular adhesion molecule 1
IPTG	Isopropyl- $\beta$ -D-thiogalactopyranoside
ITC	Isothermal calorimetry
kDa	Kilo Daltons
KAHRP	Knob-associated histidine-rich protein
LDH	Lactate dehydrogenase
LogP	Logarithm of the octanol/water partition coefficient
MDH	Malate dehydrogenase
MESA	Mature parasite-infected erythrocyte surface antigen
R <sub>max</sub>	Maximal theoretical response
MSP1	Merozoite surface protein 1
mRNA	Messenger ribonucleic acid
$\mu$ g	Microgram
$\mu$ l	Microlitre
$\mu$ l/min	Microlitres per minute
$\mu$ m	Micrometre
$\mu$ M	Micromolar
mg	Milligram
mg	Milligrams
mg/ml	Milligrams per millilitre
ml	Millilitre
mM	Millimolar
Min	Minutes
M	Molar
TEMED	<i>N,N,N',N'</i> -Tetramethylethylenediamine
ng	Nanograms
nm	Nanometers
nmol	Nanomoles
NHS	N-hydroxysuccinimide
NBT	Nitro blue tetrazolium
NMR	Nuclear Magnetic Resonance
NEF	Nucleotide exchange factor
Opt	Optimised
PSA	Penicillin – streptomycin – amphotericin
%	Percentage
PBMC	peripheral blood mononuclear cells
PMSF	Phenylmethylsulphonyl fluoride
PEXEL	<i>Plasmodium</i> export element
<i>P. falciparum</i>	<i>Plasmodium falciparum</i>
PfENR	<i>Plasmodium falciparum</i> enoyl-ACP reductase
PfEMP	<i>Plasmodium falciparum</i> erythrocyte membrane protein
PfGCHI	<i>Plasmodium falciparum</i> GTP cyclohydrolase I
PfHsp70	<i>Plasmodium falciparum</i> Hsp70
PfHsp90	<i>Plasmodium falciparum</i> Hsp90
PTEX	<i>Plasmodium</i> Translocon of Exported proteins
PEI	Polyethyleneimine
KCl	Potassium chloride
RU	Response units / resonance units
RTS,S	RTS,S/AS01 <i>Plasmodium falciparum</i> vaccine
SMILE	Simplified Molecular-Input Line-Entry

siRNA	Small interfering ribonucleic acid
NaCl	Sodium chloride
SDS	Sodium dodecyl sulphate
SDS-PAGE	Sodium dodecyl sulphate polyacrylamide gel electrophoresis
SD	Standard deviation
SE	Standard error
$R_{eq}$	Steady-state response
SBD	Substrate binding domain
SPR	Surface Plasmon resonance
3D	Three dimensional
TBS-T	Tris buffered saline with Tween
TBS	Tris-buffered saline
UV	Ultraviolet
U	Units
VCAM	Vascular cell adhesion molecule
v/v	Volume per volume
w/v	Weight per volume
Wt	Wild type

**CHAPTER 1:**

---

**Introduction**

---



## 1.1. LITERATURE REVIEW

---

### 1.1.1. *Malaria and Plasmodium falciparum*

---

#### 1.1.1.1. *The Global burden of malaria*

---

Malaria in humans is caused by five species of *Plasmodium* parasites: *P. falciparum*, *P. vivax*, *P. ovale*, *P. malariae* and *P. knowlesi* (Tuteja, 2007; Vythilingam *et al.*, 2006). *Plasmodium* parasites, transmitted to humans by female mosquitoes belonging to the *Anopheles* genus (Tuteja, 2007), are eukaryotic, intracellular, unicellular parasites belonging to the phylum *Apicomplexa* (Levine, 1971), characterised by the presence of an apical complex – a collection of structures at the anterior end of the organisms which allows for invasion of host cells (Lim and McFadden, 2010).

It was estimated in the 2011 World Malaria Report by the World Health Organisation's (WHO) Global Malaria Programme that in the year 2010 there were 216 million malaria cases worldwide and 655 000 deaths due to malaria (WHO, 2011). Africa is by far the area worst affected by malaria with 81 % of malaria cases and 91 % of deaths being in Africa. In 2010, 86 % of malaria deaths were of children under the age of five (WHO, 2011). Pregnant women, too, are significantly affected by malaria. Pregnancy alters the immune system, thus women have an increased susceptibility to *P. falciparum* malaria during pregnancy and if untreated, the infection results in higher mortality rates compared to other groups (Reuben, 1993). Compared to the statistics for 2006 (247 million malaria cases, 881 000 deaths), reported in the 2008 World Malaria Report (WHO, 2008), there has been a decrease in the global impact of malaria; however, with resistance of the parasite to current therapies as well as resistance of the *Anopheles* mosquito to commonly used insecticides, the malaria problem is by no means under control (WHO, 2011).

#### 1.1.1.2. *Plasmodium falciparum* biology

---

Of the 247 million malaria cases in 2006, an estimated 91 % of these were caused by *P. falciparum* (WHO, 2008). *P. falciparum* can cause cerebral malaria, the most lethal form of malaria (Haldar and Mohandas, 2007), and has the highest mortality rate compared to the other *Plasmodium* species (Adams *et al.*, 2002). *P. falciparum*'s life cycle (shown schematically in Figure 1.1) is extremely complex,

including stages in both an invertebrate (*Anopheles* spp mosquito) host and a vertebrate (human) host (Sinnis and Sim, 1997). Briefly (as reviewed by Sinnis and Sim, 1997; Wirth, 2002; Fujioka and Aikawa, 2007), a *P. falciparum* infected female *Anopheles* mosquito injects parasites in the form of sporozoites into the human host while feeding. Sporozoites invade liver cells, where they develop into merozoites. As many as 20 000 merozoites can develop from a single sporozoite. Merozoites eventually rupture from hepatocytes and enter the bloodstream where they invade erythrocytes and begin a continuous asexual cycle. In the erythrocytes, the parasite goes through several stages, developing from ring to trophozoite and finally to schizont stage. At the schizont stage, the parasite contains approximately 16 merozoites (Bannister, 2001), which are released into the bloodstream upon erythrocyte rupture, and are able to infect new erythrocytes. From asexual stages, some parasites may differentiate into male and female gametocytes, which can be taken up by a female *Anopheles* mosquito feeding on an infected human. In the midgut of the mosquito, the gametocytes become gametes and fertilisation occurs. The zygote develops into an ookinete, which subsequently forms an oocyst on the midgut wall. The oocyst contains sporozoites, which, when released invade the salivary gland of the mosquito, enabling it to infect a human and continue the *P. falciparum* life cycle in a new host (Sinnis and Sim, 1997).

During the asexual stages of the parasite in the human erythrocyte, the host cell undergoes a number of changes critical to the parasite's survival as well as to the pathology of the malaria disease (Craig and Scherf, 2001; Haldar and Mohandas, 2007). These changes include the appearance of protrusions on the erythrocyte surface, which have been termed knobs (Kilejian, 1979). The knobs consist of knob associated histidine-rich protein (KAHRP) (Culvenor *et al.*, 1987; Pologe *et al.*, 1987) shown to form stable complexes with spectrin and actin, two skeletal proteins in the erythrocyte (Kilejian, 1991). Anchored to the erythrocyte surface by knobs is *P. falciparum* erythrocyte membrane protein 1 (PfEMP1) (Baruch *et al.*, 1995), a member of a family of antigenically-variant proteins encoded by approximately 60 genes of the *var* family (Gardner *et al.*, 2002; Flick and Chen, 2004). PfEMP1 plays an important role in both the immune evasion of *P. falciparum* (Craig and Scherf, 2001) and in mediating the adhesion of infected erythrocytes to each other and to vascular endothelial cells, a process known as sequestration (Barnwell *et al.*, 1989). During the initial stages of the erythrocyte life cycle, *P. falciparum*-infected host cells are able to freely circulate through the human bloodstream, however, at later trophozoite stages, sequestration occurs, resulting in the clustering of infected erythrocytes in smaller blood vessels (Barnwell *et al.*, 1989). Sequestration is mediated by interactions between receptors on human cells, including intercellular adhesion molecule 1 (ICAM-1), CD36, thrombospondin and vascular

cell adhesion molecule (VCAM) with the infected erythrocyte surface (Smith *et al.*, 1995), in particular with knobs (Barnwell *et al.*, 1989). Cells involved in adherence to infected erythrocytes during sequestration include endothelial cells, blood cells, platelets as well as uninfected erythrocytes (Buffet *et al.*, 2011). PfEMP1 has been identified as the mediating protein in sequestration and has been shown to bind to the CD36 receptor (Baruch *et al.*, 1997). The interaction between PfEMP1 and CD36 is reinforced by actin in both the parasite and the human endothelial cells, where, upon binding, an intracellular event triggers processes including kinase activation and subsequent actin filament formation at the point of adhesion. The resulting reorganisation of the actin cytoskeleton as well as a loss in negative charges by CD36 molecules leads to a clustering of CD36 on the endothelial cell surface, and thus a reinforced interaction between CD36 and PfEMP1 (Cyrklaff *et al.*, 2012).

The sequestration of infected erythrocytes is pivotal to the virulence of *P. falciparum* and in the pathology of the malaria disease (Adams *et al.*, 2002). It has been suggested that the adherence of the infected host cells to small blood vessels is a way for the parasite to evade the human immune system (Buffet *et al.*, 2011). The human spleen generally functions to filter out and retain altered, modified or old erythrocytes, which are destroyed and recycled predominantly by macrophages (Buffet *et al.*, 2011). *P. falciparum*-infected erythrocytes, therefore, are able to avoid clearance from the body by clustering and avoiding transit through the spleen (Craig and Scherf, 2001). Sequestration plays a major role in cerebral malaria, a severe form of malaria affecting the brain causing neurological symptoms including fits and coma (Adams *et al.*, 2002). An estimated 30 % of cerebral malaria cases lead to mortality caused by damage of the blood-brain barrier and subsequent leakage of cerebral vessels (Adams *et al.*, 2002). The mechanisms leading to this damage are not fully understood; however, sequestration and subsequent obstruction of cerebral blood vessels is thought to be involved in the process (Adams *et al.*, 2002). In the case of pregnant women, it is the sequestration of infected erythrocytes in the placental blood vessels which is responsible for the severe effects of pregnancy-associated malaria, including mortality of the foetus, mortality of the mother and a number of less severe complications (Gamain *et al.*, 2007)

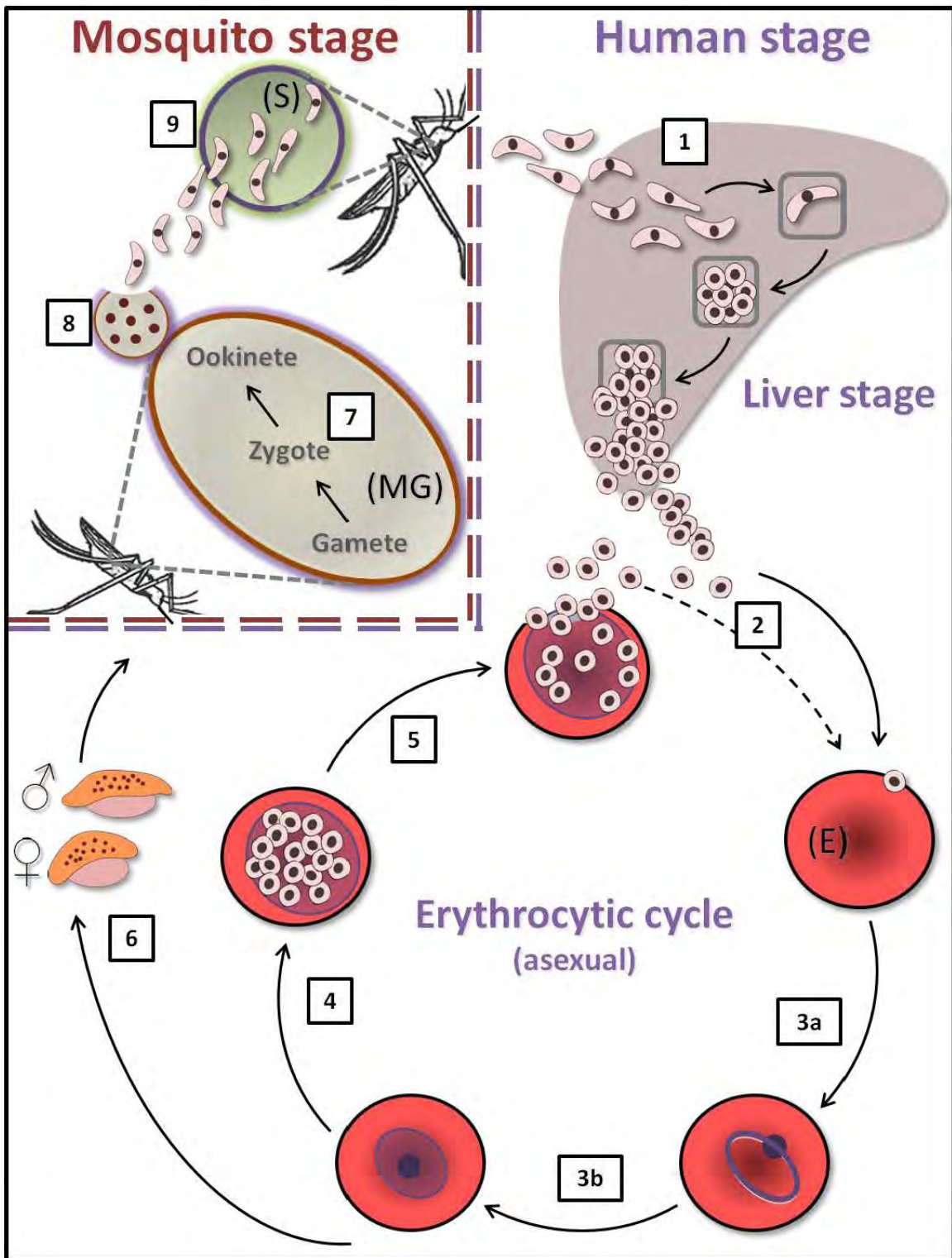


(Figure 1.1: Figure legend on the following page)

**Figure 1.1: Life cycle of *P. falciparum*** (adapted from Sinnis and Sim, 1997; Fujioka and Aikawa, 2002; Wirth, 2002). (1) An infected female *Anopheles* mosquito feeds on a human, releasing parasites in the form of sporozoites into the bloodstream. The sporozoites invade liver cells, where each sporozoite develops into thousands of merozoites. (2) Merozoite-infected liver cells rupture, releasing merozoites into the bloodstream, where they invade erythrocytes (E) and undergo their asexual life cycle. In the erythrocyte, the parasite develops from a merozoite into ring stage (3a), then a trophozoite (3b), and finally into a schizont containing merozoites (4). Merozoites rupture from the erythrocyte (5), and are released in the bloodstream where they can invade new erythrocytes. From the asexual stages in the erythrocytic cycle, parasites can differentiate into male and female gametocytes (6), initiating the sexual stages of the life cycle. Upon feeding on an infected human, the mosquito takes up gametocytes into its midgut (7), where they develop into gametes and fertilization occurs. The zygote develops into an ookinete (7). The ookinete forms an oocyst containing sporozoites on the midgut wall (8), which ruptures, releasing sporozoites which invade the mosquito salivary glands (S, 9) enabling the mosquito to infect a human and continue the parasite life cycle.

PfEMP1 is only one of a large set of parasite proteins – termed the secretome or exportome – that are exported to the erythrocyte cytosol (Hiller *et al.*, 2004; Marti *et al.*, 2004). A conserved signal peptide motif, termed the host targeting (HT; Hiller *et al.*, 2004) or *Plasmodium* export element (PEXEL; Marti *et al.*, 2004), has been identified in over 300 proteins, and has been predicted, and in many cases shown, to target these proteins to the erythrocyte cytosol (Hiller *et al.*, 2004; Marti *et al.*, 2004). PEXEL motifs are recognised and cleaved by the aspartic protease plasmepsin V, localised to the ER, allowing for further export of PEXEL proteins to the parasitophorous vacuole (Russo *et al.*, 2010; Boddey *et al.*, 2010). Most of the proteins containing the PEXEL motif are involved in either parasite virulence or remodelling of the erythrocyte (Marti *et al.*, 2004). Effective trafficking mechanisms are extremely important to the parasite's survival in the host cell, especially considering the fact that the host cell, the erythrocyte, is a denuded, metabolically inactive cell lacking the basic transport systems that most other eukaryotic cells possess, apart from simple transporters and channels allowing for the exchange of solutes across the plasma membrane (reviewed by Kirk, 2004 and Lanzer *et al.*, 2006). For this reason, nutrient acquisition required for growth and reproduction by the parasite needs to be carried out in an alternative manner to that used in most other eukaryotic systems (as reviewed by Lanzer *et al.*, 2006). In addition to the factors described above, trafficking of proteins to the erythrocyte cytosol is further complicated by the presence of the parasitophorous vacuole (PV). The PV is a membrane bound vacuole in which the parasite resides after erythrocyte invasion, and, formed during erythrocyte invasion, is thought to consist primarily of host cell lipids and possibly additional molecules of parasite origin (Ansorge *et al.*, 1996; Cowman and Crabb, 2006; Eksi and Williamson, 2011). The implications of the parasite's existence within the PV in the erythrocyte are that the parasite is separated from the

erythrocyte cytosol by its plasma membrane as well as the PV membrane, and is separated from the extracellular space by a third membrane: the erythrocyte membrane.

Before 2009 the trafficking mechanism or machinery of export of parasite proteins was unknown, despite the identification of the PEXEL or HT sequence. A large protein complex located on the PV membrane has since been identified, and has been termed the *Plasmodium* Translocon of Exported proteins (PTEX). PTEX has been proposed to be a translocon exporting parasite proteins in an ATP-dependent manner to the erythrocyte, and is considered a key discovery in deciphering parasite transport mechanisms (de Koning-Ward *et al.*, 2009).

### 1.1.1.3. Current antimalarials, drug resistance and vaccine research

---

Ideally, the first line of defence against malaria infection of humans is a preventative one: prophylaxis. Prophylaxis (prevention of illness) in the case of malaria can take two basic forms: practical or behavioural prophylaxis, and chemoprophylaxis, and is extensively reviewed in an article by Castelli and colleagues (2010). Practical preventative measures simply include using bed nets and insect repellent to avoid mosquito bites and thus infection with *Plasmodium*. Additional preventative measures can be taken in the form of chemoprophylaxis. A number of drugs are prescribed by doctors for the prevention of malaria infection in humans, including chloroquine, proguanil, atovaquone, mefloquine, doxycycline, primaquine and tefenoquine, as well as various combinations of these (Castelli *et al.*, 2010).

Antimalarial drugs for the treatment of malaria include the well-known agents chloroquine and artemisinin. As early as in the 1600s, quinine, found in the bark of cinchona trees, was used to treat malaria and was used as its primary treatment until the 1920s, when more effective, synthetic derivatives of quinine were identified (Achan *et al.*, 2011). One such derivative is chloroquine, a 4-aminoquinolone, which, like most other related drugs such as pamaquine, primaquine, tafenoquine, mefloquine, halofantrine and lumefantrine, acts by preventing the parasite from polymerising the haem pigment (toxic product of haemoglobin metabolism) to non-toxic haematin crystals (Hobbs and Duffy, 2011; Butler *et al.*, 2010). Unfortunately *P. falciparum* parasites have developed resistance to chloroquine through mutations in the chloroquine resistance transporter (PfCRT), a digestive vacuolar membrane protein in *P. falciparum* (Bennett *et al.*, 2007). With the increase of chloroquine resistance, quinine re-emerged as an effective antimalarial (Bennett *et al.*, 2007) despite its adverse side-effects;

however, drug resistance to quinine, though less severe and at a slower rate compared with other antimalarials, is also emerging (Achan *et al.*, 2011). A second class of antimalarial drugs, the antifolates, act specifically by inhibiting the enzymes dihydrofolate reductase (DHFR) and dihydropteroate synthase (DHPS), both involved in the folate pathway, which is essential to DNA synthesis and amino acid metabolism in the parasite (Bloland, 2001; Hyde, 2005). Antifolate drugs include the DHFR inhibitors proguanil and pyrimethamine (Bloland, 2001). Resistance to proguanil emerged within only a year after its introduction (Achan *et al.*, 2011), resulting in the use of antifolate combination treatments, in which DHFR inhibitors are used in combination with sulfa drugs such as sulfamethoxazole and sulfadoxine (Bloland, 2001). Resistance to these combinations, such as the sulfadoxine/pyrimethamine has also arisen (Bloland, 2001). Proguanil is often used in combination with the hydroxynaphthoquinone atovaquone as Malarone™, since atovaquone, though effective against chloroquine resistant *P. falciparum*, is prone to rapid resistance when used alone (Bloland, 2001). A drug which functions in a related but distinct way to chloroquine is artemisinin. Artemisinin was developed as an antimalarial treatment by the Chinese during the Vietnam War in 1972 (Hobbs and Duffy, 2011), and was originally isolated from the *Artemisia annua* plant, though is artificially synthesised today (Sá *et al.*, 2011). The drug functions by reacting with the iron atom in the haem to form highly destructive free radical molecules lethal to parasites (Butler *et al.*, 2010). Artemisinin is an extremely potent and fast-acting antimalarial, found to be more effective even than quinine. A number of synthetic derivatives of artemisinin have been developed for improved solubility, and these include dihydroartemisinin, artesunate and artemether (Sá *et al.*, 2011). In recent years, artemisinin resistance has emerged in the Mekong region on the Cambodia-Thailand border, with evidence for possible spread of this resistance. As a result, and as a means of preventing the further spread of artemisinin resistance, there has been an urgent call for withdrawal of all artemisinin monotherapies from the market. Artemisinin-based combination therapy is the recommended first line therapy in confirmed uncomplicated malaria cases, and replacement of monotherapies by such combination therapies is part of the Global Plan for Artemisinin Resistance Containment (GPARC) laid out by the World Health Organisation (WHO, 2011).

In addition to prophylaxis and chemotherapeutics, vaccines are another potential way of lowering the global impact of malaria. However, there are no successful, licensed malaria vaccines in use as yet (WHO, 2011). Furthermore, there are no successful vaccines against any human parasites (Hill, 2011). Research into potential malaria vaccines is targeted at the different stages of *Plasmodium*. In addition to multi-stage vaccines, vaccines against the pre-erythrocytic stage, the blood stage and the transmission

stage of the parasite are being investigated (Thera and Plowe, 2012). Parasite vaccines generally belong to one of two vaccine types: protein antigen-based or whole organism-based vaccines, where protein antigen-based vaccines most commonly use immunogenic surface proteins as antigens, and whole organism vaccines make use of attenuated or inactivated (for example by radiation) whole parasites (Crampton and Vanniasinkam, 2007; Luke and Hoffman, 2003). Around 20 malaria vaccines are currently in either phase I or phase II clinical trials, and one very promising vaccine against *P. falciparum*, RTS,S/AS01 (RTS,S), is in phase III clinical trials (WHO, 2011; The RTS,S Clinical Trials Partnership, 2012). RTS,S is a pre-erythrocytic vaccine. The vaccine contains components of circumsporozoite protein (CSP), a surface protein of sporozoites, sections of which are known to elicit an immune response. Antibodies against specifically a central repeat region of CSP block hepatocyte invasion by *P. falciparum*, thus the hope is that RTS,S could induce antibodies in vaccinated individuals to block infection by *P. falciparum* (Thera and Plowe, 2012). Initial results from the phase III RTS,S clinical trial have been promising, lowering the incidence of clinical malaria by 55 % in 6000 children considered to be at risk for infection in Africa (WHO, 2011).

### ***1.1.2. Molecular chaperones and heat shock proteins***

---

Heat shock proteins (Hsps) are a large group of proteins induced by cellular stress, and include many molecular chaperones (Nonaka *et al.*, 2006). Molecular chaperones, of which there are both stress-inducible as well as constitutively expressed proteins, function to facilitate the correct folding and assembly of polypeptides, thus preventing the formation of misfolded or incorrectly assembled proteins (Ellis, 1987; Hendrick and Hartl, 1993). The constitutively expressed counterparts of Hsps are referred to as the heat shock cognate proteins (Hscs) (Ingolia and Craig, 1982).

Hsps proteins are classified according to their size in kDa, the Hsps of ~ 90 kDa being termed Hsp90s. Hsp90, the structure of which (in complex with the Hsp70-Hsp90 organising protein, Hop) was recently determined by electron cryomicroscopy (Southworth and Agard, 2011), consists of highly conserved domains: an N-terminal 25 kDa ATP binding domain, a middle domain of 35 kDa and a 12 kDa C-terminal domain (Terasawa *et al.*, 2005). A charged linker region between the ATP binding domain and the middle domain plays a role in modulating Hsp90 function *in vivo* (Tsutsumi *et al.*, 2012). The C-terminal



domain facilitates the dimerisation of Hsp90 (Nemoto *et al.*, 1995), which has been found to be essential to the *in vivo* function of the chaperone (Wayne and Bolon, 2007). Apart from a molecular chaperone role in protein folding and stabilization, Hsp90 has been found to be central in signal transduction pathways in eukaryotes (Caplan, 1999).

Hsp70s (Hsps of ~ 70 kDa) carry out a wide range of cellular roles associated with proteins, including facilitating the correct folding and assembly of newly synthesized proteins, refolding incorrectly folded or aggregated proteins, and translocation of proteins across membranes (Mayer and Bukau, 2005). Hsp70s consist of an N-terminal ~44 kDa ATPase domain, a ~15 kDa substrate-binding domain, and a ~10 kDa C-terminal domain. The C-termini of cytosolic Hsp70s in eukaryotes most often end in a highly conserved EEVD sequence motif (Freeman *et al.*, 1995), which mediates the interaction with proteins containing a tetratricopeptide repeat (TPR) domain (Scheufler *et al.*, 2000), such as Hop, which facilitates the interactions between Hsp70 and Hsp90 (Blatch and Lässle, 1999; Odunuga *et al.*, 2004). The ATPase domain of Hsp70s is common to actin and hexokinase, and consists of four subdomains (IA, IB, IIA and IIB), with subdomains IA and IB forming one structural lobe, and subdomains IIA and IIB forming a second and structurally similar lobe. A three-dimensional structure of the ATPase domain of Hsp70 (bovine Hsc70) revealed the binding site for ATP to be located in the deep cleft formed by the two lobes of the ATPase domain (Bork *et al.*, 1992; Flaherty *et al.*, 1990). Crystal structures of the ATPase domains of four isoforms of human Hsp70s revealed a high level of structural conservation between the functionally diverse Hsp70s, supporting the idea that the functional diversity and specificity of Hsp70s is determined by the substrate-binding domains and interacting co-chaperones (Wisniewska *et al.*, 2010). Examples of such divergent functions between highly homologous proteins have recently been reported on: the constitutively expressed Hsc70 and heat inducible HSPA1A (Hsp72) human Hsp70s were found to have complete opposite effects (slowing and accelerating, respectively) on the clearance of tau, the protein associated with human neurodegenerative disease (Jinwal *et al.*, 2012), and in *in vitro* experiments, overexpression of HSPA1A in cells effectively prevented heat-induced cell death, whereas HSPA6 was not able to do so (Hageman *et al.*, 2011).

From various structural studies, it has become evident that allostery between the ATPase and substrate-binding domains plays an essential part in Hsp70 function. Specifically, ATP binding and hydrolysis by the ATPase domain regulates the conformation (open vs. closed) and therefore function of the substrate-binding domain (Jiang *et al.*, 2005; Swain *et al.*, 2007; Bhattacharya *et al.*, 2009; Zhuravleva and

Gierasch, 2011; Zuiderweg *et al.*, 2012; Kityk *et al.*, 2012). Hsp70s have been implicated in human disease and have thus emerged as a potential drug target (see Section 1.1.4).

The Hsp40s (Hsps of ~ 40 kDa) are known to interact with and regulate the function of Hsp70s, and are characterized by the presence of a highly conserved and functionally important J-domain. The J-domain is a highly conserved ~70 amino acid sequence consisting of four  $\alpha$ -helices (helices I – IV) and a highly conserved histidine-proline-aspartic acid (HPD) motif between helices II and III (Cheetham and Caplan, 1998). Based on the presence and organization of four domains, Hsp40s are generally classed into three types: type I, type II and III (Cheetham and Caplan, 1998), as illustrated in Figure 1.2. Type I Hsp40s possess the four conserved domains: the N-terminal J-domain, a glycine/phenylalanine-rich (GF-rich) domain, a Zinc-finger domain containing four cysteine repeat (CXXCXGXG) sequences and a C-terminal substrate binding domain (Cheetham and Caplan, 1998). Type II Hsp40s contain the N-terminal J-domain, the flanking GF-rich region as well as the C-terminal substrate binding domain; however, they lack the Zinc-finger domain. Type III Hsp40s possess only the J-domain, which is not necessarily at the N-terminus (Cheetham and Caplan, 1998). More recently, a fourth type (type IV) of Hsp40s has been described, which can be seen as a sub-class of the type III Hsp40s, also shown in Figure 1.2. The type IV Hsp40s possess a J-domain, at a position not necessary N-terminal, that lacks the highly conserved HPD motif (Botha *et al.*, 2007). Type I and II Hsp40s have been found to play a major role (together with Hsp70 partners) in protein folding and related functions, including protein degradation and re-folding of misfolded proteins, and their localisations are generally limited to the cytosol, nucleus and the ER (Walsh *et al.*, 2004; Qiu *et al.*, 2006). Type III Hsp40s have been found to be more functionally diverse, displaying a wider range of localizations than type I and II Hsp40s (including transmembrane, endoplasmic reticulum [ER], mitochondrial, ribosome-associated and cytosolic) and biological functions (including mitochondrial biogenesis, mRNA splicing and protein translation), a number of which remain unknown, and none of which have been found to include protein folding functions (Walsh *et al.*, 2004). More recent literature has identified further functions for various Hsp40s, including cell wall assembly and integrity, functions as redox partner proteins with electron transport properties (yeast Hsp40s, Gillies *et al.*, 2012) and stabilization of activation-induced deaminase, a process essential to antibody affinity maturation in immune responses (human DNAJA1, Orthwein *et al.*, 2011). In many cases the functions of these Hsp40s were found to be non-redundant amongst Hsp40s (Gillies *et al.*, 2012; Orthwein *et al.*, 2011).

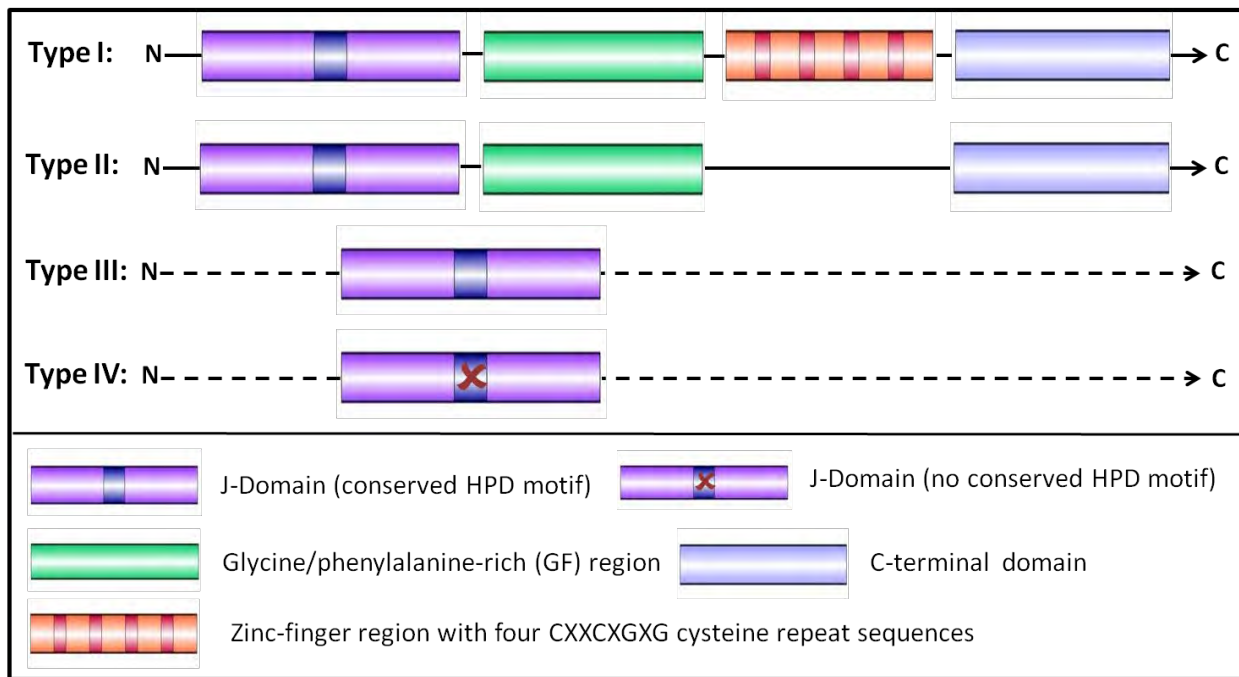


**Figure 1.2: The classification of Hsp40s according to the presence and organization of conserved domains.** Type I – IV Hsp40s represented schematically showing the organizations of one or more of four characteristic domains: the J-domain, the GF-rich region, the Zinc-finger region and the C-terminal region. The position of domains flanked by dotted lines is variable (Cheetham and Caplan, 1998; Botha *et al.*, 2007).

The protein folding activity of Hsp70s is a tightly regulated process in which Hsp40s play a central role, as illustrated by the ATPase cycle in Figure 1.3 (adapted from Szabo *et al.*, 1994, Hennessy *et al.*, 2005, Kampinga and Craig, 2010). In its role as a “protein folding (refolding) machine”, Hsp70 alternates between adenosine triphosphate (ATP) - and adenosine diphosphate (ADP) -bound states. In its ATP-bound state, Hsp70 has a lowered affinity for substrate peptides. Incorrectly folded and nascent substrate proteins are bound by Hsp40, and delivered to ATP-bound Hsp70 molecules. The Hsp40-Hsp70 interaction is a low-affinity, transient one, but allows for the stimulation of the rate of hydrolysis of ATP to ADP by Hsp70 (Schröder *et al.*, 1993; Szabo *et al.*, 1994, Kampinga and Craig, 2010). The stimulation of Hsp70 ATPase activity occurs via an interaction between the ATPase domain of the Hsp70 and the J-domain of the Hsp40, and rather than directly stimulating the Hsp70 ATPase activity, Hsp40s are thought to cause a conformational change in Hsp70, resulting in the increased ATP hydrolysis rate (Cheetham *et al.*, 1994). In the ADP-bound state, Hsp70 exhibits an increased affinity for the substrate peptide resulting in stabilization of the Hsp70-substrate interaction, allowing refolding to occur. In a process mediated by cofactors termed nucleotide exchange factors (NEF), the Hsp70-bound ADP is

exchanged for ATP, essentially “recycling” the Hsp70 molecule to be able to start a new cycle (Szabo *et al.*, 1994, Hennessy *et al.*, 2005, Kampinga and Craig, 2010). The regulation of the nucleotide and substrate binding and release of Hsp70 has been found to be regulated by Hsp40 and substrates in a synergistic manner, in which Hsp40-stimulation of Hsp70 ATPase activity is significantly decreased in the absence of bound substrate, thus substrates bound in the Hsp70 substrate-binding domain are partly responsible for stabilising their interaction with Hsp70 (Laufen *et al.*, 1999). It has been suggested that it is the Hsp40 co-chaperone that determines the “choice” of peptide substrate to be bound by Hsp70, and that Hsp40 co-chaperones allow for Hsp70s to bind a wide and diverse range of substrates (Misselwitz *et al.*, 1998).

The J-domain was previously thought to be essential to the functional interaction of Hsp40s with Hsp70s, and in particular it is the HPD motif that was thought to mediate the Hsp70-Hsp40 association (Tsai and Douglas, 1996; Suh *et al.*, 1998). There was, however, contrasting evidence regarding the region or residues on Hsp70 involved in interactions between Hsp70s and Hsp40s. Studies toward deciphering the exact mechanisms involved in Hsp70-Hsp40 interactions have been conducted most often in two systems: the bacterial DnaK-DnaJ system (DnaK and DnaJ being prokaryotic Hsp70 and Hsp40 respectively; Suh *et al.*, 1998; Laufen *et al.*, 1999; Gässler *et al.*, 1999; Landry, 2003; Ahmad *et al.*, 2011) and the mammalian Hsc70-auxilin system (Jiang *et al.*, 2007), auxilin being a neuronal J-domain containing Hsp40 (Ungewickell *et al.*, 1995). For DnaK, there has been evidence of DnaJ interacting via a binding surface in the DnaK ATPase domain (Landry, 2003) as well as of DnaJ binding to residues on both the ATPase and substrate binding domains (Suh *et al.*, 1998). A different study identified residues in the ATPase domain as well as the presence of the two linked domains (ATPase and substrate binding) of DnaK to be essential to DnaJ interacting (Gässler *et al.*, 1999). In the case of mammalian Hsc70, crystallised in complex with auxilin, residues in the ATPase domain of Hsc70, as well as in the substrate-binding domain, specifically those forming the interface between the ATPase and substrate-binding domains, were identified to be involved in mediating the Hsc70-auxilin interaction (Jiang *et al.*, 2007). More recent structural data, however, propose the HPD motif only to be involved in the interaction of Hsp40s with Hsp70s in their ATP-bound state (Ahmad *et al.*, 2011). Nuclear magnetic resonance spectroscopy experiments by Ahmad and colleagues also revealed that the interaction between DnaJ and DnaK is a multivalent one – with both the J-domain (in particular helix II, not the HPD motif) and the glycine-phenylalanine rich (GF) region interacting with DnaK. The GF region was found to interact with the DnaK substrate binding domain, whereas, in the ADP-bound state, positively charged, conserved

residues in helix II of the J-domain interact via electrostatic interactions with the ATPase domain of DnaK, specifically with negatively charged residues in the region 206-221 (Ahmad *et al.*, 2011). Considering that the work by Jiang and colleagues is based on a covalently-linked Hsc70-auxilin complex (Jiang *et al.*, 2007), the more recent work, on a non-covalent DnaK-DnaJ complex in solution (Ahmad *et al.*, 2011), is probably a more physiological-like system and therefore is potentially a more accurate model of the Hsp70-Hsp40 interaction.

In addition to the mechanisms involved in Hsp70-Hsp40 interactions, the aspect of substrate binding by the Hsp70-Hsp40 machinery has been extensively studied. In a study by the Bukau group, a peptide binding motif for recognition by a type I Hsp40 (yeast Hsp40, Ydj1p) was identified, and was found to be present in multiple copies in many yeast proteins. The identified consensus binding motif, described as G[LMQ]L{P}X{P}{CIPMVW}, where [XY] denotes the presence of one of those residues, and {} denotes none of those residues, at that position. Based on these findings and further experiments with the identified sequence, a model was proposed for Hsp40 substrate binding and subsequent delivery to Hsp70, in which a non-native polypeptide substrate is bound in a two-site binding process by both the peptide-binding motif and the zinc-finger domain of the Hsp40, and is extended between the two sites. The Hsp40, to which the substrate is now bound via two sites, is then thought to be delivered to Hsp70 for refolding by interaction with Hsp70 via its J-domain. Though this sequence and the model of substrate binding and delivery were described for the yeast type I Hsp40 Ydj1p, it is considered feasible that it may apply to other systems too, such as the human Hsp40 Hdj2, as well as other type I Hsp40s (Kota *et al.* 2009).

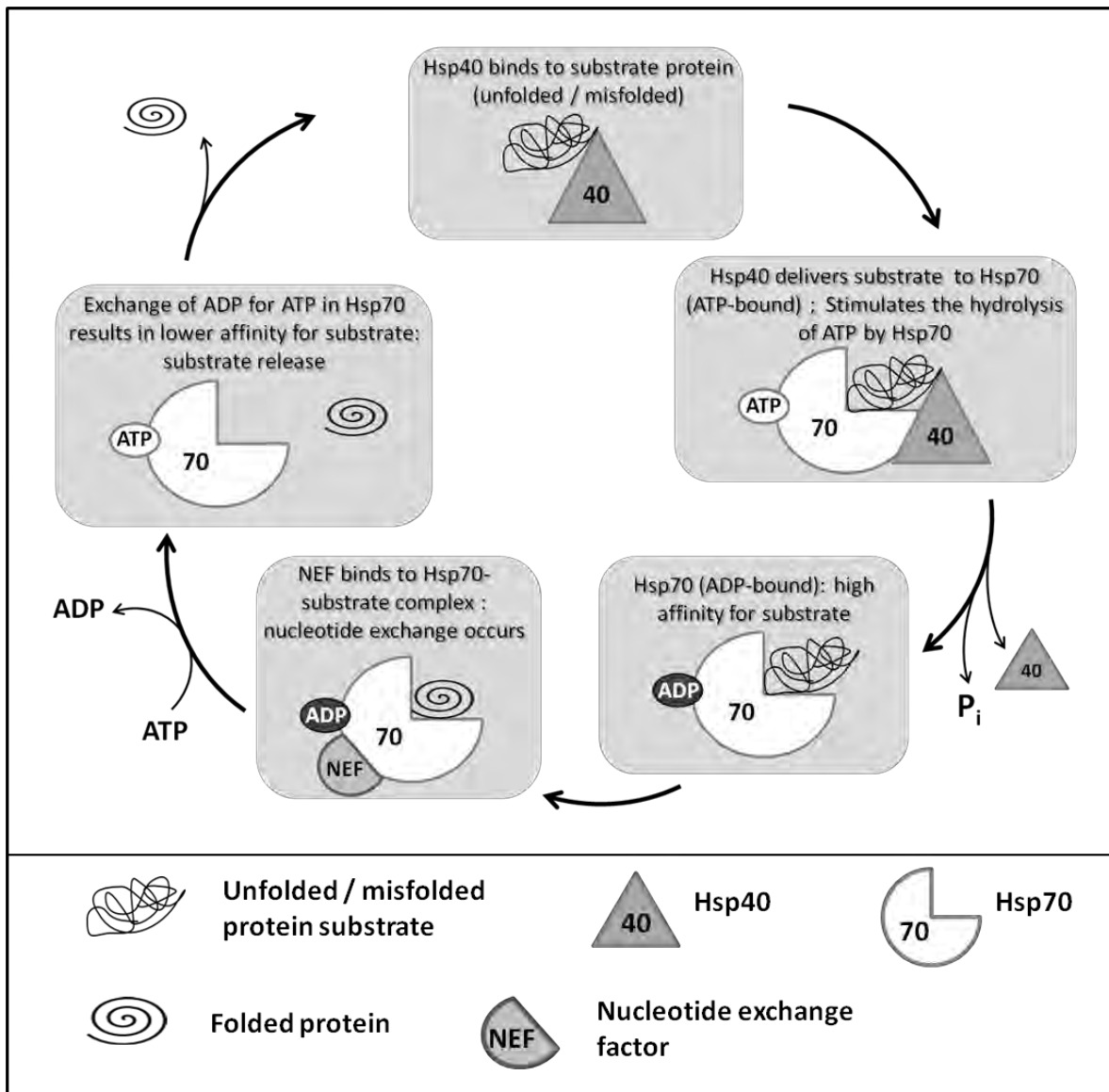


**Figure 1.3: The ATPase cycle associated with Hsp70-mediated protein folding.** An unfolded / misfolded substrate peptide is bound by Hsp40 and delivered to ATP-bound Hsp70. The ATPase activity of Hsp70 is stimulated by Hsp40, resulting in Hsp70 being ADP-bound, undergoing a conformational change, and exhibiting an increased affinity for the substrate peptide, stabilizing the peptide-Hsp70 binding. A nucleotide exchange factor facilitates the exchange of ADP bound to Hsp70 for ATP, with which substrate affinity is lowered, releasing the substrate (Szabo *et al.*, 1994, Hennessy *et al.*, 2005).

In co-operation with the Hsp70-Hsp40 chaperone systems, the Hsp100 or Clp family of chaperones, also a highly conserved group of chaperone proteins, functions to reverse stress-induced protein aggregates, specifically by solubilisation and subsequent unfolding of aggregates in an ATP-driven process. Hsp100 (called ClpB in eukaryotes and Hsp104 in eukaryotes) thus plays an important role in the thermotolerance of organisms (Schlieker *et al.*, 2004; Glover and Lindquist, 1998).

It must be noted that a lot of the work done on elucidating mechanisms of chaperone machinery and interactions between chaperones and co-chaperones has been done on bacterial systems, and though the conserved nature of chaperones means that a lot can be inferred from the bacterial system for other systems, significant differences between the bacterial and eukaryotic systems have been identified.

### **1.1.3. *P. falciparum* heat shock proteins**

---

The life cycle of *P. falciparum* (described in section 1.1.1.2) includes stages both in cold-blooded mosquito and warm-blooded human hosts (Sinnis and Sim, 1997). The transition between the cold-blooded and warm-blooded environments means that the parasite is subjected to a potential temperature increase of more than 10°C (as reviewed by Acharya *et al.*, 2007). In addition to this initial temperature increase *P. falciparum* is also exposed to further, periodical temperature increases in the form of fevers experienced by the malaria patient (Oakley *et al.*, 2007). These fevers have been found to coincide with and therefore likely to be a result of the rupture of schizont-bearing erythrocytes and consequent release of merozoites into the bloodstream. The human body's response, in the form of significantly elevated body temperature (fever), not only does not impair parasite survival, but promotes *P. falciparum* development (Pavithra *et al.*, 2004). The parasite is thus regularly exposed to temperature changes: from ~ 25 °C in the mosquito, to 37 °C in the human and ~41 °C during fever (Pavithra *et al.*, 2004), and in addition to heat shock, *P. falciparum* is exposed to a number of other stresses such as attack by host defence mechanisms (as reviewed by Sharma, 1992), and oxidative stress (Clark *et al.*, 1989). *P. falciparum* therefore needs an efficient mechanism to survive despite these stresses. The parasite's survival in the adverse and diverse conditions of its lifecycle has been attributed to the presence and activity of molecular chaperones - specifically heat shock proteins (Kumar *et al.*, 2003; Pavithra *et al.*, 2004), which are known to play an important role in the survival and virulence of a number of protozoan parasites (Neckers and Tatu, 2008). Considering the above conditions, as well as

the parasite's need to synthesize, with the help of chaperones, a large number of correctly folded proteins necessary for host-cell remodelling and other processes (Section 1.1.1.2), it is not surprising that as much as 2 % of the *P. falciparum* genome encodes chaperones (Acharya et al., 2007). Interestingly, *P. falciparum* Hsp90 has been suggested to be involved in conferring drug resistance to the parasite (Shonhai, 2010), based on the *PFHSP90* gene's location on a chromosomal segment associated with chloroquine resistance (Su and Wellem, 1994).

#### 1.1.3.1. *P. falciparum* Hsp70s

---

The *P. falciparum* genome encodes six Hsp70s (Sargeant et al., 2006; Shonhai et al., 2007), details of which are summarized in Table 1.1. PfHsp70-1, considered the major cytosolic Hsp70 and found in the parasite nucleus and cytosol (Kumar et al., 1991; Pesce et al., 2008), is the most studied of the PfHsp70s (Kumar et al., 1991; Sharma et al., 1992; Matambo et al., 2004; Ramya et al., 2006; Shonhai et al., 2005; Shonhai et al., 2008; Pesce et al., 2008; Bell et al., 2011; Botha et al., 2011; Cockburn et al., 2011). Attention has recently also been drawn to PfHsp70-x in an extensive bioinformatic and cell biological study on the protein (Külzer et al., 2012). Of the six PfHsp70s, the highest sequence identity (75 %) is shared between PfHsp70-1 and PfHsp70-x (see Chapter 3, Section 3.3.4).

PfHsp70-y and PfHsp70-z, both significantly larger than the other Hsp70s in *P. falciparum* (Table 1.1), are highly homologous to the Hsp110/Grp170-like proteins, a sub-family of Hsp70 chaperones, and have been suggested to function as nucleotide exchange factors in the malarial system (Shonhai et al., 2007). PfHsp70-z (PfHsp110c) was recently reported to play an important role in preventing the thermal aggregation of proteins in malaria parasites and, in particular, aggregation prone proteins characterised by the presence of asparagine repeats. This aggregation prevention function was suggested to be carried out in co-operation with Hsp70. Knockout experiments were used to show that PfHsp70-z was essential in the parasite (Muralidharan et al., 2012).

Little is known about PfHsp70-2, PfHsp70-3 and PfHsp70-y. PfHsp70-2 and PfHsp70-y both have a C-terminal ER-retrieval sequence, and PfHsp70-2, also known as PfBiP, is a homologue of the human binding immunoglobulin protein (BiP) (Sargeant et al., 2006; Shonhai et al., 2007). PfHsp70-3 is localised in the mitochondrion, targeted there by a mitochondrial transit peptide (Sargeant et al., 2006; Šlapeta and Keithly, 2004).



**Table 1.1: *Plasmodium falciparum* Hsp70s** (adapted and updated from Shonhai *et al.*, 2007).

	PlasmoDB notation	Predicted Localisation	Predicted size (kDa)	Expression in <i>P. falciparum</i> life cycle
<b>PfHsp70-1</b>	PF08_0054	Cytosolic <sup>(P:1; E:2)</sup> , nuclear <sup>(E:2)</sup> , PV <sup>(P:3)</sup>	74	All erythrocytic stages <sup>(5)</sup>
<b>PfHsp70-2</b>	PFI0875w	ER <sup>(P:1; E:2)</sup>	73	All erythrocytic stages <sup>(5)</sup>
<b>PfHsp70-3</b>	PF11_0351	Mitochondrial <sup>(P:1)</sup>	73	-
<b>PfHsp70-x</b>	MAL7P1.228	Cytosolic <sup>(P:1)</sup> , exported <sup>(E:4)</sup> , PV <sup>(E:4)</sup>	75	-
<b>PfHsp70-y</b>	MAL13P1.540	ER <sup>(P:1)</sup>	108	-
<b>PfHsp70-z</b>	PF07_0033	Cytosolic <sup>(P:1)</sup>	100	-

P: Predicted localisation, E: experimentally confirmed localisation. 1: Sargeant *et al.*, 2006; 2: Kumar *et al.*, 1991; 3: Nyalwidhe *et al.*, 2006; 4: Külzer *et al.*, 2012; 5: PlasmoDB (Aurrecochea *et al.*, 2009).

PfHsp70-1 (PF08\_0054) is highly expressed in all blood stages of the parasite's life cycle, with increased expression after heat shock, and is thus thought to play an important if not essential role in the survival of the parasite (Kumar *et al.*, 1991). To our knowledge, apart from the knockout study showing PfHsp70-z to be essential in parasites, no knockout or knockdown studies have been carried out to determine whether any other Hsp70 is essential in *P. falciparum*. The chaperone activity of recombinant PfHsp70-1 has been confirmed experimentally, in terms of ATPase, aggregation suppression and refolding activities (Matambo *et al.*, 2004; Ramya *et al.*, 2006; Shonhai *et al.*, 2008; Misra and Ramachandran, 2009). In addition to exhibiting *in vitro* chaperone activity, PfHsp70-1 has been found to functionally replace DnaK in a mutant strain of *E. coli*, reversing its thermosensitivity (Shonhai *et al.*, 2005). Similarly, PfHsp70-1 has recently been found to be able to repair mutant growth phenotypes in yeast strains lacking the primary endogenous Hsp70s, Ssa1 and Ssa2 (Bell *et al.*, 2011). Aside from its nuclear and cytoplasmic localizations, proteomic studies have also suggested a possible localization of PfHsp70-1 in the parasitophorous vacuole (Nyalwidhe and Lingelbach, 2006). This localization, though not confirmed by localisation studies using for example antibodies, suggests an involvement of PfHsp70-1 in the translocation of proteins, further emphasizing its importance to the survival of *P. falciparum* survival (de Koning-Ward *et al.*, 2009). Interestingly, levels of PfHsp70-1 were found to be elevated in an artemisinin-resistant *P. falciparum* strain, suggesting a role for PfHsp70-1 in artemisinin tolerance (Witkowski *et al.*, 2010). A recent study confirmed the role of PfHsp70-1 in protein trafficking,

specifically of proteins targeted to the apicoplast by the presence of an N-terminal transit peptide: PfHsp70-1 was shown, by co-immunoprecipitation, to interact with positively charged residues in the signal peptide (Banerjee *et al.*, 2012). A number of malarial Hsp40s have been predicted or shown to interact with PfHsp70-1 (Section 1.1.4.2), and in a bioinformatic analysis of PfHsp70-1, homology modelling and sequence analyses were carried out to predict residues in the ATPase domain of the protein important to interactions of PfHsp70-1 with Hsp40 partners (Shonhai *et al.*, 2008).

PfHsp70-x was recently discovered to be exported to the erythrocyte (Külzer *et al.*, 2012), contrary to the previously predicted cytosolic localisation (Sargeant *et al.*, 2006). Up until this discovery, it was generally assumed that Hsp40s exported by *P. falciparum* into the erythrocyte interacted with human Hsp70. The study by Külzer and colleagues, however, shows not only that PfHsp70-x is exported, but that it associates in complexes with exported PfHsp40s in mobile structures in infected erythrocytes termed J-dots (Külzer *et al.*, 2012; Külzer *et al.*, 2010). Interestingly, PfHsp70-x was also found to partially co-localise and thus potentially interact with PfEMP1 in infected erythrocytes. Therefore, PfHsp70-x is likely to be involved in protein transport and thus parasite pathogenicity of *P. falciparum* in the infected host cell, making it an attractive drug target (Külzer *et al.*, 2012).

### 1.1.3.2. *P. falciparum* Hsp40s

---

The *P. falciparum* genome encodes at least 49 Hsp40 proteins, representing a structurally and functionally diverse group of proteins, 19 of which are predicted to be exported to the host cell (Botha *et al.*, 2007; Njunge *et al.*, 2012), and are possibly involved in host cell remodelling (Sargeant *et al.*, 2006). Of the 49 Hsp40s, only two are type I, nine are type II, twenty five are type III and thirteen are type IV Hsp40s (Njunge *et al.*, 2012).

Hsp40s have also been found to play pathogenically important roles in *P. falciparum*: the mature parasite-infected erythrocyte surface antigen (MESA), or PfEMP2 (PFE0040c), is involved in knob formation in infected erythrocytes (Sharma, 1991), and recently, a type II Hsp40 termed KAHsp40 (PFB0090c/PF3D7\_0201800) was proposed to play a role in chaperoning knob assembly, co-localising with both KAHRP and PfEMP1 (Acharya *et al.*, 2012).

In a large-scale gene knockout study in *P. falciparum*, three Hsp40s were suggested to be essential to the parasite's survival, including a type II (PFA0660w) and two type IV (PF11\_0034; PF11\_0509) Hsp40s, all predicted to be exported due to the presence of the PEXEL sequence (Maier *et al.*, 2008). Interestingly, PFA0660w was found to co-localise with PfHsp70-x in the erythrocyte cytosol (Külzer *et al.*, 2012), suggestive of a chaperone/co-chaperone complex between the two exported proteins. Eleven Hsp40s were found to be non-essential to *P. falciparum* in the study by Maier and colleagues, and were suggested to have redundant functions, or function overlapping with other Hsp40s of the many encoded by the parasite (Maier *et al.*, 2008).

A number of potential Hsp70-Hsp40 chaperone interactions exist in *P. falciparum*. One of the two type I Hsp40s in the parasite, PfHsp40 (PF14\_0359), typical type I Hsp40, has been found to be up-regulated by heat shock, and functionally interacts with PfHsp70-1 *in vitro*, stimulating the ATPase (both single-turnover and steady state) and aggregation suppression activities of PfHsp70-1 (Botha *et al.*, 2011), suggesting a role for PfHsp40 as a co-chaperone to PfHsp70-1 in the cytosol. Pfj4, a heat-inducible type II Hsp40, has been suggested to have a possible interaction with PfHsp70-1, based on its cytosolic and nuclear localization (Pesce *et al.*, 2008), its induction upon heat shock (Watanabe *et al.*, 1997), as well as experimental evidence suggestive of an association between the two proteins (Pesce *et al.*, 2008). Though not experimentally validated, a possible interaction between PfHsp70-1 and PFB0595w, a type II Hsp40, has been predicted, based on a combination of *in silico* and yeast two-hybrid analyses (Pavithra *et al.*, 2007).

#### **1.1.4. Hsp70 as a drug target**

---

In light of the fact that chaperones do not function in isolation, but rather in conjunction with a number of co-chaperones and co-factors, chaperones have been proposed to represent a potentially attractive class of drug targets in a recent review on plasmodial chaperones as antimalarial drug targets, the rationale being that specific modulation of a single chaperone would likely have far-reaching effects on a biological system (Shonhai, 2010). Based on the implication of Hsp70 in numerous human diseases including cancer, viral infection and protein conformational diseases such as Parkinson's disease, the chaperone is considered a potential drug target in various systems (Brodsky and Chiosis, 2006), including malaria (Pesce *et al.*, 2010; Shonhai, 2010). Disease pathologies involving Hsp70 have been found to

have inappropriate levels of Hsp70 in both directions – either too much Hsp70 or too little Hsp70 can be problematic (Patury *et al.*, 2009). For this reason, various attempts at identifying modulators of Hsp70 chaperone function have been made, and several classes of Hsp70 modulators have subsequently been identified (Fewell *et al.*, 2004; Ramya *et al.*, 2006; Wright *et al.*, 2008; Chiang *et al.*, 2009). In the modulation of Hsp70, it is the ATPase activity of the protein that is of particular interest and is targeted (Fewell *et al.*, 2004; Chiang *et al.*, 2009; Botha *et al.*, 2011), based on the fact that the ATPase activity is central to regulating the biological protein folding function of Hsp70, as reviewed in Section 1.1.3 and illustrated in Figure 1.3. A review on inhibitors of Hsp90 and Hsp70 ATPase activities published in 2010 (Massey *et al.*, 2010) discussed the difficulties in inhibiting the ATPase activity of Hsp70 compared to Hsp90, an important drug target in cancer (as reviewed by Patury *et al.*, 2009). Software which, using algorithms, determines the “druggability” of biological molecules, showed that Hsp90 ATPase activity is considerably easier to inhibit than Hsp70 ATPase activity. This difference in “druggability” has been attributed to structural differences in the ATPase domains of the two chaperones – including the ATP binding site of Hsp70 being significantly more hydrophilic than that of Hsp90, reducing the likelihood of potent inhibitors of Hsp70 being cell permeable. Hsp70 ATPase activity inhibition is further complicated by the higher affinity for ATP and ADP displayed by Hsp70 compared to Hsp90, making inhibition by competitive binding more difficult (as reviewed by Massey *et al.*, 2010). In addition to these complications, studies have found that inhibition of Hsp90 in cancer in clinical trials is less effective than expected, explained by the increased expression of Hsp70 in response to the Hsp90 inhibitor, compensating for loss of Hsp90 function and reversing the effects of the compound (as reviewed by Jegu *et al.*, 2010). Furthermore, treatment of cancer cells with 17-AAG, a known Hsp90 inhibitor, has been found to be more effective when combined with the knockdown of Hsp70 by siRNA (Guo *et al.*, 2005), suggesting that Hsp70 does in fact compensate for loss of Hsp90 function. This is an important factor to consider in the targeting of Hsps and in particular in cancer systems, it has been suggested that combination treatments of Hsp90 and Hsp70 inhibitors may be a more effective approach (Patury *et al.*, 2009). As reviewed in an article on malarial heat shock proteins as chemotherapeutic targets, Hsp90 in *P. falciparum* (PfHsp90) has been found to have many interacting partners in the parasite, and is essential to parasite survival. In addition to this, PfHsp90 also has a number of roles in the parasite in common with Hsp70s (Shonhai, 2010). For these reasons, like in the case of cancer described above, potential antimalarials targeting malarial Hsp70s could be more effective in conjunction with the inhibition of PfHsp90.

#### 1.1.4.1. Hsp70 modulation

---

Hsp70 modulators identified to date were recently reviewed by Evans *et al.* (2010). Classes of molecules identified as inhibitors of Hsp70 currently include spergualins, dihydropyrimidines, fatty acids, peptides and ATP mimics. An example of a well-known spergualin Hsp70 inhibitor is 15-deoxyspergualin (DSG, Figure 1.4A), an immunosuppressive drug which has also been found to have suppressive or inhibitory effects on malaria parasite growth, both *in vivo* (rodent malaria in mice) (Midorikawa and Haque, 1997) and *in vitro* (cultured *P. falciparum*) (Midorikawa *et al.*, 1998). DSG has been found to modulate Hsp70 chaperone activity, both the ATPase (stimulation of mammalian and yeast Hsc70; Brodsky, 1999) and aggregation suppression activity (stimulation of ATP-enhanced activity of PfHsp70-1; Ramya *et al.*, 2006). DSG is thought to interact with Hsp70 via its EEVD motif (Nadeau *et al.*, 1994; Nadler *et al.*, 1998; Ramya *et al.*, 2006). Interestingly, DSG has recently been shown to disrupt the interaction between PfHsp70-1 and the hydrophobic residues of the N-terminal signal sequence targeting *PfENR*, an enoyl-ACP reductase, to the *P. falciparum* apicoplast. The disruption of this interaction was proposed to be due to binding of DSG to the EEVD motif and subsequent blockage of the nearby substrate-binding domain of PfHsp70-1 (Banerjee *et al.*, 2012).

Pyrimidinone compounds, structurally related to DSG, have also been tested as modulators of Hsp70 chaperone activity (Wright *et al.*, 2008; Fewell *et al.*, 2004; Chiang *et al.*, 2009; Botha *et al.*, 2011), resulting in the identification of modulators of the basal and/or the Hsp40-stimulated ATPase activity of various Hsp70s (yeast Hsp70 Ssa1p: Wright *et al.*, 2008; Fewell *et al.*, 2008; Chiang *et al.*, 2009; Human Hsp70: Chiang *et al.*, 2009 and PfHsp70-1: Chiang *et al.*, 2009; Botha *et al.*, 2011). Examples of such pyrimidinone compounds are MAL3-39 and DMT002264 (Figures 1.4B and 1.4C). Both MAL3-39 and DMT002264 have been found to modulate Hsp70 function, including PfHsp70-1 function, and additionally also have growth inhibitory effects on cultured *P. falciparum* parasites (Botha *et al.*, 2011; Chiang *et al.*, 2009). MAL3-39 and DMT002264 have also been shown to affect different Hsp70-Hsp40 partnerships in distinct manners: a malarial Hsp70-Hsp40 system (PfHsp70-1-PfHsp40), for example, was inhibited by DMT002264, whereas a human Hsp70-Hsp40 system (Human Hsp70-Hdj2), was unaffected in single-turnover ATPase assays, further illustrating the potential for different (but highly homologous) chaperone systems to be specifically and differentially modulated by small molecules (Botha *et al.*, 2011). In addition to having different effects on different proteins, compounds have been found to have differential effects on Hsp70 ATPase activity depending on whether Hsp70 was acting alone, or was

stimulated by an Hsp40 partner (Fewell *et al.*, 2004). MAL 3-39, for example, had no significant effect on the basal or endogenous Hsp70 ATP hydrolysis activity, but it showed significant inhibition of the Hsp40-stimulated Hsp70 ATPase activity, depending on the Hsp40 protein used (Fewell *et al.*, 2004). The mechanism by which pyrimidinone compounds modulate Hsp70 chaperone activity is not known, however, functional data interpreted together with structural features of structurally related compounds in this class led to the suggestion of the importance of both the pyrimidinone and the peptoid (present in DSG) components of the compounds (Wright *et al.*, 2008). Structural features of interest are highlighted in Figure 1.4.

In a study in which a number of peptide-linked dihydropyrimidines, compounds structurally closely related to the pyrimidinone compounds described above, were tested on Hsp70 (*E. coli* DnaK) activity, a number of molecules, including 116-5c (Figure 1.4D), were found to significantly modulate the luciferase refolding activity of DnaK, in both directions (stimulation and inhibition) (Wisén *et al.*, 2008). In this study, it was also shown that compounds with a high degree of structural similarity can have opposite (inhibitory vs. stimulatory) effects on Hsp70 function (Wisén *et al.*, 2008). Interestingly, a second peptide-linked dihydropyrimidine compound, 115-7c (Figure 1.4E), has been found to act as an “artificial chaperone” to DnaK, acting like an Hsp40 partner would, stimulating the chaperone activity (both ATPase and protein folding) of DnaK, and even compensated for a mutation in a yeast Hsp40, reversing the loss of function of the Hsp40 (Wisén *et al.*, 2010). The observed effects were found to be due to the binding of the compound on a region adjoining the J-domain binding site on DnaK (Wisén *et al.*, 2010). Dihydropyrimidines were also included in a study in which dihydropyrimidines, benzothiazines and flavones were tested as Hsp70 inhibitors as potential treatment of Alzheimer’s disease. A number of compounds screened resulted in the degradation of tau peptides (responsible for Alzheimer’s disease symptoms) due to Hsp70 inhibition, and were deemed promising alternative anti-Alzheimer’s disease drug candidates (Jinwal *et al.*, 2009). Interestingly, as part of the study by Jinwal and colleagues, methylene blue, a well-documented and effective antimalarial agent (Schirmer *et al.*, 2011) significantly inhibited the ATPase activity of Hsp70 (Jinwal *et al.*, 2009). Hsp70 inhibition as potential cancer treatment is also a growing research area. Adenosine-derived inhibitors (ATP mimics) of Hsp70 have been found to be relatively selective, and have been shown to have cytotoxic effects on HCT116 (human colon cancer) cells, which in some cases was attributed to Hsp70 modulation by these compounds (Williamson *et al.*, 2009).

Modulation of Hsp70 *in vitro* can be analysed using a number of different assays measuring various aspects of chaperone activity. How any modulation of activity observed in these assays relates to the desired *in vivo* effects, however, is not clear. Not only in the case of Hsp70 modulations, but in many other systems too, it is not possible, simply from *in vitro* studies, to know what the effects of metabolism in *in vivo* systems would be on compounds. It is thus essential that *in vitro* work is complemented with suitable *in vivo* studies (Evans *et al.*, 2010). In the case of malarial Hsp70 (and heat shock proteins in general), criticism of Hsp70 as a drug target lies in that Hsp70s across organisms are highly conserved, which makes designing or identifying compounds that have a high enough degree of specificity to inhibit the malarial Hsps and not the human equivalent difficult (Pesce *et al.*, 2010; Shonhai, 2010). The fact that this group of proteins is so highly conserved, however, and that they are essential for cell survival, means that Hsp70s are likely to evolve much slower than other less conserved and less essential protein families, and thus would be likely to be less susceptible to drug resistance (Edkins and Blatch, 2012). Ideally, for a malarial protein to be a good drug target candidate, there have to be substantial structural differences between the drug target and the corresponding human protein. PfHsp70-1 and its human homologue (HSPA1A) share a very high sequence identity of 72 % (see Chapter 3, Section 3.3.4); however, the two proteins have been differentially modulated by certain compounds (Chiang *et al.*, 2009), thus the identification of compounds specific enough to modulate only a malarial Hsp70 is conceivable.

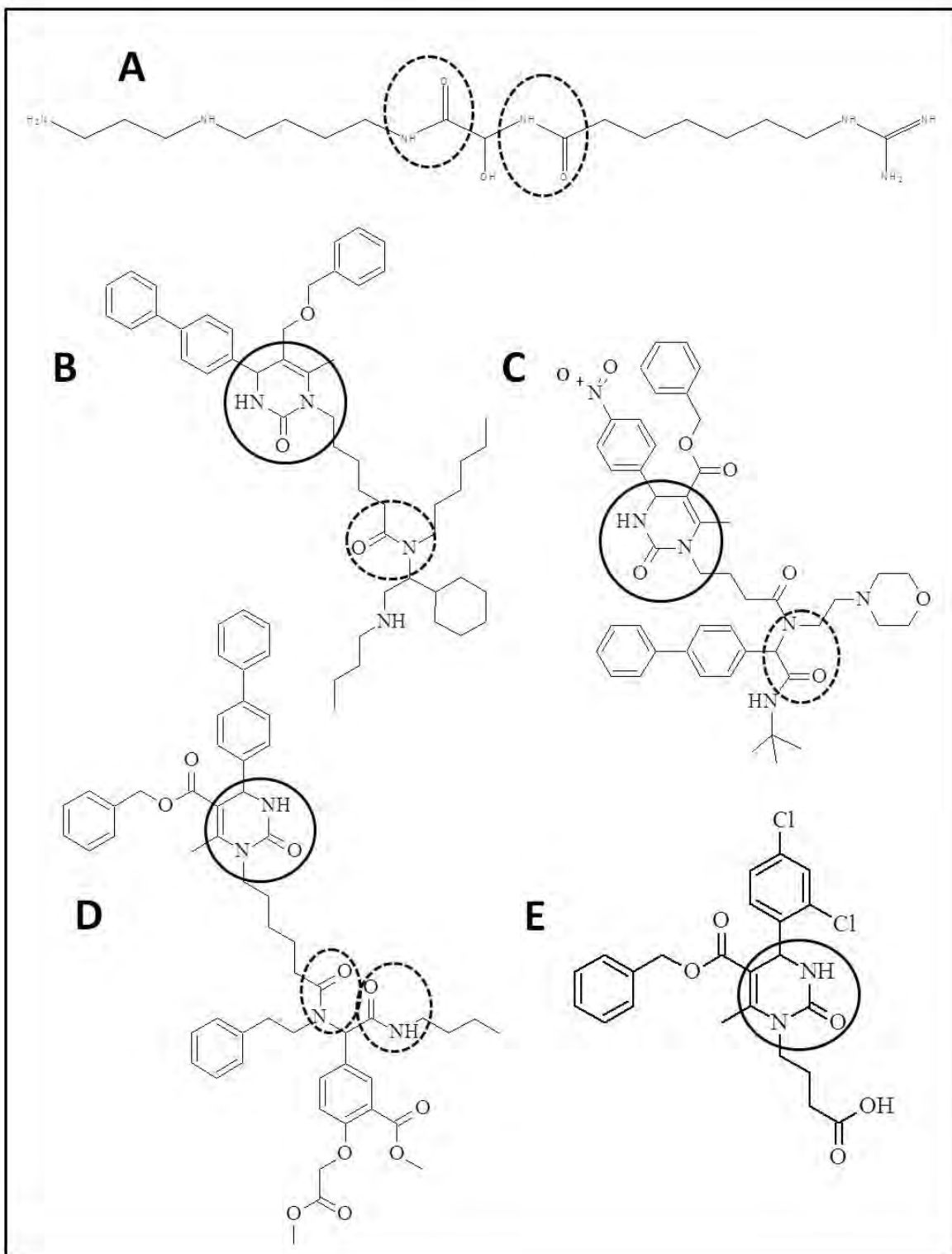


**Figure 1.4: Structures of previously identified Hsp70 modulators 15-deoxyspergualin (A), MAL-3-39 (B) DMT002264 (C), 116-5c (D) and 115-7c (E).** The structural features of the compounds thought to be important in their function as Hsp70 modulators, the pyrimidinones and peptoid components, are circled in solid and dashed lines respectively (structures re-drawn from Wright *et al.*, 2008; Chiang *et al.*, 2008, Wisén *et al.*, 2008).



## **1.2. RESEARCH MOTIVATION**

---

The ever increasing resistance of *Plasmodium falciparum* to current therapeutic agents (Section 1.1.1.3) has given rise to an urgent need for novel anti-malarial drugs with novel mechanisms and targets. PfHsp70-1 and PfHsp70-x both play important roles in the survival and virulence of the malaria parasite in the human body after infection, and in addition, PfHsp70-1 may play a role in drug resistance (Section 1.1.4.1). The two chaperones thus represent potential drug targets, assuming they can be specifically modulated in a way that does not interfere with the highly homologous human Hsp70s. Research findings reviewed in Section 1.1.4.1 show that Hsp70s, and in particular PfHsp70-1, can be differentially modulated (compared to human Hsp70) by small molecules. The identification of small molecule modulators that can alter or impair the correct functioning of PfHsp70-1 and/or PfHsp70-x (either in isolation or in their Hsp40-assisted activities) in a specific manner, and that subsequently compromise *P. falciparum* growth and virulence, would significantly contribute to the development of novel anti-malarial compounds.

## **1.3. HYPOTHESIS**

---

The basal and/or Hsp40-stimulated *in vitro* chaperone activity of PfHsp70-1 and/or PfHsp70-x can be selectively modulated by small molecules, which inhibit the growth of *P. falciparum* parasites in culture.

## 1.4. OBJECTIVES

---

The broad research objective of this project is to test the effects of a set of compounds of natural origin on the *P. falciparum* and human Hsp70-Hsp40 chaperone systems, with the aim of finding compounds that significantly and selectively modulate the chaperone function of PfHsp70-1 and/or PfHsp70-x, and inhibit *in vitro* parasite growth. Specific research objectives include:

1. Recombinant production and purification of malarial (PfHsp70-1, PfHsp70-x, PfHsp40) and human (HsHsp70 and Hsj1) Hsp70 and Hsp40 proteins of interest.

*Strategy: Transformation of hexa-histidine-tagged chaperone-encoding plasmids into E. coli, overexpression of recombinant proteins, purification of overexpressed proteins by nickel-affinity chromatography.*

2. Assessment of the effects of test compounds on the *in vitro* chaperone activities of PfHsp70-1, PfHsp70-x and HsHsp70 (basal and Hsp40-stimulated).

*Strategy: Screening of compounds for effects on the chaperone activities of Hsp70s (in the presence and absence of Hsp40s) using in vitro aggregation suppression and steady-state ATPase assays.*

3. Assessment of the affinities of compounds of interest for PfHsp70-1, PfHsp70-x and HsHs70 as well as the potential disruption of Hsp70-Hsp40 interactions by compounds.

*Strategy: Surface Plasmon resonance (SPR) spectroscopy to establish and quantify Hsp70-compound and Hsp70-Hsp40 interactions, as well as to investigate the effects of compounds on any established Hsp70-Hsp40 interactions.*

4. Testing compounds of interest as potential inhibitors of growth of *P. falciparum* parasites in culture, and determining the toxicity of any such compounds to mammalian cell lines.

*Strategy: Screening of compounds of interest as inhibitors of in vitro P. falciparum growth using a growth inhibition assay and P. falciparum-infected erythrocytes, and assessing the toxicity of compounds to cultured mammalian cells using a cell proliferation assay.*

**CHAPTER 2:**

---

**Heterologous expression and purification of recombinant heat shock proteins**

---

## 2.1. INTRODUCTION

---

A significant milestone in the modern biotechnology industry was the successful production of the first human protein, somatostatin, in a bacterial system, by Genentech and their collaborators in 1977. Itakura and colleagues were able to produce the 14 amino acid human growth hormone in *E. coli*, achieving the first ever successful production of a functional polypeptide from a synthetic gene (Itakura *et al.*, 1977). Soon after this historical achievement, in 1978, the second and hugely significant recombinant production of a human hormone was achieved: human insulin was produced in *E. coli* (Genentech press release, 1978), another milestone not only in biotechnology but also in modern medicine. Since then, a large amount of research on heterologous protein production has been carried out, both in medical or therapeutic contexts as well as for the characterisation of proteins of interest in fundamental research.

There are a large number of possible expression host systems which can be considered for the production of heterologous proteins, including bacteria (e.g. *E. coli*, *Bacillus* spp., *Pseudomonas* spp.), yeasts, fungi, insect cells, mammalian cells, transgenic animals (in which proteins of interest are expressed in and purified from milk, egg white, blood, urine or plasma) and transgenic plants (reviewed by Demain and Vaishnav, 2009). Of these host systems, *E. coli* is the most widely used system for several reasons. The genome and genetic mechanisms of *E. coli* have been extensively studied and characterised; growth rates as well as protein expression rates in *E. coli* are rapid, allowing for large-scale production of recombinant proteins; and the growth and maintenance of *E. coli* in culture is relatively inexpensive (Demain and Vaishnav, 2009). Disadvantages, however, include the inability of the *E. coli* cells to carry out post-translational modification of eukaryotic proteins (Makrides, 1996), as well as the tendency of the bacterial cells to produce recombinant proteins in the form of insoluble inclusion bodies of inactive protein, complicating subsequent protein purification procedures (Kane and Hartley, 1988).

In addition to host expression systems, there are also many commercially available heterologous expression vector systems to choose from, which allow for the over-expression of recombinant proteins, as well as the control of this expression by the presence of a specific promoter included on the expression vector (Nicoll *et al.*, 2006). Each of these different promoter systems has different advantages. The expression system used in the purification of all but one protein in this study was the

pQE30 vector (Qiagen, U.S.A.), containing a T5 phage promoter, which is readily recognised by *E. coli* polymerase, and can be tightly regulated (Nicoll *et al.*, 2006).

In light of increasing malaria drug resistance and hence the need for the identification and characterisation of novel plasmodial proteins as drug targets, there is an increasing need to obtain large amounts of pure and functional plasmodial proteins by heterologous gene expression (Birkholtz *et al.*, 2008). The expression of recombinant plasmodial proteins has proven somewhat problematic, as illustrated by the attempted heterologous expression of 1000 *P. falciparum* open reading frames in *E. coli* by the Structural Genomics of Pathogenic Protozoa (SGPP) group (Washington, U.S.A.), which resulted in only about a third of the target proteins being successfully expressed, and of these, only 63 proteins were obtained in a soluble form (Mehlin *et al.*, 2006).

A consideration with heterologous or recombinant protein expression in a non-native host expression system is the matter of rare codons (Gustafsson *et al.*, 2004). Coding regions from heterologous organisms, such as the human and malarial genes expressed in *E. coli* in the case of this study, can sometimes contain certain codons that are rare in *E. coli*. This can result in slow, inefficient production of the protein of interest, and even in early termination of translation, resulting in truncated protein products (Gustafsson *et al.*, 2004). *P. falciparum* has an AT-rich genome (~ 80 % AT content, Musto *et al.*, 1999), and this phenomenon, as well as the rare codons used by *Plasmodium*, have previously resulted in problems when expressing malarial genes in *E. coli* (Baca and Hol, 2000; Matambo *et al.*, 2004). To overcome the problem of rare codons in *P. falciparum* protein production in *E. coli*, Baca and Hol (2000) constructed a plasmid referred to as the RIG plasmid, which encodes codons for arginine (R), isoleucine (I) and glycine (G) that are rare in *E. coli*. In their study, Baca and Hol found that co-expression of the RIG plasmid with the expression vectors encoding malarial proteins in *E. coli* significantly improved the expression of the malarial proteins (Baca and Hol, 2000). Another approach to overcome the matter of rare codons is the use of codon optimisation, a technology in which rare codons in a heterologous coding sequence are replaced with codons more frequently used by the expression host, without altering the amino acid sequence. This is achieved either by site-directed mutagenesis, or by synthesis of an entire gene with the modified codons (Gustafsson *et al.*, 2004). Alternatively, instead of codon optimisation, a more recent technique referred to as codon harmonisation can be used for the expression of a heterologous gene containing rare codons. Codon harmonisation is based on the idea that the pattern of codon frequency along a gene regulates the gene translation rate, employing less

frequently used codons, for example, to slow the translation rate and allow for correct folding of the nascent polypeptide at certain points (Angov *et al.*, 2008). Codon harmonisation, therefore, involves “harmonising” the sequential codon frequency pattern of a heterologous gene in a host system with the codon frequency of a wild type gene in its native system to emulate the rate of translation of a gene in its native environment (Angov *et al.*, 2008). Both codon optimisation and codon harmonisation have been shown to greatly improve expression levels of heterologous proteins in *E. coli* (Gustafsson *et al.*, 2004; Angov *et al.*, 2008). Codon harmonisation of the coding region of *P. falciparum* merozoite surface protein 1 (MSP1), an important malaria vaccine candidate, resulted in a significant increase (~ 1000 fold increase) in the expression level of MSP1 in *E. coli* compared to the wild type coding region (Angov *et al.*, 2011a; Angov *et al.*, 2011b).

The study by the SGPP group revealed that the matter of rare codons and AT content in *P. falciparum* genes played a less significant role in the problems associated with the heterologous expression of soluble plasmodial proteins than protein characteristics including high molecular weight, high pI, high degree of protein disorder as well as a lack of homology to *E. coli* proteins (Mehlin *et al.*, 2006). Some simple and often successful ways of improving the solubility of recombinant proteins expressed in *E. coli* include using expression temperatures lower than the typical 37 °C, as well as the use of bioreactors for *E. coli* growth (Birkholtz *et al.*, 2008).

Molecular chaperones (either of the same species as the target protein or of the same species as the expression host) have also been shown to aid in the expression of soluble recombinant proteins. Chaperones, either one or a combination of chaperones and co-chaperones, have been found to successfully facilitate the correct folding of recombinant proteins when co-expressed with the target gene in a given expression host, resulting in higher yields of soluble target protein. This strategy has been successfully demonstrated in literature. In one study, a number of yeast proteins co-expressed with *E. coli* chaperones in an *E. coli* expression system resulted in significantly increased solubility of the majority of the target proteins (Trésaugues *et al.*, 2004), as did the co-expression of a number of eukaryotic proteins (human, yeast, *Xenopus laevis* and *Anopheles* spp. origin) co-expressed with *E. coli* chaperones in *E. coli* in another study (de Marco and De Marco, 2004). Co-expression of a human target protein (argonaute) with human Hsp90 in *E. coli* was also found to result in significantly increased yields of soluble target protein (Tolia and Joshua-Tor, 2006). More recently, this strategy of co-expressing target proteins with chaperones for improved solubility has been applied to a malaria drug target: the

co-expression of PfHsp70-1 with the drug target GTP cyclohydrolase I (PfGCHI), involved in the plasmodial folate biosynthetic pathway, was shown to significantly improve yields of soluble recombinant PfGCHI expressed in *E. coli* (Stephens *et al.*, 2011).

Examples of therapeutically important *P. falciparum* proteins which have recently been successfully produced in *E. coli* are given in Table 2.1, along with the special conditions applied in the expression.

**Table 2.1: Recently produced recombinant *P. falciparum* proteins of therapeutic interest.** Special expression conditions (where specified) are described.

Protein	Therapeutic relevance	Special expression conditions	Reference
Circumsporozoite protein (CSP)	Vaccine candidate: hepatocyte invasion	Codon optimisation, bioreactor <i>E. coli</i> growth, low temperatures (25 °C)	Plassmeyer <i>et al.</i> , 2009
Pfs48/45	Vaccine candidate: transmission blocking	Codon harmonisation	Chowdhury <i>et al.</i> , 2009
1-deoxy-D-xylulose-5-phosphate reductoisomerase (PFDXR)	Drug target: role in isoprenoid biosynthesis, absent in humans	Codon harmonisation	Goble <i>et al.</i> , 2012
Orotate phosphoribosyltransferase / orotidine 5'-monophosphate decarboxylase complex (PfOPRT/PfOMPDC)	Drug target: pyrimidine biosynthesis	Low temperatures (18 °C)	Kanchanaphum and Krungkrai, 2010
GTP cyclohydrolase I (PfGCHI)	Drug target: folate biosynthesis	Co-expression with <i>P. falciparum</i> chaperone (PfHsp70-1)	Stephens <i>et al.</i> , 2011
PfHsp90	Drug target: asexual stage parasite development	None specified	Pallavi <i>et al.</i> , 2010
PfHsp40	Drug target: suggested cytosolic Hsp70 co-chaperone	Codon harmonisation, 26 °C and 30 °C.	Botha <i>et al.</i> , 2011

To be able to study and work with a recombinantly produced protein, it needs to be obtained in a pure form, free of any contaminating proteins. Various approaches can be considered for the isolation or purification of proteins from a whole cell lysate. In the case of Hsp70s, which bind ATP or ADP, immobilised ATP or ADP can be used to purify the proteins. However, this can result in the co-purification of endogenous Hsp70s, such as DnaK in *E. coli* (Blond-Elguindi *et al.*, 1993), contaminating the heterologous protein; a problem commonly encountered in Hsp70 purification (Rial and Ceccarelli, 2002). The co-purification of native chaperones along with recombinant chaperones can be overcome by the use of affinity tags in affinity chromatography. The pQE30 expression vector mentioned above is engineered to produce the protein of interest as a fusion protein, bearing an N-terminal hexa-histidine (His)<sub>6</sub> tag, allowing for relatively simple purification by nickel-affinity chromatography (Porath *et al.*, 1975; Sulkowski *et al.*, 1985). An additional advantage to using hexa-histidine tags is that protein

characteristics are rarely altered by histidine tags, compared, for example, to glutathione S-transferase (GST) tags, which, due to the GST protein itself being a dimer, can cause dimerisation of recombinant GST fusion proteins (Structural Genomics Consortium *et al.*, 2008). In addition, hexa-histidine tags are relatively small, and, unlike some other fusion tags, do not alter the solubility of recombinant fusion proteins (Structural Genomics Consortium *et al.*, 2008). Despite the use of an affinity tag such as a hexa-histidine tag, co-purification of bacterial proteins together with recombinant proteins is not an uncommon problem, and bacterial contaminants that commonly co-purify with hexa-histidine proteins purified by nickel-affinity chromatography include the chaperones and co-chaperones GroES (10.4 kDa), DnaJ (41.1 kDa), GroEL (57.4 kDa) and DnaK (69.1 kDa), which may co-purify by binding to either the chromatographic resin or the recombinant target protein (Structural Genomics Consortium *et al.*, 2008).

The successful expression and purification of a number of *P. falciparum* chaperones or co-chaperones has been reported in literature. Recombinant PfHsp70-1 (Matambo *et al.*, 2004; Ramya *et al.*, 2006; Shonhai *et al.*, 2008; Chiang *et al.*, 2009; Misra and Ramachandran, 2009), PfHsp70-2 (Ramya *et al.*, 2006), PfHip (Ramya *et al.*, 2006), PfHsp40 (Botha *et al.*, 2011), PfHop (Gitau *et al.*, 2012) and PfHsp90 (Pallavi *et al.*, 2010) have all been expressed in and purified from *E. coli*. PfHsp70-1, included in this study, has previously been successfully purified by both native (Ramya *et al.*, 2006; Shonhai *et al.*, 2008) and denaturing (Matambo *et al.*, 2004; Shonhai *et al.*, 2008; Chiang *et al.*, 2009; Misra and Ramachandran, 2009) methods, as well as in the presence (Matambo *et al.*, 2004; Shonhai *et al.*, 2008; Misra and Ramachandran, 2009) and the absence (Ramya *et al.*, 2006) of the RIG plasmid. PfHsp40, the purification of which has only been reported once, is also included in this study. PfHsp40 was purified by denaturing methods, and was expressed at lower temperatures (Botha *et al.*, 2011). Denaturing methods of purification of the above proteins have generally involved the inclusion of urea (typically 4 M or 8 M) during the lysis step of the purification, followed by attempts at refolding the protein *in vitro* by the use of native wash and /or elution buffers (Matambo *et al.*, 2004; Hamada *et al.*, 2009; Botha *et al.*, 2011).

The aim of the work reported in this chapter was to produce the human and malarial Hsp70 and Hsp40 proteins of interest to this project (PfHsp70-1, PfHsp70-x, HsHsp70, PfHsp40 and Hsj1a) in *E. coli*, and subsequently to purify each protein in high enough yields and at sufficiently high levels of purity for *in vitro* assays.



## 2.2. MATERIALS AND METHODS

---

### 2.2.1. Materials

---

Expression plasmids (pQE30-PfHsp70-1(wt), pQE30-PfHsp70-1(opt), pQE30-PfHsp70-x, pQE30-PfHsp40, pQE30-Hsj1a and pMSHsp70) were obtained from various sources described in Section 2.2.2. All restriction enzymes (*Bam*HI, *Hind*III, *Xba*I and *Pst*I), restriction digest reaction buffers and  $\lambda$  DNA were purchased from Promega (U.S.A.). Unstained molecular weight protein marker, O'GeneRuler 1 kb DNA Ladder and SnakeSkin Dialysis Tubing (10 kDa molecular weight cut-off) were from ThermoScientific (U.S.A.). MassRuler™ Express HR Forward DNA Ladder and Bradford reagent (ready to use) were purchased from Fermentas (U.S.A.). Antibiotics (ampicillin, kanamycin and chloramphenicol), glycerol, sodium chloride (NaCl), tris-(hydroxymethyl)-aminomethane (Trizma® base: Tris), imidazole, yeast extract, bromophenol blue, urea, polyethyleneimine (PEI), sodium dodecyl sulphate (SDS), ammonium persulphate (APS), acrylamide/bisacrylamide, *N,N,N',N'*-Tetramethylethylenediamine (TEMED), glycine, ponceau S and dimethyl-sulfoxide (DMSO) were purchased from Sigma-Aldrich (U.S.A.). Hydrochloric acid (HCl), ethanol, methanol, glacial acetic acid, and Tween®20 were purchased from Saarchem, Merck (Germany). Tryptone powder (pancreatic digest of casein) and bacteriological agar were purchased from Biolab, Merck (Germany). Isopropyl- $\beta$ -D-thiogalactopyranoside (IPTG) and PeqGold Protein marker IV were purchased from PEQLAB (Germany), and lysozyme and phenylmethylsulphonyl fluoride (PMSF) were purchased from Roche (Switzerland). Nickel sulphate (NiSO<sub>4</sub>), disodium hydrogen phosphate (Na<sub>2</sub>HPO<sub>4</sub>), potassium hydrogen phosphate (KH<sub>2</sub>PO<sub>4</sub>) and potassium chloride (KCl) were purchased from Merck and chelating sepharose beads (Fast Flow, R10) were purchased from GE Healthcare (Germany). Coomassie brilliant blue R-250 was purchased from USB (U.S.A.). Amicon® Ultra Centrifugal filters (30 kDa molecular weight cut-off) were purchased from Millipore (Ireland). Polyclonal rabbit anti-PfHsp40 antibodies were raised against a peptide immunogen designed by Dr. Melissa Botha (Botha *et al.*, 2011), and were produced by Dr. R. Zimmerman (Universität des Saarlandes, Germany). Polyclonal rabbit anti-PfHsp70-1 antibodies were raised against recombinant hexa-histidine tagged full-length PfHsp70-1 (Pesce *et al.*, 2008). Monoclonal mouse His-Probe (H-3) primary antibody (sc-8036) and UltraCruz™ Nitrocellulose Pure Transfer western blotting membrane (0.45 $\mu$ m) were purchased from Santa Cruz Biotechnology Inc. (U.S.A.), and horse radish peroxidase (HRP) -conjugated goat anti-mouse and HRP-conjugated goat anti-rabbit secondary antibodies were purchased from Sigma-Aldrich (U.S.A.).

## 2.2.2. Expression of recombinant proteins in *E. coli*: induction and solubility studies

---

Details of the expression plasmids used in the expression of proteins of interest in this study and the confirmation of the identities of the expression plasmids are given in Appendix B (Section 7.2.1). As described in Section 7.2.1, PfHsp70-1 was purified from *E. coli* strains transformed with two different plasmids: pQE30-PfHsp70-1(wt) and pQE30-PfHsp70-1(opt) containing the wild type and the codon optimized coding regions for PfHsp70-1 respectively.

### 2.2.2.1. Induction studies for the assessment of target protein expression in *E. coli*

---

The expression profile of each recombinant protein of interest was assessed by carrying out an induction study in one or more *E. coli* strains. Competent *E. coli* cells (Appendix A, Section 7.1.1) were transformed (Appendix A, Section 7.1.2) with plasmid DNA. A volume of 25 ml of 2 x yeast-tryptone (YT) broth (1.6 % w/v tryptone, 1.0 % w/v yeast extract, 0.5 % w/v sodium chloride) containing the appropriate antibiotic(s) (Appendix B, Section 7.2.1, Table 7.1) was inoculated with a single transformant colony and grown overnight at 37 °C with shaking at 200 rpm. The overnight starter colony was diluted into 250 ml of 2 x YT broth, containing antibiotic(s) (Appendix B, Section 7.2.1, Table 7.1). The cultures were grown with shaking at 37 °C until ready for induction at mid-log phase ( $A_{600}$  of ~0.6 – 0.8). Recombinant protein expression was induced by the addition of isopropyl- $\beta$ -D-thiogalactopyranoside (IPTG) to a final concentration of 1 mM. A pre-induction sample was collected prior to induction for SDS-PAGE and Western analysis. The sample was centrifuged at 16000 *g* for one minute, after which the supernatant was discarded and the remaining cell pellet was resuspended in a volume of PBS determined by the following equation:

$$A_{600} \div 0.5 \times 75 = \text{volume PBS } (\mu\text{l}) \quad (\text{Equation 2.1})$$

Cultures were grown and hourly samples were collected until five hours after induction. The following morning, an overnight sample was collected. All post-induction samples were prepared as described for the pre-induction sample above using equation 2.1. Samples were analysed by SDS-PAGE and Western analysis and, based on the results, the optimum induction time was chosen to give the maximum yield of the protein of interest.

### 2.2.2.2. Solubility studies for the assessment of the solubility of target protein expressed in *E. coli*

---

In order to determine the solubility of the proteins of interest, and thus the best approach for the purification of each protein, solubility studies were carried out. After induction by IPTG for the pre-determined amount of time for each protein, cultures were harvested at 2700 *g* for 20 minutes at 4 °C, after which cell pellets were resuspended in native lysis buffer (10 mM Tris-HCl, pH 7.5, 300 mM NaCl, 50 mM imidazole, 1 mM phenylmethylsulphonyl fluoride (PMSF), 1 mg/ml lysozyme). Lysis was allowed to proceed on ice for 20 minutes after which the lysate was frozen at – 80 °C overnight. Thawed lysates were sonicated (5 x 15 second sonication at an amplitude of 50 µm using a VibraCell sonicator, Sonics & Materials Inc., U.S.A., with 30 second incubation on ice between each pulse), and lysates cleared by centrifugation at 12000 *g* for 30 minutes at 4 °C. Samples were taken of the three fractions: total lysate (after lysis but prior to centrifugation), soluble fraction (supernatant after centrifugation) and insoluble fraction (pellet after centrifugation). These samples were analysed by SDS-PAGE (Appendix A, Section 7.1.3) and Western analysis (Appendix A, Section 7.1.4).

### 2.2.3. Purification of recombinant proteins from *E. coli*

---

The PfHsp70-1, PfHsp70-x, HsHsp70, Hsj1a and PfHs40 proteins used in this study are all hexa-histidine tagged proteins and thus purification was achieved by nickel-affinity chromatography performed in batch under either native or denaturing conditions, depending on the solubility of the protein as determined by the solubility study. HsHsp70 was C-terminally tagged, whereas PfHsp70-1, PfHsp70-x, PfHsp40 and Hsj1a were N-terminally tagged. Histidine tags were not cleaved off after purification.

PfHsp70-1, PfHsp70-x and Hsj1a were purified using the same native purification procedure, adapted from the method used to purify PfHsp70-1 by Matambo *et al.* (2004) and Shonhai *et al.* (2008), and the method used to purify Hsj1a by McNamara (2006). After induction of recombinant protein expression by IPTG for a given number of hours (based on the induction studies), cells were harvested by centrifugation at 2700 *g* for 20 minutes at 4 °C. Native lysis buffer (10 mM Tris-HCl, pH 7.5, 300 mM NaCl, 50 mM imidazole, 1 mM PMSF, 1 mg/ml lysozyme) was used to resuspend the cell pellet, and lysis was allowed to proceed for 20 minutes on ice. The resulting lysate was frozen overnight at -80 °C, then thawed on ice. In the case of PfHsp70-1(wt), polyethyleneimine (PEI) was added to the lysate to a final

concentration of 0.1 % (v/v). The addition of PEI, followed by centrifugation at high speeds, is thought to cause precipitation and thus removal of nucleic acids from the cleared lysate during protein isolation, aiding in the solubilisation of recombinant proteins without compromising protein structure or function (Trabbic-Carlson *et al.*, 2004; Shonhai *et al.*, 2008). The thawed lysate was subjected to sonication (5 x 15 second sonication at an amplitude of 50  $\mu$ m, with 30 second incubation on ice between each pulse). The final lysate was cleared by centrifugation at 12000 *g* for 30 minutes at 4 °C. Nickel-charged sepharose beads (250 - 400  $\mu$ l of 50 % [v/v] slurry) (Section 7.1.5) were added to the resulting supernatant, and binding was allowed with gentle agitation at 4 °C for 4 hours or overnight. Beads were collected by centrifugation at 1500 *g* for 1 minute, and the supernatant (unbound fraction) discarded. Three washes (6 ml) with native wash buffer (10 mM Tris-HCl, pH 7.5, 300 mM NaCl, 50 mM imidazole, 1 mM PMSF) were carried out, after which bound proteins were eluted from the beads three times (6 ml, 4 ml and 2 ml) using native elution buffer (10 mM Tris-HCl, pH 7.5, 300 mM NaCl, 500 mM imidazole, 1 mM PMSF).

The purification procedure used to isolate HsHsp70 was adapted from the protocol provided by Prof. J. Brodsky's research group (University of Pittsburgh, U.S.A.). HsHsp70 cultures were induced with IPTG, and cells were harvested four hours post-induction by centrifugation at 2700 *g* for 15 minutes at 4 °C. Cell pellets were resuspended in wash buffer (20 mM Tris-HCl, pH 8.0, 0.1 mM EDTA, 50 mM KCl). After a second centrifugation of 10 minutes at 5000 *g*, the cell pellets were frozen at - 80 °C overnight. Pellets were thawed on ice and resuspended in lysis buffer (20 mM Tris-HCl, pH 8.0, 0.1 mM EDTA, 50 mM KCl, 1 mM PMSF and 1 mg/ml lysozyme). The cell lysate was incubated on ice for 30 minutes, after which three freeze-thaw cycles (3 minutes in liquid nitrogen, 10 minutes in a 30 °C water bath) were carried out to achieve lysis. The lysate was sonicated (7 x 15 second sonication at an amplitude of 50  $\mu$ m, with 30 second incubation on ice between each pulse), and centrifuged at 12000 *g* for 30 minutes at 4°C. The supernatant was stored on ice. The insoluble fraction was resuspended in buffer (20 mM Tris-HCl, pH 8.0, 0.1 mM EDTA, 50 mM KCl) and sonicated a second time (as above). The second sonicated fraction was centrifuged at 12000 *g* for 30 min. The supernatants from the two sonications were pooled and incubated with 300  $\mu$ l nickel-charged sepharose beads (50 % v/v slurry) for 4 hours or overnight at 4 °C. Native washes and elutions were carried out as described previously.

PfHsp40 was purified under denaturing conditions. Cultures were harvested four hours post-induction, at 2700 *g* for 20 minutes at 4 °C. Cell pellets were resuspended in denaturing lysis buffer (10 mM Tris-

HCl, pH 8.0, 300 mM NaCl, 50 mM imidazole, 8 M urea, 1 mM PMSF, 1 mg/ml lysozyme), and frozen overnight at -80 °C. The frozen lysate was thawed on ice and sonicated (5 x 15 second sonication at an amplitude of 50 µm, with 30 second incubation on ice between each pulse). The resulting lysate was cleared by centrifugation at 12000 *g* for 30 minutes at 4 °C, and the supernatant incubated with nickel-charged sepharose beads (150 µl of 50 % v/v slurry) for 4 hours or overnight at 4 °C. Three washes (4 ml each) of decreasing urea concentrations were carried out, using wash buffer (10 mM Tris-HCl, pH 8.0, 300 mM NaCl, 50 mM imidazole, containing 4 M urea [wash 1], 2 M urea [wash 2] and finally no urea [wash 3]). PfHsp40 was eluted off the beads with native elution buffer (10 mM Tris-HCl, pH 7.5, 300 mM NaCl, 500 mM imidazole). To increase the concentration and improve the purity of PfHsp40 eluted off the beads, the elution fractions were pooled and passed through a centrifugal column filter as described in Appendix A (Section 7.1.6.2).

Subsequent to purification and prior to use in *in vitro* work, all recombinant proteins were subjected to buffer exchange to facilitate the removal of imidazole. In the case of PfHsp70-1(wt), this was achieved using dialysis (Appendix A, Section 7.1.6.1), and for all other proteins (PfHsp70-1(opt), PfHsp70-x, HsHsp70, Hsj1a and PfHsp40), centrifugal column filters (Appendix A, Section 7.1.6.2) were used. The integrity and degree of purity of the proteins following buffer exchange was assessed using SDS-PAGE. Proteins were quantified by one of two methods. Protein used in ATPase and aggregation suppression assays (Chapter 3) was quantified spectrophotometrically using a NanoDrop instrument (Appendix A, Section 7.1.7), and protein used in surface plasmon resonance spectroscopy experiments (Chapter 4) were quantified using the Bradford's method of protein quantification (Appendix A, Section 7.1.8). Recombinant PfHsp70-1, PfHsp70-x, HsHsp70 and Hsj1a were stored at 4 °C until use, and recombinant PfHsp40 was aliquoted and stored at - 80 °C until use.

## 2.3. RESULTS

---

### 2.3.1. Expression and purification

---

The results of the SDS-PAGE and Western analyses of the expression and purification of each of the proteins of interest in various *E. coli* strains are given in sections 2.3.1.1 – 2.3.1.6.

#### 2.3.1.1. PfHsp70-1 wild type

---

A side-by-side induction study of PfHsp70-1(wt) production in *E. coli* XL1 Blue was carried out, in which one of two cultures was co-transformed with the RIG plasmid (Figure 2.1). An increase in the intensity of the band at 72 kDa between the pre-induction and the overnight induction samples (Figure 2.1A lanes 1 and 7; Figure 2.1B, lanes 1 and 2) indicated successful induction of PfHsp70-1 by IPTG both in the presence and absence of the RIG plasmid. The identity of the band was confirmed to be PfHsp70-1(wt) by Western analysis (Figures 2.1A and 2.1B; lower panels). The similarity between the expression profiles of PfHsp70-1(wt) in the two SDS-PAGE gels (the distinct 72 kDa bands) in Figure 2.1A indicated that the RIG plasmid had little to no effect on the expression levels of PfHsp70-1(wt) in *E. coli* XL1 Blue cells, and thus the protein was purified in the absence of the RIG plasmid under native conditions. Based on the induction study (Figure 2.1A), in which the intensity of the 72 kDa band representing PfHsp70-1(wt) in lane 7 (overnight post-induction sample) of each of the SDS-PAGE gels was markedly greater than in any of the other lanes, expression was induced overnight for maximum protein yield in the purification. The intensity of the 72 kDa bands in the soluble fraction sample (Figure 2.1B, lane 5) suggested that the over-expressed protein was relatively soluble, based on a prominent band on both the SDS-PAGE and Western blot analyses at the expected size. The elution samples in the SDS-PAGE analysis (Figure 2.1B, lanes 10 – 12) showed that PfHsp70-1(wt) was obtained at a high level of purity, estimated at > 90 %. Despite a significant amount of target protein being lost in the unbound fraction (Figure 2.1B, lane 6), as well as remaining bound to beads following elution (Figure 2.1B, lane 13) high yields of PfHsp70-1(wt) were routinely obtained (Table 2.2).

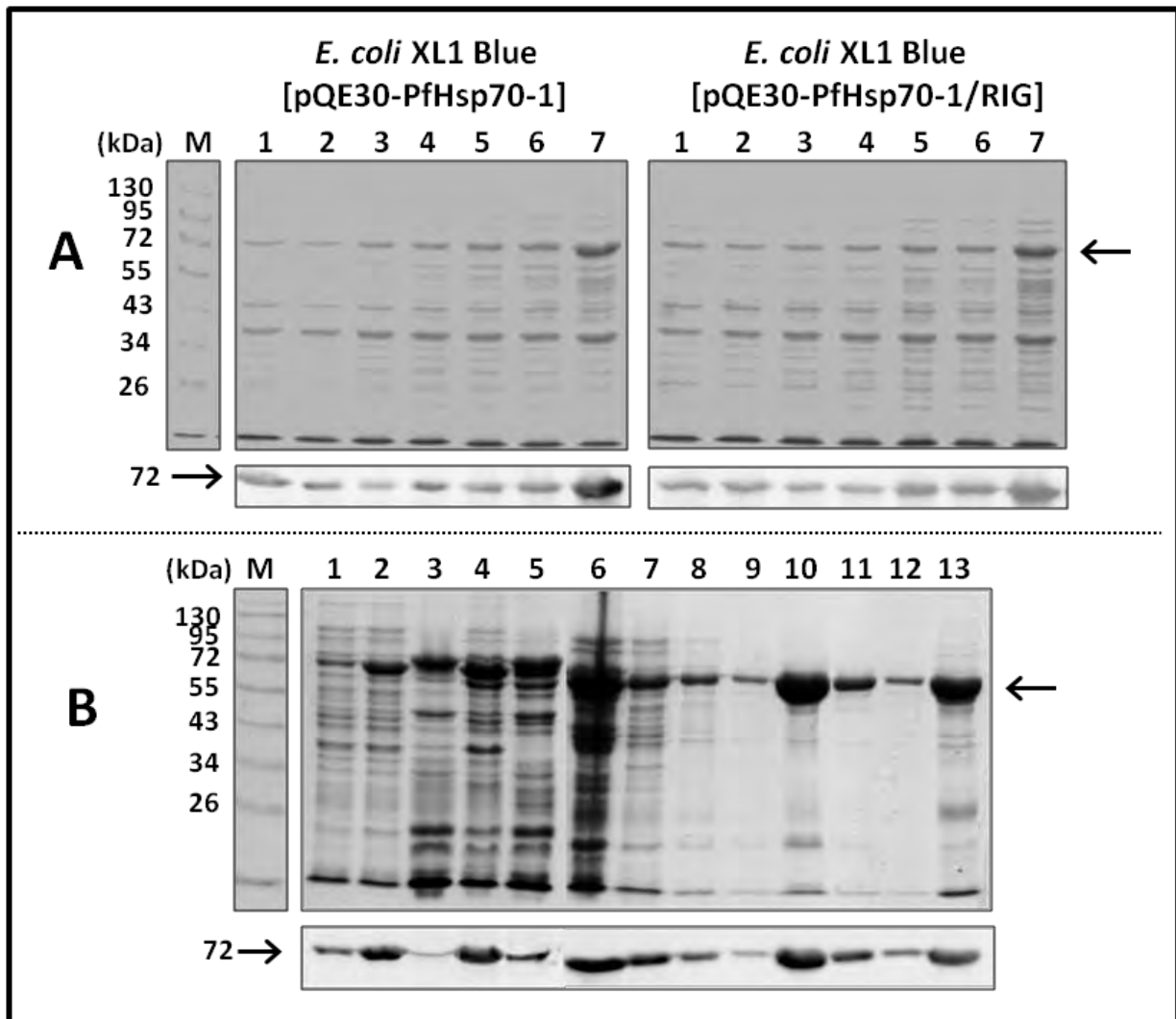


**Figure 2.1: Expression and purification of PfHsp70-1(wt) from *E. coli* XL1 Blue.** (A) SDS-PAGE (upper panel) and Western analysis (lower panel) of the expression of PfHsp70-1(wt) (72 kDa) in *E. coli* XL1 Blue cells, in the absence (left-hand panel) and presence (right-hand panel) of the RIG plasmid. Lanes – M: PeqGold Protein Marker IV (sizes indicated on the left), 1: Pre-induction sample (total protein extract), 2-6: Hourly samples one to five hours post-induction (total protein extracts), 7: Overnight induction sample (total protein extracts). (B) SDS-PAGE (upper panel) and Western analyses (lower panel) of the purification of PfHsp70-1(wt) from *E. coli* XL1 Blue. Lanes - M: PeqGold Protein Marker IV (sizes indicated on the left), 1: Pre-induction sample (total protein extract); 2: Overnight induction sample (total protein extract); 3: Lysate; 4: Insoluble fraction; 5: Soluble fraction; 6: Unbound fraction; 7 - 9: Wash fractions using native wash buffer; 10 - 12: Elutions using native elution buffer; 13: Fraction bound to the beads after elutions. Arrows on the right hand side of the figure indicate the expected size in kDa of over-expressed and purified PfHsp70-1(wt). Western analysis was performed with primary rabbit polyclonal anti-PfHsp70-1 (1:5000) antibody and HRP-conjugated goat anti rabbit IgG secondary antibody (1:10 000).

### 2.3.1.2. PfHsp70-1 (codon optimized)

---

An induction study of the production of PfHsp70-1(opt) in *E. coli* XL1 Blue was carried out and a prominent band of over-expressed protein at the expected size of 72 kDa (Figure 2.2A, upper panel), confirmed by Western analysis to be PfHsp70-1(opt) (Figure 2.2A, lower panel) was present in all samples in the SDS-PAGE gel. However, the intensity of this band seemed to diminish slightly after three hours of induction, and thus, for the purification of PfHsp70-1(opt), expression was induced by IPTG for three hours. A side-by-side solubility study was carried out, in which the effect of PEI (added to the lysate before sonication) on the solubility of PfHsp70-1(opt) was assessed. Both the SDS-PAGE gel (upper panel) and the Western analysis (lower panel) in Figure 2.2B show no obvious differences in the intensities of the 72 kDa bands of over-expressed PfHsp70 in the insoluble and soluble fraction samples (lanes 4 and 5 compared to lanes 6 and 7), and thus PEI was not included in the purification protocol for PfHsp70-1(opt). PfHsp70-1(opt) was purified from *E. coli* XL1 Blue under native conditions after three hour induction of expression with IPTG. PfHsp70-1(opt) was generally obtained at high yields, exceeding those of PfHsp70-1(wt) (Table 2.2). As with PfHsp70-1(wt), the high PfHsp70-1(opt) yields were obtained despite significant losses of target protein in the unbound fraction in the purification, as well as loss of protein remaining bound to the beads after elution (Figure 2.2C, lanes 6 and 13 respectively). PfHsp70-1(opt) was purified to a reasonable degree of purity (estimated at ~ 80 % from SDS-PAGE analysis, Figure 2.2C, lanes 10-12), however, a prominent contaminating band of ~ 23 kDa was observed in the elution fractions of PfHsp70-1(opt) (Figure 2.2C, lanes 10-12). The purity of PfHsp70-1(opt) was notably improved following buffer exchange (using centrifugal filter columns), as seen by the lack of contaminating proteins in the SDS-PAGE analysis of the protein after buffer exchange, shown in Figure 2.2C, lane BE, from which the purity of PfHsp70-1(opt) was estimated to be > 95 %.



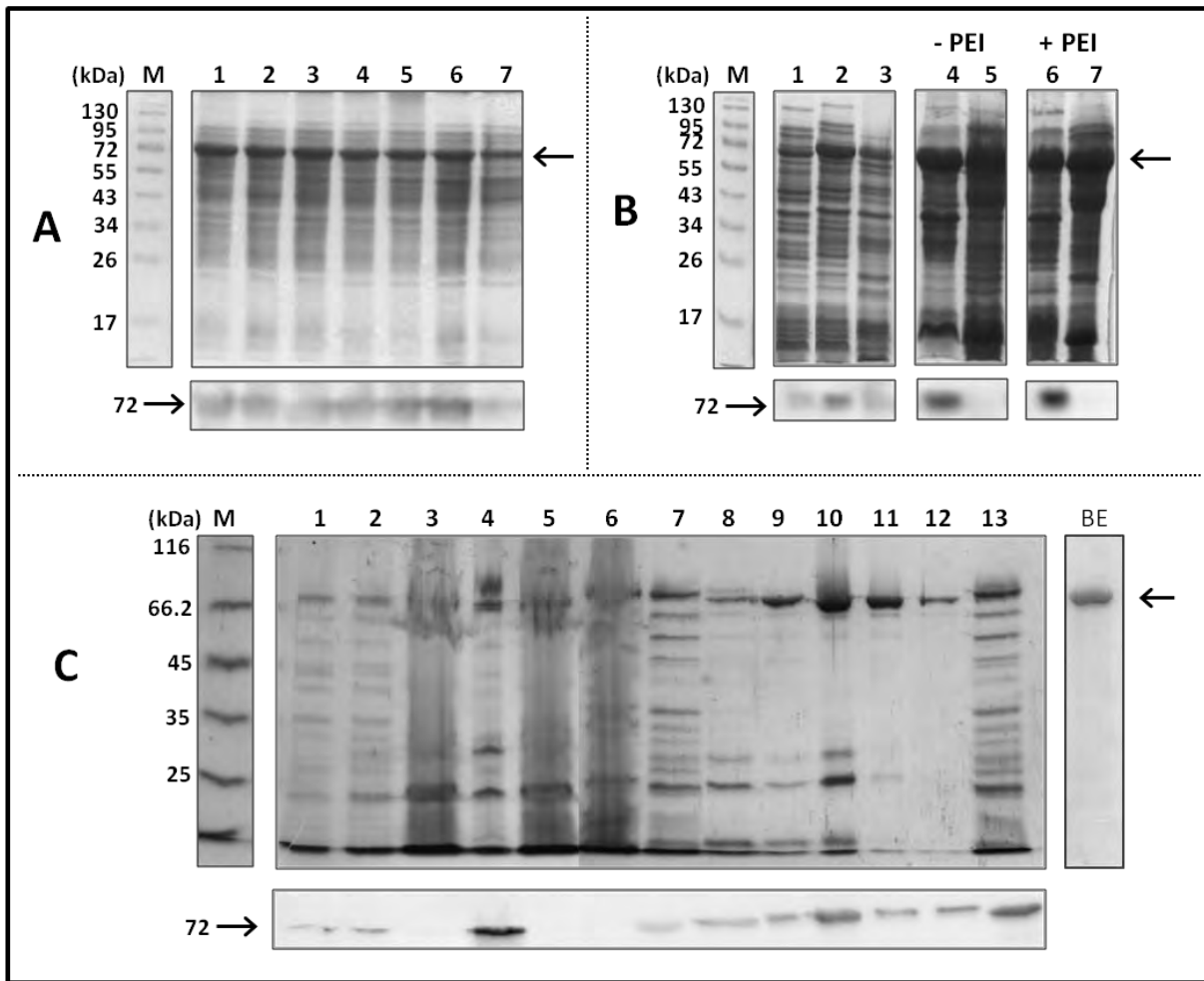


**Figure 2.2: Expression, solubility and purification of PfHsp70-1(opt) from *E. coli* XL1 Blue.** (A) SDS-PAGE (upper panel) and Western analysis (lower panel) of the expression of PfHsp70-1(opt) (72 kDa) in *E. coli* XL1 Blue cells. Lanes – M: PeqGold Protein Marker IV (sizes indicated on the left), 1: Pre-induction sample (total protein extract), 2-6: Hourly samples one to five hours post-induction (total protein extracts), 7: Overnight induction sample (total protein extract). (B) SDS-PAGE (upper panel) and Western analysis (lower panel) of the solubility of PfHsp70-1(opt) in *E. coli* XL1 Blue cells in the absence (lanes 4 & 5) and presence (lanes 6 & 7) of 0.1 % (v/v) polyethyleneimine (PEI). Lanes – M: PeqGold Protein Marker IV (sizes indicated on the left), 1: Pre-induction sample, 2: Three hour post-induction sample, 3: Total lysate, 4 & 6: Insoluble fractions, 5 & 7: Soluble fractions. (C) SDS-PAGE (upper panel) and Western analysis (lower panel) of the purification of PfHsp70-1(opt) from *E. coli* XL1 Blue cells. Lanes - M: Thermo Scientific Unstained Molecular Weight Marker (sizes indicated on the left), 1: Pre-induction sample (total protein extract); 2: Four hour post-induction sample (total protein extract); 3: Lysate; 4: Insoluble fraction; 5: Soluble fraction; 6: Unbound fraction; 7 - 9: Wash fractions using native wash buffer; 10 - 12: Elution fractions using native elution buffer; 13: Fraction bound to beads after elutions; BE: Sample of target protein following buffer exchange by centrifugal filter column. Arrows on the right hand side of the figure indicate the expected size of over-expressed and purified PfHsp70-1 (optimized). Western analysis was performed with primary rabbit polyclonal anti-PfHsp70-1 (1:5000) and HRP-conjugated goat anti-rabbit secondary antibody (1:10 000).

### 2.3.1.3. PfHsp70-x

---

The second malarial Hsp70, PfHsp70-x, was produced in the *E. coli* M15[pRep4] strain. The pRep4 plasmid resident in this *E. coli* strain expresses, in addition to kanamycin resistance, a 360 amino acid *lac* repressor protein encoded by the *lac I* gene. Until the addition of IPTG, the *lac* repressor protein halts the expression of the protein encoded by the co-transformed pQE30-PfHsp70-x plasmid. This ensures that leaky or basal expression of the protein of interest does not occur (Farabaugh, 1978). The effect of the pRep4 plasmid is evident in the SDS-PAGE and Western analyses of the expression of PfHsp70-x in the M15[pRep4] cells (Figure 2.3A), where the 74 kDa band shown to be PfHsp70-x by the Western analysis was not present in the pre-induction sample (Figure 2.3A, lane 1), but was prominent in all post-induction samples (Figure 2.3A, lanes 2 - 7). As with the optimised form of PfHsp70-1, the effect of PEI on the solubility of PfHsp70-x was assessed (Figure 2.3B), and PEI was found to have no detectable effect on the solubility of PfHsp70-x as the amount of soluble PfHsp70-x (lane 4) relative to insoluble PfHsp70-x (lane 3) in the absence of PEI is comparable to the amount of soluble PfHsp70-x (lane 6) relative to insoluble PfHsp70-x (lane 5) in the presence of PEI. PfHsp70-x was thus purified from *E. coli* M15[pRep4] cells under native conditions in the absence of PEI. As with PfHsp70-1, significant amounts of target protein were lost in the unbound fraction (Figure 2.3C, lane 6) during the purification of PfHsp70-x, and a significant amount of target protein also remained bound to the beads following the elution steps (Figure 2.3C, lane 13); however, high yields (Table 2.2) of PfHsp70-x were obtained despite these losses. The purity of PfHsp70-x was estimated to be > 90 % from the SDS-PAGE analysis of the purification (Figure 2.3C, lanes 10-12).

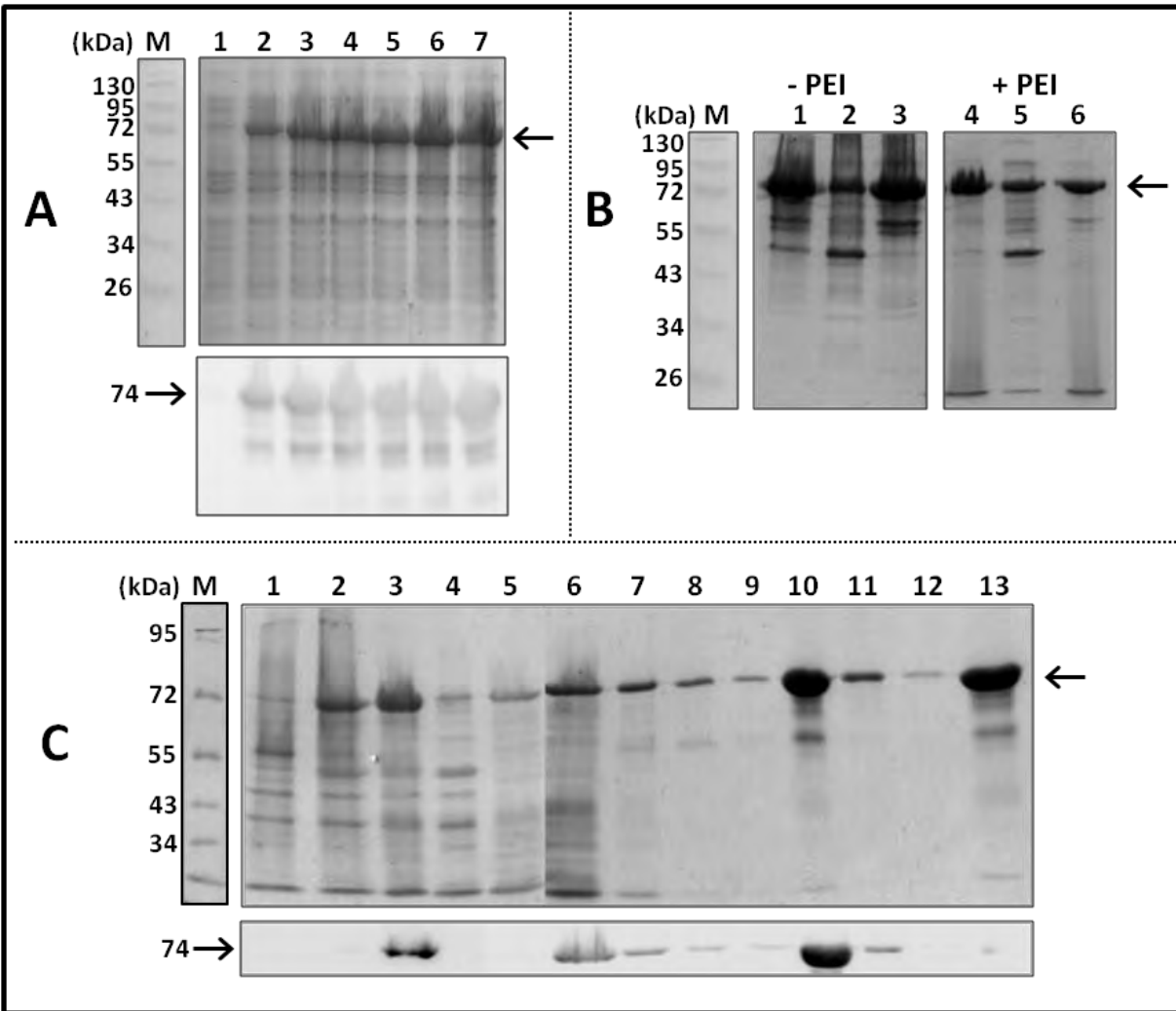


**Figure 2.3: Expression, solubility and purification of PfHsp70-x from *E. coli* M15[pRep4].** (A) SDS-PAGE (upper panel) and Western analysis (lower panel) of the expression of PfHsp70-x (74 kDa) in *E. coli* M15[pRep4] Blue cells. Lanes – M: PeqGold Protein Marker IV (sizes indicated on the left), 1: Pre-induction sample (total protein extract), 2-6: Hourly samples one to five hours post-induction (total protein extracts), 7: Overnight induction sample (total protein extract). (B) SDS-PAGE analysis of the solubility of PfHsp70-x in *E. coli* M15[pRep4] cells in the presence and absence of 0.1 % (v/v) polyethyleneimine (PEI). Lanes – M: PeqGold Protein Marker IV (sizes indicated on the left), 1 & 4: Lysate, 2 & 5: Insoluble fraction, 3 & 6: Soluble fraction. (C) SDS-PAGE (upper panel) and Western (lower panel) analyses of the purification of PfHsp70-x from *E. coli* M15[pRep4] cells. Lanes - M: PeqGold Protein Marker IV (sizes indicated on the left), 1: Pre-induction sample (total protein extract); 2: Overnight induction sample (total protein extract); 3: Lysate; 4: Insoluble fraction; 5: Soluble fraction; 6: Unbound fraction; 7 - 9: Wash fractions using native wash buffer; 10 - 12: Elution fractions using native elution buffer; 13: Fraction bound to beads after elutions. Arrows on the right hand side of the figure indicate the expected size of over-expressed and purified PfHsp70-x. Western analysis was performed with primary monoclonal mouse His-probe (1:1000) and HRP-conjugated goat anti-mouse secondary antibody (1:10 000).

#### 2.3.1.4. HsHsp70

---

HsHsp70 was expressed in *E. coli* BL21 cells, and based on the induction study (Figure 2.4A), in which the Western analysis showed the highest intensity band for the four hour post-induction sample (lane 5), cultures were harvested after four hours of induction by IPTG. The method used consisted of lysis steps (freeze-thaw cycles and sonication), after which the insoluble fraction was further processed, being subjected to a second sonication step, in an attempt to recover protein from the insoluble fraction. The analysis of the purification of HsHsp70, and in particular the Western analysis (Figure 2.4B, lower panel), showed that the first insoluble fraction (lane 4) clearly still contained a significant amount of target protein, represented as a 72 kDa band, especially compared to the first soluble fraction (lane 5). This method of recovering protein from the insoluble fraction was shown to be extremely effective, as was evident from the second soluble fraction (lane 8), in which there was considerably more HsHsp70 than in the initial soluble fraction shown in lane 5. Some target protein was lost in the unbound fraction (Figure 2.4B, lane 9) during the purification procedure, and as with the malarial Hsp70s purified, a significant amount of protein remained bound to the beads following the elution steps (Figure 2.4B, lane 16). Nevertheless, large yields of HsHsp70 (Table 2.2) were purified from *E. coli* BL21, at a high degree of purity of > 90 % as estimated from the SDS-PAGE analysis of the purification (Figure 2.4B, lanes 13-15). Buffer exchange by centrifugal filter columns resulted in a marked increase in the degree of purity of HsHsp70 (estimated at > 95 %), as shown by the SDS-PAGE analysis of the buffer exchanged protein in Figure 2.4 B (lane BE).

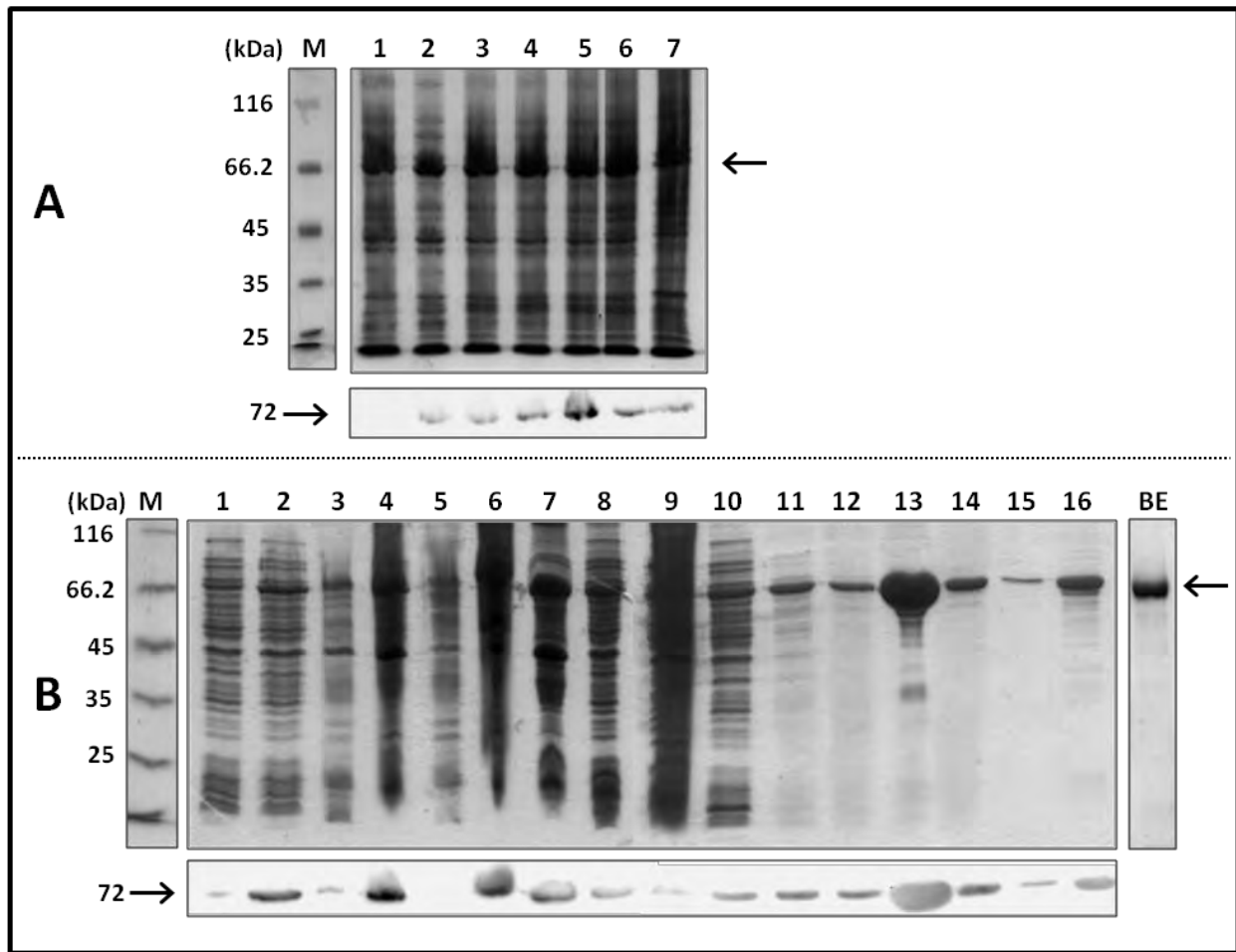


**Figure 2.4: Expression and purification of HsHsp70 from *E. coli* BL21.** (A) SDS-PAGE (upper panel) and Western analysis (lower panel) of the expression of HsHsp70 (72 kDa) in *E. coli* BL21 cells. Lanes - M: Thermo Scientific Unstained MW Protein Marker (sizes indicated on the left), 1: Pre-induction sample (total protein extract), 2-6: Hourly samples one to five hours post-induction (total protein extracts), 7: Overnight induction sample (total protein extract). (B) SDS-PAGE (upper panel) and Western analysis (lower panel) of the purification of HsHsp70 from *E. coli* BL21 cells. Lanes - M: PeqGold Protein Marker IV (sizes indicated on the left), 1: Pre-induction sample (total protein extract); 2: Four hour post-induction sample (total protein extract); 3: Lysate after first sonication; 4: Insoluble fraction after first sonication; 5: Soluble fraction after first sonication; 6: Lysate after second sonication; 7: Insoluble fraction after second sonication; 8: Soluble fraction after second sonication; 9: Unbound fraction; 10 – 12: Wash fractions using native wash buffer; 13 -15: Elution fractions using native elution buffer; 16: Fraction bound to beads after elutions; BE: Sample of target protein following buffer exchange by centrifugal filter column. Arrows on the right hand side of the figure indicate the expected size of over-expressed and purified HsHsp70. Western analysis was performed with primary monoclonal mouse His-probe (1:1000) and HRP-conjugated goat anti-mouse secondary antibody (1:10000).

### 2.3.1.5. PfHsp40

---

The successful purification of PfHsp40 from *E. coli* XL1 Blue cells by denaturing methods was recently published (Botha *et al.*, 2011), and the purification reported here was adapted from these published methods (Figure 2.5). Three different *E. coli* strains (XL1 Blue, BL21 and M15[pRep4]) were transformed with the pQE30-PfHsp40 plasmid, and induction studies were carried out in all three strains to identify the strain which yielded the highest expression levels of the protein of interest. Comparing the expression levels of PfHsp40 in the M15[pRep4] cell line (Figure 2.5A) to the levels obtained in the other two *E. coli* strains, it was evident that the best expression was obtained in the M15[pRep4] strain, since in the SDS-PAGE gels, PfHsp40 was present as a distinct, over-expressed band of ~ 55 kDa only in the *E. coli* M15 strain. The Western analysis for the *E. coli* XL1 Blue strain in Figure 2.5A shows, in addition to the PfHsp40 at the expected size of ~55 kDa, a secondary but prominent lower molecular weight band of ~ 36 kDa, possibly a product of either degradation or early termination of transcription. In the case of the *E. coli* BL21 strain, Western analysis showed that there was no product at the expected size of ~55 kDa, but only a smaller product, again possibly a degradation or early transcription product. In the case of the *E. coli* M15 strain, PfHsp40 was clearly visible at the correct expected size of ~ 55 kDa in the SDS-PAGE gel, as well as in the Western analysis, where the major species detected is of the correct size, and there are no other major or prominent bands showing degradation or early termination of transcription of the protein. The bands above and below the band of interest in the Western analysis of PfHsp40 expression in *E. coli* M15[pRep4] cells were accounted for as non-specific bands, shown by the similar banding pattern detected in an untransformed *E. coli* M15[pRep4] cell lysate probed with anti-PfHs40 antibody (Figure 2.5C). In addition to this side-by-side expression study, a side-by-side solubility study in the three *E. coli* strains was carried out (Figure 2.5B), and in the resulting Western analysis, the correct PfHsp40 band of ~ 55 kDa was only detected in the *E. coli* M15[pRep4] fractions, though only in very low levels in the soluble fraction.

Based on both the expression studies as well as the solubility study, the *E. coli* M15[pRep4] strain was selected as the expression system for the recombinant production of PfHsp40. The low levels of PfHsp40 detected in the soluble fraction of the *E. coli* M15[pRep4/pQE30-PfHsp40] lysate by Western analysis of the solubility study (Figure 2.5B, lower panel, lane 3) meant that, like the published approach, a denaturing purification was carried out and, as with the purification of HsHsp70, an attempt was made to recover protein from the insoluble pellet fraction. The lysis in the described purification procedure

was performed under denaturing conditions (8 M urea included in the lysis buffer). The denaturant (urea) was gradually eliminated by the use of three wash steps with wash buffer containing decreasing concentrations of urea, the third wash containing no urea. The SDS-PAGE and Western analyses of the elution samples from the purification of PfHsp40 (Figure 2.5D, lanes 10 - 12) showed that the target protein was isolated to only a moderate degree of purity, based on the number of contaminating bands observed in the elution fractions analysed by SDS-PAGE (Figure 2.5D, lanes 10-12). To improve the purity of the protein, and to try to concentrate the protein, the pooled protein elutions were passed through a 30 kDa cut-off centrifugal filter column (Appendix A, Section 7.1.6.2). This step also served as a buffer exchange step to facilitate the removal of imidazole from the protein solution. SDS-PAGE analysis (Figure 2.5D, lane BE) showed that this process was relatively successful in further purifying the protein, as a number of the contaminating lower molecular weight proteins present in the initial elutions of PfHsp40 were no longer present in the concentrated sample, however, the purity of the protein was estimated to be no more than 80 %. PfHsp40 was purified in only moderate amounts (Table 2.2).

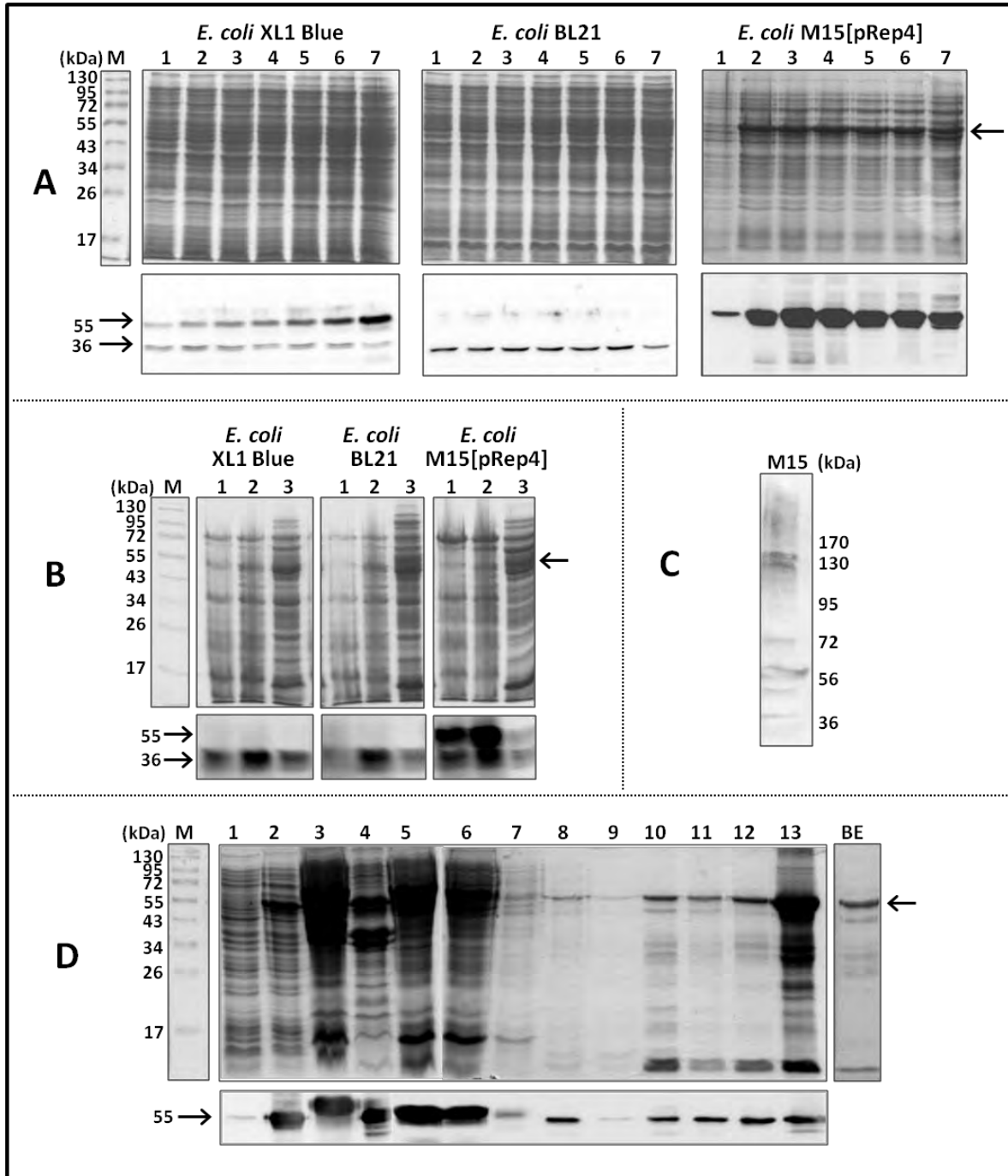


**Figure 2.5: Expression, solubility and purification of PfHsp40.** (A) SDS PAGE (upper panel) and Western analysis (lower panel) of induction studies of the expression of PfHsp40 (55 kDa) in three *E. coli* strains: XL1 Blue (left panel), BL21 (middle panel) and M15[pRep4] (right panel). Lanes – M: PeqGold Protein Marker IV (sizes indicated on the left), 1: Pre-induction sample (total protein extract), 2-6: Hourly samples one to five hours post-induction (total protein extracts), 7: Overnight induction sample (total protein extract). (B) SDS-PAGE (upper panel) and Western analysis (lower panel) of the solubility of PfHsp40 in three *E. coli* strains. XL1 Blue (left panel), BL21 (middle panel) and M15[pRep4] (right panel). Lanes – M: PeqGold Protein Marker IV (sizes indicated on the left), 1: Total lysate, 2: Insoluble fraction, 3: Soluble fraction. (C) Control Western of an untransformed *E. coli* M15[pRep4] cell lysate, with protein



sizes indicated to the right. (D) SDS-PAGE (upper panel) and Western analysis (lower panel) of the purification of PfHsp40 from *E. coli* M15[pRep4]. Lanes - M: PeqGold Protein Marker IV (sizes indicated on the left), 1: Pre-induction sample (total protein extract); 2: Four hour post-induction sample (total protein extracts); 3: Lysate; 4: Insoluble fraction; 5: Soluble fraction; 6: Unbound fraction; 7: Wash fraction using 4 M urea wash buffer; 8: Wash fraction using 2 M urea wash buffer; 9: Wash fraction using native wash buffer; 10 - 12: Elution fractions using native elution buffer; 13: Fraction bound to beads after elution; BE: Pooled, buffer exchanged and concentrated PfHsp40 elutions. Arrows on the right hand side of the figure indicate the expected size of over-expressed and purified PfHsp40. Western analysis was performed with primary rabbit polyclonal anti-PfHsp40 (1:5000) and HRP-conjugated goat anti-rabbit secondary antibody (1:10 000).

#### 2.3.1.6. *Hsj1a*

---

Hsj1a, previously purified and characterised by Ms. Caryn McNamara, was purified according to the methods described in her thesis (McNamara, 2006). An induction study of the expression of Hsj1a in *E. coli* XL1 Blue was carried out and assessed by SDS-PAGE and Western analyses (Figure 2.6A). The prominent 36 kDa band present in all lanes on the SDS-PAGE gel of Hsj1a expression in *E. coli* XL1 Blue (Figure 2.6A, upper panel) showed that the recombinant protein was highly expressed in the cells even before induction with IPTG right through to the overnight culture at a similar expression level. Western analysis of the induction study (Figure 2.6A, lower panel), however, showed a gradual increase in expression after IPTG induction. For the purification of Hsj1a from *E. coli* XL1 Blue, cells were harvested four hours post-induction, and native purification was carried out. The SDS-PAGE and Western analyses of the purification of Hsj1a (Figure 2.6B) showed despite significant losses of target protein coming off the beads in the unbound fraction (Figure 2.6B, lane 6) as well as a significant amount of protein remaining bound to the beads following the elutions steps of the purification (Figure 2.6B, lane 13), Hsj1a was purified in large yields (Table 2.2). The SDS-PAGE analysis of the purification procedure shows that a number of low molecular weight contaminants (Figure 2.6B, lanes 10-12) were co-purified with Hsj1a, however, as shown for PfHsp70-1(opt), the purity of Hsj1a following buffer exchange by centrifugal columns was significantly improved (data not shown), and the purity was estimated at > 90 %.

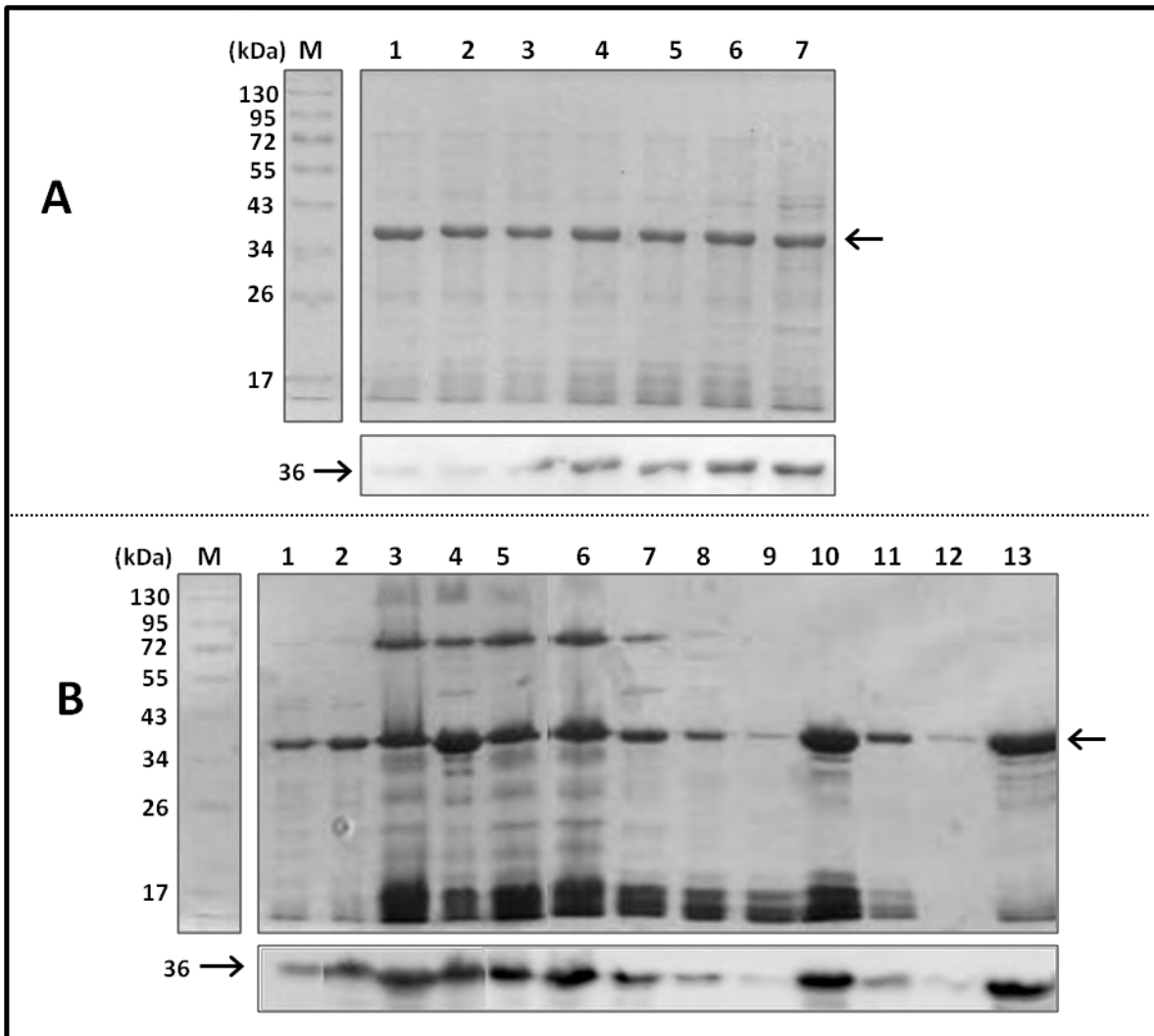


**Figure 2.6: Expression and purification of Hsj1a from *E. coli* XL1 Blue.** (A) SDS-PAGE (upper panel) and Western analysis (lower panel) of the expression of Hsj1a (36 kDa) in *E. coli* XL1 Blue cells. Lanes – M: PeqGold Protein Marker IV (sizes indicated on the left), 1: Pre-induction sample (total protein extract), 2-6: Hourly post-induction samples (total protein extracts), 7: Overnight induction sample (total protein extract). (B) SDS-PAGE (upper panel) and Western analysis (lower panel) of the purification of Hsj1a from *E. coli* XL1 Blue cells. Lanes - M: PeqGold Protein Marker IV (sizes indicated on the left), 1: Pre-induction sample (total protein extract); 2: Four hour post-induction sample (total protein extract); 3: Lysate; 4: Insoluble fraction; 5: Soluble fraction; 6: Unbound fraction; 7 - 9: Wash fractions using native wash buffer; 10 - 12: Elution fractions using native elution buffer; 13: Fraction bound to beads after elution. Western analysis was performed with primary monoclonal mouse His-probe (1:1000) and HRP-conjugated goat anti-mouse secondary antibody (1:10 000).

The yields generally obtained from successful purifications of each of the proteins of interest were calculated and are shown in Table 2.2. Higher yields of PfHsp70-1(opt) were routinely obtained compared to PfHsp70-1(wt), and the highest protein yields were generally obtained from purifications of PfHsp70-x and Hsj1a (shown by the nmol yield shown in Table 2.2, which takes into consideration the size of the proteins). Of all the proteins purified, PfHsp40 was obtained at the lowest yields by far, resulting in, at most, less than 1 mg of protein per litre of culture.

**Table 2.2: Yields of recombinant proteins isolated from transformed *E. coli* cells.** Approximate yields are shown as ranges, encompassing the lowest and highest yields obtained in successful purifications of each protein.

Protein	Yield (mg protein / litre culture)	Yield (nmol protein / litre culture)
PfHsp70-1(wt)	1 -4	14 – 56
PfHsp70-1(opt)	3-6	42 – 83
PfHsp70-x	4-8	54 – 108
HsHsp70	3-6	42 – 83
PfHsp40	0.2-0.8	4 – 16
Hsj1a	2-4	55 - 111

## 2.4. DISCUSSION

---

In the case of the recombinant Hsp70s (PfHsp70-1(wt), PfHsp70-1(opt), PfHsp70-x and HsHsp70) purified in this study, reasonable to high yields (1 – 8 mg of protein per litre of culture, Table 2.2) were obtained. These yields were achieved despite significant losses of target proteins in the unbound fractions in purifications, as well as losses of protein remaining bound to nickel-charged beads following elution steps during purification. Because the degree of purity of the target proteins was not 100 %, the calculated yields of the proteins in Table 2.2 are likely to be slightly over-estimated, as the determined concentrations include the contaminating proteins too.

PfHsp70-1(wt) has been successfully purified a number of times (Matambo *et al.*, 2004; Shonhai *et al.*, 2008; Chiang *et al.*, 2009; Misra and Ramachandran, 2009). Optimisation of the purification of PfHsp70-1 by Matambo *et al.* (2004) included an investigation into the effect of the presence of the RIG plasmid on the expression of PfHsp70-1. A similar side-by-side study was conducted here (Figure 2.1A), and contrary to the findings of Matambo *et al.* (2004), co-expression of the RIG plasmid with the PfHsp70-1(wt) expression vector had no noticeable effect on the expression of PfHsp70-1(wt) in *E. coli* XL1 Blue cells, and thus the RIG plasmid was not used in the recombinant production of PfHsp70-1(wt) in this study. Though relatively high yields of PfHsp70-1(wt) were obtained from successful purifications, expression levels were inconsistent between purifications, resulting in frequent unsuccessful purifications, and thus the plasmid encoding the optimised PfHsp70-1 was purchased.

The codon optimised version of the pQE30-PfHsp70-1 plasmid resulted in consistently successful purifications of PfHsp70-1(opt) from *E. coli* XL1 Blue cells under native conditions. The SDS-PAGE analysis of the induction study of PfHsp70-1(opt) in Figure 2.2A revealed that PfHsp70-1(opt) was highly expressed throughout the induction samples, even before induction with IPTG. The side-by-side solubility study conducted to assess the effect of the addition of PEI to the cell lysate on the solubility and subsequent purification of PfHsp70-1(opt) was assessed. PEI seemed to have no effect on the solubility of PfHsp70-1(opt), and thus subsequent purifications were conducted without the addition of PEI to the cell lysate. The solubility of PfHsp70-1(wt) (Figure 2.1B, lane 5) surprisingly appeared to be greater than that of PfHsp70-1(opt) (Figure 2.2C, lane 5) relative to the insoluble fractions for each protein (lane 4 in each figure). Despite the apparent low solubility, however, high yields of PfHsp70-1(opt) were consistently obtained during purifications using native methods. As shown in Table 2.2,

higher yields of PfHsp70-1(opt) were routinely obtained compared to PfHsp70-1(wt); however, prior to buffer exchange, the degree of purity of PfHsp70-1(wt) was generally higher than that of PfHsp70-1(opt). The degree of purity of PfHsp70-1(opt) was significantly increased following buffer exchange (Figure 2.2C, lane BE).

Unlike the malarial Hsp70s, the malarial Hsp40, PfHsp40, was purified to relatively low yields (Table 2.2), as well as to a lower degree of purity; however the use of buffer exchange columns did aid in removing some of the contaminants from the isolated PfHsp40. Still, the PfHsp40 purified in this study was less pure than that previously reported (Botha *et al.*, 2011), and whereas the previous work on PfHsp40 reported typically purifying ~ 1 mg of recombinant PfHsp40 from a litre of culture (Botha *et al.*, 2011), the highest yield achieved in this study was < 1 mg per litre of culture. In the study by Botha and colleagues, PfHsp40 was expressed and purified in two different ways, using different *E. coli* strains, M15[pRep4] being used in one case. Like in the purification of PfHsp40 from *E. coli* M15[pRep4] by Botha and colleagues, PfHsp40 was purified under denaturing conditions in this study. Differences between the two methods include the use of lower expression temperatures (30 °C) and lower antibiotic concentrations (50 µg/ml ampicillin, 25 µg/ml kanamycin), compared to the expression at 37 °C with ampicillin and kanamycin concentrations of 100 and 50 respectively in this study. These modifications to the growth conditions were made in this study, however, no noticeable differences in protein expression levels were noted under the different sets of conditions (data not shown), and thus, the original conditions (30 °C, 100 µg/ml ampicillin, 50 µg/ml kanamycin) were used for routine purifications of this protein. Further strategies to improve the expression levels of soluble PfHsp40 could include the use of even lower expression temperatures than 30 °C, as well as perhaps a higher or lower concentration of IPTG. In the purification of PfHsp40, protein was eluted off the nickel-charged sepharose beads using 500 mM imidazole. A significant amount of target protein remained bound to the beads following the elution steps (Figure 2.5D, lane 13). An attempt was made to remove this bound protein from the beads using an additional elution step with an elution buffer containing 1 M imidazole; however, though this resulted in a significant amount of target protein eluting off the beads, a large number of contaminants co-eluted, resulting in highly impure and thus unusable PfHsp40 (data not shown). To improve the purity of PfHsp40, further purification steps, including, perhaps, ion exchange chromatography using fast protein liquid chromatography (FPLC) could be employed. PfHsp40 was purified under denaturing conditions (8 M urea), and the denaturant was gradually eliminated from the system by using washes of decreasing urea concentrations and finally a wash containing no urea, as a

means of refolding the recombinant PfHsp40 *in vitro*. Urea, like guanidine, is commonly used in the purification of insoluble recombinant proteins. By disrupting the inter- and intra-molecular interactions in the overexpressed protein, unfolding and thus denaturation of the protein occur, resulting in solubilisation of the protein. Renaturation of the unfolded protein can be achieved by non-denaturing concentrations of the denaturant (Hamada *et al.*, 2009). This approach of refolding a denatured protein *in vitro* is generally considered to have a low success rate (Structural Genomics Consortium *et al.*, 2008). Because the purified recombinant PfHsp40 in this study was not assessed in terms of the portion of protein that was in a native conformation vs. remaining denatured, by for example Fourier Transform Infrared Resonance (FTIR) spectroscopy or tryptophan fluorescence spectroscopy, it cannot be determined to what extent the target protein was refolded during the purification procedure (Haris and Severcan, 1999). However, because the protein was later found to be active in its role as a co-chaperone (Chapter 3), it can be assumed that a significant proportion of the protein was in a native and active state.

The purification of recombinant HsHsp70 produced in this study differed significantly from the methods used to purify the malarial Hsp70s, particularly by the inclusion of second sonication step in the protocol. Based on the SDS-PAGE and Western analyses of the HsHsp70 purification, a large proportion of HsHsp70 remained in the insoluble fraction compared to the soluble fraction (Figure 2.4B, lanes 4 and 5 respectively) of the cell lysate after the first sonication step. The insoluble fraction was thus subjected to a second sonication step, which, based on the increased amount of target protein in the soluble fraction after the first sonication compared to the amount in the soluble fraction after the second sonication (Figure 2.4B, lane 8 compared to lane 5), resulted in the recovery of a significant amount of HsHsp70 from the insoluble fraction of the first lysate. This observation suggests that a significant amount of target protein was still contained within incompletely lysed cells, or, alternatively, was trapped within cell debris and thus sedimenting into the pellet along with cell debris upon centrifugation. The method used to purify HsHsp70 resulted in the purification of high yields (Table 2.2) of HsHsp70 from transformed *E. coli* BL21 cells, with a high degree of purity (estimated at > 90 %). The degree of purity of the protein was significantly improved by the removal of lower molecular weight contaminants following buffer exchange by centrifugal filter columns (Figure 2.4B, lane BE).

Recombinant Hsj1a, which was highly expressed in and purified from *E. coli* XL1 Blue by previously described methods (McNamara, 2006), was obtained in higher yields than any of the other recombinant proteins (nmol yields, Table 2.2), but was purified to only a moderate degree of purity (~ 75 %, Figure 2.6B, lanes 10-12). The degree of purity; however, was significantly improved (to > 90 %) following buffer exchange by centrifugal filter columns (data not shown).

Despite the non-denaturing or native purification protocols used to isolate the recombinant malarial Hsp70s, HsHsp70 and Hsj1a, it cannot be assumed that these proteins were all isolated in a completely native and correctly folded state: it is possible that in the case of some or all recombinant proteins isolated, there was a component that was in an unfolded or misfolded state. As discussed for PfHsp40, techniques such as FTIR spectroscopy or circular dichroism (CD) could have been employed to determine the conformational state of the isolated proteins.

As alluded to in Section 2.1, contamination of purified recombinant chaperones by DnaK is a common problem, particularly in the purification of recombinant Hsp70s (Rial and Ceccarelli, 2002). In this study, the presence of DnaK in the preparations of Hsp70s used in particular in *in vitro* ATPase assays could potentially have confounding effects on results, since DnaK itself has ATPase activity (Liberek *et al.*, 1991). Potential DnaK contamination can be confirmed by Western analysis probing for DnaK. The possible contamination of the purified recombinant proteins in this study was not assessed, and can therefore not be ruled out. In the case of Hsp70s, it would not be possible to observe potential DnaK contamination on an SDS-PAGE gel of the purified protein, since DnaK (69.1 kDa; Structural Genomics Consortium *et al.*, 2008) is very similar in size to the Hsp70s purified in this study. For the Hsp40s, though Western analysis was not carried out to probe for DnaK, DnaK contamination is unlikely to have occurred, based on two pieces of evidence. Firstly, in the SDS-PAGE analyses of the purifications of both Hsj1a (Figure 2.6B) and PfHsp40 (Figure 2.5D), no contaminating bands are visible at DnaK's expected size of ~ 70 kDa. Secondly, in later *in vitro* ATPase assays (Chapter 3), control reactions in which Hsj1a and PfHsp40 were assessed in the absence of Hsp70s, showed that neither of the Hsp40s exhibited any ATPase activity. If any contaminating DnaK was present in the Hsp40 preparations, a low level of ATPase activity due to DnaK would most likely have been detected.

PfHsp70-1(wt), PfHsp70-1(opt), PfHsp70-x, HsHsp70 and Hsj1a were successfully purified at relatively high yields and to high degrees of purity (following buffer exchange), which allowed for extensive *in*

*in vitro* work to be carried out on the effects of small molecules and the chaperone and/or chaperone-co-chaperone activities of these proteins. PfHsp40 was purified to a lower degree of purity and in low yields; however, enough recombinant PfHsp40 was purified to allow for *in vitro* work on PfHsp40 as a co-chaperone to be carried out.



**CHAPTER 3:**

---

**Small molecule modulation of the *in vitro* chaperone activity of *Plasmodium falciparum* and human Hsp70 and Hsp70-Hsp40 systems**

---

Note: some of the work described in this chapter has been published in the following article:

**Cockburn, I.L.**, Pesce, E.-R., Pryzborski, J.M., Davies-Coleman, M.T., Clark, P.G.K., Keyzers, R.A., Stephens, L.L. and Blatch, G.L. (2011). **Screening for small molecule modulators of Hsp70 chaperone activity using protein aggregation suppression assays: inhibition of the plasmodial chaperone PfHsp70-1.** *Biological Chemistry*, 382, 431-438.

The published data has been reproduced as part of this thesis with written permission of the publishers of the article (De Gruyter: [www.degruyter.com/view/j/bchm](http://www.degruyter.com/view/j/bchm)). Data that has been reproduced from the publication in this chapter shall be indicated as such by reference to Cockburn *et al.*, 2011.

### 3.1. INTRODUCTION

---

Purified recombinant PfHsp70-1 has been shown to possess *in vitro* aggregation suppression activity (Ramya *et al.*, 2006; Shonhai *et al.*, 2008; Botha *et al.*, 2011), as well as steady-state (Matambo *et al.*, 2004; Shonhai *et al.*, 2008) and single turnover (Chiang *et al.*, 2009; Botha *et al.*, 2011) ATPase activity. The aggregation suppression activity of PfHsp70-1 has been demonstrated with the use of malate dehydrogenase (MDH) as a substrate protein (Shonhai *et al.*, 2008), based on methods previously described for the bacterial Hsp70 DnaK (Boshoff *et al.*, 2008). There has been one report of the use of an aggregation suppression assay for the identification of an Hsp70 inhibitor, specifically the stimulation of the ATP-enhanced suppression of glutamate dehydrogenase aggregation by PfHsp70-1 in the presence of the immunosuppressant compound DSG (Ramya *et al.*, 2006). The use of MDH aggregation suppression assays as a tool for the identification of Hsp70 inhibitors has not been previously described.

ATPase assays as a means of screening for small molecule modulators of Hsp70s has been demonstrated for a number of Hsp70s including DnaK (Wisén *et al.*, 2010), the yeast Hsp70 Ssa1p (Fewell *et al.*, 2004; Wright *et al.*, 2008; Chiang *et al.*, 2009), human Hsp70 (Chiang *et al.*, 2009, Botha *et al.*, 2011) as well as PfHsp70-1 (Chiang *et al.*, 2009; Botha *et al.*, 2011). The effect of small molecules has been assessed on both the basal and the Hsp40-stimulated Hsp70 activity of these Hsp70s, Hsp40-stimulation being achieved by a wide range of Hsp40s including bacterial DnaJ (Wisén *et al.*, 2010), human Hdj1 (Chiang *et al.*, 2009), human Hdj2 and Hsj1a (Botha *et al.*, 2011), and yeast Ydj1 (Chiang *et al.*, 2009; Fewell *et al.*, 2004; Botha *et al.*, 2011). In these studies very varied effects have been observed. The study by Wright and colleagues (2004), in which the effects of pyrimidinones-peptoid compounds on the ATPase activity of Ssa1p alone and stimulated by the J-domain containing viral T-antigen (TAg), were assessed, presents an interesting and diverse set of results. In many cases, the same compound was found to have opposite effects on the basal vs. the J-domain stimulated ATPase activity. Compounds were identified that either stimulated or inhibited both the basal and the J-domain-stimulated ATPase activity of Ssa1p, whereas other compounds were found to stimulate the basal activity, but inhibit the J-domain stimulated activity, or alternatively, inhibit the basal activity and stimulate the J-domain stimulated activity (Wright *et al.*, 2004).

The study by Botha and colleagues (2011) also yielded interesting results: not only were differences observed in the effects of compounds (MAL3-39 and DMT002264, previously found to have antimalarial activity: Chiang *et al.*, 2009) on Hsp70 and Hsp70-Hsp40 systems when comparing chaperones from different species (comparing malarial and human chaperone / co-chaperone partnerships), but interestingly, differences in the small molecule modulation of the ATPase activities of Hsp70 and Hsp70-Hsp40 systems between steady-state and single-turnover ATPase assays was observed (Botha *et al.*, 2011).

The compounds included in this study are all either natural products, or synthetic derivatives of these, and belong to two sets of compounds: 1,4 naphthoquinones and marine prenylated alkaloids. Compounds belonging to these classes have previously been shown to have various biological activities. The 1,4 naphthoquinone series includes lapachol, a natural product first isolated from a tree species of the bigonaceous family in 1882 (Paterno, 1882). Lapachol, along with a number of its derivatives, has been shown to have anticancer (Bonifazi *et al.*, 2010) and antimalarial (Pérez-Sacau *et al.*, 2005) activity. Bonifazi and colleagues synthesized a series of 1,4 naphthoquinone analogues and tested them for antiproliferative activity against six human cell lines, including ovarian, breast, cervical, lung and colon cancer cell lines. A number of the test compounds were found to have IC<sub>50</sub> values in the low micromolar range (< 1 µM) against one or more cell lines (Bonifazi *et al.*, 2010). Pérez-Sacau and colleagues found lapachol to have moderate antimalarial activity against *P. falciparum* (strain F32) with an IC<sub>50</sub> of 24 µM, and several of its derivatives having lower IC<sub>50</sub> values (< 5 µM). Furthermore, 26 structurally related compounds were assessed, allowing the authors to make inferences about structure-activity relationships within the series. Most notably, the presence of a pyran or furan ring fused to the core double-ring skeleton of the naphthoquinones appeared to increase antimalarial activity of the compounds (Pérez-Sacau *et al.*, 2005). In the context of malaria, the most well-known 1,4 naphthoquinone is the drug known as atovaquone, which is used in combination with proguanil (in the form of Malarone™ tablets) for both treatment and prevention of malaria (Looareesuwan *et al.*, 1999; Fidock, 2010), as well as a number of other protozoan diseases (Baggish and Hill, 2002). Atovaquone was synthesized based on the structure and activity of lapachol (Wells, 2011). Several of the marine prenylated alkaloids included in this study have also been found to have biological activities. The malonganenone A – C group of compounds, natural products extracted from a Mozambican sea fan, *Leptogorgia gilchristi*, were found to possess activity against several oesophageal cancer cell lines (Keyzers *et al.*, 2006).

The Hsp40 used in this study to assess the effects of compounds on the Hsp40-stimulated ATPase activity of Hsp70s is a human type II Hsp40, Hsj1a (DNAJB2). Hsj1a is preferentially expressed in the brain (Cheetham *et al.*, 1992), and plays a role in the ER-associated degradation (ERAD) of proteins via the ubiquitination pathway. Hsj1a, in addition to a J-domain, has two ubiquitin interaction motifs through which it interacts with ubiquitylated proteins targeted for degradation, preventing their aggregation and thus the toxic effects of protein aggregation in neurons (Westhoff *et al.*, 2005). Hsj1a has previously been shown to stimulate the *in vitro* ATPase activities of mammalian Hsc70 (Cheetham *et al.*, 1994), human Hsp70 (Botha *et al.*, 2011; Gao *et al.*, 2012) as well as PfHsp70-1 (Botha *et al.*, 2011), and was thus used in this study as a model J-domain containing protein for the assessment of Hsp70-Hsp40 ATPase activities of PfHsp70-1, PfHsp70-x and HsHsp70. In the case of PfHsp70-1, PfHsp40, a suggested co-chaperone of PfHsp70-1 (Botha *et al.*, 2011), was also used to show J-domain stimulated ATPase activity. Interestingly, a recent study on the interaction between Hsj1a and human Hsp70 revealed that the C-terminal alpha-helical domain of Hsp70 is essential for the Hsj1a-stimulation of Hsp70 ATPase activity and activation of the allosteric response of Hsp70 to Hsj1a (Gao *et al.*, 2012).

The aims of the experiments in this chapter, toward completion of Objective 2 (Section 1.4) were to assess the effects of compounds on the aggregation suppression activity of PfHsp70-1 and PfHsp70-x, as well as on the basal and Hsp40-stimulated ATPase activities of PfHsp70-1 and PfHsp70-x (compared to that of HsHsp70), with the hope of identifying modulators specific to PfHsp70-1 and/or PfHsp70-x, and not to HsHsp70. An additional aim was to carry out a kinetic characterization of the steady-state ATPase activity of PfHsp70-x, which was previously uncharacterized. Recombinant chaperones (PfHsp70-1, PfHsp70-x, HsHsp70, PfHsp40 and Hsj1a) whose purification was described in Chapter 2 were used in the study.

## 3.2. MATERIALS AND METHODS

---

### 3.2.1. Materials

---

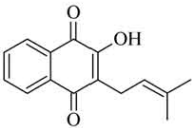
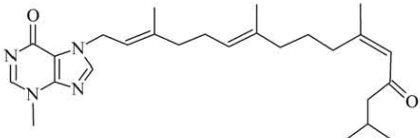
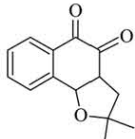
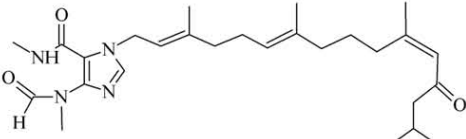
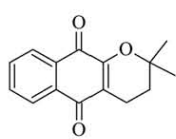
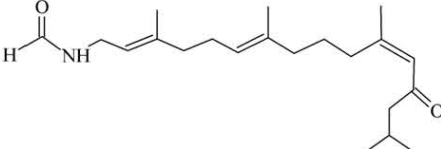
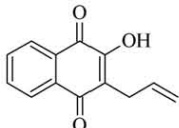
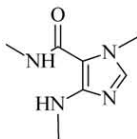
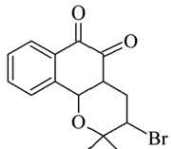
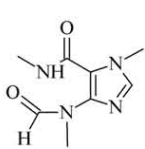
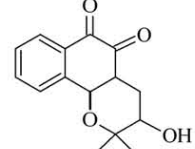
Pig heart malate dehydrogenase (MDH), bovine serum albumin (BSA, Fraction V) and adenosine-5'-triphosphate (ATP) were purchased from Roche (Switzerland). Sodium chloride, tris-(hydroxymethyl)-aminomethane (Trizma® base: Tris), dithiothreitol (DTT), Hepes, sodium dodecyl sulphate (SDS), potassium chloride (KCl), and dimethyl-sulfoxide (DMSO) were purchased from Sigma-Aldrich (U.S.A), and potassium dihydrogen phosphate (KH<sub>2</sub>PO<sub>4</sub>), magnesium chloride (MgCl<sub>2</sub>), ascorbic acid, ammonium molybdate, hydrochloric acid (HCl), glacial acetic acid and tri-sodium citrate were supplied by Saarchem, Merck (Germany). 96-well plates were purchased from Greiner Bio-One (Germany). Lapachol,  $\alpha$ -lapachona, hydroxy- $\beta$ -lapachona, nor- $\beta$ -lapachona, bromo- $\beta$ -lapachona, c-alil-laurosona, malonganenone A, malonganenone B, malonganenone C, PGKC4\_7C and PGKC4\_4I were received from project collaborator Professor M. Davies-Coleman (Rhodes University, South Africa). The lapachol series of compounds (lapachol,  $\alpha$ -lapachona, hydroxy- $\beta$ -lapachona, nor- $\beta$ -lapachona, bromo- $\beta$ -lapachona, c-alil-laurosona) was received by Professor M. Davies-Coleman as a gift from Professor Antonio Ventura Pinto (Núcleo de Pesquisas em Produtos Naturais, UFRJ, 21944-971 Rio de Janeiro, RJ, Brazil). Compounds of the malonganenone series (malonganenone A, malonganenone B, malonganenone C, PGKC4\_7C and PGKC4\_4I) (Rhodes University, South Africa) were isolated (malonganenones) or synthesized (PGKC4\_7C and PGKC4\_4I) by Dr. Robert Keyzers, under the supervision of Professor M. Davies-Coleman, as previously described (Keyzers *et al.*, 2006; Cockburn *et al.*, 2011).

### 3.2.2. Preparation of test compounds

---

All compounds were resuspended to stocks of 30 mM in DMSO and stored at – 80 °C. Prior to use in any experiments, spectral scans of all compounds were carried out at 200 – 900 nm to ensure that they had no significant absorbance at wavelengths relevant to any spectrophotometric assays used in this study. All compounds had minor absorbance peaks at ~ 250 nm (data not shown), which was well below the wavelengths used in *in vitro* chaperone assays (360 nm and 850 nm, Sections 3.2.3 and 3.2.4 respectively) as well as in growth assays (650 nm and 550 nm, Sections 5.2.4 and 5.2.6 respectively). Table 3.1 shows the structures of the compounds.

**Table 3.1: Names and structures of compounds of interest.**

Lapachol and synthetic derivatives (1,4-naphthoquinones)		Prenylated alkaloids and synthetic derivatives	
Common name	Structure	Common name	Structure
Lapachol		Malonganenone A	
Nor-β-lapachona		Malonganenone B	
α-Lapachona		Malonganenone C	
C-Alil-lausona		PGKC4_7C	
Bromo-β-lapachona		PGKC4_4I	
Hydroxy-β-lapachona		-	-

### 3.2.3. MDH aggregation suppression assays

---

MDH aggregation suppression assays were carried out as previously described (Boshoff *et al.*, 2008; Shonhai *et al.*, 2008). The thermal aggregation of MDH, a model substrate protein, and the suppression of such aggregation by chaperones, were monitored spectrophotometrically. Assay buffer (50 mM Tris, pH 7.4, 100 mM NaCl) was heated to 48 °C in a Peltier-heated cell of a Helios Alpha DB spectrophotometer. MDH (0.72 µM final concentration) was added to the heated buffer and the temperature was maintained at 48 °C for 30 minutes during which the light scatter due to protein aggregates was monitored at 360 nm. To measure the aggregation suppression chaperone activity of Hsp70s, purified recombinant Hsp70s (Chapter 2) were included in the reaction mixture (PfHsp70-1(wt): 0.36 µM; PfHsp70-x: 0.18 µM). The human Hsp70 (HsHsp70) was not suitable for the assay, as the protein formed aggregates at 48 °C. HsHsp70 was thus not included in MDH aggregation suppression experiments. PfHsp70-1 and PfHsp70-x seemed to retain a high level of activity at 48 °C. The proteins themselves did not aggregate under the assay conditions (data not shown), and consistently exhibited a high level of aggregation suppression activity. In the case of PfHsp70-1, the chaperone has been shown to be highly thermostable, and PfHsp70-1 has in fact been shown to have optimum ATPase activity at 50 °C (Misra and Ramachandran, 2009).

For the purposes of this study the described assay was further adapted as a tool to screen compounds as modulators of the aggregation suppression activity of Hsp70s (as described by Cockburn *et al.*, 2011). Compounds were included in the assay by addition to heated buffer (48 °C) together with chaperones for a brief incubation period to allow the reaction mixture to re-equilibrate to 48 °C, after which, to initiate the reaction, MDH was added to the reaction mixture. As an initial screening for modulatory effects of compounds on the aggregation suppression activity of Hsp70s, compounds were used at a final concentration of 300 µM. For any compounds found to have modulatory effects on Hsp70 activity, a concentration-dependency experiment was carried out in which the screening was expanded to include a concentration range of 300 µM, 200 µM, 100 µM, 10 µM, 1 µM and a stoichiometrically equivalent concentration to the Hsp70 used (0.36 µM for PfHsp70-1, 0.18 µM for PfHsp70-x) of compound. These experiments were carried out with three independently purified batches of protein; however, due to limited availability of compounds, only a single replicate of each experiment was conducted for each protein batch. A number of controls were included in the assays described above. A reaction in which BSA (0.72 µM) was included instead of Hsp70 was carried out to show that



suppression of the thermal aggregation of MDH was due to the chaperone activity of Hsp70 and not simply due to the presence of a second protein in the system. DMSO was also included in the assay (together with MDH and Hsp70) at the maximum concentration (1 %, v/v) used in any compound screening to assess whether the solvent had any effect on chaperone activity. Compounds were also assayed (at the maximum concentration: 300  $\mu$ M) together with MDH (no chaperone) to rule out that the compounds were causing an increase or decrease in MDH aggregation; and together with chaperones (no MDH) to ensure that apparent inhibition of aggregation suppression activity was not due to aggregation of the Hsp70 in the presence of compounds. Assays were performed with at least two independently purified batches of recombinant proteins.

#### **3.2.4. ATPase assays**

---

Steady-state ATPase activity assays were carried out according to previously described methods (Matambo *et al.*, 2004). Since the ATPase activity of PfHsp70-x has not been characterised before, a kinetic study was carried out for this protein. PfHsp70-x (1.6  $\mu$ M) in HEPES buffer (10 mM HEPES, pH 8.0, 100 mM KCl, 2 mM MgCl<sub>2</sub>, 0.5 mM DTT) was allowed to equilibrate to 37 °C. Reactions were initiated by the addition of ATP at different concentrations (0, 100, 200, 400, 800 and 1000  $\mu$ M). Reactions were allowed to proceed at 37 °C for 30 minutes (predetermined to be in the initial linear stage of the reaction, and as can be seen in Figure 3.5A), after which 50  $\mu$ l samples (in triplicate for each reaction) were collected and added to 50  $\mu$ l 10 % (w/v) SDS in 96-well plates to terminate reactions. Addition of 50  $\mu$ l 1 % (w/v) ammonium molybdate in 1 M HCl, then 50  $\mu$ l 6 % (w/v) ascorbic acid in distilled water, and finally 125  $\mu$ l 2 % (w/v) trisodium citrate in 2 % (v/v) glacial acetic acid, followed by 3-6 hours of colour development at 37 °C, allowed for the quantification of inorganic phosphate. The absorbance of samples was measured at 850 nm using a Powerwave 96-well plate reader (BioTek Instruments Inc., U.S.A.), and absorbance values were converted to phosphate concentrations using a standard curve of absorbance vs. phosphate concentration (Figure 3.3B) based on a set of KH<sub>2</sub>PO<sub>4</sub> standards assayed along with the samples. All samples were corrected for spontaneous ATP hydrolysis. A Michaelis-Menten kinetic plot was constructed and used to determine the specific activity ( $V_{max}$ ) and  $K_m$  for the basal ATPase activity of PfHsp70-x. A non-linear regression curve was fitted to the Michaelis-Menten plot using GraphPad Prism® (v. 4.03; San Diego, CA, U.S.A.) software.

For the assessment of the effects of compounds on the basal and Hsp40-stimulated steady state ATPase activity of Hsp70s, PfHsp70-1(opt) was used at 2.4  $\mu\text{M}$ , PfHsp70-x and HsHsp70 at 1.6  $\mu\text{M}$ , Hsj1a at 0.8  $\mu\text{M}$  and PfHsp40 at 0.54  $\mu\text{M}$ . The concentrations of Hsp40s relative to Hsp70s were chosen based on previous studies, and gave a sufficient amount of stimulation of ATPase activity to be able to observe both positive and negative modulation by compounds. Hsp70s (in the presence or absence of Hsp40) were briefly incubated with compounds (100  $\mu\text{M}$  for screening) on ice, and then the reaction mixtures were equilibrated to 37  $^{\circ}\text{C}$ . As in the kinetic experiment described above, the reactions were initiated by the addition of ATP (600  $\mu\text{M}$ ). Samples were taken upon ATP addition ( $T=0$ ) and every 10 minutes thereafter for 60 minutes and immediately added to 10 % (w/v) SDS in 96-well plates.  $\text{KH}_2\text{PO}_4$  standards were included in the experiments for the quantification of ATP hydrolysis by Hsp70s. The colour development and absorbance measurement procedures described above were carried out in the same way as for the kinetic study. The initial slope of each reaction was plotted, and used to calculate the fold activity of either the basal or Hsp40-stimulated Hsp70 ATPase activity, relative to the “no compound” reactions. Control reactions assessing the effect of DMSO on ATPase activity were included and showed that DMSO had no significant effect on the basal and Hsj1a-stimulated ATPase activity of any of the Hsp70s (Appendix B, Section 7.2.2.1, Figure 7.3) and the “no compound” reactions were thus taken as the 100 % activity values. A statistical analysis (unpaired, two-tailed T-test, 95 % confidence interval) of the data was carried out to assess whether apparent fold differences in ATPase activities (relative to “no compound” reactions) were statistically significant.

### **3.2.5. Sequence alignments of Hsp70s**

---

Multiple sequence alignments were performed for PfHsp70-1, PfHsp70-x and HsHsp70. The three proteins were globally aligned with each other to determine the homology between them. In addition, the three proteins were aligned with DnaK to allow for the identification of differences in key residues known to play a role in DnaK interactions with DnaJ (Ahmad *et al.*, 2011), as well as those thought to facilitate the interaction between Hsc70 and auxilin (Jiang *et al.*, 2007). These alignments were carried out in an attempt to relate any differences in the effects of compounds on the three Hsp70-Hsp40 systems to key sequence differences in regions or residues on the Hsp70s known to be essential for interactions. Amino acid sequences were obtained from the National Center for Biotechnology (NCBI) (DnaK, HsHsp70) and PlasmoDB (PfHsp70-1, PfHsp70-x), and were aligned using ClustalW multiple sequence alignment tool ([www.ebi.ac.uk/Tools/msa/clustalw2](http://www.ebi.ac.uk/Tools/msa/clustalw2)).

### 3.3. RESULTS

---

#### 3.3.1. *Inhibition of the aggregation suppression activity of PfHsp70-1 and PfHsp70-x*

---

Control aggregation suppression assays were carried out and the results are shown in Figure 3.1A. DMSO (1 %, v/v) and BSA had no effect on the aggregation of MDH at 48 °C over 30 minutes. Figure 3.1A also shows the significant suppression of the thermal aggregation of MDH by PfHsp70-1 and PfHsp70-x. The initial screening of compounds for effects on PfHsp70-1 chaperone activity was carried out with 300  $\mu$ M of each compound. A range of effects was observed in the assay including compounds suppressing MDH aggregation (in the absence of Hsp70, Appendix B, Section 7.2.2.2, Figure 7.4), acting as chemical chaperones and therefore being unsuitable for screening in the MDH assay. These compounds (nor- $\beta$ -lapachona, hydroxy- $\beta$ -lapachona, c-alil-lauserona and PGKC4\_7C) were disregarded for further assessment, as their effects in control reactions would confound screening results. Of the compounds found to have no confounding effects in control reactions, five (lapachol, bromo- $\beta$ -lapachona, malonganenone A, malonganenone B, malonganenone C) were found to inhibit the aggregation suppression activity of PfHsp70-1 at 300  $\mu$ M (Figure 3.1B), and two ( $\alpha$ -lapachona and PGKC4\_4I), had no effect on either MDH aggregation or PfHsp70-1 aggregation suppression activity (data not shown). Since the assays used in the work described in this chapter are not conducive to high-throughput screening, and require large amounts of compound, the set of eleven test compounds was limited to the five above-mentioned active compounds for the purposes of screening for modulatory effects of compounds in both aggregation suppression and ATPase assays. Of the five compounds, only two (bromo- $\beta$ -lapachona and malonganenone A) were found to have an effect on the aggregation suppression activity of PfHsp70-x at 300  $\mu$ M.

For compounds found to inhibit the aggregation suppression activity of PfHsp70-1 and PfHsp70-x, dose-response experiments were carried out. The results of these experiments are illustrated in Figures 3.2 and 3.3. Figure 3.2A shows the progress curves (i-v) of the dose response experiments assessing the effects of lapachol, bromo- $\beta$ -lapachona, and malonganenones A, B and C on the aggregation suppression activity of PfHsp70-1. Figures 3.2A(i-v) are single, representative replicates of the experiments, illustrating the concentration-dependency of the inhibitory effects of compounds on PfHsp70-1. Concentration dependency was especially evident for bromo- $\beta$ -lapachona, malonganenone A and malonganenone C, particularly from 10  $\mu$ M onward for malonganenones A and C, and for bromo-

$\beta$ -lapachona the effects was only evident at 100 and 300  $\mu$ M. For lapachol and malonganenone B, the inhibitory effect was only clear at the highest compound concentration (300  $\mu$ M). The bar graph in Figure 3.2B shows the averaged data for experiments carried out with three independent batches of PfHsp70-1. Due to batch-to-batch variations in aggregation suppression activity, the data showed a large degree of variation (shown as error bars, standard deviation), masking the overall dose-dependent effect seen in the progress curves. However, looking simply at the bars in Figure 3.2B, and not taking into account the error bars, a general increase in MDH aggregation can be seen with increasing compound concentrations. For PfHsp70-x, progress curves for dose-response experiments with bromo- $\beta$ -lapachona and malonganenone A are shown in Figure 3.3A (i and ii respectively). Data in the progress curves again represents only a single replicate of one batch of PfHsp70-x. A concentration dependent effect was observed for bromo- $\beta$ -lapachona (at 100  $\mu$ M and 300  $\mu$ M, no notable differences at 1  $\mu$ M and 10  $\mu$ M), whereas the inhibition of PfHsp70-x by malonganenone A was only evident at 300  $\mu$ M. As with PfHsp70-1, the overall dose-response effects of compounds shown in Figure 3.3B was somewhat masked by the large error bars (standard deviation) shown for the data, again due to variations in activity of independently purified batches of PfHsp70-x.

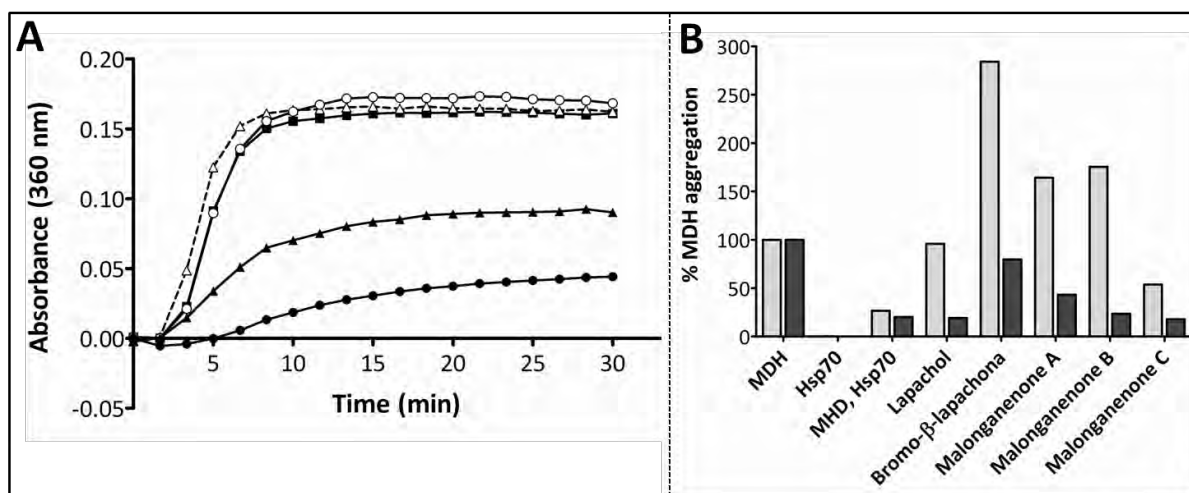


**Figure 3.1: MDH aggregation assays – control reactions and compound screening.** (A) Control reactions included 0.72  $\mu$ M MDH alone (closed squares, solid line), MDH (0.72  $\mu$ M) and BSA (0.72  $\mu$ M) (open triangles, dashed line), MDH (0.72  $\mu$ M) and 1 % (v/v) DMSO (open circles, solid line), MDH (0.72  $\mu$ M) and PfHsp70-1 (0.36  $\mu$ M) (closed triangles, solid line), MDH (0.72  $\mu$ M) and PfHsp70-x (0.18  $\mu$ M) (closed circles, solid line). (B) Effects of compounds on the aggregation suppression activity of PfHsp70-1 and PfHsp70-x where the final absorbance of MDH alone is taken as 100 %. Bars labelled with compound names include 300  $\mu$ M compound, MDH (0.72  $\mu$ M) and either PfHsp70-1 (0.36  $\mu$ M; light bars) or PfHsp70-x (0.18  $\mu$ M; dark bars). Data in A is published in Cockburn *et al.*, 2011.

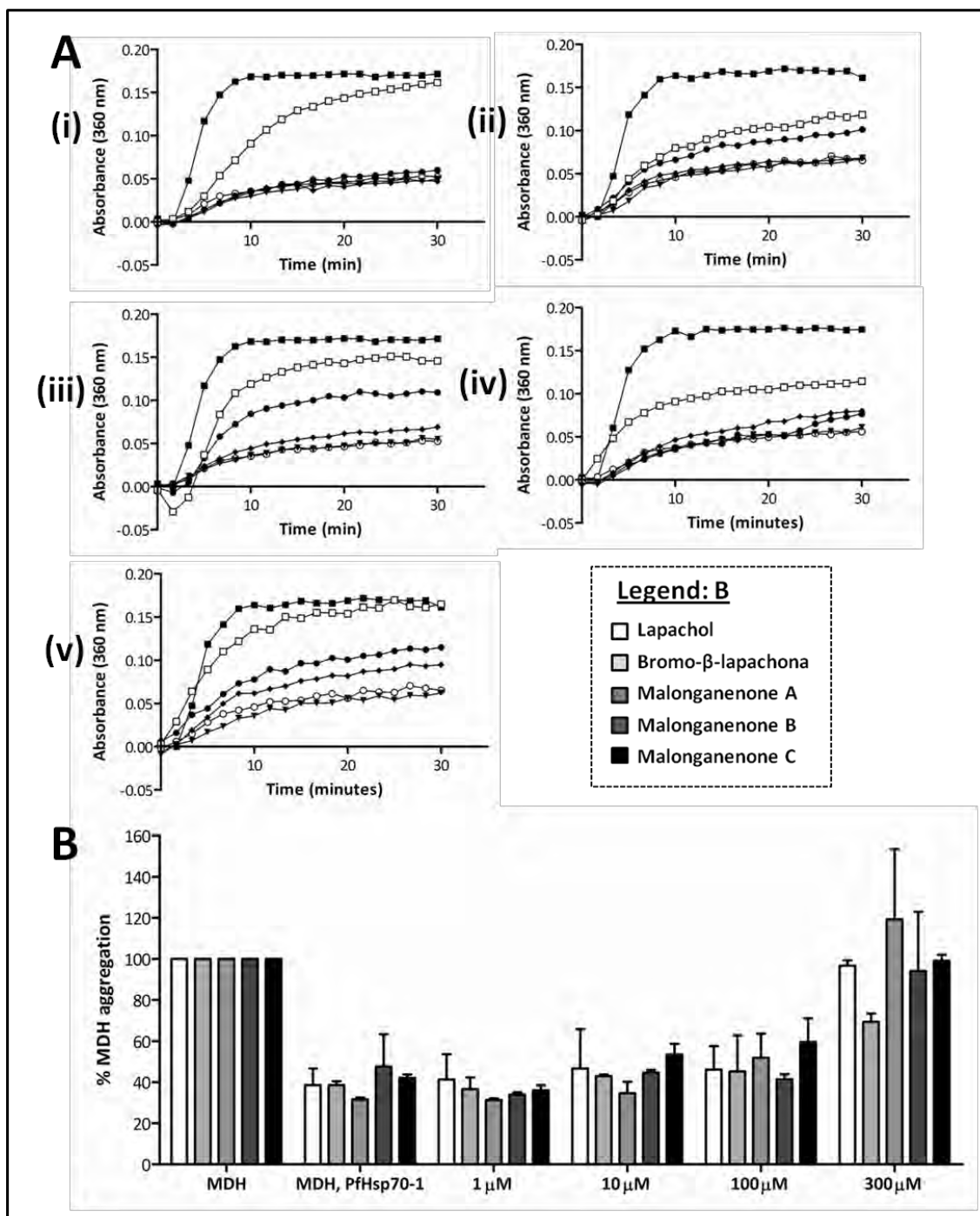


**Figure 3.2: Concentration-dependent effects of compounds on the aggregation suppression activity of PfHsp70-1.** Progress curves of absorbance vs. time (A) showing inhibition of PfHsp70-1 by lapachol (i), bromo-β-lapachona (ii), malonganenone A (iii), malonganenone B (iv) and malonganenone C (v). Reactions include MDH alone (0.72 μM) (closed squares), MDH (0.72 μM) and PfHsp70-1 (0.36 μM) (open circles), and MDH, PfHsp70-1 and compounds, at 1 μM (closed downward triangles), 10 μM (closed diamonds), 100 μM (closed circles) and 300 μM (open squares). Data from three independently purified batches of PfHsp70-1 (B) is shown as a percentage of the MDH only reaction. Concentrations on the x-axis indicate compound concentration in the presence of MDH and PfHsp70-1. Data in A is published in Cockburn *et al.*, 2011.

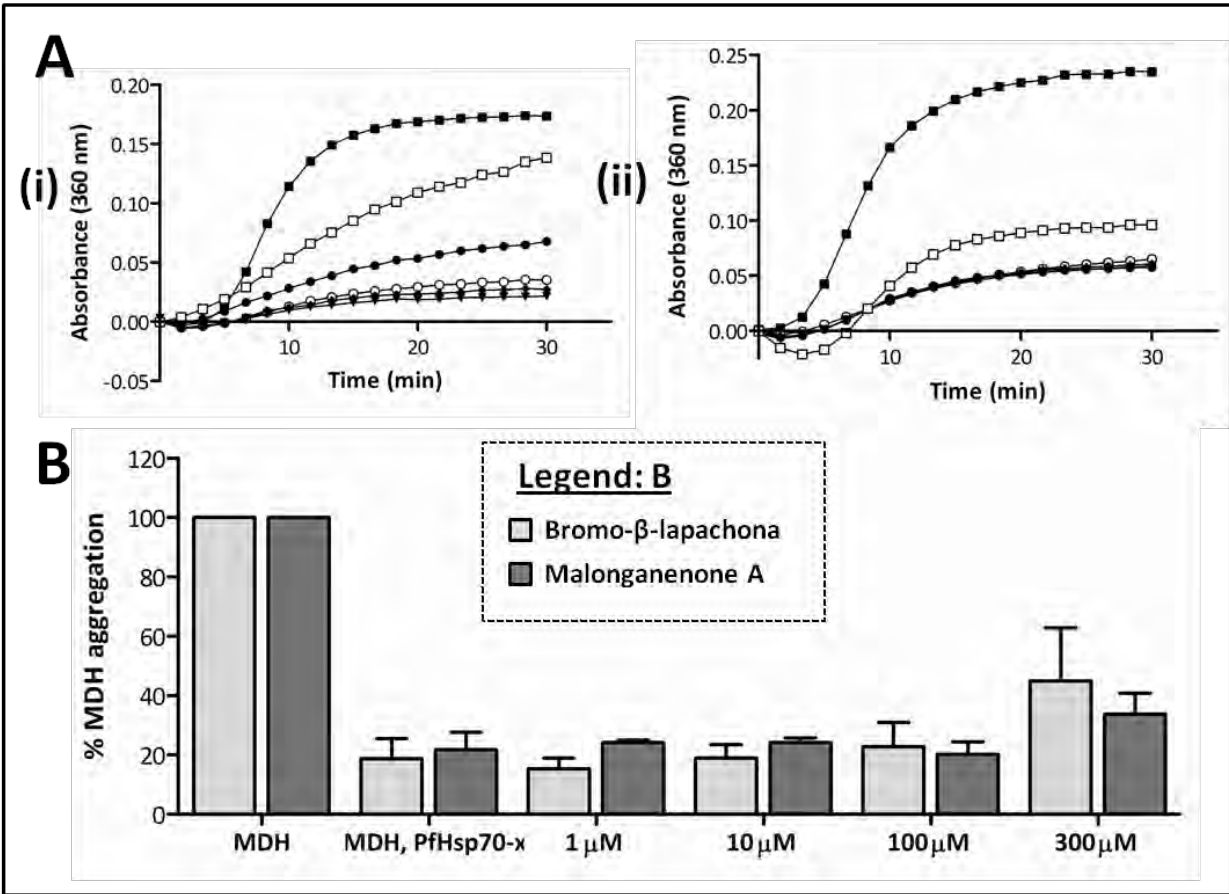


**Figure 3.3: Concentration dependent effects of compounds on the aggregation suppression activity of PfHsp70-x.** Progress curves of absorbance vs. time (A) showing inhibition of PfHsp70-x by bromo-β-lapachona (i) and malonganenone A (ii). Reactions include MDH alone (0.72 μM) (closed squares), MDH (0.72 μM) and PfHsp70-x (0.18 μM) (open circles), and MDH, PfHsp70-x and compounds, at 1 μM (closed downward triangles), 10 μM (closed diamonds), 100 μM (closed circles) and 300 μM (open squares). Data from three independently purified batches of PfHsp70-x (B) is shown as a percentage of the MDH only reaction. Concentrations on the x-axis indicate compound concentration in the presence of MDH and PfHsp70-x.

### 3.3.2. Characterisation of the steady-state ATPase activity of PfHsp70-x

The results of the kinetic characterisation of the steady-state ATPase activity of PfHsp70-x are shown in Figure 3.4. The Michaelis-Menten plot of specific activity (mmol ATP hydrolysed / min / mol PfHsp70-x) vs. ATP concentration (Figure 3.4A) shows that the steady-state ATPase activity of PfHsp70-x follows conventional Michaelis-Menten kinetics, allowing for the determination of kinetic parameters ( $V_{\max}$  and  $K_m$ ) by fitting a non-linear regression curve to the data. Using this method,  $V_{\max}$  and  $K_m$  were determined to be  $0.21 \pm 0.02$  mmol ATP/min/mol PfHsp70-x and  $393.9 \pm 92.3$   $\mu$ M respectively (values represent the average of triplicate experiments,  $\pm$  standard deviation).

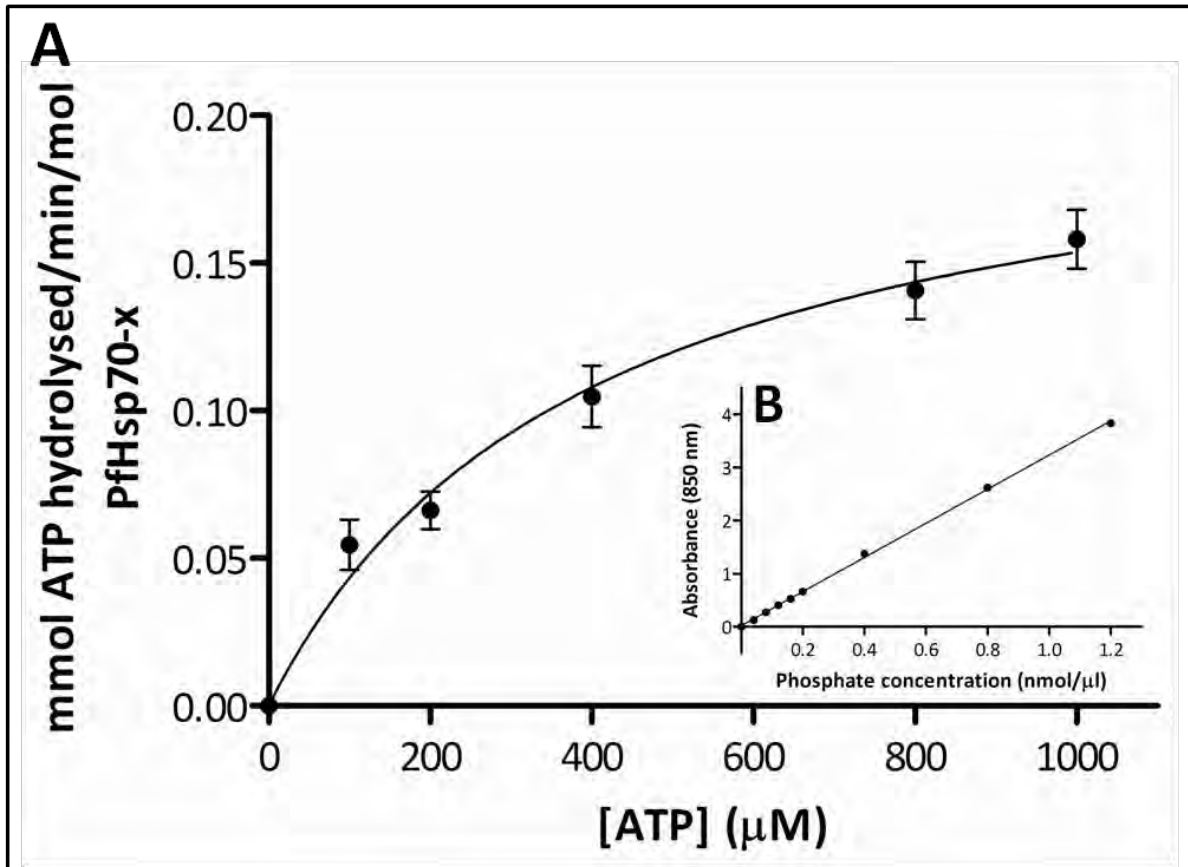


**Figure 3.4: Kinetic characterisation of the steady-state ATPase activity of PfHsp70-x.** A: Michaelis-Menten kinetic plot of the steady-state ATPase activity of PfHsp70-x in the presence of increasing substrate (ATP) concentration. B: Standard curve of absorbance vs. phosphate concentration used to calculate ATP hydrolysis rates.  $V_{\max}$  ( $0.21 \pm 0.02$  mmol ATP/min/mol PfHsp70-x) and  $K_m$  ( $393.9 \pm 92.3$   $\mu$ M ATP) values were determined from a non-linear regression curve fitted to the data in A. ATPase activity of PfHsp70-x was calculated assuming the protein to be in the monomeric state, with a molecular weight of 74 kDa.

### **3.3.3. Modulation of the basal and Hsp40-stimulated ATPase activity of PfHsp70-1, PfHsp70-x and HsHsp70 by small molecules**

---

The effects of compounds on the basal and Hsp40-stimulated steady state ATPase activity of PfHsp70-1, PfHsp70-x and HsHsp70 are shown in Figures 3.5 and 3.6 and 3.7, and the data is summarised in Table 3.2. Hsp40-stimulated ATPase activity the three Hsp70s was shown using Hsj1a, and in the case of PfHsp70-1, additional experiments were carried out showing stimulation of ATPase activity by PfHsp40, thought to be an *in vivo* co-chaperone to PfHsp70-1 (Botha *et al.*, 2011). For PfHsp70-1/PfHsp40 experiments, only compounds found to significantly modulate the basal (malonganenone A) or Hsj1a-stimulated (lapachol and bromo- $\beta$ -lapachona) ATPase activity of PfHsp70-1 were screened due to limiting amounts of recombinant PfHsp40 (Figure 3.7). The basal ATPase activity (Figure 3.5B) of PfHsp70-1 was significantly stimulated by malonganenone A (~15 % increase in activity), and none of the other four compounds had any significant effects. The Hsj1a-stimulated activity of PfHsp70-1 (Figure 3.6B) was significantly ( $P < 0.001$ ) stimulated by both lapachol and bromo- $\beta$ -lapachona (~20 % and ~30 % increase in activity respectively). Interestingly, in contrast to the Hsj1a-stimulated PfHsp70-1 activity, the PfHsp40-stimulated ATPase activity of PfHsp70-1 (Figure 3.7B) was significantly inhibited by bromo- $\beta$ -lapachona (~75 % inhibition) malonganenone A (~65 % inhibition), and appeared to also be notable inhibited by lapachol (~35 % inhibition), however this apparent inhibition was not statistically significant ( $P > 0.05$ ). The basal ATPase activity of PfHsp70-x (Figure 3.5C) was significantly ( $P < 0.001$ ) inhibited by both lapachol and bromo- $\beta$ -lapachona (~40 % and ~80 % decrease in activity). Similarly, the Hsj1a-stimulated ATPase activity of PfHsp70-x (Figure 3.6D) too was significantly ( $P < 0.001$ ) inhibited by lapachol and bromo- $\beta$ -lapachona (~50 % and 90 % decrease in activity respectively), as well as by malonganenone A (~20 % decrease in activity;  $P < 0.001$ ). Malonganenone B and C also inhibited the Hsj1a-stimulated ATPase activity of PfHsp70-x significantly ( $P < 0.05$ ), though to a lesser extent (~ 10 % decrease in activity). The basal ATPase activity of HsHsp70 (Figure 3.5D) was significantly ( $P < 0.05$ ) inhibited by bromo- $\beta$ -lapachona (~15 % decrease in activity), which was, on the contrary, found to stimulate the Hsj1a-stimulated HsHsp70 activity (~ 10 % increase,  $P < 0.001$ , Figure 3.6F). None of the other four compounds had any significant effects on either the basal or Hsj1a-stimulated HsHsp70 ATPase activity.



The data shown in Figures 3.5 - 3.7 is summarised in Table 3.2. For PfHsp70-1, only malonganenone A was found to affect (stimulate) basal ATPase activity. Contrasting effects by compounds were observed for the Hsj1a-stimulated vs. PfHsp40-stimulated ATPase activity of PfHsp70-1: malonganenone A had no effect on the Hsj1a-stimulated activity, but significantly inhibited and PfHsp40-stimulated activity, and lapachol and bromo- $\beta$ -lapachona stimulated the Hsj1a-stimulated activity, but inhibited (non-significant effect for lapachol) the PfHsp40-stimulated activity of PfHsp70-1. For PfHsp70-x, compounds had an inhibitory effect or no effect on the basal or Hsj1a-stimulated activity. For HsHsp70, both inhibition (basal activity) and stimulation (Hsj1a-stimulated activity) were observed. The compound with the broadest effects across all Hsp70 or Hsp70-Hsp40 systems assayed was bromo- $\beta$ -lapachona, modulating all but one (basal PfHsp70-1 activity) reaction.

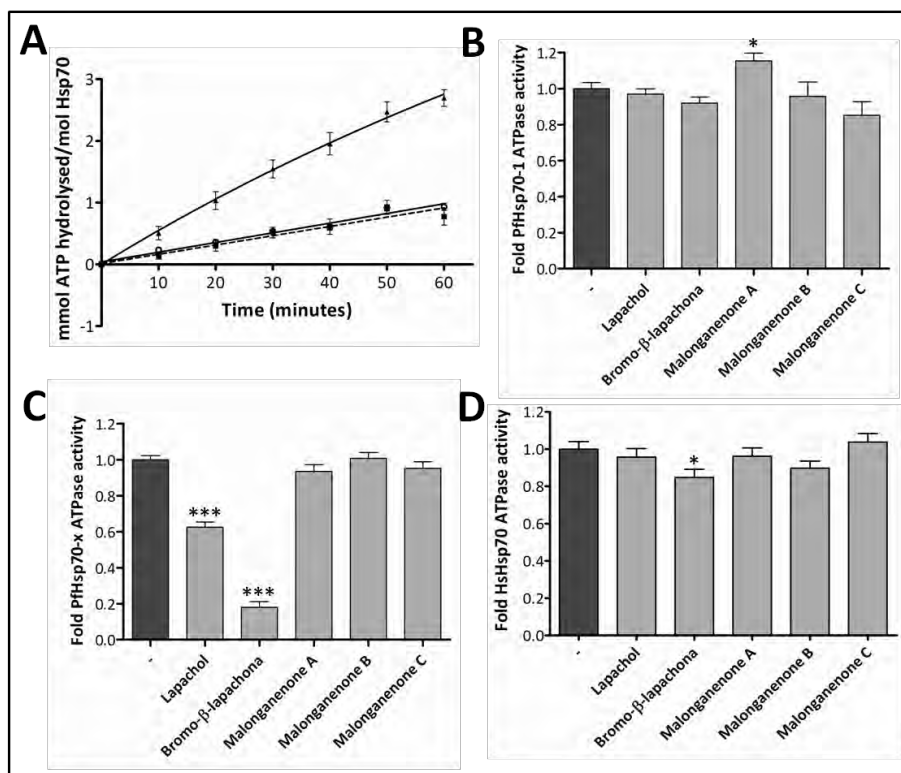


**Figure 3.5. Effects of compounds on the basal steady-state activities of PfHsp70-1, PfHsp70-x and HsHsp70.** A: Progress curves (ATP hydrolysis vs. time) for PfHsp70-1 (open circles, solid line), PfHsp70-x (closed triangles, solid line) and HsHsp70 (closed squares, dashed line). Fold Hsp70 ATPase activity relative to a “no compound” control reaction (dark bar) in the presence of test compounds is shown for PfHsp70-1 (B), PfHsp70-x (C) and HsHsp70 (D). All data represents the average of nine replicates, where error bars show standard deviation. Significant differences relative to the “no compound” reaction are indicated by \* ( $P < 0.05$ ) or \*\*\* ( $P < 0.001$ ) as determined by a two-tailed T-test with a 95 % confidence interval.

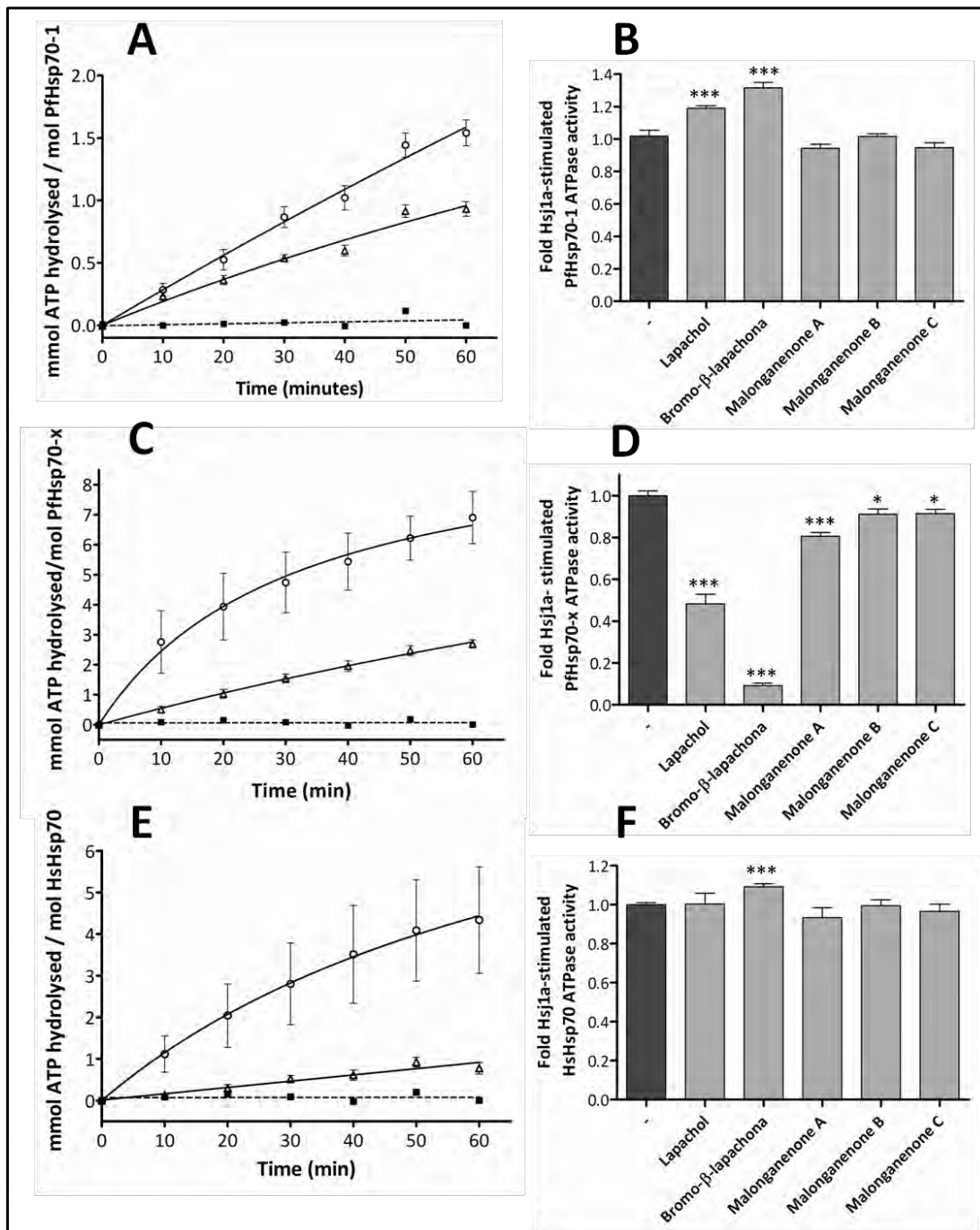


**Figure 3.6: Effects of compounds on the Hsj1a-stimulated steady-state ATPase activities of PfHsp70-1, PfHsp70-x and HsHsp70.** The stimulation of ATPase activity by Hsj1a is shown for PfHsp70-1 (A), PfHsp70-x (C) and HsHsp70 (E), where closed squares and dashed lines represent Hsj1a alone, open triangles and solid lines represent Hsp70 alone, and open circles and solid line represent Hsj1a-stimulated Hsp70. The effects of compounds on the Hsj1a-stimulated ATPase activity of each Hsp70 is shown in B (PfHsp70-1), D (PfHsp70-x) and F (HsHsp70) in terms of fold activity relative to the “no compound” control reaction (dark bars). All data represents the average of nine replicates, where error bars show standard deviation. Significant differences relative to the “no compound” reaction are indicated by \* ( $P < 0.05$ ) or \*\*\* ( $P < 0.001$ ) as determined by a two-tailed T-test with a 95 % confidence interval. For ATPase activity calculations, all Hsp70s were assumed to be in a monomeric state.

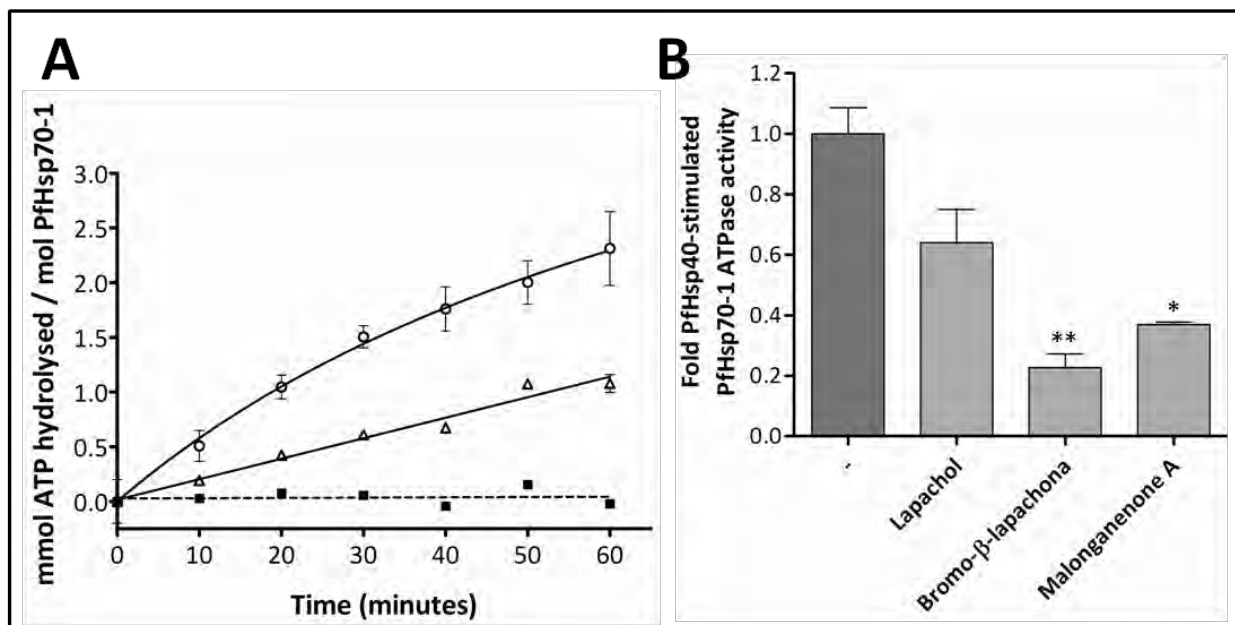


**Figure 3.7: Effects of compounds on the PfHsp40-stimulated steady-state ATPase activity of PfHsp70-1.** The stimulation of the ATPase activity of PfHsp70-1 (2.4  $\mu$ M) by PfHsp40 (0.54  $\mu$ M) is shown (A), where closed squares and dashed lines represent PfHsp40 alone, open triangles and solid lines represent Hsp70 alone, and open circles and solid lines represent PfHsp40-stimulated PfHsp70-1. The effects of compounds on the PfHsp40-stimulated ATPase activity of PfHsp70-1 is shown in (B) in terms of fold activity relative to the “no compound” control reaction (dark bar). The data represents the average of three replicates, where error bars show standard deviation. Significant differences relative to the “no compound” reaction are indicated by \* ( $P < 0.05$ ) and \*\* ( $P < 0.01$ ) as determined by a two-tailed T-test with a 95 % confidence interval.

**Table 3.2: Summary of the effects of test compounds (100  $\mu$ M) on the basal and Hsp40-stimulated ATPase activities of PfHsp70-1, PfHsp70-x and HsHsp70.** Data represents averages of at least nine replicates in the case of basal and Hsj1a-stimulated activities, including three independently purified batches of each protein, and in the case of PfHsp40-stimulated activities, data represents three replicates. All data represents the fold ATPase activity, relative to a “no compound” control reaction,  $\pm$  standard deviation.

	PfHsp70-1			PfHsp70-x		HsHsp70	
	Basal	Hjs1a-stimulated	PfHsp40-stimulated	Basal	Hjs1a-stimulated	Basal	Hjs1a-stimulated
Lapachol	0.97 $\pm$ 0.09	<u>1.19 <math>\pm</math> 0.04</u>	0.64 $\pm$ 0.16	<u>0.63 <math>\pm</math> 0.08</u>	<u>0.48 <math>\pm</math> 0.14</u>	0.96 $\pm$ 0.13	1.00 $\pm$ 0.15
Bromo-β-lapachona	0.92 $\pm$ 0.09	<u>1.32 <math>\pm</math> 0.10</u>	<u>0.23 <math>\pm</math> 0.06</u>	<u>0.18 <math>\pm</math> 0.09</u>	<u>0.09 <math>\pm</math> 0.03</u>	<u>0.85 <math>\pm</math> 0.13</u>	<u>1.09 <math>\pm</math> 0.04</u>
Malonganenone A	<u>1.15 <math>\pm</math> 0.12</u>	0.94 $\pm$ 0.06	<u>0.37 <math>\pm</math> 0.01</u>	0.93 $\pm$ 0.11	<u>0.81 <math>\pm</math> 0.05</u>	0.96 $\pm$ 0.13	0.93 $\pm$ 0.12
Malonganenone B	0.96 $\pm$ 0.23	1.02 $\pm$ 0.05	ND	1.00 $\pm$ 0.08	<u>0.91 <math>\pm</math> 0.07</u>	0.90 $\pm$ 0.11	1.00 $\pm$ 0.09
Malonganenone C	0.85 $\pm$ 0.21	0.95 $\pm$ 0.09	ND	0.95 $\pm$ 0.11	<u>0.92 <math>\pm</math> 0.06</u>	1.04 $\pm$ 0.14	0.97 $\pm$ 0.11

ND: not determined. Statistically significant differences are shown in underlined bold type and significant inhibition and significant stimulation of ATPase activity are shown in red and green respectively.

The very strong inhibitory effects of lapachol (~ 40 % inhibition) and bromo- $\beta$ -lapachona (~80 % inhibition) at 100  $\mu$ M on the basal ATPase activity of PfHsp70-x were further investigated by dose-response experiments. Basal steady-state ATPase activity assays were carried out using a range of compound concentrations (25, 50 and 100  $\mu$ M). The results of these experiments are shown in Figure 3.8 below, and show that at 25  $\mu$ M, neither lapachol nor bromo- $\beta$ -lapachona have an effect on the ATPase activity of PfHsp70-x; however, at 50 and 100  $\mu$ M, both compounds show a notable decrease in activity, though the fold activities at 50  $\mu$ M are not significantly ( $P > 0.05$ ) different from those at 25 or 0  $\mu$ M.

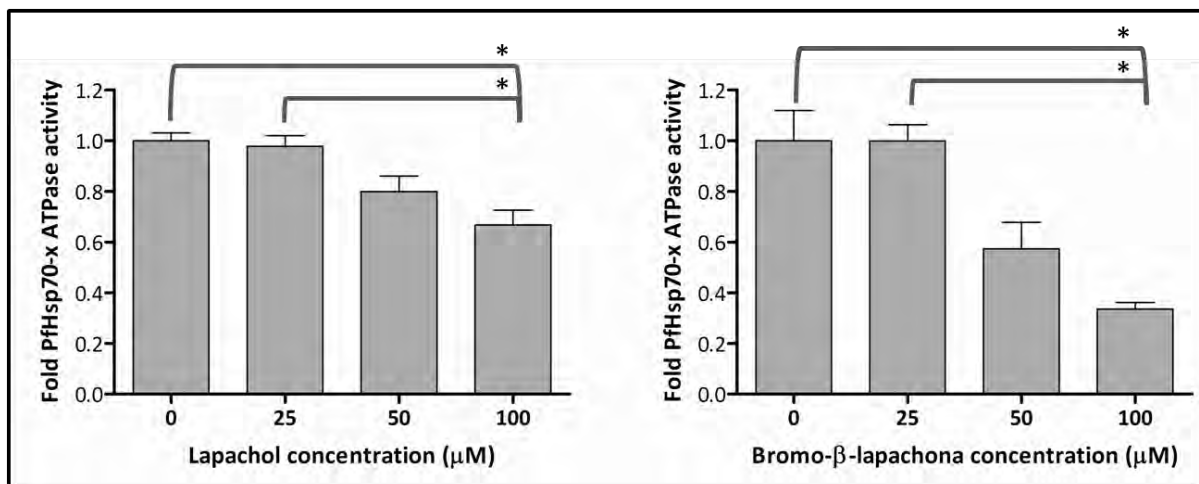


**Figure 3.8: Concentration-dependent effects of compounds on the basal ATPase activity of PfHsp70-x.** Effects of lapachol (A) and bromo- $\beta$ -lapachona (B) at a range of concentrations on the basal steady-state ATPase activity of PfHsp70-x (1.6  $\mu$ M) in terms of fold activity relative to the “no compound” control reaction (0  $\mu$ M compound). The data represents the average of three replicates, where error bars show standard deviation. Significant differences relative to either the “no compound” reaction or the 25  $\mu$ M compound reaction are indicated by \* ( $P < 0.05$ ) as determined by a two-tailed T-test with a 95 % confidence interval.

The effect of malonganenone A on the ATPase activity of PfHsp70-x shown in Table 3.2 was of particular interest, as the basal ATPase activity of PfHsp70-x was unaltered in the presence of malonganenone A, whereas the Hsj1a-stimulated activity was inhibited. Additional experiments were thus conducted to further investigate the effect of malonganenone A on the Hsj1a-stimulated activity of PfHsp70-x, and included an investigation into the effects of varying the order of addition of reaction components in the assay, as well as the effects of varying concentrations of Hsj1a and malonganenone A relative to each other. The results are shown in Figure 3.9. Figure 3.9A shows the effects of altering the order of addition of reactions components: as previously shown (Figure 3.6D), the ability of Hsj1 to stimulate PfHsp70-x ATPase activity was diminished in the presence of 100  $\mu$ M malonganenone A, as can be seen comparing the lower two bars in Figure 3.9A with the top bar, regardless of the order of addition of reaction components. When PfHsp70-x and Hsj1a were pre-incubated together before the addition of malonganenone A, the ATPase activity was significantly ( $P < 0.05$ ) higher than when PfHsp70-x and malonganenone A were pre-incubated together before the addition of Hsj1a. Next, the significant inhibition of Hsj1a-stimulated ATPase activity of PfHsp70-x activity was further investigated with an attempt to titrate malonganenone A and Hsj1a against each other. Figure 3.9B shows that the ability of malonganenone A to decrease Hsj1a-stimulation of ATPase activity of PfHsp70-x is concentration – dependent, shown by the decrease in Hsj1a-stimulated PfHsp70-x ATPase activity with increasing malonganenone A concentration. Furthermore, when the malonganenone A concentration was fixed (100  $\mu$ M), increasing Hsj1a-concentration resulting in increasing Hsj1a-stimulated ATPase activity of PfHsp70-x (Figure 3.9C).

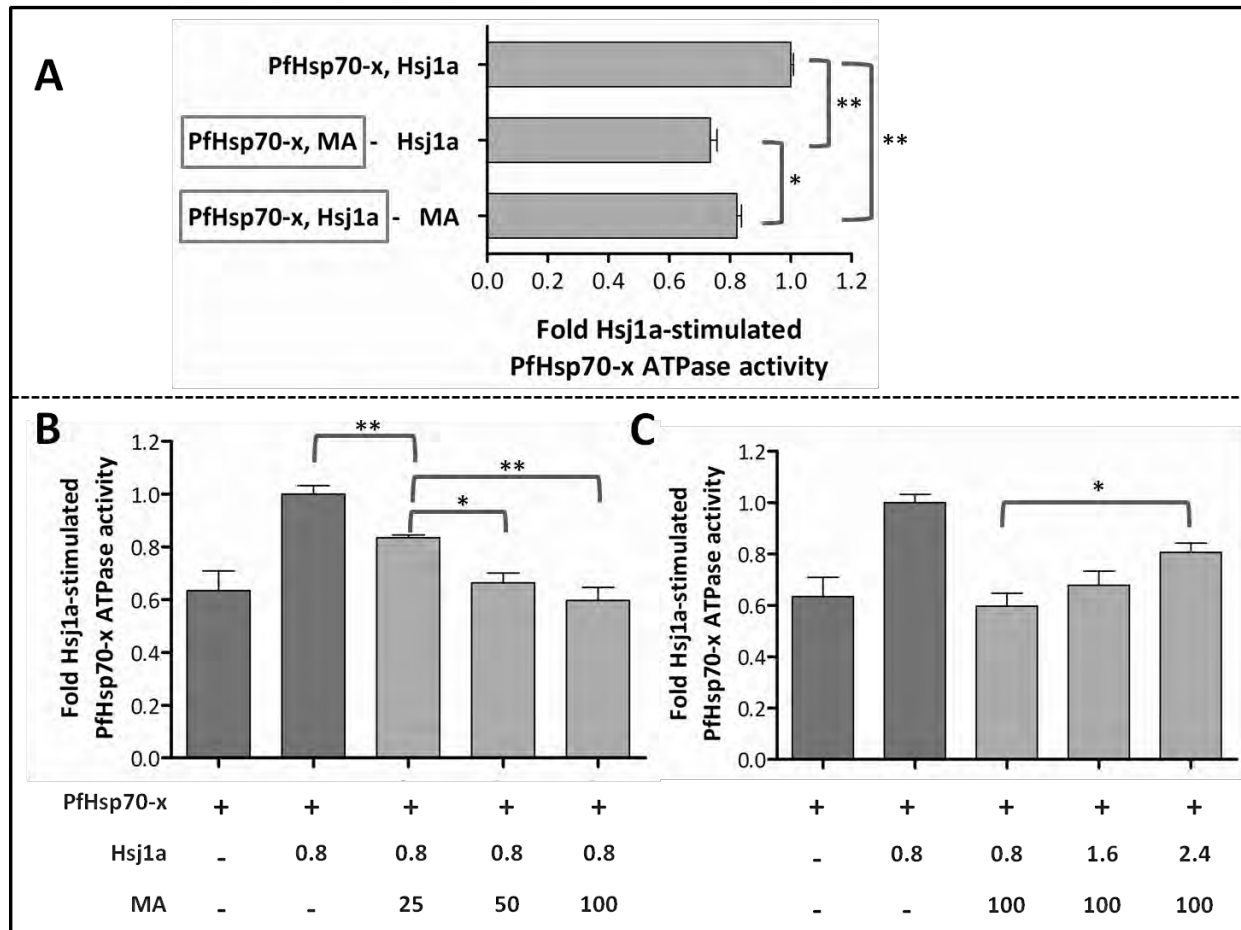


**Figure 3.9: Effects of malonganenone A on the stimulation of PfHsp70-x ATPase activity by Hsj1a.** A: The fold Hsj1a-stimulated ATPase activity in the absence (top bar) and presence (two lower bars) of malonganenone A (MA) is shown. The middle bar represents data for the reaction in which PfHsp70-x was pre-incubated with malonganenone A before the addition of Hsj1a, and the bottom bar represents data for the reaction in which PfHsp70-x and Hsj1a were pre-incubated together for 10 minutes before the addition of malonganenone A. Reaction components pre-incubated together before the addition of the third component are shown in grey boxes. B: Malonganenone A diminishes the stimulatory effect of Hsj1a on the ATPase activity of PfHsp70-x in a dose-dependent manner (constant PfHsp70-x and Hsj1a concentration). C: In the presence of 100  $\mu$ M malonganenone A, the stimulatory effect on the ATPase activity of PfHsp70-x by Hsj1a was concentration-dependent. In all experiments PfHsp70-x concentration was fixed at 1.6  $\mu$ M. Statistically significant differences are indicated by \* ( $P < 0.05$ ) and \*\* ( $P < 0.01$ ), as determined by paired, two-tailed T-tests with a 95 % confidence interval.

### 3.3.4. Sequence alignments of PfHsp70-1, PfHsp70-x and HsHsp70

In a global alignment of PfHsp70-1, PfHsp70-x and HsHsp70, a high degree of sequence identity ( $\geq 70\%$ ; Table 3.3) was found between the three proteins, the highest identity being shared between PfHsp70-1 and PfHsp70-x. Of the three Hsp70s, PfHsp70-1 and PfHsp70-x were also found to share the highest identities in their ATPase (82%) and substrate binding (69%) domains. HsHsp70 was found to have a substantially lower identity with the two malarial proteins. Identity was generally found to be higher in the ATPase domains than the substrate binding domains of the three proteins.

**Table 3.3: Pairwise homologies between PfHsp70-1, PfHsp70-x and HsHsp70.** Homology, determined by multiple sequence alignments of the protein sequences using ClustalW, represent % amino acid identity. Alignments of the complete proteins (global), the ATPase domains (ATPase) and their substrate binding domains (SBD) are shown.

	PfHsp70-1	PfHsp70-x	HsHsp70
<b>Global</b>	PfHsp70-1	-	75
	PfHsp70-x	75	-
	HsHsp70	72	70
<b>ATPase</b>	PfHsp70-1	-	82
	PfHsp70-x	82	-
	HsHsp70	76	75
<b>SBD</b>	PfHsp70-1	-	69
	PfHsp70-x	69	-
	HsHsp70	66	63

A number of studies have been conducted to determine which amino acids in Hsp70s are essential for interactions with both peptide substrates (Zhu *et al.*, 1996) and Hsp40 co-chaperones (Suh *et al.*, 1998; Gässler *et al.*, 1998; Ahmad *et al.*, 2011; Jiang *et al.*, 2007). Peptide substrates have been found to interact with a number of residues in the substrate-binding domain of DnaK: I401, T403, M404, V407, T409, F426, S427, A429, G433, A435, V436, I438 (Zhu *et al.*, 1996). The region(s) on Hsp70s important in interactions with Hsp40s are somewhat disputed (Section 1.1.2): a predominantly negatively charged portion of DnaK (206-221) has been found to be important for Hsp40 interactions, specifically thought to interact with positively charged residues in helix II of the J-domains of Hsp40s (Ahmad *et al.*, 2011). Bovine Hsc70, on the other hand, was thought to interact with Hsp40 (auxilin) via a different region to that described for DnaK (Jiang *et al.*, 2007).

Sequence alignments (as described in Section 3.2.5) were carried out in an attempt to attribute differences in modulation of activity of different Hsp70 or Hsp70-Hsp40 systems to differences in key residues suggested to be involved in substrate or peptide binding. The residues identified in Hsc70 by Jiang and colleagues (2007) have previously been compared to the corresponding residues in PfHsp70-1 (Shonhai *et al.*, 2008), and here, have been compared to the corresponding residues in PfHsp70-1, PfHsp70-x and HsHsp70 (Figure 3.10). The alignment and comparison previously carried out facilitated the identification of an amino acid substitution in PfHsp70-1 (H198: positively charged), where human and bovine Hsc70s both possessed a negatively charged aspartic acid residue, suggesting a difference in the interaction of PfHsp70-1 with Hsp40 partners compared to other Hsp70-Hsp40 interactions (Shonhai *et al.*, 2008). In the alignment depicted in Figure 3.10, the substitution of H198 is shown for PfHsp70-1, and, interestingly, neither PfHsp70-x or HsHsp70 share this substitution, but, at the position corresponding to 198<sup>PfHsp70-1</sup>, PfHsp70-x and HsHsp70 have, like the Hsc70s (not shown), an aspartic acid residue. An additional substitution in PfHsp70-1 relative to the Hsc70s, also shown by Shonhai and colleagues (2008), is at position 182<sup>PfHsp70-1</sup>, where PfHsp70-1 possesses a methionine residue, and the Hsc70s (not shown), had leucine residues: a conservative substitution. Again, HsHsp70 and PfHsp70-x were found to have leucine residues at the corresponding position. PfHsp70-x was also found to differ in one of the residues identified by Jiang and colleagues (2007) to be involved in Hsp70-Hsp40 interactions: at position 220, PfHsp70-x had a lysine residue (as did DnaK), where PfHsp70-1 and HsHsp70 (like the Hsc70s: not shown) had glutamine residues. Though the substitution in PfHsp70-x is a conservative one, the substitution is of an uncharged residue to a charged one, and thus, like the H198 substitution in



PfHsp70-1, may suggest a difference in the nature of the interaction of PfHsp70-x with Hsp40s and other Hsp70s (including PfHsp70-1 and HsHsp70) and Hsp40.

In terms of residues thought to be important in binding peptide substrates (Figure 3.10, blue boxes), PfHsp70-1, PfHsp70-x and HsHsp70 do show both conservative (I401L, S427T, A435G: grey shading, Figure 3.10) and non-conservative (M404A, A429Y: black shading, Figure 3.10) differences in these key residues relative to DnaK, however, in all cases, these differences are completely conserved across the three Hsp70s of interest, and thus PfHsp70-1, PfHsp70-x and HsHsp70 show no differences between them in the residues involved in substrate binding. In the case of residues corresponding to residues 206-221 in DnaK thought to be important in interactions with Hsp40s based on the study by Achmad and colleagues (2011), there are several sequence differences when comparing the three proteins of interest to DnaK and to each other. There are four non-conservative changes in amino acid residues compared to DnaK (E206T, V210G, T215I, L219K: black shading, Figure 3.10); however, again, these changes are conserved across the three proteins of interest. Of the amino acid substitutions in this region compared to DnaK, two were not conserved across all three Hsp70s of interest. At position 207<sup>DnaK</sup>, the isoleucine residue was conserved in all four Hsp70s except for PfHsp70-x, which had leucine instead; and at position 208<sup>DnaK</sup>, HsHsp70 and DnaK shared the same residue (aspartic acid), and PfHsp70-1 and PfHsp70-x had a glutamic acid at that position. Both these changes; however, are conservative. Additional residues found to be important in DnaK interactions with DnaJ (Ahmad *et al.*, 2011), D326 and T417, were conserved across all four Hsp70s.

In terms of residues involved in substrate binding, therefore, there are no differences between PfHsp70-1, PfHsp70-x and HsHsp70. In the regions on Hsp70s involved in interactions with Hsp40s (based on DnaK-DnaJ interaction, Ahmad *et al.*, 2011); however, no two of the three Hsp70s of interest (PfHsp70-1, PfHsp70-x and HsHsp70) share an identical sequence – differences occurring in the second and third residues (207<sup>DnaK</sup> and 208<sup>DnaK</sup>) of the functionally important region 206-221<sup>DnaK</sup>.



### 3.4. DISCUSSION

---

The levels of suppression of MDH aggregation at 48 °C by PfHsp70-1 are similar to those previously observed (Shonhai *et al.*, 2008). The aggregation suppression of PfHsp70-x (not previously characterised) was found to be higher than that of PfHsp70-1 in this study. The ATPase activity of PfHsp70-x has not been previously shown or characterised. The specific activity of PfHsp70-x determined in this study ( $0.21 \pm 0.02$  mmol ATP / min / mol protein =  $15.9 \pm 1.5$  nmol ATP / min / mg protein) is very similar to that previously reported for PfHsp70-1 (14.6 nmol ATP / min / mg protein), as is the  $K_m$  for ATP ( $393.9 \pm 92.3$   $\mu$ M ATP in this study compared to 616.5  $\mu$ M) (Matambo *et al.*, 2004). When comparing the ATPase activities of PfHsp70-1 and PfHsp70-x in this study, however, PfHsp70-x was found to have a significantly higher basal ATPase activity than PfHsp70-1 (Figure 3.5 A). The basal and Hsj1a-stimulated ATPase activities of both PfHsp70-1 and HsHsp70 were higher than those observed in a recent study (Botha *et al.*, 2011). In the case of PfHsp70-1, the higher ATPase activity observed in this study compared to the study by Botha and colleagues (2011) could be due to the purification methods used: PfHsp70-1 used in ATPase assays by Botha and colleagues was purified under denaturing conditions (Botha *et al.*, 2011), in contrast to the non-denaturing methods used in this study.

The results of the MDH aggregation suppression and steady-state ATPase assays of PfHsp70-1, PfHsp70-x and HsHsp70 in the presence of test compounds overall illustrate that differential modulation of Hsp70 chaperone function is possible even in Hsp70s sharing high identity such as that ( $\geq 70$  %) shared by PfHsp70-1, PfHsp70-x and HsHsp70, and in particular by the two malarial Hsp70s, PfHsp70-1 and PfHsp70-x (75 %). Significant differences in modulation by different compounds were observed in the three Hsp70s, as well as between the basal and the Hsj1a-stimulated ATPase activities of the chaperones, and the Hsj1a and PfHsp40-stimulated ATPase activities of PfHsp70-1.

In the case of the aggregation suppression assays, PfHsp70-1 and PfHsp70-x, despite sharing 69 % identity in their substrate binding domains, were differentially modulated by compounds. Five compounds (lapachol, bromo- $\beta$ -lapachona and malonganenones A-C) were found to inhibit the aggregation suppression activity of PfHsp70-1, however in the case of two of these compounds (lapachol and malonganenone B), this effect was only observed at the highest compound concentration used (300  $\mu$ M). The aggregation suppression activity of PfHsp70-x was only inhibited by two (bromo- $\beta$ -lapachona and malonganenone A) of the five compounds found to inhibit PfHsp70-1, and in the case of

malonganenone A, a slight inhibition was only observed at the highest compound concentration (300  $\mu$ M).

Similar to the study of pyrimidinone-peptoid regulation of Hsp70 and Hsp70-Hsp40 ATPase activity (Wright *et al.*, 2004), a wide range of effects on ATPase activity was observed in this study (Table 3.2). In some cases compounds had no effect on the basal ATPase activity of Hsp70, but significantly modulated (either inhibition or stimulation) the Hsj1a-stimulated ATPase activity (lapachol with PfHsp70-1 and malonganenones A-C with PfHsp70-x). In other instances compounds significantly inhibited both the basal and the Hsj1a-stimulated activity (lapachol and bromo- $\beta$ -lapachona with PfHsp70-x), and in the case of malonganenone A and PfHsp70-1, compound stimulated the basal activity but had no effect on the Hsj1a-stimulated activity (malonganenone A with PfHsp70-1). Bromo- $\beta$ -lapachona, surprisingly, inhibited the basal activity of HsHsp70, but enhanced the Hsj1a-stimulated HsHsp70 ATPase activity. The most pronounced effects on basal ATPase activity was the inhibition of PfHsp70-x by lapachol and bromo- $\beta$ -lapachona, and thus these effects were further investigated by conducting dose-response experiments, showing that the inhibition of PfHsp70-x by lapachol and bromo- $\beta$ -lapachona is concentration-dependent.

In the case of inhibition of the Hsj1a-stimulated ATPase activity of PfHsp70-x by malonganenone A, which had no effect on the basal ATPase activity of the protein, the compound was found to have a more pronounced inhibitory effect on activity when added before the Hsj1a, suggesting perhaps that the malonganenone A, when pre-incubated with PfHsp70-x binds more stably to the Hsp70 than Hsj1a does. Hsp70-Hsp40 interactions are generally considered to be dynamic or transient, and therefore it is possible that these data show a more stable complex between PfHsp70-x and malonganenone A, which can be overcome by Hsj1a to a lesser extent than the dynamic PfHsp70-x-Hsj1a complex can be overcome by malonganenone A. The experiment in which Hsj1a and malonganenone A were titrated against each other showed that the effects of malonganenone A on the Hsj1a-stimulated ATPase activity of PfHsp70-x can to some extent be overcome by increasing Hsj1a concentrations, and similarly, the stimulatory effects of Hsj1a on the ATPase activity of PfHsp70-x can to some extent be overcome by increasing concentrations of malonganenone A. Higher concentrations of Hsj1a would have to be included in the experiment to assess whether Hsj1a can completely outcompete the malonganenone A. In the case of PfHsp70-x, malonganenone A and to a lesser extent malonganenones B and C, which had no effect on basal ATPase activity, but inhibited the Hsj1a-stimulated activity of the chaperone, may be

physically disrupting the interaction between PfHsp70-x and Hsj1a; an effect which, presumably due to the transient nature of Hsp70-Hsp40 interactions, could not be overcome by pre-incubation of PfHsp70-x with Hsj1a. The Hsj1a-stimulated ATPase activities of both PfHsp70-1 and HsHsp70 were unaffected by malonganenones A-C. This could potentially be attributed to differences in the interaction of these three proteins with Hsp40s. In the region of the ATPase domain of PfHsp70-x involved in interaction with Hsp40s (based on structural studies of DnaK-DnaJ interaction, Ahmad *et al.*, 2011), PfHsp70-x has a leucine residue at position 207<sup>DnaK</sup> (Figure 3.10) where PfHsp70-1 and HsHsp70 have an isoleucine residue. Though this difference is a conservative one (both isoleucine and leucine are non-polar residues), and neither residue is likely to be involved in direct interactions with the positively charged residues on helix II of Hsp40s, a leucine residue would contribute slightly less bulk to the binding region than isoleucine would, and thus may mean that the interaction of PfHsp70-x with Hsj1a is slightly different to that of HsHsp70 or PfHsp70-1 with Hsj1a, and could account for the effect of the malonganenones on PfHsp70-x compared to the other two Hsp70s.

Findings in MDH aggregation suppression assays for PfHsp70-x correlate with those observed in ATPase assays, as illustrated by two compounds with profound effects on PfHsp70-x chaperone activity: bromo- $\beta$ -lapachona and malonganenone A. Bromo- $\beta$ -lapachona had a significant effect on the basal and Hsj1a-stimulated ATPase activity of PfHsp70-x, and also, not surprisingly, on the aggregation suppression activity of the protein. Based on its structure (Table 3.1), bromo- $\beta$ -lapachona is potentially acting as an ATP mimic, binding in the ATP binding site of the ATPase domain of PfHsp70-x, resulting in decreased ATPase activity as well as an allosteric effect on the substrate-binding domain causing decreased substrate recognition or binding. This proposed mechanism could be tested by assessing the ATPase activity at various ATP concentrations, both in the presence and absence of compound. An increase in the  $K_m$  (decreased affinity) for ATP in the presence of the inhibiting compound would suggest that the compound is indeed competing with ATP by binding in the ATPase domain. Malonganenone A, on the other hand, is probably not binding in the ATP binding site, as it has no effect on the basal ATPase activity of PfHsp70-x, but rather binds at the region in the ATPase domain facilitating Hsp40 interactions. At lower concentrations malonganenone A therefore does not affect aggregation suppression activity. The effect of malonganenone A on aggregation suppression activity of PfHsp70-x (at 300  $\mu$ M) as well as the effects of malonganenones A-C on the aggregation suppression activity of PfHsp70-1 could be explained by likening the malonganenone compounds to peptide substrates. Peptide substrate motifs recognised by Hsp70s have been described as having a central hydrophobic region of four to five

residues (most often leucine residues), flanked by basic residues (Rüdiger *et al.*, 1997). It is therefore conceivable that the malonganenone compounds, with their highly hydrophobic hydrocarbon chains, are, not necessarily being recognised as substrate peptides, but are binding in the hydrophobic pocket of the substrate binding domains, preventing MDH from binding and thus inhibiting the ability of PfHsp70-x and PfHsp70-1 to prevent the aggregation of MDH.

A very interesting effect by compounds was observed in the comparison between PfHsp40-stimulated and Hsj1a-stimulated ATPase activity of PfHsp70-1. Lapachol, which significantly stimulated the Hsj1a-stimulated ATPase activity of PfHsp70-1, seemed to inhibit the PfHsp40-stimulated ATPase activity of PfHsp70-1, though this effect was not statistically significant. Similarly, bromo- $\beta$ -lapachona significantly stimulated the Hsj1a-stimulated activity, but significantly inhibited the PfHsp40-stimulated activity of PfHsp70-1. Malonganenone A, which, though stimulating the basal ATPase activity of PfHsp70-1, had no effect on the Hsj1a-stimulated activity, but significantly inhibited the PfHsp40-stimulated activity. These contrasting effects of compounds on PfHsp70-1 stimulated by two different Hsp40s is very intriguing, though not unknown: a similar effect was found in the study by Fewell and colleagues (2004), where two DSG analogues, MAL3-39 and MAL3-101, were found to inhibit the ATPase activity of Hsp70 stimulated by TAG, but had no effect on the ATPase activity stimulated by Ydj1. These findings suggest that the nature of the PfHsp70-1-PfHsp40 and PfHsp70-1-Hsj1a interactions is different, which, considering that Hsj1a and PfHsp40 represent Hsp40s of two different types (type II and type I respectively), and are of very different origins (human and *P. falciparum*), is highly probable.

Overall, in the work in this chapter, two compounds stand out: bromo- $\beta$ -lapachona and malonganenone A. Bromo- $\beta$ -lapachona seemed to be the most active compound of all, inhibiting the aggregation suppression activities of PfHsp70-1 and PfHsp70-x, and modulating the ATPase activities of all Hsp70 and Hsp70-Hsp40 systems apart from the basal activity of PfHsp70-1. Malonganenone A, on the other hand, exhibited the most desired effects in terms of the aims of this chapter - namely to identify Hsp70 modulators specific to PfHsp70-1 and/or PfHsp70-x and not to HsHsp70. Malonganenone A fulfilled these criteria, by inhibiting the aggregation suppression of PfHsp70-1 and PfHsp70-x, and modulating the ATPase activities of PfHsp70-1 (basal and PfHsp40-stimulated activities) and PfHsp70-x (Hsj1a-stimulated), and not HsHsp70. Malonganenone A therefore represents a relatively specific modulator of the chaperone activities of key malarial Hsp70s.

An important note in interpreting the data in this study is that the recombinant HsHsp70 used in this work lacks the EEVD motif (Section 2.2.1), as the HsHsp70 expression plasmid available for this study was designed as such by the project collaborators. The EEVD motif has been implicated in several facets of Hsp70 function, including substrate recognition, ATPase activity and interaction with co-chaperones. In addition to functional roles, the EEVD is also thought to play a role in maintaining the correct conformation of Hsp70 (Freeman *et al.*, 1995), and thus the recombinant HsHsp70 used may not be a biologically relevant form of the protein, a possibility that must be considered when interpreting the data at hand.

The experiments carried out in this study resulted in interesting and varied data, showing in some cases modulatory effects of compounds very specific to selected systems, however, without further investigation, the exact mechanisms of the Hsp70 modulation by these compounds cannot be determined, but only speculated on. This could potentially be achieved by the use of biophysical binding studies to investigate the interactions of compounds with Hsp70s (Chapter 4). Binding studies could also be complemented by *in silico* docking of compounds to homology models of the Hsp70s of interest, which would give an idea of the nature or mechanisms of the interactions between Hsp70s and compounds. A limitation of this study was the small number of test compounds included. Because the methods employed to assess potential Hsp70 modulation by compounds were not conducive to high throughput screening, it was not feasible to include more compounds. A larger set of structurally related test compounds would have allowed for an in-depth assessment of structure-activity relationships.

An important consideration in the context of the ATPase activity modulation by small molecules is that this study included only steady-state ATPase assays, and not single-turnover assays. Because the two assays assess different aspects of the ATPase cycle of Hsp70s, different effects of compounds may be observed in the two methods, as found by Botha *et al.*, (2011). Further assessment of the effects of these compounds on Hsp70 chaperone function should thus include single-turnover ATPase assays, as well as perhaps luciferase refolding assays, which, as described by Nicoll and colleagues (2007), is, besides ATPase assays, an effective means of assessing the *in vitro* chaperone activity of Hsp70s (Nicoll *et al.*, 2007).

**CHAPTER 4:**

---

**Hsp70-Hsp40 and Hsp70-small molecule *in vitro*  
binding studies**

---



## 4.1. INTRODUCTION

---

Biophysical binding assays can be carried out using a number of technologies including isothermal titration calorimetry (ITC), nuclear magnetic resonance (NMR) spectroscopy and surface plasmon resonance (SPR) spectroscopy. These techniques are a means of providing insight into the interactions between molecules (Huber and Mueller, 2006). Since the release of the first commercially available SPR instrument in 1990 (Jönsson *et al.*, 1991), the technology has continued to gain popularity as an effective tool for the analysis of biomolecular interactions. Compared to other methods used to characterise interactions between molecules, SPR has distinct advantages. When compared to ITC, for example, SPR requires less ligand for immobilisation, less analyte for injections, is less time consuming both in terms of experiments and data analysis, and has a greater sensitivity (Jecklin *et al.*, 2009). SPR has successfully been used to investigate a wide range of interactions, including protein-protein, protein-peptide, protein-DNA, antibody-antigen and protein-drug or protein-small molecule interactions (Karlsson and Fält, 1997; Rich and Myszka, 2004; Willander and Al-Hilli, 2009).

SPR is a spectroscopic biosensor method in which one binding partner (the ligand) is immobilised onto a sensor surface, and the second binding partner (the analyte) is passed over the immobilised ligand in a microfluidic flow cell (O'Shannessy *et al.*, 1993; Szabo *et al.*, 1995). Sensor chips used in SPR consist of a glass prism, upon which a thin film of gold is deposited. The metal surface is coated with an organic polymer layer (commonly carboxymethyl dextran), onto which protein ligands can be immobilised (Szabo *et al.*, 1995). SPR spectroscopy is based on changes in refractive index due to binding events. *p*-Polarised light is directed through the glass prism, and is reflected off the gold surface. Changes in the refractive index of the ligand layer in contact with the gold surface due to binding events and thus an accumulation of material (analyte) at the surface result in changes in the reflected light in the glass prism. These changes are detected as changes in arbitrary response or resonance units (RU) (De Crescenzo *et al.*, 2008). The association and dissociation of analytes onto and off ligands in SPR is monitored in real-time on a sensorgram – a progress curve of response vs. time, where the observed response is proportional to the amount of analyte (mass) bound per surface area of immobilised ligand on the sensor surface. An example of a sensorgram is shown in Figure 4.1.

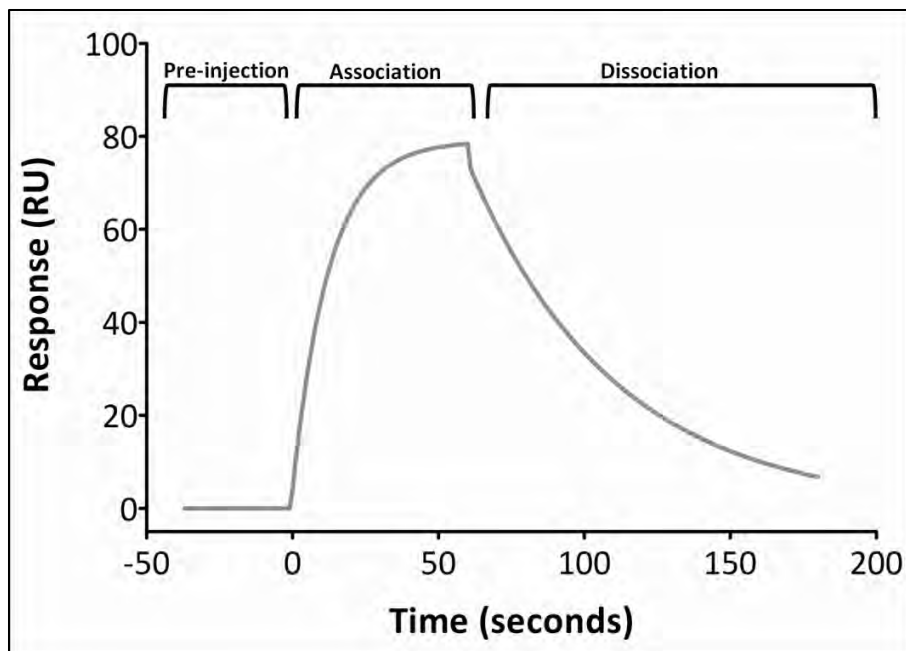


**Figure 4.1: Example of an SPR sensorgram.** Pre-injection, association and dissociation phases of a simulated SPR curve are shown (Rich and Myszka, 2004). The SPR curve was simulated using BIAevaluation software (v. 4.1.1, GE Healthcare, U.K.) and graphed using GraphPad Prism® software (v. 4.03; San Diego, CA, U.S.A.)

To allow an observed interaction between two molecules to be quantified in terms of kinetic rates of association and dissociation, one of a number of known binding models can be fit to SPR data generated (Szabo *et al.*, 1995; Myszka and Rich, 2000; Myszka, 2000). The Langmuir model of binding, which assumes a 1:1 interaction between the immobilised ligand and injected analyte, is described by equation 4.1, where  $k_a$  and  $k_d$  describe association and dissociation rate constants respectively.



From the  $k_a$  and  $k_d$  observed for an interaction, the affinity constant ( $K_D$ ) for an interaction can be determined (equation 4.2) (O'Shannessy *et al.*, 1993; Myszka, 1997; De Crescenzo *et al.*, 2008).

$$K_D = \frac{k_d \text{ (s}^{-1}\text{)}}{k_a \text{ (M}^{-1}\text{s}^{-1}\text{)}} \quad (\text{Equation 4.2})$$

As an alternative to assessing the association and dissociation rates of an interaction, experiments can be carried out such that the association phase of the interaction is long enough to allow a steady-state plateau to be reached in the interaction, observed as no change in signal with time. The response at steady-state or at equilibrium ( $R_{eq}$ ) can be plotted against analyte concentrations for the determination of  $K_D$  (Nguyen *et al.*, 2007).

The technology of SPR is constantly improving, specifically in terms of the sensitivity of instruments, increased sample handling capacities and throughput, as well as improved data processing and analysing capacity. These developments have led to an increased use of SPR in protein-small molecule interaction analyses (Myszka, 2004), including many drug discovery applications (Myszka and Rich, 2000; Huber and Mueller, 2006). These applications of SPR also include investigations into different chaperones and their interactions with each other, with substrates and with modulators of their activity (Szabo *et al.*, 1995).

The interactions between Hsp70, Hsp90 and Hop and in particular the molecular basis of these interactions have been extensively investigated using SPR, commonly in combination with mutational studies. Among other techniques, SPR was used to identify the contact residues of the TPR1 domain of mSTI (murine Hop) that facilitate interactions with Hsc70, and which determine specificity for either Hsc70 or Hsp90 (Odunuga *et al.*, 2004). The interaction between Hsp90 and Hop was further investigated in a later study using mutational studies and SPR, showing the interaction to be facilitated by residues on the nuclear localisation signal of the Hsp90-binding domain of Hop (Daniel *et al.*, 2008). The mechanisms of Hsp70-Hsp40 interactions have also been determined to a great extent using SPR. A study by Mayer and colleagues in 1999 made use of SPR to identify residues in Hsp40 (DnaK) functionally important in its interactions with Hsp70 (DnaK). DnaJ (immobilised) was shown to specifically interact with DnaK passed over the sensor chip, and this interaction was not observed when a mutant DnaJ (mutated in the functionally important HPD motif) was used (Mayer *et al.*, 1999).

Mutational studies and SPR were also used to identify residue R26 on helix II of the J-domain of the murine Hsp40 ERj1 as an essential contact residue in the interaction between ERj1 and the ER Hsp70, BiP, supporting the idea that not only the HPD motif, but also helix II of Hsp40s are essential for Hsp70-Hsp40 interactions (Nicoll *et al.*, 2007). More recently, the mechanism by which the Hsp70-Hsp40 chaperone machinery binds to peptide substrates has been investigated by the use of SPR, revealing that multiple Hsc70 molecules and a single dimer of a type I Hsp40 recognise and bind to an unfolded

protein substrate independently of each other, facilitating the refolding of the substrate (Terada and Oike, 2010).

Hsp70 has also been studied in terms of small-molecule modulators using SPR. Gentamicin, an aminoglycoside antibiotic used to treat Gram-negative bacteria, has been shown to modulate the chaperone activity of Hsp70. Subsequently, the effect of gentamicin on the interactions between Hsp70 and substrate peptide and Hsp70 and Hsp40 was assessed using SPR. Hsp40 and substrate peptides were immobilised onto separate sensor chips, over which Hsp70 was passed in the presence and absence of gentamicin, and the compound was found to disrupt the Hsp70-peptide interaction, but not the Hsp70-Hsp40 interaction (Yamamoto *et al.*, 2010). A series of adenosine-derived inhibitors of Hsp70 have also been assessed in terms of their affinities for Hsp70 using SPR, leading to the identification of Hsp70-small molecule affinities of as high as 0.3  $\mu\text{M}$  (Williamson *et al.*, 2009). Similarly, novel small-molecule inhibitors of Hsp90 with high affinities for Hsp90 (high nanomolar range) have been identified (Zhou *et al.*, 2004).

Chaperones are known to play a role in protein misfolding and subsequent amyloid formation, and thus, as recently reviewed, interactions between amyloids and chaperones are commonly studied using various biophysical techniques including SPR (Zhang *et al.*, 2011). The yeast Hsp40 Ydj1, for example, has been shown to interact with Ure2, a yeast prion protein using SPR (Zhang *et al.*, 2011).

This large volume of publications describing the use of SPR in chaperone-co-chaperone and chaperone-small molecule interactions highlights the applicability of this technique in the current study.

The work described in the previous chapter (Chapter 3) shows that a number of compounds (lapachol, bromo- $\beta$ -lapachona, malonganenones A, B and C) belonging to the 1,4 naphthoquinone and prenylated alkaloid compound classes modulate malarial (PfHsp70-1, PfHsp70-x) and human (HsHsp70) Hsp70s to varying degrees and with varying specificities *in vitro*, both in terms of their basal and co-chaperone-stimulated chaperone activities. The aims of the work described in this chapter, toward completion of Objective 3 (Section 1.4), lead on from the findings in Chapter 3, as a further investigation into these compounds as Hsp70 modulators, by biophysical binding studies. The first aim was to assess the potential interactions between the five above-mentioned compounds of interest with PfHsp70-1, PfHsp70-x and HsHsp70; and secondly, to establish interactions between Hsp70s (PfHsp70-1, PfHsp70-x

and HsHsp70) and the human Hsp40, Hsj1a, and assess the effect of malonganenone A on such interactions, based on findings in Chapter 3 suggestive of disruption of Hsp70-Hsp40 interactions by malonganenone A. Surface Plasmon resonance spectroscopy was used toward the completion of these aims.

## **4.2. MATERIALS AND METHODS**

---

### **4.2.1. Materials**

---

CM5 (carboxymethylated dextran) sensor chips were purchased from GE Healthcare (U.K.). N-hydroxysuccinimide (NHS), 1-ethyl-3-(3-dimethylaminopropyl) carbodiimide hydrochloride (EDC) and ethanolamine-HCl were purchased from GE Healthcare (U.K.) as well as from Bio-Rad laboratories Inc. (U.S.A.). Hepes, glycine, sodium hydroxide (NaOH), sodium chloride (NaCl), sodium acetate, dimethyl sulfoxide (DMSO) and sodium dodecyl sulphate (SDS) were from Sigma-Aldrich (U.S.A.), and hydrochloric acid (HCl) and phosphoric acid were from Saarchem, Merck (Germany). Membrane filters (0.45  $\mu\text{m}$ ) were purchased from Sartorius Stedim Biotech (Germany). Bovine serum albumin (BSA, Fraction V) and adenosine-5'-triphosphate (ATP) were purchased from Roche (Switzerland). The GLH sensor chip was purchased from Bio-Rad Laboratories Inc. (U.S.A.). Recombinant proteins purified as described in Chapter 2, and compounds described in Chapter 3 (Section 3.2.1) were used.

### **4.2.2. Surface Plasmon resonance spectroscopy: *BIAcore*<sup>®</sup>X system**

---

A *BIAcore*<sup>®</sup>X SPR instrument (GE Healthcare, Sweden) was used to assess the potential interactions between Hsp70s and compounds.

#### 4.2.2.1. Protein preparation

---

Recombinant PfHsp70-1(opt) and PfHsp70-x, the production and purification of which are detailed in Chapter 2, were subjected to buffer exchange into Hepes running buffer (10 mM Hepes-NaOH, pH 7.4, 150 mM NaCl, filter sterilised through 0.45 µm membrane filters and de-gassed at ~ 25 °C, for 60 minutes) using Amicon® Ultra Centrifugal Filters (Appendix A, Section 7.1.6.2). Following buffer exchange, the integrity of proteins to be immobilised on the sensor chip was assessed using SDS-PAGE analysis, by which proteins were estimated to be > 90 % pure (examples shown in Chapter 2: PfHsp70-1 – Figure 2.2; HsHsp70 – Figure 2.4).

#### 4.2.2.2. Docking, priming and preconditioning of sensor chips

---

Subsequent to docking of a CM5 sensor chip into the Biacore®X instrument, the chip was primed with seven injections (3 minutes each) of Hepes running buffer. In preparation for the immobilisation of Hsp70s onto sensor chip surfaces, docked and primed sensor chips were subjected to a series of preconditioning steps: two injections each of NaOH (100 mM), HCl (10 mM), SDS (0.1 %) and phosphoric acid (0.085 %) at a flow rate of 100 µl/min.

#### 4.2.2.3. Protein pre-concentration

---

Immobilisation of a protein onto a CM5 chip via amine coupling requires the protein to be in a protonated state to allow for an accumulation of the protein on the negatively charged dextran matrix. Generally, therefore, proteins are immobilised in buffers with pH values of one unit below the protein pI, which for PfHsp70-1 (pI = 5.5) and PfHsp70-x (pI = 5.0) was pH 4.5 and pH 4.0. These pH values were used as a starting point to further optimise the immobilisation conditions for each protein. Sodium acetate buffers (10 mM) were used for protein immobilisation, and were also used in a set of pre-concentration steps. Three different preparations of the Hsp70s, (20 µg/ml in 10 mM sodium acetate, pH 4.0, pH 4.5 and pH 5.0), were injected over the sensor chip surface consecutively (each followed by a wash step of a Hepes running buffer injection) at a flow rate of 10 µl/min. Based on the relative gradients of observed responses (Appendix B: Section 7.2.2) upon protein injections at different pHs, pH 4.5 was chosen as the most suitable immobilisation buffer for both PfHsp70-1 and PfHsp70-x.

#### 4.2.2.4. Protein immobilisation

---

Directly prior to immobilisation by amine coupling, frozen aliquots of EDC (0.4 M in deionised water) and NHS (0.1 M in deionised water) were thawed and mixed in a ratio (volumes) of 1:1. The EDC/NHS mixture was injected over the sensor chip surface at a flow rate of 5  $\mu\text{l}/\text{min}$  to activate the chip surface, followed by a wash step with HEPES running buffer. Hsp70 (5  $\mu\text{g}/\text{ml}$  in pH 4.5 acetate buffer) was injected at 5  $\mu\text{l}/\text{min}$ , followed by a wash step with running buffer. Any free amine sites were deactivated by an injection of ethanolamine-HCl (1.0 M, pH 8.5). The second reference flow cells of the CM5 chips were subjected to the same immobilisation procedures described above; however, the protein injection step was omitted. This reference flow cell allowed for the correction of data for any non-specific binding effects. The PfHsp70-x sensor chip used was prepared by Dr. Eva-Rachele Pesce.

#### 4.2.2.5. Assessment of Hsp70-compound interactions

---

For the assessment of potential Hsp70-compound interactions between malarial Hsp70s (PfHsp70-1 and PfHsp70-x) and compounds of interest (lapachol, bromo- $\beta$ -lapachona, malonganenones A, B and C), and to allow for the quantification of any such interactions, each compound was passed over the immobilised Hsp70s at a range of concentrations (1, 6.25, 12.5, 25, 50 and 100  $\mu\text{M}$ ). A range of buffer blanks containing DMSO at concentrations corresponding to the compound injections (0.003, 0.021, 0.042, 0.083, 0.166 and 0.333 %) were included so that the bulk effect of DMSO on the chips could be accounted for in the analysis of data. Compounds and DMSO were injected over the chips at a flow rate of 5  $\mu\text{l}/\text{min}$  allowing for a 60 second contact time and 250 second dissociation time. The low flow rate was selected to allow for any interactions between Hsp70s and small molecules to reach equilibrium, thus allowing interactions to be observed under steady-state conditions. After each compound injection, a regeneration step (injection of 10 mM Glycine-HCl, pH 1.5 for 60 seconds at 5  $\mu\text{l}/\text{min}$ ) was carried out to ensure no compound remained bound to the chip surface. Resulting SPR sensorgrams were analysed using BIAevaluation software (v. 4.1.1, GE Healthcare, U.K.), and visualised using Microsoft® Office Excel 2007. For each compound concentration, the sensorgram was double referenced against both the corresponding DMSO control sensorgram as well as the reference flow cell. Corrected sensorgrams were then assessed using the Langmuir model of 1:1 binding, with simultaneous determination of association and dissociation rate constants,  $k_a$  and  $k_d$ . Fitting of the Langmuir model to the data generated a calculated  $R_{\text{eq}}$  value (Equation 4.3) and, using GraphPad Prism® (v. 4.03; San Diego, CA, U.S.A.) software,

steady-state analyses were carried out by plotting saturation curves of the resulting  $R_{eq}$  values vs. compound concentration. To determine the interaction affinity ( $K_D$ ), non-linear regression curves described by equation 4.3 (a steady-state affinity model), where  $K_A$  is the equilibrium association constant,  $C$  is the analyte concentration,  $R_{max}$  is the theoretical maximum binding capacity of the immobilised protein and  $n$  is the steric interference factor (BIAevaluation v. 4.1.1, GE Healthcare, U.K.), were fitted to the data.

$$R_{eq} = \frac{K_A \cdot C \cdot R_{max}}{1 + K_A \cdot C \cdot n} \quad \text{(Equation 4.3)}$$

#### **4.2.3. Surface Plasmon resonance spectroscopy: ProteOn™ XPR36 system**

---

A ProteOn™ XPR36 Protein interaction array SPR system (Bio-Rad Laboratories Inc., U.S.A.) was used in the assessment of both Hsp70-compound and Hsp70-Hsp40 interactions. The ProteOn™ XPR36 system makes use of sensor chips comprising six parallel channels for immobilisation of ligands, and the instrument contains six channels for injection of analytes. Analytes are injected over the six ligand channels in a direction perpendicular to the ligand channels, thus allowing for 36 possible interactions to be monitored simultaneously (Bio-Rad Laboratories, Inc., Bulletin 5390C). This concept is illustrated in Figure 4.2.

In this study, a GLH sensor chip was used, which, unlike the CM5 chip used with the BIAcore®X instrument, consisting of a carboxymethyl dextran surface, consists of a modified alginate polymer layer bound to the surface of the sensor prism, also designed for amine coupling of ligands to the surface. Immobilisation of proteins onto the GLH chip surface can result in very high levels of immobilisation of ligands, and is thus amenable to both protein-small molecule and protein-protein work (Bio-Rad Laboratories Inc., product information: <http://www.bio-rad.com/prd/en/US/LSR/SKU/176-5013/ProteOn-GLH-Sensor-Chip>; Bio-Rad Laboratories Inc., Bulletin 5390C).



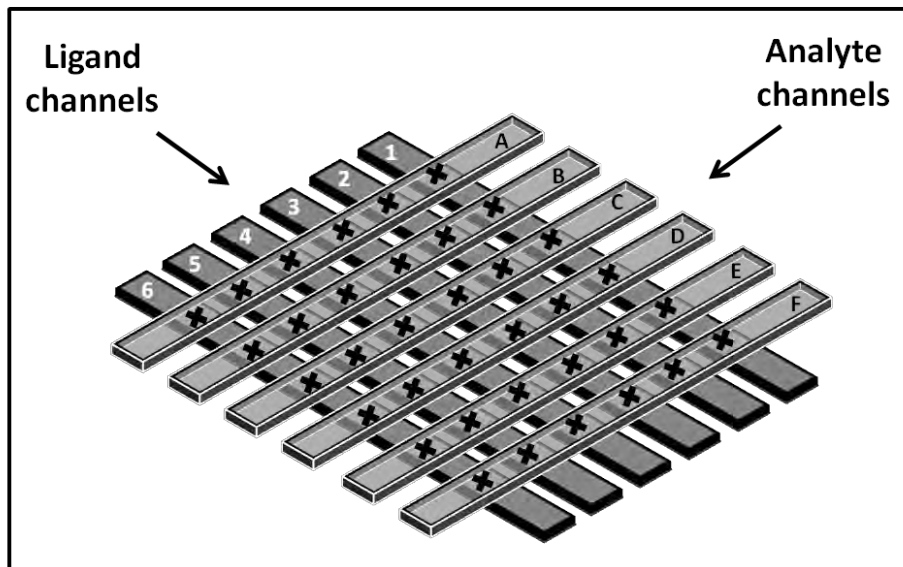


**Figure 4.2: Schematic representation of the configuration of ProteOn™ XPR36 sensor chips.** Analyte channels (clear, A-F) pass perpendicularly over immobilised ligand channels (grey, 1-6), creating 36 points of interaction, represented as black crosses (adapted from Bio-Rad Laboratories Inc., Bulletins 5412, 5413B and 5390C).

#### 4.2.3.1. Protein preparation

---

Recombinant PfHsp70-1(opt), PfHsp70-x and HsHsp70 were prepared for immobilisation onto GLH sensor chips as described for PfHsp70-1 and PfHsp70-x in Section 4.2.2.1.

#### 4.2.3.2. Docking, preconditioning and stabilisation of sensor chip

---

Subsequent to docking of the GLH chip in the ProteOn™ XPR36 instrument, the chip was initialised – an automated process driven by the ProteOn™ Manager software (Bio-Rad laboratories Inc., U.S.A.) which prepares the sensor surface as well as the detection and fluidic systems for an experiment. Prior to immobilisation of proteins by amine coupling, the six ligand channels of the GLH chip were conditioned with 30 µl injections of NaOH (50 mM), SDS (0.5 %) and phosphoric acid (0.85 %) at 100 µl/min (18 seconds contact time). The ligand channel surfaces were then stabilised by injection of HEPES running buffer (100 µl, 100 µl/min, 60 seconds contact time).

#### 4.2.3.3. Protein immobilisation

---

Chip surfaces were activated by 150  $\mu\text{l}$  injections of a NHS (10 mM) / EDC (40 mM) mixture (1:1 volumetric ratio) prepared immediately prior to injection, at a flow rate of 30  $\mu\text{l}/\text{min}$  (300 seconds contact time). Proteins, diluted (to concentrations indicated below) in sodium acetate buffers (10 mM) of pHs of approximately one unit below the pI of each protein (PfHsp70-1 and HsHsp70: pH 4.5, PfHsp70-x: pH 4.0) were then injected over the activated chip, after which the chip was deactivated with an injection of ethanolamine-HCl (1 M). Protein and ethanolamine-HCl injections were carried out at a flow rate of 30  $\mu\text{l}/\text{min}$ , injecting 30  $\mu\text{l}$  to allow for a contact time of 300 seconds. Any unbound protein was removed by a regeneration step: injection of 30  $\mu\text{l}$  glycine-HCl (10 mM, pH 1.5) at 100  $\mu\text{l}/\text{min}$  (18 seconds contact time), after which an additional stabilisation step (injection of Hepes running buffer as above) was carried out.

#### 4.2.3.4. Assessment of Hsp70-compound interactions

---

As with the BIAcore<sup>®</sup>X system, compounds were passed over recombinant Hsp70s immobilised to the GLH sensor chip to assess the potential interactions between Hsp70s and compounds. As before, the experiments were carried out at 25 °C using a Hepes running buffer, a range of compound concentrations, and a set of DMSO control injections at dilutions corresponding to the compound concentrations used. After each compound or DMSO injection, a regeneration step was carried out by injecting 30  $\mu\text{l}$  glycine-HCl (10 mM, pH 1.5) over the chip for 18 seconds (100  $\mu\text{l}/\text{min}$ ). As described in Section 4.2.2.5, a low flow rate of 5  $\mu\text{l}/\text{min}$  was used in BIAcore<sup>®</sup>X experiments to allow for the assessment of interactions under steady-state conditions. On the ProteOn<sup>™</sup> XPR36 system, the minimum flow rate is 25  $\mu\text{l}/\text{min}$ , and thus Hsp70-small molecule interactions could not be assessed in the same way as they were using the BIAcore<sup>®</sup>X system. For compound injections on the ProteOn<sup>™</sup> XPR36 system, therefore, different sets and combinations of parameters (flow rates, concentration ranges, contact times, dissociation times) were used in an attempt to optimise the conditions that would allow for the generation of data that could be fitted to the Langmuir model of binding for quantification. In the case of lapachol and bromo- $\beta$ -lapachona, the conditions resulting in the best data were 100  $\mu\text{l}$  injections at a flow rate of 100  $\mu\text{l}/\text{min}$ , contact and dissociation times of 60 seconds and 250 seconds respectively, and a concentration range of 12.5, 25, 50, 100 and 200  $\mu\text{M}$ . For malonganenones A, B and

C, a flow rate of 50  $\mu\text{l}/\text{min}$ , contact and dissociation times as above and concentrations of 25, 50, 100, 125 and 150  $\mu\text{M}$  yielded the best data. These higher flow rates of 50 and 100  $\mu\text{l}/\text{min}$  were selected as a means of eliminating or minimising the effect of mass transfer (also termed mass transport). Mass transfer is an effect observed when the rate of analyte binding to the immobilised ligand exceeds the rate at which analyte can diffuse to the surface. The resulting effect can significantly alter the apparent kinetics of an interaction. Mass transport can be controlled experimentally by either avoiding very high ligand immobilisation densities, as well as by using higher flow rates to ensure that the rate of transport of analyte to the sensor chip surface is not exceeded by the binding rate (Rich and Myszka, 2000).

All data generated for small-molecule interactions with Hsp70s were corrected by double referencing using the blank ligand channel as well as a corresponding set of DMSO control injections. Data was exported from the ProteOn™ Manager software (Bio-Rad laboratories Inc., U.S.A.) into the BIAevaluation (GE Healthcare, U.K.) software for analysis by the Langmuir model of binding. Unlike the data generated with the BIAcore®X instrument, for which steady-state analyses were carried out for the quantification of interactions, the ProteOn™ XPR36 results were quantified ( $K_D$ ) based purely on the model (Langmuir) fit to the data.

#### 4.2.3.5. Assessment of the effect of malonganenone A on Hsp70-Hsp40 interactions

---

Using the ProteOn™ XPR36 system and the GLH chip described in Section 4.2.3.1, the potential interaction of Hsj1a with each of PfHsp70-1, PfHsp70-x and HsHsp70 was assessed. As for the small molecule assessments, Hepes running buffer was used, and the temperature was maintained at 25 °C. A flow rate of 100  $\mu\text{l}/\text{min}$  was applied to avoid the effect of mass transfer (described in Section 4.2.3.4), and contact and dissociation times of 90 seconds and 600 seconds respectively were allowed. In previously described SPR experiments involving Hsp70-Hsp40 interactions, Hsp40 was immobilised and Hsp70 was injected over the sensor surface. The concentration of Hsj1a to inject over the immobilised Hsp70s was thus based on DnaJ concentrations used in literature (Yamamoto *et al.*, 2010: 0.03 – 4  $\mu\text{M}$ ; Gässler *et al.*, 1998 and Mayer *et al.*, 1999: 1.25  $\mu\text{M}$ ). Hsj1a was injected over immobilised Hsp70s at 1.6  $\mu\text{M}$ , and due to the importance of ATP in assessing Hsp70-Hsp40 interactions as described in Section 4.1, Hsj1a injections were carried out both in the presence and absence of ATP (1 mM). BSA, also at 1.6  $\mu\text{M}$  was also passed over the chip as a control for potential non-specific binding to Hsp70s.

In *in vitro* studies described in chapter 3, malonganenone A was found to significantly inhibit the Hsj1a-stimulated and not the basal ATPase activity PfHsp70-x, suggesting that the compound was disrupting the interaction between PfHsp70-x and Hsj1a. To further investigate this observation, the effect of malonganenone A on Hsp70-Hsp40 interactions was assessed using SPR, by injection of Hsj1a over Hsp70s in the presence of ATP, and in the presence and absence of malonganenone A (50  $\mu$ M). In this experiment, Hsj1a was pre-incubated with ATP (1 mM) and either malonganenone A (50  $\mu$ M) or DMSO (0.166 %) before injection over the sensor chip surface. Following each injection of protein, a regeneration step was carried out, in which glycine-HCl (10 mM, pH 1.5) was injected over the chip at a flow rate of 100  $\mu$ l/min for 18 seconds. All experiments were carried out in triplicate and data representing the average of triplicate results was generated. Sensorgrams were corrected by double referencing against both the reference channel of the sensor chip and a blank buffer injection, containing, where appropriate, ATP and/or malonganenone A. Sensorgrams were processed using the ProteOn Manager<sup>TM</sup> Software (v. 3.1.0.6, Bio-Rad Laboratories Inc, U.S.A.) and visualised using Microsoft<sup>®</sup> Office Excel.

## **4.3. RESULTS**

---

### **4.3.1. Protein Immobilisation**

---

Recombinant proteins were successfully immobilised onto both CM5 sensor chips for BIAcore<sup>®</sup>X experiments, and onto a GLH sensor chip for ProteOn<sup>TM</sup> XPR36 experiments. The resulting levels of immobilisation of each protein are shown in Table 7.3 (Appendix B, Section 7.2.3). The sensorgrams of the pre-concentration (BIAcore<sup>®</sup>X) and immobilisation (BIAcore<sup>®</sup>X and ProteOn<sup>TM</sup> XPR36) procedures are shown in Appendix B (Section 7.2.2). On the GLH chip, HsHsp70 was immobilised at two different concentrations. As expected, the higher concentration (25  $\mu$ g/ml) resulted in a higher level of immobilisation than the lower concentration (10  $\mu$ g/ml), and since this higher level of immobilisation (~ 6400 RU) was more comparable to those achieved for PfHsp70-1 and PfHsp70-x (~ 12 000 RU and ~ 11 000 RU respectively), this channel was considered the active HsHsp70 channel, and all data shown for HsHsp70 refers to this channel. The resulting levels of immobilisation on the CM5 and GLH chips are shown in Appendix B (Section 7.2.3; Table 7.2).

The level of immobilisation of a ligand onto a sensor chip surface determines the  $R_{\max}$  values for interactions assessed on that surface- the  $R_{\max}$  value being the theoretical maximal response for an analyte injected over immobilised ligand (De Crescenzo *et al.*, 2008).  $R_{\max}$  is dependent on the level of immobilisation of ligand ( $R_{\text{lig}}$ ), the molecular weight of both ligand and analyte ( $MR_{\text{lig}}$  and  $MR_{\text{ana}}$  respectively), as well as the valency of the ligand ( $V_{\text{lig}}$ ), as described by Equation 4.4 below.

$$R_{\max} = \frac{R_{\text{lig}} \cdot MR_{\text{ana}} \cdot V_{\text{lig}}}{MR_{\text{lig}}} \quad (\text{Equation 4.4})$$

### 4.3.2. Interactions of compounds with Hsp70s

---

#### 4.3.2.1. BIAcore®X system

---

The results of the BIAcore®X SPR assessment of the potential interactions between small molecules (lapachol, bromo- $\beta$ -lapachona and malonganenones A, B and C) and Hsp70s (PfHsp70-1 and PfHsp70-x) are shown in Figures 4.3 – 4.5 and in Figures 7.7-7.11, Appendix B.

In each figure, the sensorgram of response (RU) vs. time resulting from the injection of compounds at various concentrations over immobilised Hsp70 is shown. Overlaid onto the sensorgrams in each figure is the Langmuir model fitted to the data (shown as dashed lines in colours corresponding to those used to represent each compound concentration in the sensorgrams).  $R_{\max}$  and  $\chi^2$  ( $\text{Chi}^2$ ) values for each data set are also shown in each figure. The  $\chi^2$  value, which is a statistical measure of the closeness of the fit to the data, is derived from the fitted and experimental values at a given point, as well as the total number of points.  $\chi^2$  values of < 10 % of the  $R_{\max}$  value are generally considered acceptable (Bio-Rad Laboratories, Inc., Bulletin 6044).  $R_{\max}$  values for each interaction were calculated using Equation 4.4 above. Along with the sensorgram, a residual plot is shown for each data set, which shows the degree of deviation of the data from the fitted model, and is thus a measure of how well the model fits the data. In a good fit, the residual points, which represent the difference between the fitted and the experimental data for each data point, are randomly distributed about the x-axis of the plot, and show

no distinct trends (BIAevaluation v. 3.0 software handbook, 1997). The residual plots as well as the  $\chi^2$  values were used to assess the suitability of the model fit to the data.

In assessing whether a specific interaction between a compound and an immobilised Hsp70 existed based on the SPR data obtained, compounds were said to interact specifically with the immobilised protein if a dose-dependent response of increasing response with increasing compound concentration was observed. Quantification of such interactions (affinity:  $K_D$ ) was deemed accurate where data fitted satisfactorily (based on  $\chi^2$  values and residual plots) to the Langmuir model of 1:1 binding. Where a compound was found to show no interaction with immobilised Hsp70s (no dose-dependent increase in response with increasing compound concentration), a single, representative replicate of data is shown. Where a specific interaction was observed, the sensorgram, residual plot and resulting saturation curve of a single replicate are shown, as well as a saturation curve showing the average result of all replicates (Figures 4.3 – 4.5).

Saturation curves for specific interactions were generated using calculated  $R_{eq}$  values derived from the kinetic assessment of the data by the Langmuir model.  $R_{eq}$  values for each concentration of each compound were calculated according to Equation 4.5 below, where  $k_a$  and  $k_d$  (association and dissociation rate constants respectively) were determined from the kinetic assessment of the data, and  $R_{max}$  was calculated as described.

$$R_{eq} = \frac{k_a \cdot C \cdot R_{max}}{k_a \cdot C + k_d} \quad (\text{Equation 4.5})$$

Due to technical problems with the BIAcore®X instrument, specifically failure of the integrated microfluidics cartridge (IFC), the effects of malonganenone B and C on PfHsp70-x were not assessed, nor was binding of any compounds with HsHsp70. This failure also meant that the data for some interactions was not replicated.

As can be seen in Figures 4.3 - 4.5 and Figures 7.7-7.11 (Appendix B), the low flow rate (5  $\mu$ l/min) used in the BIAcore®X experiments was effective in allowing potential interactions to be assessed under steady-state conditions, based on the observation of little to no change in response with time between ~ 10 and 50 seconds on each sensorgram. Based on the fact that for all compounds and for both PfHsp70-1 and PfHsp70-x, measurable responses were obtained (ranging from ~ 15 to ~ 90 RU at 100  $\mu$ M of

compounds, excluding negative values which are explained later), with distinctions between different concentrations of compounds, the levels of immobilisation of each protein were sufficiently high to be able to assess interactions with small molecules.

Based on observed dose-dependent increases in steady-state responses with compound concentration, specific interactions were observed between lapachol and PfHsp70-1 (Figure 4.3), malonganenone A and PfHsp70-1 (Figure 4.4), and malonganenone A and PfHsp70-x (Figure 4.5).

Only two replicates of the experiment assessing the interaction between PfHsp70-1 and lapachol were carried out. As shown in the sensorgram in Figure 4.3A, lapachol was found to bind to PfHsp70-1 in a dose-dependent manner. The sensorgram shows injection spikes at the injection start (time = 0 seconds) and end (time = 60 seconds) points; however, these points were excluded from the data range used in quantification of the interaction and thus are inconsequential to the assessment. The data showing the interaction between lapachol and PfHsp70-1 fitted well to the Langmuir model, based on randomly distributed residual points on the residual plot (Figure 4.3B), as well as a very low  $\chi^2$  value (0.273). The interaction could thus be accurately quantified:  $K_D = (1.25 \pm 0.34) \times 10^{-6}$  M (average of two replicates). Compounds were assessed in a concentration range of  $1 \times 10^{-6}$  to  $100 \times 10^{-6}$  M. The affinity measured between lapachol and PfHsp70-1 falls within this range, further validating the accuracy of the measured affinity.

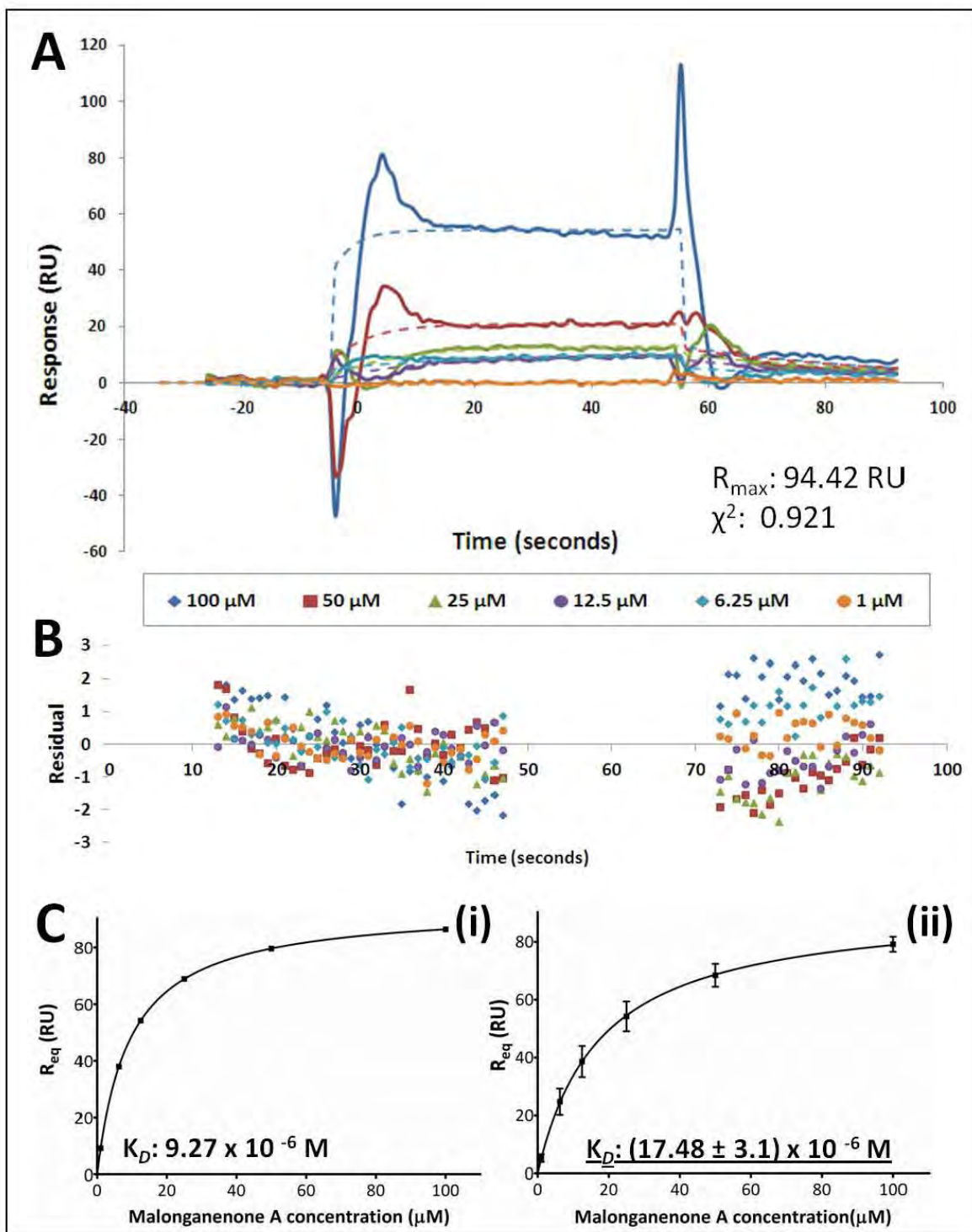


**Figure 4.3: SPR analysis of the interaction between lapachol and PfHsp70-1.** SPR sensorgram of a range of concentrations of lapachol binding to immobilised PfHsp70-1 (solid lines) at 5  $\mu\text{l}/\text{min}$ , with the Langmuir model (dashed lines, corresponding colours) fitted to the data, including the resulting theoretical  $R_{\max}$  and  $\chi^2$  values (A). The residual plot shows deviation from the Langmuir model (B). Saturation curves and resulting  $K_D$  values  $\pm$  SE (C) for a single replicate (i) and the average of two replicates (ii) are shown.



Malonganenone A was found to bind in a dose-dependent manner to both PfHsp70-1 (Figure 4.4A) and PfHsp70-x (Figure 4.5A). Due to the problems with the IFC mentioned earlier, the data for malonganenone A and PfHsp70-x was not replicated, and thus was considered preliminary; however, the experiment for malonganenone A and PfHsp70-1 was replicated four times, and was found to be highly reproducible. In the sensorgrams shown for malonganenone A injected over PfHsp70-1 (Figure 4.4A) and PfHsp70-x (Figure 4.5A), a dip in the sensorgrams can be seen immediately subsequent to injection (time  $\sim$  0-5 seconds), which was attributed to the low flow rate causing a delay in the observed response, and therefore perhaps a mass transport effect, in which the compound was binding to the sensor surface at a faster rate than it was delivered to the surface. The very rapid increase in response after the initial delay at higher malonganenone A concentrations is also indicative of a possible mass transport effect, however, since mass transport effects generally only affect the association and dissociation rates of interactions, this possible effect was not a confounding one in these experiments, as a steady-state assessment was carried out, which was not reliant on association and dissociation rates for affinity quantifications. For malonganenone A binding to both PfHsp70s, the  $\chi^2$  values were well within the acceptable range (0.921 and 4.65 for PfHsp70-1 and PfHsp70-x respectively: both  $< 10\%$  of corresponding  $R_{\max}$  values), suggesting the data fit was accurate. The residual plot for PfHsp70-1 (Figure 4.4B) shows a fairly random distribution of residuals about the x-axis; however, for PfHsp70-x (Figure 4.5B), residuals show very clear trends relative to the x-axis, suggesting that the affinity calculated for malonganenone A binding to PfHsp70-x ( $K_D = 1.57 \times 10^{-6}$  M) may not be accurate. The fact that the measured affinity is outside of the compound concentration range assessed also indicates a possible inaccuracy of the result, and thus further experimentation would be required to validate the result. In the case of PfHsp70-x (Figure 4.5), the measured response due to malonganenone A injection at 100  $\mu$ M exceeds the calculated  $R_{\max}$  for the interaction (64.61 RU). This could be attributed to one of two possible scenarios. Firstly, non-specific binding by the compound on the sensor surface could result in responses higher than the theoretical maximum response, and secondly, the observed discrepancy could be due to multiple valency of the immobilised protein.  $R_{\max}$  values were calculated from equation 4.4, in which one of the terms describes the valency of the ligand. This term was assumed to be "1" for all calculations, and thus  $R_{\max}$  values are based on the assumption that ligands did not have multiple valencies. Higher responses, therefore, could be indicative of multiple valency of the ligand. The calculated affinity of malonganenone A for PfHsp70-1 ( $K_D = 17.48 \times 10^{-6}$  M) was considered accurate based in the reproducibility of the data, the low  $\chi^2$  value, the randomly distributed residuals as well as the fact that the affinity was well within the experimental concentration range.

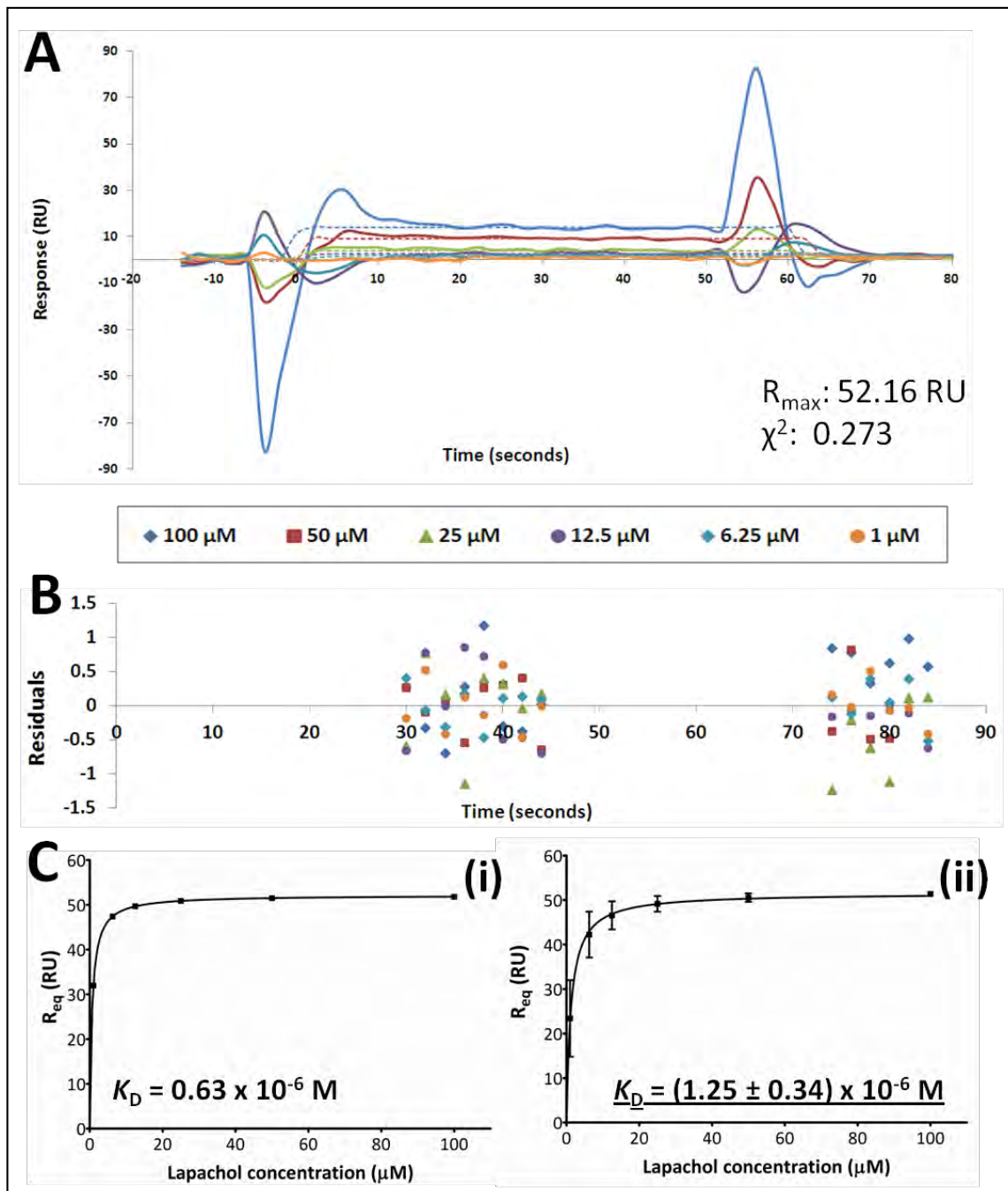


**Figure 4.4: SPR analysis of the interaction between malonganenone A and PfHsp70-1.** SPR sensorgram of a range of concentrations of malonganenone A binding to immobilised PfHsp70-1 (solid lines) at 5  $\mu\text{l}/\text{min}$ , with the Langmuir model (dashed lines, corresponding colours) fitted to the data, including the resulting theoretical  $R_{\max}$  and  $\chi^2$  values (A). The residual plot shows deviation from the Langmuir model (B). Saturation curves and resulting  $K_D$  values  $\pm$  SE (C) for a single replicate (i) and the average of four replicates (ii) are shown.

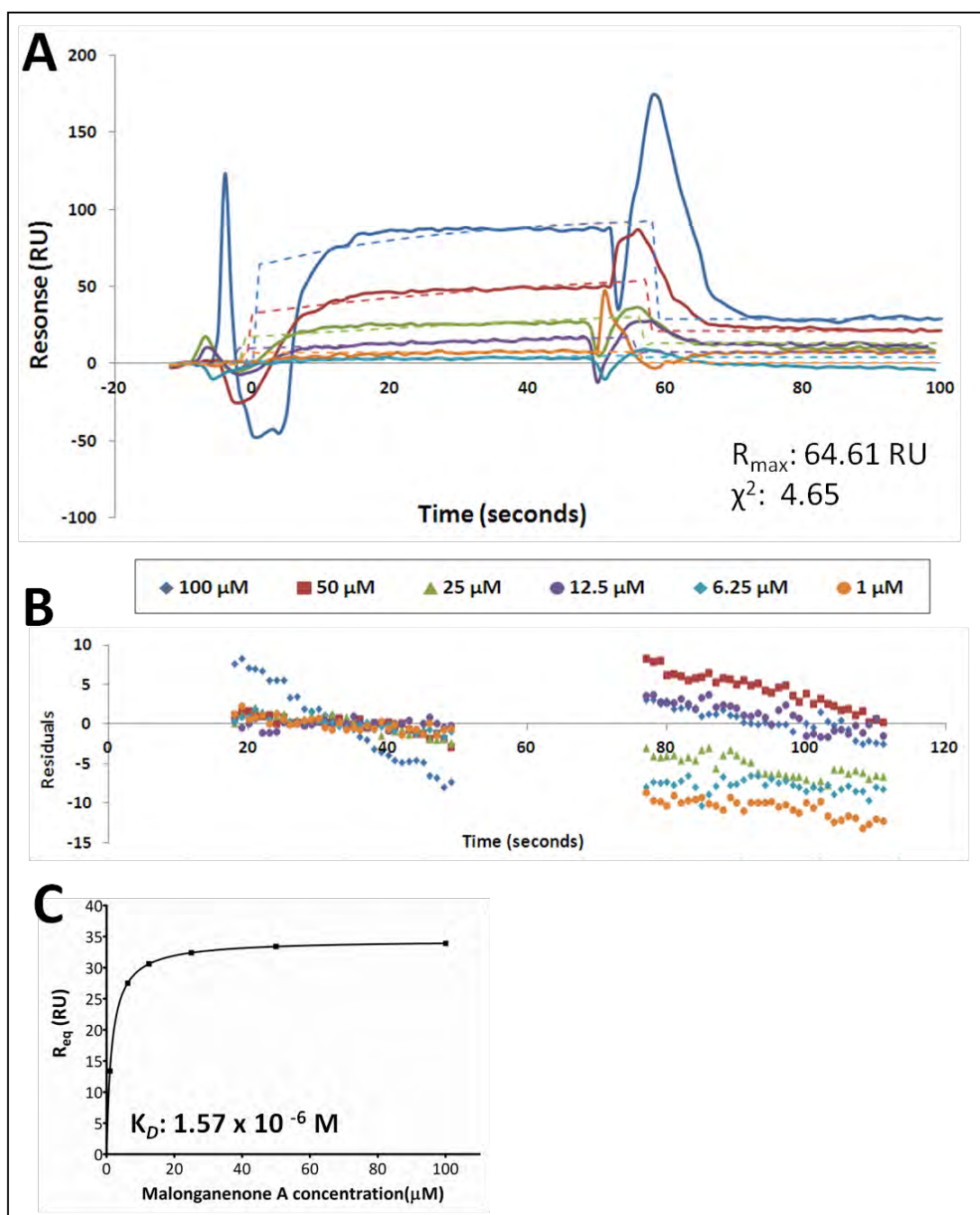


**Figure 4.5: SPR analysis of the interaction between malonganenone A and PfHsp70-x.** SPR sensorgram of a range of concentrations of malonganenone A binding to immobilised PfHsp70-x (solid lines) at 5  $\mu\text{l}/\text{min}$ , with the Langmuir model (dashed lines, corresponding colours) fitted to the data, including the resulting theoretical  $R_{\text{max}}$  and  $\chi^2$  values (A). The residual plot shows deviation from the Langmuir model (B). The saturation curve and resulting  $K_D$  value  $\pm$  SE (C) for a single replicate are shown.

All other potential interactions assessed using the BIAcore®X system (lapachol and PfHsp70-x: Appendix B, Figure 7.7; bromo-β-lapachona and PfHsp70-1: Appendix B, Figure 7.8; bromo-β-lapachona and PfHsp70-x: Appendix B, Figure 7.9; malonganenone B and PfHsp70-1: Appendix B, Figure 7.10; malonganenone C and PfHsp70-1: Appendix B, Figure 7.11) showed no specific interaction between the compound and immobilised protein, based on the lack of a concentration-dependent response. These experiments also resulted in unacceptably high  $\chi^2$  values when the Langmuir model was fitted to the data, and in all cases, the residual plots (part B of each of the figures mentioned above) for these experiments showed points which are not randomly distributed about the x-axis, but rather, showing clear trends of deviation from the fitted model for each compound concentration. The results of all the Hsp70-compound SPR assessments carried out using the BIAcore®X system are summarised in Table 4.1.

#### 4.3.2.2. *ProteOn™ XPR36 system*

---

The results of the experiments assessing the potential interactions between Hsp70s (PfHsp70-1, PfHsp70-x and HsHsp70) and small molecules (lapachol, bromo-β-lapachona and malonganenones A, B and C) by the ProteOn™ XPR36 system are shown in Figures 7.12 – 7.16 in Appendix B. As described in Section 4.2.4.1 for the BIAcore®X experiments, a sensorgram of response (RU) vs. time is shown for each potential interaction, onto which the Langmuir model fitted to the data is overlaid. As before,  $R_{max}$  and  $\chi^2$  values as well as a residual plot are shown for each data set. The residual plots and  $\chi^2$  values were again used to assess the suitability of the model fit to the data.

In the assessment of the potential interactions between small molecules and Hsp70s by the ProteOn™ XPR36 SPR system, all five compounds appear to bind specifically to all three Hsp70s based on the dose-dependent increases in responses with increasing compound concentrations in all cases, however, the reported data is considered preliminary, and needs significant optimisation and repeating in order to be validated. The preliminary results of these experiments are summarised in Table 4.1. Experiments required for validation of the apparent interactions and quantification of such interactions is further discussed in Section 4.4.

Table 4.1 below summarises the data obtained on both the BIAcore®X and ProteOn™ XPR36 in the assessment of the potential interactions between Hsp70s and small molecules. It must be noted that, for reasons discussed in Section 4.4, as well as in the text accompanying SPR data in this section and in Appendix B, the results below are considered preliminary, and further experiments (detailed in Section 4.4) would be required for validation of the results. The results, however, though needing validation, do allow for some speculation and discussion (section 4.4) regarding these potential Hsp70-compound interactions.

**Table 4.1: Summary of the preliminary results of the assessment of the potential interactions between small molecules and Hsp70s.** Where applicable, affinities ( $K_D$ , M) are reported as either accurate (black type) or inaccurate (grey type).

	Interactions between small molecules and Hsp70s				
	BIAcore®X instrument		ProteOn™ XPR36 instrument		
	PfHsp70-1	PfHsp70-x	PfHsp70-1	PfHsp70-x	HsHsp70
Lapachol	(1.25 ± 0.34) × 10 <sup>-6</sup>	X	Suggested interaction, NQ	0.79 × 10 <sup>-6</sup>	1.70 × 10 <sup>-6</sup>
Bromo-β-lapachona	X	X	Suggested interaction, NQ	Suggested interaction, NQ	Suggested interaction, NQ
Malonganenone A	(17.48 ± 3.12) × 10 <sup>-6</sup>	(1.57 ± 0.01) × 10 <sup>-6</sup>	(10.20 ± 10.10) × 10 <sup>-6</sup>	(62.63 ± 45.54) × 10 <sup>-6</sup>	(186.83 ± 227.37) × 10 <sup>-6</sup>
Malonganenone B	X	ND	Suggested interaction, NQ	Suggested interaction, NQ	Suggested interaction, NQ
Malonganenone C	X	ND	6.48 × 10 <sup>-6</sup>	411 × 10 <sup>-6</sup>	1.36 × 10 <sup>-6</sup>

X: no apparent interaction; ND: not determined; NQ: not quantifiable. Variation (±) is reported as either SE (BiaCore®X) or SD (Proteon™ XPR36).

### 4.3.3. Hsp70-Hsp40 interactions

The sensorgrams of the assessment of interactions between Hsj1a and immobilised Hsp70s in the presence and absence of ATP are shown in Figure 4.6. In the case of all three Hsp70s, a significant increase in response units with time was observed in the association phase of each sensorgram, and a gradual decrease in response units in the dissociation phase, indicative of an interaction between Hsj1a and each of the Hsp70s, both in the presence and absence of ATP. BSA (1.6 μM), used as a non-specific binding control (Figure 4.6, grey line), resulted in no increase in response when passed over the Hsp70s, thus indicating that there was no interaction between BSA and the Hsp70 and thus that the interaction

observed between Hsj1a and Hsp70s was a specific one. In the absence (Figure 4.6, dashed black line) of ATP, a greater response due to Hsj1a binding was observed compared to in the presence (Figure 4.6, solid black line) of ATP.

ATP itself did bind to each of the Hsp70s (data not shown), however, this effect was corrected for by subtraction of sensorgrams of ATP binding (in the absence of protein analyte) over each Hsp70 channel from sensorgrams of protein analyte binding in the presence of ATP.

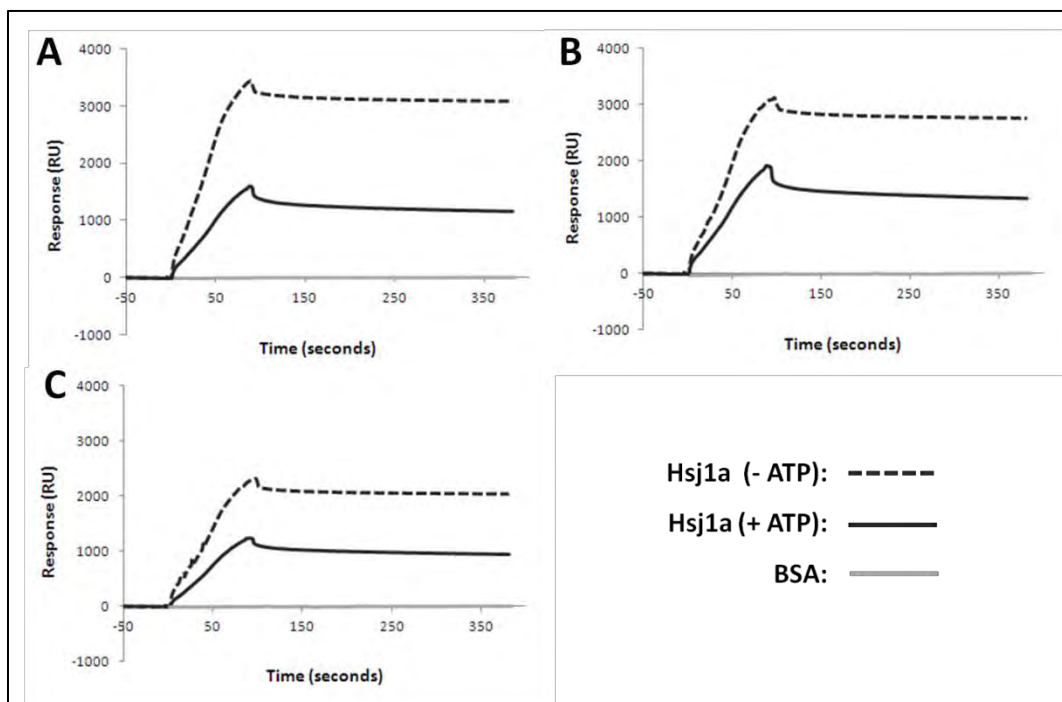


**Figure 4.6: SPR sensorgrams of the analysis Hsp70-Hsj1a interactions.** Sensorgrams of Hsj1a (1.6  $\mu$ M) binding to immobilised PfHsp70-1 (A), PfHsp70-x (B) and HsHsp70 (C) both in the presence (solid black lines) and absence (dashed black lines) of ATP (1 mM). BSA (solid grey line) was included as a non-specific binding control.

#### 4.3.3.1. Effects of malonganenone A on Hsp70-Hsj1a interactions

The effect of malonganenone A on the interactions between Hsj1a and Hsp70s was assessed in the presence of ATP (1 mM), since the observed Hsp70-Hsj1a interactions (Section 4.3.3) were only considered physiologically relevant interactions in the presence of ATP (discussed in Section 4.3).

The results of the assessment of the effects of malonganenone A on Hsp70-Hsj1a interactions are shown in Figure 4.7. In the case of all three Hsp70s, a difference in the response due to Hsj1a was observed between the absence (Figure 4.7, solid black lines) and the presence (Figure 4.7, solid grey lines) of malonganenone A. As expected, based on the interaction between Hsp70s and malonganenone A shown in both Section 4.2.4, a binding response was observed from a control injections of malonganenone A too (Figure 4.7, dashed black lines), however, this effect was corrected for in the injection of Hsj1a in the presence of the compound. The response due to Hsj1a binding was decreased in the presence of malonganenone A for all three Hsp70s, and the most pronounced decrease was observed for Hsj1a binding to PfHsp70-x (Figure 4.7B).

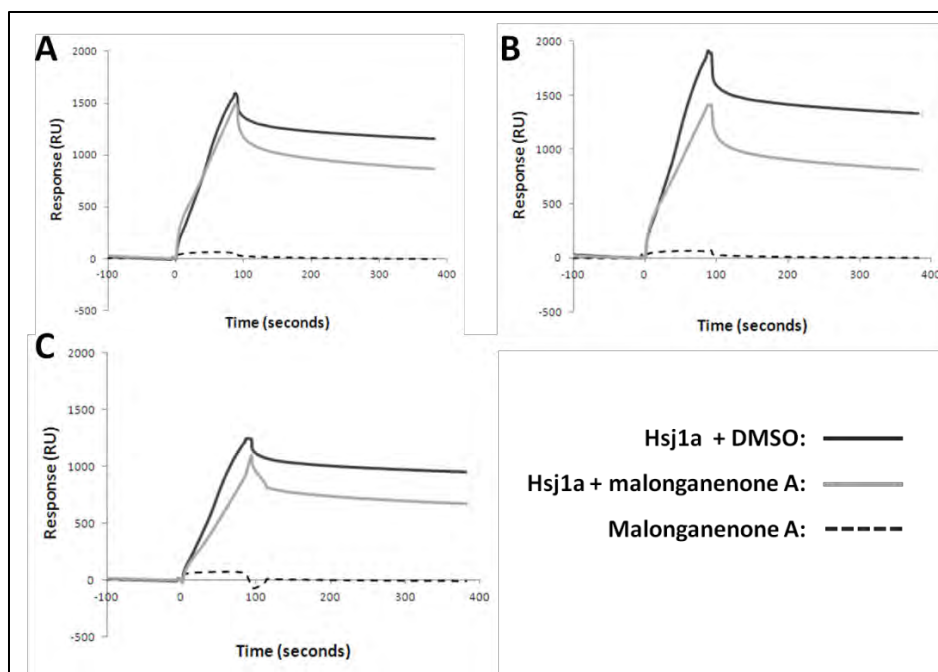


**Figure 4.7: The effects of malonganenone A on the interaction between Hsj1a and Hsp70s determined by surface plasmon resonance.** Sensorgrams of Hsj1a (1.6  $\mu$ M) binding to immobilised PfHsp70-1 (A), PfHsp70-x (B) and HsHsp70 (C) in the presence of 1 mM ATP. Hsj1a was pre-incubated with either DMSO (0.166 %, solid black lines) or malonganenone A (50  $\mu$ M, solid grey lines). The response of Hsj1a in the presence of malonganenone A was corrected for the binding effect of malonganenone A (dashed black lines).

#### 4.4. DISCUSSION

---

SPR was used in this study to complement the *in vitro* work on small molecule modulation of Hsp70s described in Chapter 3. The results of the experiments carried out to assess the potential interactions between Hsp70s and small molecules (Section 4.3.2) are highly comparable between the two SPR instruments used; for example affinities of  $(17.48 \pm 3.12) \times 10^{-6}$  M vs.  $(10.20 \pm 10.06) \times 10^{-6}$  M being measured for the interaction between malonganenone A and PfHsp70-1 on the BIAcore®X and ProteOn™ XPR36 systems respectively. Using the ProteOn™ XPR36 system, all five compounds were found to interact with each of the three Hsp70s to some extent, based on the concentration-dependency of the observed responses (Section 4.3.2.2). These findings were not surprising, bearing in mind the extremely high level of identity between the Hsp70s (Chapter 3, Section 3.3.4), and the significant modulatory effects that each compounds was found to have on at least one of the Hsp70s in *in vitro* assays (Chapter 3). Because all five compounds assessed did appear to bind to all three Hsp70s, however, it would have been useful to assess a small molecule that could act as a negative control or a non-specific binding control, showing no specific interaction with any of the Hsp70s.

On the BIAcore®X instrument, of the Hsp70-small molecule pairs assessed, several were found to have no specific interaction (bromo-β-lapachona, malonganenone B and malonganenone C with PfHsp70-1; lapachol and bromo-β-lapachona with PfHsp70-x). These contrasting results can potentially be attributed to the relative sensitivities of the two instruments. The BIAcore®X instrument has a low molecular weight detection limit of < 180 Da (BIAcore®X Product Information, BR-9000-72), and thus sensitivity should not have been a problem in detecting the small molecules included in this study, the smallest of which is lapachol (242 Da). The BIAcore®X instrument was made available on the market in 1996, and only a year later, a new BIAcore instrument, the BIAcore 2000, was said to have improved sensitivity for detection of low molecular weight analytes as well as weak affinity interactions due to improved signal-to-noise ratios and greater reliability of the measurements (Karlsson *et al.*, 1997). Considering the ProteOn™ XPR36 system was introduced 10 years after the BIAcore®X instrument, it is highly probable that the newer system has significantly improved sensitivity and thus detection limits compared to the earlier instrument. A benchmark study published a few years ago, in which 150 participating researchers used, between them, 18 different SPR systems or instruments to measure the affinity between two proteins (Fab and glutathione S-transferase), showed that despite differences between the instruments used, experimental design was generally responsible for differences in the



results obtained from the 150 researchers, rather than the instrumentation, and that generally, very similar results were obtained from the different groups using a wide range of instruments, including the two used in this study. The benchmark study does therefore suggest that similar results should be obtained on two very different systems, however, the interaction assessed in the benchmark study was a protein-protein one, studying two proteins of > 40 kDa each, and thus relative sensitivity limitations of any of the instruments used would have been inconsequential to the study, and were not discussed (Rich *et al.*, 2009).

Some of the non-interacting Hsp70-small molecule pairs on the BIAcore®X in this study were found to have significant non-specific binding effects resulting in various artifacts such as negative association slopes as shown in Section 4.3.2.1. Since the polymer surface chemistry on the sensor chip surfaces differs between the ProteOn™ XPR36 GLH chips and the BIAcore® CM5 chips, it is also possible that the non-specific binding effect was greater on the CM5 reference flow cell surface than on the GLH chip alginate surface.

The only Hsp70-small molecule interactions which were confirmed and quantified in both systems were those between malonganenone A and both PfHsp70s. In the case of the interaction between malonganenone A with PfHsp70-1, the affinities determined by the two systems are very similar (within one order or magnitude of each other: Table 4.1). The affinity between malonganenone A and Pfsp70-x; however, differs somewhat between the two systems, though the affinity determined by the ProteOn™ XPR system, representing a triplicate result, has a high degree of variation (SD), and the affinity range when taking into consideration the variation includes the affinity determined in the BIAcore®X experiment.

Besides possible improved sensitivity and the capacity for high throughput assessments to be carried out, the advantage of the Proteon™ XPR36 system in the analysis of small molecule interactions with the three Hsp70s of interest over the BIAcore®X system is that compounds could be assessed on all three Hsp70s simultaneously under identical conditions and using the exact same compound samples, making it possible to make direct comparisons between the effects observed across the different ligand channels. The data generated by the ProteOn™ XPR system thus represents a complete and side-by-side data set comparing the binding of compounds between the three Hsp70s of interest. The only inconsistency in the comparison in this case is that PfHsp70-1 and PfHsp70-x were immobilised to very

similar levels on the GLH chip (~12 000 and ~11 000 RU respectively), while HsHsp70 was immobilised to a significantly lower level in comparison (~6400 RU). This difference may have resulted in a lower sensitivity for small molecules in the HsHsp70 channel compared to the malarial Hsp70 channels.

When comparing the affinities of compounds for different Hsp70s as determined by the Proteon™ XPR36 system, some interesting differences were noted. Malonganenone C was found to bind to PfHsp70-1 with a higher affinity (two orders of magnitude difference, Table 4.1) than to PfHsp70-x. This difference correlates well with the findings described in Chapter 3, showing that malonganenone C significantly inhibited the aggregation suppression activity of PfHsp70-1, and had no effect on the aggregation suppression activity of PfHsp70-x. The results for lapachol were considered preliminary, and would have to be further explored to be validated, however, based on the preliminary affinities, lapachol had a higher affinity for PfHsp70-x than for HsHsp70 (the affinity for PfHsp70-1 could not be quantified accurately), which again correlates to findings described in Chapter 3, showing that the ATPase activity of PfHsp70-x is significantly inhibited by lapachol, whereas that of HsHsp70 is unaffected.

The degree of variation (SD: Table 4.1) in the affinities between malonganenone A and Hsp70s as determined by the Proteon™ XPR36 system made a comparison between the three proteins somewhat difficult. Taking into consideration the standard deviations in the affinity values, there seem to be no significant differences between the reported affinities. The high degree of variability between the replicates suggests that the regeneration conditions used in the SPR experiments were not suitable. Regeneration that is too harsh (extreme pHs, high concentrations of denaturants) can result in removal of not only bound analyte, but of some immobilized ligand, altering the sensor chip surface for subsequent analyte injections. Regeneration that is not stringent enough can result in accumulation of analytes on the ligand surface, also altering the surface for subsequent injections. The data could perhaps have been improved upon by optimisation of the regeneration conditions used. Intermittent testing of the integrity of chip surface could have been carried out with known interacting partners of Hsp70 to confirm that the surface used in experiments was not being altered or destroyed by the regeneration conditions used.

A comparison of the interactions of malonganenone A with PfHsp70-1 compared to PfHsp70-x using the BIAcore®X data generated shows that the compound had a higher affinity for PfHsp70-x than for PfHsp70-1 (Table 4.1). Malonganenone A was found to modulate both the aggregation suppression and

ATPase activities of both PfHsp70s (Chapter 3); however, affected only the Hsp40-stimulated ATPase activity of PfHsp70-x, and the basal ATPase activity of PfHsp70-1. The results of biophysical assessment of these Hsp70-small molecule interactions and their implications will be further discussed in Chapter 6.

There are a number of limitations in the small molecule work reported on in this chapter, and thus, as stated previously, the data is considered preliminary. One such limitation is that the effect of DMSO on the chip surface was accounted for using inappropriate methods. In this study, data was double referenced by subtraction of the response on the reference flow cell from that on the active flow cell, as well as by subtraction of a series of DMSO injections corresponding in concentration to compound injections. A more appropriate method to correct for the effect by DMSO, however, would have been to use a solvent correction protocol, in which a series of DMSO dilutions are injected over the sensor surface and a calibration curve is generated and used by the SPR software to correct for the DMSO bulk effect.

Another concern with the small molecule work, particularly in the case of the ProteOn™ XPR36 system (Figures 7.12-7.16), is that in many cases the curves did not reach saturation before the end of the association phase. Toward more accurately assessing and quantifying these interactions, conditions should be optimised to allow for saturation to be reached. This would also potentially allow for the compounds to be assessed under steady-state conditions, which is often considered more suitable for small molecule work than kinetic quantification. In addition to assessing Hsp70-compound interactions under steady-state conditions, experiments in which lower levels of ligand immobilisation are used could be carried out to further validate the preliminary results reported in this study. In both the BIAcore®X and the ProteOn™ XPR36 systems, high levels of immobilisation of both PfHsp70-1 and PfHsp70-x were used. Though higher protein loads are often necessary for the system to be sensitive enough for small molecule work, these high loads can also contribute to undesired re-binding and mass transport effects which can confound data interpretations, as seemed to be the case in some of the results shown in this chapter. Before binding between these small molecules and Hsp70s can be concluded with certainty and can be quantified, the experiments would have to be repeated using lower levels of protein immobilisation.

As mentioned for a number of the Hsp70-compound interactions, the quantification of apparent interactions would need to be validated by more rigorous testing, including carrying out more replicates

of experiments, and using more suitable concentration ranges. Ideally, to be able to quantify affinities with certainty, three concentrations below the determined  $K_D$ , and three concentrations above saturation would have to be included.

Binding studies of chaperone-co-chaperone and chaperone-substrate interactions are commonly carried out in the presence of ATP (Suh *et al.*, 1998; Gässler *et al.*, 1998), or for comparative purposes, in both the presence and absence of ATP or presence of ADP (Gamer *et al.*, 1996; Mayer *et al.*, 1999). The relevance of the inclusion of ATP in these systems is illustrated by the study by Mayer and colleagues (1999). In their study on the interaction between DnaK and DnaJ, Mayer and colleagues found that, in the presence of ATP, the DnaK ATPase domain alone showed no interaction with DnaJ, compared with a significant interaction observed for full-length DnaK injected over immobilised DnaJ in the presence of ATP. As reviewed in Chapter 1, Hsp70 interacts with Hsp40 co-chaperones in the ATP bound state. Hsp40 then stimulates the hydrolysis of ATP by Hsp70, and Hsp70, now in an ADP bound state, has an increased affinity for peptide substrates and a lowered affinity for Hsp40s (Section 1.1.2). Considering these conditions under which Hsp70s bind either substrates or co-chaperones, the ATPase domain of DnaK would be expected to bind DnaJ in the presence of ATP. The contrary findings, therefore, suggested that the observed interaction between full-length DnaK and DnaJ was not a chaperone-co-chaperone interaction, but rather a chaperone-substrate one, in which DnaJ was being recognised as a substrate by DnaK. The observed DnaK-DnaJ interaction was thus considered a non-physiological one (Mayer *et al.*, 1999).

Figure 4.13 shows that, for all three Hsp70s, binding of Hsj1a to Hsp70s was greater in the absence of ATP compared to in the presence of ATP. Since, in the presence of ATP, Hsp70s are in a closed conformation, with a low affinity for peptide substrate, only co-chaperones (and not substrates) would be expected to bind (Section 1.1.2). In the absence of ATP, however, both peptide substrates as well as co-chaperones would likely bind to Hsp70. The results shown in Figure 4.13 can thus be explained by the fact that, in the absence of ATP, all the injected Hsj1a was binding to the Hsp70s, both as a co-chaperone (the native, correctly folded portion of the recombinant protein preparation) and as a peptide substrate (the non-native or misfolded portion of the protein preparation). In the presence of ATP, however, only the correctly folded portion of the Hsj1a preparation was able to bind to the Hsp70 (as a co-chaperone). Thus, in assessing the Hsp70-Hsj1a interactions as chaperone-co-chaperone interactions and not as chaperone-substrate interactions, the interaction in the presence of ATP was

considered the physiologically relevant interaction, and further experiments were carried out in the presence of ATP. The notion that in absence of ATP Hsj1a is binding as both a substrate and a co-chaperone could be investigated by the use of high affinity peptide substrates of Hsp70, such as NR (NRLLLTGC; Gässler *et al.*, 2001), which, when supplied at saturating levels, would eliminate any Hsj1a binding as substrate.

The effect of malonganenone A on the interactions between Hsj1a and Hsp70s is shown in Figure 4.14, and shows, for all three Hsp70s, that Hsj1a binding to Hsp70s is decreased in the presence of malonganenone A. This effect was more pronounced for PfHsp70-1 and PfHsp70-x. In *in vitro* ATPase assays, malonganenone A was found to inhibit the Hsj1a-stimulated ATPase activity of PfHsp70-x, but not the basal activity, suggesting that the compound disrupted the interaction between PfHsp70-x and Hsj1a. The decreased binding of Hsj1a to Hsp70s shown in Figure 4.14 further supports this hypothesis; however, the results are considered preliminary. To validate the observed effect of diminished interactions of Hsj1a with Hsp70s due to malonganenone A, further experiments including a range of concentrations of Hsj1a, as well as a range of concentrations of malonganenone A would have to be carried out, allowing for a quantification of the Hsj1a-Hsp70 interactions both in the presence and the absence of malonganenone A.

In Figures 4.6 and 4.7, the binding responses of Hsj1a on Hsp70s do not reach saturation, even after a relatively long association time of 100 seconds. This could potentially be due to the high level of Hsp70 immobilisation on the sensor chip, or non-specific accumulation of protein on the sensor surface, which could have confounding effects on data interpretation. It would therefore be necessary to repeat these experiments and to use conditions (level of Hsp70 immobilisation, flow-rate and interaction times) which would allow saturation to be reached.

An important consideration in these experiments assessing interactions between Hsp70s and either compounds or co-chaperones is the nucleotide state of the Hsp70s. Purified Hsp70s generally exist in an ADP-saturated state. The nucleotide state is very likely to affect the affinity of Hsp70s for potential interacting partners, especially those thought to interact in the nucleotide binding domain, and thus, for a greater understanding of potential binding mechanisms, it would be beneficial to assess all potential Hsp70 interaction in different nucleotide states in future experiments.

Having successfully shown specific interactions between the three Hsp70s of interest to this study (PfHsp70-1, PfHsp70-x and HsHsp70), and Hsp40, as well as between the Hsp70s and small molecules, the aims of this chapter toward completion of Objective 3 (Section 1.4) were successfully achieved. These findings must, however, be considered in light of possible limitations of the use of SPR technology in binding studies of chaperones and their interactions: a finding in the study by Mayer and colleagues on DnaK-DnaJ interactions by SPR showed that DnaJ immobilised to a sensor chip had compromised function, specifically reduced substrate-binding ability. The authors concluded from this observation that the immobilisation of DnaJ caused steric obstruction of the substrate binding site of DnaJ, thus making it inaccessible to the substrate (the heat shock transcription factor  $\sigma^{32}$ ; Mayer *et al.*, 1999). This altered or compromised function of DnaJ illustrates a limitation in that the immobilisation of chaperones, generally considered highly mobile molecules, is likely to affect function and thus interactions of chaperones. This is an important point to bear in mind when in the context of the data presented in this chapter: due to the immobilisation of the Hsp70s of interest, the nature of observed interactions may not necessarily be completely native or physiologically accurate.

In addition to a number of additional experiments and repeats of described SPR experiments, additional techniques such as NMR or ITC in the case of protein-compound interactions and tryptophan fluorescence in the case of protein-protein interactions would be useful in validating the reported data and further quantifying potential interactions.

**CHAPTER 5:**

---

**Toxicity of compounds to *Plasmodium falciparum*  
and human cell lines**

---

Note: some of the work described in this chapter has been published in the following article:

**Cockburn, I.L.**, Pesce, E.-R., Pryzborski, J.M., Davies-Coleman, M.T., Clark, P.G.K., Keyzers, R.A., Stephens, L.L. and Blatch, G.L. (2011). **Screening for small molecule modulators of Hsp70 chaperone activity using protein aggregation suppression assays: inhibition of the plasmodial chaperone PfHsp70-1.** *Biological Chemistry*, 382, 431-438.

The published data has been reproduced as part of this thesis with written permission of the publishers of the article (De Gruyter: [www.degruyter.com/view/j/bchm](http://www.degruyter.com/view/j/bchm)). Data that has been reproduced from the publication in this chapter shall be indicated as such by reference to Cockburn *et al.*, 2011.



## 5.1. INTRODUCTION

---

Almost 400 years ago, quinine, a natural product extracted from the bark of the *Cinchona* tree, was successfully used to treat malaria, and with that was the first ever successful treatment of an infectious disease with a chemical compound (as reviewed by Achan *et al.*, 2011). This important and historical anti-malarial compound is still used to treat malaria today, however, it has been found to have undesirable properties and side-effects, and has largely been replaced by newer and more effective anti-malarials (Achan *et al.*, 2011). *Malaria Journal* recently published two review articles highlighting the importance of investigating natural products as future anti-malarial therapies. The authors of both reviews stressed the need for new classes of medicines due to the increasing challenge of resistance of *P. falciparum* to existing therapies, and both reviews urged researchers to look to natural products for new compounds (Ginsburg and Deharo, 2011; Wells, 2011). Ginsburg and Deharo pointed out that, although 62 % of small-molecule human drugs introduced between 1981 and 2006 are either natural products or derivatives or analogues of natural products, recent drug discovery research has been focused on synthetic compounds, presumably due to the increased capacity for the synthesis and high throughput screening of large synthetic chemical libraries (Ginsburg and Deharo, 2011). Apart from natural compounds historically representing a large proportion of active and successful human drugs, it has been suggested that natural products are, on average, found to be better ligands for target proteins than new synthetic compounds. This fact has been attributed to the fact that all primary and secondary metabolites, receptors, enzymes, transporters and regulatory proteins native to living organisms originated from the same limited set of molecules present in early life forms, and have thus co-evolved to interact (Ganesan, 2008; Ginsburg and Deharo, 2011).

The aims of the experiments in this chapter, toward completion of Objective 4 (Section 1.4) were to screen compounds previously shown to be compounds of interest, i.e. inhibitors of the *in vitro* chaperone activity of PfHsp70-1 and PfHsp70-x (as determined by work in Chapter 3) as potential inhibitors of *P. falciparum* growth in culture, and to determine the toxicity (IC<sub>50</sub> values) of any such inhibitors towards the parasites using a colorimetric lactate dehydrogenase growth inhibition assay (Makler *et al.*, 1993). The compounds found to be toxic to parasites were tested for toxicity towards mammalian cells. A cell proliferation assay was used for toxicity determination, using both a cancerous (MDA-MB-231) and a non-malignant (MCF12A) breast cell line. An assessment of the predicted oral

bioavailability of each of the test compounds was also carried out, using Lipinski's "Rule of Five" (Lipinski, *et al.*, 2001).

## 5.2. METHODS AND MATERIALS

---

### 5.2.1. Materials

---

Dulbecco's Modified Eagle Medium (DMEM) containing Glutamax<sup>TM</sup>, Ham's F10 medium containing Glutamax<sup>TM</sup>, fetal calf serum (FCS) and Penicillin (10 U/ml) – streptomycin (100 µg/ml) – amphotericin (12.5 µg/ml) (PSA) were purchased from Gibco (Invitrogen, U.K.). Epidermal growth factor (EGF), hydrocortisone, trypsin, gentamycin, dimethyl-sulfoxide (DMSO), cyclohexamide, sodium-L-lactate, nitro blue tetrazolium (NBT), 3-acetylpyridine dinucleotide (APAD), diaphorase and paclitaxel were supplied by Sigma-Aldrich. Insulin was obtained from NovoRapid (Novo Nordisk Pharmaceuticals, Denmark), and the MTT (3-[4,5-dimethylthiazol-2-yl]-2,5-diphenyl tetrazolium bromide) Cell Proliferation assay Kit I was purchased from Roche (Switzerland). RPMI 1640 medium was obtained from PAA Laboratories (GE Healthcare), and human type A<sup>+</sup> serum and erythrocytes were sourced from the Marburg blood bank (Germany). Sorbitol was supplied by Carl Roth (Germany), and blasticidin S by InvivoGen (U.S.A.). Hypoxanthine was purchased from CC-Pro (Germany). WR99210 was a kind gift from Jacobus Pharmaceuticals (U.S.A.). Tissue culture vessels and 96-well assay plates were purchased from Corning® (U.S.A.).

### 5.2.2. Assessment of the potential permeability and solubility of test compounds

---

In the past, many lead compounds have failed clinical trials purely based on unfavourable pharmacokinetic properties and hence unsuitability as potential drugs (Keller *et al.*, 2006). The need for a way of predicting such properties based on compound structure gave rise to Lipinski's "Rule of 5", by which the potential of compounds to be "drug-like" in terms of oral bioavailability can be assessed (Lipinski *et al.*, 2001). The rule states that if a compound does not fulfil more than two of four criteria (described below), it can be considered to be unlikely to be well absorbed in the body (Lipinski *et al.*, 2001). The criteria were:

1. The sum of hydrogen-bond donors (OH and NH molecules) should not exceed 5
2. The sum of hydrogen-bond acceptors (O and N atoms) should not exceed 10
3. The molecular weight should not exceed 500 g/mol
4. The LogP value should not exceed 5, or the MLogP should not exceed 4.15

The “Rule of 5” was named based on the numbers in the above criteria all being multiples of five. The LogP (logarithm of the octanol/water partition coefficient) of a compound is calculated from the distribution of a compound between a polar or aqueous medium (water) and a non-polar or lipophilic one (octanol), based on the structure of the compound. Hence the LogP is a measure of the lipophilicity or hydrophobicity of a compound, which relates to the potential absorption and oral bioavailability of a compound in the body (Lipinski *et al.*, 2001). The MLogP, too, describes the lipophilicity of compounds, simply calculated in a different way, as described by Moriguchi and colleagues (Moriguchi *et al.*, 1992; Moriguchi *et al.*, 1994). It has been suggested that LogP or MLogP values are insufficient to give a good idea of the hydrophobicity of a compound, as the calculation does not take into account the ionic state of compounds at various biological or physiological pHs (Bhal *et al.*, 2007). The suggested improvement on Lipinski’s Rule of Five by Bhal and colleagues is the use of LogD rather than LogP (also with a cut-off value of 5), where LogD takes into account the ionic state of a compound at a specified pH (Bhal *et al.*, 2007). Therefore, for the purposes of this study, LogP values were calculated in the Rule of Five assessment of compounds, and additionally the LogD values were calculated. Because, as previously discussed, physiological pH in the blood is 7.4, but drugs are absorbed in the small intestine at pH ~ 5.5 (Bhal *et al.*, 2007), LogD values were calculated for the compounds at both pH 7.4 and 5.5.

A basic assessment of the eleven compounds included in this study was carried out. A Simplified Molecular-Input Line-Entry (SMILE) notation for each compound was generated using ChemSketch® Software (v. 11.01, Advanced Chemistry Development, Inc., Canada), and LogP and LogD values were calculated using the ChemAxon MarvinSketch LogP calculator ([www.chemaxon.com/marvin/sketch](http://www.chemaxon.com/marvin/sketch)).

### 5.2.3. Growth and maintenance of *P. falciparum* cultures

---

*Plasmodium falciparum* 3D7 parasites were grown and maintained in continuous culture according to Trager and Jensen (1976) with minor modifications. RPMI 1640 growth medium was supplemented with 10 % heat inactivated serum (human, type A<sup>+</sup>), 200 mM hypoxanthine and 20 mg/ml gentamicin. A haematocrit of 4% (v/v) of human erythrocytes (type A<sup>+</sup>) was used, and parasites were grown at 37 °C, 5 % (v/v) CO<sub>2</sub> and 5 % (v/v) O<sub>2</sub>. Synchronisation of cultures to ring stage was achieved by sorbitol lysis (Lambros and Vanderberg, 1979).

### 5.2.4. LDH growth inhibition assay

---

Growth inhibition assays were conducted on *P. falciparum* 3D7-infected erythrocytes using the lactate dehydrogenase (LDH) method (Makler *et al.*, 1993). To ensure that the LDH growth assay was working correctly, two compounds, 4,6-diamino-1,2-dihydro-2,2-dimethyl-1-[(2,4,5-trichlorophenoxy)propyloxy]-1,3,5-triazine (WR99210) and blasticidin S, known to be toxic to *P. falciparum*, were used as positive controls (Kinyanjui *et al.*, 1999; Hill *et al.*, 2006; Yamaguchi *et al.*, 1965). In addition to the two positive control compounds, the effect of DMSO, used to resuspend each of the test compounds, was also assessed at a range of concentrations in the assay as a vehicle control.

Serial dilutions of all test compounds, WR99210, blasticidin S and DMSO in were prepared in culture medium in 96-well assay plates. Test compounds and blasticidin S were used at final concentrations of 0.01, 0.1, 1 and 10 µM, and WR99210 was made up to final concentrations of 0.009, 0.09, 0.9 and 9 µM. Cyclohexamide (final concentration 25 µM) was added to an additional set of wells to measure the background LDH levels (see below). A 'no compound' control (untreated parasites) was included on each assay plate (only culture medium, no compound) and was taken as the '100% growth' value for that plate. After the additions and dilutions of all test compounds, control compounds and DMSO were made, ring-stage *P. falciparum*-infected erythrocytes in culture medium were added to the assay wells at a starting parasitaemia of 0.1% and a haematocrit of 1 %. The final assay volume in each well was 200 µl, and after gentle mixing, plates were incubated in a gassed incubator (5 % (v/v) CO<sub>2</sub>, 5 % (v/v) O<sub>2</sub>) at 37 °C for 72 hours.

After the 72 hour treatment period, 50  $\mu$ l from each well in each assay plate (after gentle mixing) was transferred row-by-row into the corresponding well of a second set of 96-well plates, which contained 230  $\mu$ l cold PBS in each well. The newly prepared plates containing the 50  $\mu$ l samples were centrifuged at 1100  $g$  for 10 minutes at 4  $^{\circ}$ C, and 200  $\mu$ l of supernatant was carefully removed from each well. The plates containing the erythrocyte pellets were frozen at  $-20$   $^{\circ}$ C overnight or until needed. After the assay plates were allowed to thaw for 30 minutes at room temperature, 50  $\mu$ l of the *P. falciparum* infected erythrocytes were transferred row-by-row from each well into the corresponding wells of a third set of 96-well plates. Complete LDH substrate was prepared immediately before use, and consisted of the following components, each prepared separately: LDH substrate buffer (5.6 mg/ml sodium L-lactate, 0.25 % (v/v) Triton X-100, 100 mM Tris-HCl, pH 8.0), nitro blue tetrazolium (NBT) solution (0.2 mg/ml NBT in LDH substrate buffer), 3-acetylpyridine adenine dinucleotide (APAD) stock solution (10 mg/ml APAD in distilled water) and diaphorase stock solution (50 units/ml in distilled water). Complete LDH substrate was prepared by combining NBT, APAD and diaphorase solutions in a ratio (volumes) of 1:5:20. A volume of 100  $\mu$ l complete LDH substrate was added to every well of every plate, after which the plates were briefly shaken to mix the substrate with the samples, and centrifuged at 1100  $g$  for 1 minute to eliminate air bubbles. Plates were kept at room temperature in the dark until absorbance readings were taken using a Ledetect96 96-well plate reader (Labexim Products, Germany), at 650 nm. Absorbance readings were taken at 15, 30 and 45 minutes after substrate addition.

Analysis of the LDH growth inhibition assay data was carried out using Microsoft<sup>®</sup> Office Excel and GraphPad Prism<sup>®</sup> (v. 4.03; San Diego, CA, U.S.A.) software. All raw data were corrected for the average cyclohexamide absorbance readings for each plate to account for any background LDH levels present before treatment of parasites, since cyclohexamide, a potent inhibitor of protein synthesis in eukaryotes is able to kill all parasites immediately and completely (Schneider-Poetsch *et al.*, 2010). The absorbance readings for the untreated parasites were averaged and used as the maximum (100 %) value. Reported IC<sub>50</sub> values (Table 5.2) and the accompanying variation representing the 95% confidence interval of IC<sub>50</sub> values were calculated using a non-linear regression fit of the data.

### **5.2.5. Growth and maintenance of human cell lines**

---

MDA-MB-231 breast cancer cells were maintained in DMEM containing Glutamax™ supplemented with 5 % (v/v) heat-inactivated FCS and PSA. MCF12A cells were cultured in a 1:1 ratio of Ham's F10 medium and DMEM (both containing Glutamax™), supplemented with PSA, 10 % heat inactivated FCS, 20 µg/ml EGF, 500 ng/ml hydrocortisone, and 10 µg/ml insulin. Both cell lines were grown at 37 °C and 9 % CO<sub>2</sub> in a humidified incubator. To carry out passaging of cells, cultures were treated with 1 % trypsin (w/v) to lift cells, which were then washed in phosphate buffered saline (PBS) (137 mM NaCl, 2.7 mM KCl, 10 mM Na<sub>2</sub>HPO<sub>4</sub>, 2 mM KH<sub>2</sub>PO<sub>4</sub> pH 7.4) before being re-seeded into culture flasks.

### **5.2.6. MTT cell proliferation assay**

---

To determine the effects of selected compounds in this study on the growth and survival of human cell lines, as an indication of the toxicity of the compounds, MTT cell proliferation assays were carried out. The assay was conducted according to the manufacturer's instructions (Roche, Switzerland). Cells were seeded into 96-well plates (6000 cells / well), and allowed to adhere overnight. Cells were treated with either DMSO (at the highest concentration used in any compound dilutions: maximum 1 %) or compounds at selected concentrations, for 72 hours. Cells were also treated with paclitaxel, which served as a positive control (Section 5.3.3), and was used at final concentrations of 25, 50, 100 and 200 nM. After 72 hours of treatment, 10 µl of a 5 mg/ml MTT solution was added to each well. The addition of MTT resulted in the formation of an insoluble precipitate, which was solubilised four hours after MTT addition by the addition of 100 µl of 10 % SDS in 0.01 M HCl. Solubilisation was allowed to proceed overnight, and the following day the resulting coloured product was quantified spectrophotometrically at 550 nm, using a Powerwave 96-well plate reader (BioTek Instruments Inc., U.S.A.). Only metabolically active cells are able to convert MTT to the insoluble formazan crystals, and thus the absorbance in each well is directly proportional to the number of living cells in that well (Vistica *et al.*, 1991). The absorbance in wells treated with compounds was calculated as a percentage of the DMSO-treated control to determine the percentage survival of compound-treated cells. A statistical analysis (unpaired, two-tailed T-test, 95 % confidence interval) of the data was carried out to assess whether any observed differences in cell survivals (relative to 100 %: DMSO-treated control) were statistically significant.

### 5.3. RESULTS

#### 5.3.1. The predicted permeability and solubility of test compounds

Table 5.1 shows the results of the assessment of the potential oral bioavailability of the compounds included in this study according to Lipinski's Rule of Five (Lipinski *et al.*, 2001). All eleven compounds included in this study fulfill at least three of the four criteria forming the Rule of Five. In all compounds, the sum of both the hydrogen bond acceptors and hydrogen bond donors did not exceed the acceptable numbers of 10 and 5 respectively. The molecular weights of all compounds did not exceed the cut-off of 500 g/mol, which is an important factor in the potential permeability of compounds through membranes (Lipinski *et al.*, 2001). The only violations of any of the criteria is by malonganenone A and malonganenone C, which were both found to have logP values exceeding the cut-off value of 5 (5.16 and 5.07 respectively).

**Table 5.1: Assessment of the potential permeability and solubility of test compounds according to Lipinski's Rule of Five, based on chemical structure.**

Compound	Molecular weight (g/mol)	Number of HBDs	Number of HBAs	LogP value	Fulfilment of $\geq 2$ of 4 criteria	LogD at pH 7.4	LogD at pH 5.5
Lapachol	242.274	1	3	2.59	Yes	2.53	2.59
$\alpha$ -Lapachona	242.274	0	3	2.15	Yes	2.15	2.15
C-alil-lausona	214.22	1	3	1.96	Yes	1.87	1.96
Bromo- $\beta$ -lapachona	323.186	0	3	3.37	Yes	3.37	3.37
Hydroxy- $\beta$ -lapachona	260.289	1	4	1.051	Yes	1.83	1.83
Nor- $\beta$ -lapachona	230.263	0	3	2.46	Yes	2.46	2.46
Malonganenone A	438.616	0	6	<b><u>5.16</u></b>	Yes	<b><u>5.16</u></b>	<b><u>5.16</u></b>
Malonganenone B	470.658	1	7	4.65	Yes	4.65	4.65
Malonganenone C	333.516	1	3	<b><u>5.07</u></b>	Yes	<b><u>5.07</u></b>	<b><u>5.07</u></b>
PGKC4_7C	168.2	2	5	-0.21	Yes	-0.21	-0.22
PGKC4_41	196.21	1	6	-1.28	Yes	-1.28	-1.28

(HBD: Hydrogen bond donor; HBA: Hydrogen bond acceptor. Violations of any criteria are shown as bold figures underlined).

### 5.3.2. Effects of compounds on the growth of *P. falciparum* parasites in vitro

Figure 5.1 shows the effect of the positive and vehicle controls on the growth of *P. falciparum* 3D7. WR99201 is an inhibitor of *P. falciparum* dihydrofolate reductase (DHFR) with subnanomolar potency in wild type parasites (Kinyanjui *et al.*, 1999). Blasticidin S, a fungal toxin found to kill most prokaryotic and eukaryotic cells by inhibition of mRNA translation on ribosomes, is widely used in selective transfections in many cell types (Hill *et al.*, 2006; Yamaguchi *et al.*, 1965). Both WR99210 (Figure 5.1A) and blasticidin S (Figure 5.1B) were found to have considerable inhibitory effects on *P. falciparum* growth in a dose-dependent manner, and thus the LDH assay was considered to be working correctly. Blasticidin S had a significant ( $P \leq 0.001$ ) effect on parasite survival even at 0.01  $\mu\text{M}$  (88 % parasite survival), and at 10  $\mu\text{M}$  inhibited the parasite survival almost completely ( $\sim 2$  % survival). Similarly, WR99210 inhibited parasite growth (86 %) at 0.009  $\mu\text{M}$ , and at 9  $\mu\text{M}$  almost completely inhibited all parasite survival ( $\sim 4$  % survival). The highest concentration of DMSO in any of the test compound dilutions was  $< 0.005$  %. Based on Figure 5.1C, 0.005 % DMSO had no significant effect ( $P > 0.05$ ) on the survival of parasites (relative to the untreated parasites), and thus the percentage survival of the parasites after treatment with positive control and test compounds was calculated relative to untreated parasites, rather than relative to DMSO-treated parasites.

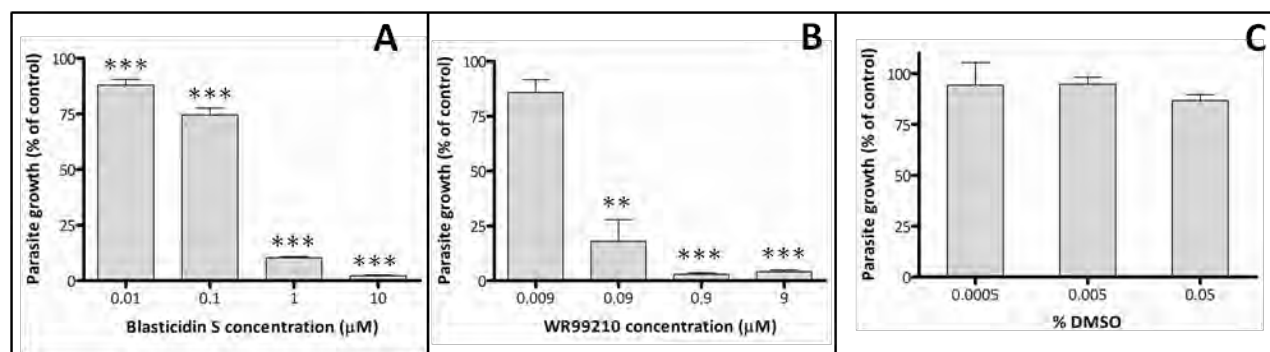


**Figure 5.1: The effects of two positive control compounds (A: blasticidin and B: WR99210) and a vehicle control (C: DMSO) on the survival of *P. falciparum* 3D7 parasites after 72 hour treatment.** Data represents mean values, with error bars showing the standard error of the experiments (A:  $n = 12$ , B:  $n = 4$ , C:  $n = 2$ , where  $n =$  no. of wells per concentration). Statistical significance of differences relative to 100 % (untreated parasites) is indicated by asterisks above bars in A and B ( $P \leq 0.001$ : \*\*\*,  $P \leq 0.01$ : \*\*). Apparent differences in C were not significant.



The results of the screening of the 1,4 naphthoquinone and marine prenylated test compounds are shown in Table 5.2. MAL3-39, a small molecule modulator of Hsp70s (including PfHsp70-1) which was previously found to have antimalarial activity against *P. falciparum* growth ( $IC_{50} = 0.8 \mu\text{M}$ ; Chiang *et al.*, 2009) was included in the compound  $IC_{50}$  screen, and was found to have an  $IC_{50}$  of  $\sim 30 \mu\text{M}$  in this study. Of the compounds screened, malonganenone A and malonganenone C showed the highest antimalarial activity, with low  $IC_{50}$  values of 0.8 and 5.2  $\mu\text{M}$  respectively. Lapachol, bromo- $\beta$ -lapachona and hydroxy- $\beta$ -lapachona showed similar and moderate toxicity to parasites ( $IC_{50}$  values of 19, 17 and 25  $\mu\text{M}$  respectively). Malonganenone B and  $\alpha$ -lapachona have the highest  $IC_{50}$  values ( $> 50 \mu\text{M}$ ), while four compounds (nor- $\beta$ -lapachona, c-alil-lausona, PGKC4\_7C and PGKC4\_41) were found to be non-toxic to parasites, showing no inhibition of the growth of *P. falciparum* in this assay at maximum concentrations of 10  $\mu\text{M}$ .

**Table 5.2: The toxicity of compounds of interest toward *P. falciparum* parasites cultured *in vitro*.** Values represent the 95% confidence interval of calculated  $IC_{50}$  concentrations towards the asexual blood stages of 3D7 *P. falciparum* parasites cultured in human erythrocytes. Some of the data shown in this table is published in Cockburn *et al.*, 2011.

Compound	$IC_{50}$ concentration ( $\mu\text{M}$ )
Lapachol	$18.67 \pm 2.27$
Nor- $\beta$ -lapachona	NT*
$\alpha$ -Lapachona	$> 50$
C-alil lausona	NT*
Bromo- $\beta$ -lapachona	$17.29 \pm 4.44$
Hydroxy- $\beta$ -lapachona	$25.10 \pm 19.47$
Malonganenone A	$0.81 \pm 0.24$
Malonganenone B	$> 50$
Malonganenone C	$5.20 \pm 2.49$
PGKC4_7C	NT*
PGKC4_41	NT*
MAL3-39	$29.58 \pm 16.03$

(\*NT: Compound found to be non-toxic to *P. falciparum* in the described assay.)

### 5.3.3. Effects of compounds on the growth of human cell lines

---

Paclitaxel, a cytotoxic agent known to cause apoptosis in breast cancer cells (Meyn *et al.*, 1995; Milas *et al.*, 1995), was used as a positive control in the MTT assays. Figure 5.2A displays a dose-dependent decrease in cell survival of both MDA-MB-231 and MCF12A cells with increasing paclitaxel concentration after 72 hours of treatment. The calculated  $IC_{50}$  of paclitaxel in the MDA-MB-231 cell line (33.73 nM) was within the range of reported values in literature (2.4 nM: Nakayama *et al.*, 2009; 10 nM: Qi *et al.*, 2012; 10-20 nM: Tassone *et al.*, 2003; 10  $\mu$ M: Meñendez *et al.*, 2001). MCF12A cells showed a lower susceptibility to the drug than MDA-MB-231 cells (Figure 5.2A:  $IC_{50}$  not determined). The compounds selected for assessment of toxicity in human cells by MTT assay were those that were found to have inhibitory effects on the *in vitro* chaperone activities of PfHsp70-1 and PfHsp70-x (Chapter 3) as well as inhibitory effects (with  $IC_{50}$  values < 20  $\mu$ M) on the growth of *P. falciparum* as determined by the LDH growth inhibition assay (Section 5.3.2). Compounds found to have significant effects in both parasites and *in vitro* work were lapachol, bromo- $\beta$ -lapachona, malonganenone A and malonganenone C. The concentrations at which the selected test compounds were assayed were based on the  $IC_{50}$  concentrations resulting from the LDH parasite growth assay (Table 5.2).

While the main cell line for the research design was the malignant cell line MDA-MB-231, the availability of the non-malignant MCF12A cell line provided an opportunity to include an additional control cell line for a preliminary comparative study. Compounds were thus screened at a single concentration (the  $IC_{50}$  concentrations in Table 5.2, rounded to 20  $\mu$ M for lapachol and bromo- $\beta$ -lapachona, 1  $\mu$ M for malonganenone A and 5  $\mu$ M for malonganenone C) in MCF12A cells, and in MDA-MB-231 cells, compounds were assayed at 1, 10 and in some cases 50 times the  $IC_{50}$  values determined for parasites. The results of the MTT assays screening test compounds at selected concentrations are illustrated in Figure 5.2B (MDA-MB-231) and C (MCF12A). At 20  $\mu$ M lapachol was found to be non-toxic to MDA-MB-231 cells and minimally toxic to MCF12A cells (90 % cell survival,  $P \leq 0.001$ ) but significantly ( $P \leq 0.001$ ) compromised the survival of MDA-MB-231 cells at 200  $\mu$ M (~ 50 % cell survival). Bromo- $\beta$ -lapachona treatment resulted in a significantly ( $P \leq 0.001$ ) low cell survival of  $\leq 20$  % in MCF12A cells (at 20  $\mu$ M) as well as MDA-MB-231 cells (at 20  $\mu$ M and 200  $\mu$ M). At 1  $\mu$ M (data not shown) and 10  $\mu$ M, malonganenone A had no significant effect on the survival of MDA-MB-231 cells, whereas at 50  $\mu$ M in MDA-MB-231 cells and at 1  $\mu$ M in MCF12A cells, malonganenone A had a slight (94 % and 92 % respectively) but significant ( $P \leq 0.01$ ) effect on cell survival. malonganenone C, assayed at 50 and 250

$\mu\text{M}$  in MDA-MB-231 cells and at 5  $\mu\text{M}$  in MCF12A cells, resulted in cell survivals of  $\geq 90\%$  in both cell lines, with only the effect on MCF12A cells (90 % cell survival,  $P \leq 0.001$ ) being statistically significant.

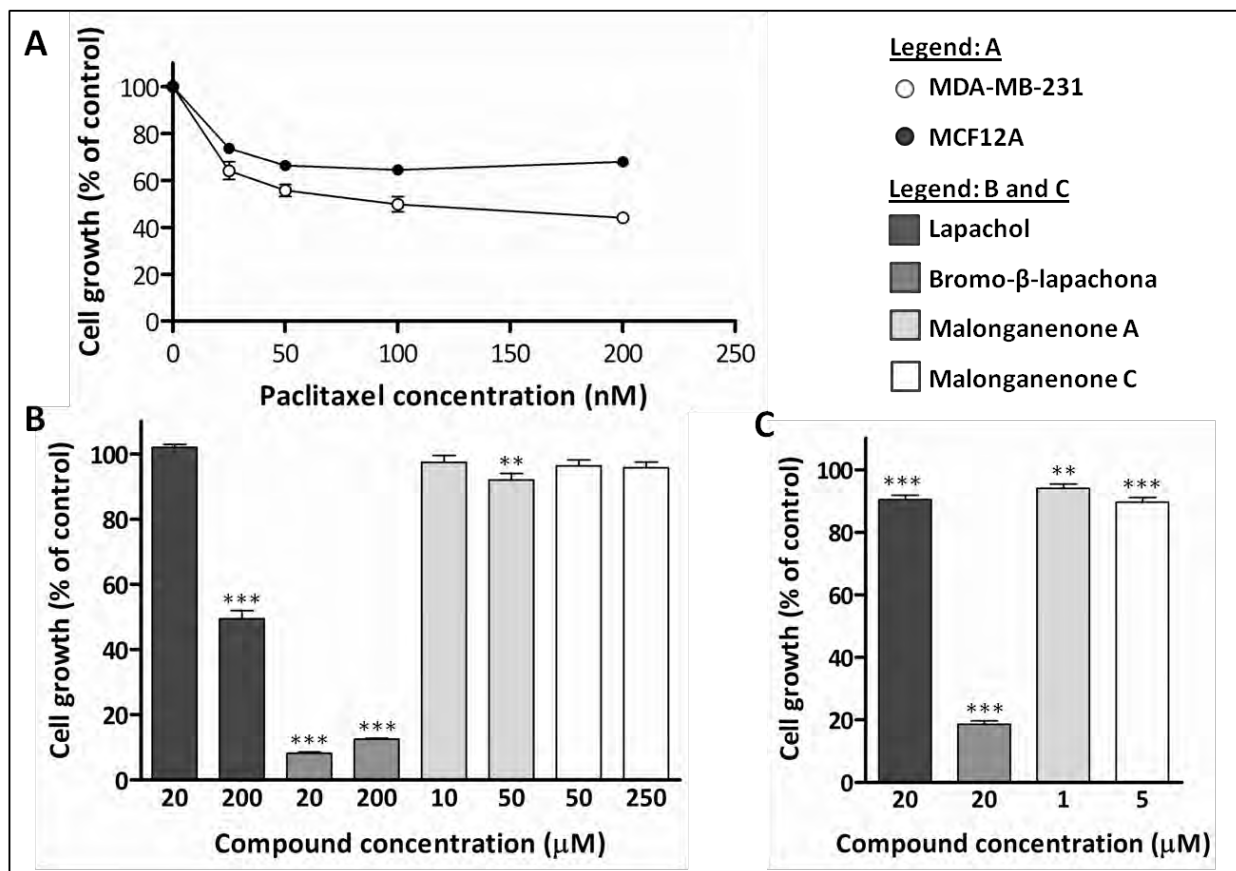


**Figure 5.2: The effect lapachol, bromo- $\beta$ -lapachona, malonganenone A and malonganenone C on the survival of two human cell lines.** (A) Percentage cell survival of MDA-MB-231 (open circles) and MCF12A (closed circles) cells after treatment with a range of concentrations of paclitaxel (positive control). (B and C) The effect of four compounds of interest at selected concentrations on the survival of MDA-MB-231 (B) and MCF12A (C) cells. In (B) and (C), the sets of bars coloured from darkest to lightest (left to right) represent data for lapachol, bromo- $\beta$ -lapachona, malonganenone A and malonganenone C respectively. All data represents percentage cell survival after 72 hour treatment measured using an MTT cell proliferation assay kit and was calculated relative to a DMSO vehicle control of a corresponding DMSO percentage (maximum 1 %). Data in A, B and C represents averages of nine replicates carried out across three assay plates and error bars indicate standard deviation. Statistical significance of differences relative to 100 % is indicated by asterisks above bars in B and C ( $P \leq 0.001$ : \*\*\*,  $P \leq 0.01$ : \*\*,  $P \leq 0.05$ : \*).

## 5.4. DISCUSSION

---

The assessment of the predicted permeability and solubility of the compounds included in this study according to Lipinski's Rule of 5 (Lipinski *et al.*, 2001) showed that all compounds were within the acceptable range for each assessment criterion, except in the case of malonganenone A and malonganenone C, which both had LogP values greater than the acceptable maximum of 5. The LogD values for malonganeones A and C, both at pH 7.4 and pH 5.5, also exceeded 5. All five compounds, however, can be predicted as being sufficiently permeable and soluble to be considered as drug candidates, since no compound had more than one violation of the Rule of Five. It is not surprising that the LogP values of two of the three malonganenone compounds assessed exceeded the acceptable range considering they all have long hydrocarbon chains in their structures (Chapter 3, Table 3.1), contributing to their high hydrophobicities.

The results of the LDH assays carried out to determine the antimalarial activity of test compounds showed that two compounds (malonganenone A and malonganenone C) had relatively high antimalarial activities ( $\leq 5 \mu\text{M}$ ), particularly malonganenone A, with an  $\text{IC}_{50}$  of  $< 1 \mu\text{M}$ . Lapachol, hydroxy- $\beta$ -lapachona and bromo- $\beta$ -lapachona have lower antimalarial activities, but still show moderate toxicity towards the parasites, with  $\text{IC}_{50}\text{s} \leq 25 \mu\text{M}$ . Lapachol and bromo- $\beta$ -lapachona have both previously been found to inhibit *P. falciparum* growth (strain F32) with reported  $\text{IC}_{50}$  values of  $24.4 \mu\text{M}$  and  $2.7 \mu\text{M}$  respectively (Pérez-Sacau *et al.*, 2005) – values comparable to those obtained in this study. Malonganenone B and  $\alpha$ -lapachona had little antimalarial activity ( $\text{IC}_{50} > 50 \mu\text{M}$ ), and four compounds were found to be completely non-toxic to *P. falciparum* parasites in the LDH assay. Mal3-39, previously found to have an  $\text{IC}_{50}$  of  $0.8 \mu\text{M}$  toward *P. falciparum* growth (Chiang *et al.*, 2009) was found to have a slightly higher  $\text{IC}_{50}$  of  $\sim 30 \mu\text{M}$  in this study. This discrepancy could be attributed to the different growth assays used, LDH assay in this case vs. a [ $^3\text{H}$ ] Hypoxanthine uptake assay used by Chiang and colleagues (2009).

Lapachol, bromo- $\beta$ -lapachona, malonganenone A and malonganenone C were considered compounds of interest in this study, since they exhibited inhibitory activities toward the *in vitro* chaperone activities of one or both of the malarial Hsp70s included in the study (PfHsp70-1 and PfHsp70-x, Chapter 3) as well as toward parasite growth as assessed by the LDH assay in this chapter. These compounds of interest were thus subjected to further assessment of toxicity toward human cell lines. The four compounds were initially screened for effects on human cells (both MDA-MB-231 and MCF12A lines) at the  $\text{IC}_{50}$

concentrations determined for each of them in *P. falciparum* growth assays. Higher concentrations (10 or 50 times the IC<sub>50</sub> values) were then tested on only the MDA-MB-231 cells (due to limited availability of MCF12A cells). At its parasite IC<sub>50</sub> value of 20 µM, lapachol was found to have little to no toxicity to either human cell line, however, at 200 µM lapachol was toxic (50 % cell survival) to MDA-MB-231 cells. Previously, lapachol has been found to have a variety of IC<sub>50</sub>s to various cancer cell lines, ranging from 1.9 µM in ovarian cancer cells (A2780), to 76 µM in breast cancer (T-47D) cells. At 20 µM (parasite IC<sub>50</sub>) bromo-β-lapachona was highly toxic (< 20 % cell survival) to both cell lines. Malonganenone A and malonganenone C displayed similar limited toxicities to MCF12A cells (> 90 % cell survival) at 1 and 5 µM respectively (parasite IC<sub>50</sub> concentrations), and at 10 and 50-fold these IC<sub>50</sub> concentrations, showed similarly low toxicities toward MDA-MB-231 cells (> 90 % cell survival). Malonganenones A-C, previously found to have moderate biological activity towards six oesophageal cell lines (IC<sub>50</sub>s ranging from 17 µM to > 100 µM) have also been reported to have IC<sub>50</sub>s towards MCF12A cells of 20.7, 18.7 and > 100 µM respectively.

Though none of the compounds tested here were found to have extremely high antimalarial activities (nanomolar range), several compounds did exhibit relatively low IC<sub>50</sub>s to parasites, as well as limited toxicities to human cell lines at 50 times the IC<sub>50</sub>s to parasites, and thus represent possible platforms for further research and rational drug design. Malonganenone A in particular is of interest, as it has a low IC<sub>50</sub> toward parasites (1 µM), low toxicity toward human cell lines (> 90 % cell survival at 50 times the parasite IC<sub>50</sub> concentration in MDA-MB-231 cells), and passes the Lipinski assessment as a “drug-like” compound.

Despite the fact that the LDH and MTT assays used in this study are a good starting point of an indication of the toxicity of the selected compounds towards parasites and mammalian cells, no cytotoxicity assays are infallible. In a study published in International Journal of Pharmaceutics in 2005, a comparison was made between different methods for cytotoxicity determination in mammalian cells. The MTT method, an LDH assay, a neutral red assay and an assay measuring the ATP content of cells were all tested in one system (mouse fibroblasts), with a number of different toxic agents with known mechanism of toxicity (Weyermann *et al.*, 2005). Significant differences (0.1 – 200 mM and 4 – 1300 mM IC<sub>50</sub> values) in results were obtained for compounds across different assays, and the conclusion was drawn that not all assays are suited to cytotoxicity assessments of all compounds (Weyermann *et al.*, 2005). An idea of the mechanism of action of a test compound as well as the mechanism of cell death (e.g. apoptosis vs.

necrosis) can help in making the right choice for an assay (Weyermann *et al.*, 2005). MTT and LDH assays, for example, were found to be unsuitable for compounds which only affect intracellular processes or targets (Weyermann *et al.*, 2005). In terms of toxicity determination in *P. falciparum* parasites, there are also a number of available methods besides the LDH assay used in this study. These include a hypoxanthine incorporation assay, assessment by light microscopy, enzyme-linked immunosorbent assays (ELISA) and flow-cytometry-based assays (Noedl *et al.*, 2003, Karl *et al.*, 2009). The LDH assay, though relatively simple and amenable to high-throughput screening, it has been found to be less sensitive than other methods (Basco *et al.*, 1995, Noedl *et al.*, 2003).

Going forward with this work, therefore, it would be important to further investigate and characterise the toxic effects of compounds of interest with more rigorously using a number of different methods, and possibly expanding the study to using multiple *P. falciparum* strains, as well as to more mammalian cell lines. In this study, breast cells were used, as these were readily available, however it would be advantageous to test the toxicity of compounds of interest towards more suitable mammalian cells such as hepatocytes and peripheral blood mononuclear cells (PBMC), since the liver and the blood stream form important stages in the *P. falciparum* life cycle (Sinnis and Sim, 1997).

**CHAPTER 6:**

---

**Conclusions, discussion and future work**

---

## 6.1. SUMMARY OF EXPERIMENTS AND KEY FINDINGS

---

The broad and overall objective of this study was to investigate a set of compounds as potential modulators of the *in vitro* chaperone activities of two malarial Hsp70s (PfHsp70-1 and PfHsp70-x) compared to the human Hsp70, HSPA1A (HsHsp70), and to assess the effects of any such modulators on *P. falciparum* and mammalian cell growth.

The purified recombinant proteins described in Chapter 2 were used to carry out *in vitro* experiments toward the completion of Objectives 2 and 3 (Section 1.4). These experiments involved assessing the effects of test compounds on the *in vitro* aggregation suppression and ATPase activities of the Hsp70s of interest. Binding studies using SPR were also carried out to establish the interactions between Hsp70s and compounds and between Hsp70s and Hsj1a. The purified recombinant human Hsp70 was not amenable to aggregation suppression assays (Section 3.2.3), and thus the effects of the compounds on the aggregation suppression activity were compared only between PfHsp70-1 and PfHsp70-x. The basal and Hsp40-stimulated ATPase assays were carried out using malarial Hsp70s and human Hsp70 allowing for a comprehensive comparison between the effects of compounds on the various chaperone / -co-chaperone systems.

From an initial set of eleven compounds, five (lapachol, bromo- $\beta$ -lapachona, malonganenone A, B and C) were chosen for further investigation based on their inhibitory effects on the aggregation suppression activity of PfHsp70-1 (Section 3.3.1). The effects of these five compounds on the aggregation suppression activities of PfHsp70-1 and PfHsp70-x and on the basal and Hsp40-stimulated ATPase activities of PfHsp70-1, PfHsp70-x and HsHsp70 are summarised in Table 6.1. To complement the *in vitro* activity assays carried out with Hsp70s and test compounds, a biophysical binding assessment was conducted using SPR to assess both the potential interactions between compounds and Hsp70s, as well as the potential disruption of Hsp70-Hsp40 interactions by compounds. These results, though preliminary, are also summarised in Table 6.1. All eleven compounds were tested for effects on the survival of *P. falciparum in vitro*. The compounds able to modulate Hsp70s *in vitro* as well as inhibit the growth of cultured malaria parasites (lapachol, bromo- $\beta$ -lapachona, malonganenone A, and C) were tested for toxicity toward two mammalian breast cell lines (MDA-MB-231 and MCF12A). To complement the toxicity experiments, the compounds were assessed *in silico* for their predicted oral bioavailabilities



using the Rule of Five based on their chemical structures (Lipinski *et al.*, 2001, Section 5.3.1). All eleven compounds were found to have acceptable predicted oral bioavailabilities as no compound had more than one violation of the four criteria described in the Rule of Five. One violation regarding the logP values, which are a measure of solubility, was identified for both malonganenone A and malonganenone C. Malonganenone A and C had logP values > 5, which are indicative of very high hydrophobicity. The results of the cell culture experiments and the Rule of Five assessment are also summarised in Table 6.1.

The biochemical features of PfHsp70-x were previously largely uncharacterised. Thus, the aggregation suppression and ATPase activities of PfHsp70-x were investigated in this study. PfHsp70-x was found to have a significant aggregation suppression activity, reducing the thermally induced aggregation of MDH to ~20 % at 0.18  $\mu\text{M}$  compared to ~40 % by PfHsp70-1 at a higher (0.36  $\mu\text{M}$ ) concentration. A kinetic assessment of the ATPase activity of PfHsp70-x was carried out, and the chaperone was found to have a basal steady-state ATPase activity of 0.21 mmol ATP/ min / mol protein, and a  $K_m$  for ATP of 393  $\mu\text{M}$  (Section 3.3.2). These values are comparable to those previously published for PfHsp70-1 (Matambo *et al.*, 2004). The stimulation of the ATPase activity of PfHsp70-x had also not been shown previously, and in this study, Hsj1a was found to significantly stimulate the ATPase activity of PfHsp70-x.

**Table 6.1: Summary of the results of the assessment of compounds in terms of Hsp70 modulation, biophysical interactions with Hsp70s, toxicities toward *P. falciparum* and mammalian cells *in vitro*, and predicted oral bioavailability.**

	Modulation of <i>in vitro</i> aggregation suppression activity of Hsp70s	Modulation of basal <i>in vitro</i> ATPase activities of Hsp70s	Modulation of Hsp40-stimulated <i>in vitro</i> ATPase activities of Hsp70s	Biophysical interactions with Hsp70s	<i>In vitro</i> toxicity to <i>P. falciparum</i> (IC <sub>50</sub> , μM)	Effects on mammalian cell growth in culture	<i>In silico</i> predicted oral bioavailability
<b>Lapachol</b>	•PfHsp70-1: inhibition only at 300 μM	•PfHsp70-x: inhibition (~ 35 %)	•PfHsp70-1 & Hsj1a: stimulation (~20 %) •PfHsp70-x & Hsj1a: inhibition (~50 %)	•Suggested interactions with all three Hsp70s, strongest affinity for PfHsp70-x (K <sub>D</sub> : 0.79 x 10 <sup>-6</sup> M)	•18.67 ± 2.27	•Moderate (~50 %) MDA-MB-231 cell survival at 10 x parasite IC <sub>50</sub>	•Good – no violation of Rule of Five
<b>Bromo-β-lapachona</b>	•PfHsp70-1 & PfHsp70-x: marked inhibition from 100 μM.	•PfHsp70-x: inhibition (~ 80 %) •HsHsp70: inhibition (~15 %)	•PfHsp70-1 & Hsj1a: stimulation (~ 30 %) •PfHsp70-1 & PfHsp40: inhibition (~ 75 %) •PfHsp70-x: inhibition (~ 90 %) •HsHsp70 & Hsj1a: stimulation (~ 10 %)	•Suggested interactions with all three Hsp70s, non-specific binding effects, non-quantifiable interactions.	•17.29 ± 4.44	•Low (~10 % and ~20 %) survival of MDA-MB-231 & MCF12A cells at parasite IC <sub>50</sub>	•Good – no violation of Rule of Five
<b>Malonganenone A</b>	•PfHsp70-1: marked inhibition from 10 μM •PfHsp70-x: inhibition only at 300 μM	•PfHsp70-1: stimulation (~ 15 %)	•PfHsp70-1 & PfHsp40: inhibition (~ 65 %) •PfHsp70-x & Hsj1a: inhibition (~ 20 %)	•Specific interactions with all three Hsp70s, highest affinity for PfHsp70-1, lowest for HsHsp70 • Abrogation of Hsj1a interaction with all three Hsp70s	•0.81 ± 0.24	•High (~90 %) MDA-MB-231 cell survival at 50 x parasite IC <sub>50</sub>	•Good: single violation of Rule of Five (high hydrophobicity)
<b>Malonganenone B</b>	•PfHsp70-1: inhibition only at 300 μM	•No significant modulation	•PfHsp70-x & Hsj1a: inhibition (~ 10 %)	•Suggested interactions with all three Hsp70s, non-quantifiable interactions.	•>50	ND	•Good – no violation of Rule of Five
<b>Malonganenone C</b>	•PfHsp70-1: marked inhibition from 10 μM	•No significant modulation	•PfHsp70-x & Hsj1a: inhibition (~ 10 %)	•Specific interactions with all three Hsp70s, lower affinity for PfHsp70-x than for PfHsp70-1 & HsHsp70.	•5.20 ± 2.49	•High (>90 %) MDA-MB-231 cell survival at 50 x parasite IC <sub>50</sub>	•Good: single violation of Rule of Five (high hydrophobicity)

## 6.2. CONCLUSIONS AND DISCUSSION

---

The desired outcome of this study was the identification of one or more compound(s) that specifically inhibit malarial Hsp70s, and not human Hsp70, and that are toxic to malaria parasites, but not to human cells. Table 6.1 allows for overall observations and comparisons to be made about the compounds of interest and their effects.

One of the most striking observations is that bromo- $\beta$ -lapachona is the most biologically active molecule of the five compounds tested based on its significant effects in the human and malarial chaperones *in vitro*, as well as on the cell viability assays of both malarial and human whole cell systems. Bromo- $\beta$ -lapachona inhibited the ATPase activity of PfHsp70-x (basal and Hsj1a-stimulated) by > 80 %, and was the only compound found to inhibit all three Hsp70s in either their basal or Hsp40-stimulated ATPase activity or both. Bromo- $\beta$ -lapachona also inhibited the aggregation suppression activities of both malarial Hsp70s. In addition to the effects on chaperone activity, bromo- $\beta$ -lapachona was moderately toxic to malaria parasites ( $IC_{50} \sim 20 \mu\text{M}$ ) and highly toxic to mammalian cells resulting in only 10 % and 20 % cell survival in MDA-MB-231 and MCF12A cell respectively at 20  $\mu\text{M}$ .

Another significant observation from Table 6.1 is that the malonganenone compounds, and in particular malonganenone A, display the most desired effects of the compounds included in this study. Malonganenone A inhibited the aggregation suppression activities of both PfHsp70-1 and PfHsp70-x, and also modulated the ATPase activities of both malarial Hsp70s (either basal or Hsp40-stimulated activity), but had no effect on either the basal or the Hsj1a-stimulated ATPase activity of HsHsp70. Malonganenone A had the most potent effect of all compounds on *P. falciparum* growth *in vitro* ( $IC_{50} \sim 1 \mu\text{M}$ ); however, at the parasite  $IC_{50}$  (MCF12A cells) and at 50 times the parasite  $IC_{50}$  (MDA-MB-231 cells), the compound inhibited mammalian cell growth by < 10 %. Malonganenones B and C had similar but less pronounced effects than malonganenone A. Both compounds inhibited the aggregation suppression activity of PfHsp70-1 as well as the Hsj1a-stimulated ATPase activity of PfHsp70-x but had no effect on the ATPase activity of HsHsp70. Malonganenone B had low toxicity toward parasites ( $IC_{50} > 50 \mu\text{M}$ ) and was therefore not tested on mammalian cells. Malonganenone C had a higher toxicity toward parasites ( $IC_{50} \sim 5 \mu\text{M}$ ) and very little toxicity toward mammalian cells at the parasite  $IC_{50}$  ( $\sim 90$  % MCF12A cell survival) and at 50 times the parasite  $IC_{50}$  ( $> 90$  % MDA-MB-231 cell survival). Malonganenone A (and to

a lesser extent malonganenones B and C) thus affects malarial systems but not (or too a much lesser extent) human systems (*in vitro* chaperones and cell systems) and is therefore a novel candidate for further potential antimalarial drug design. Though the potency of the compound's antimalarial activity is relatively low, a review on compound screening in antimalarial drug discovery deemed compounds with  $IC_{50}$ s of between 1 and 5  $\mu$ M worthy of further testing and development, where the next step would be to test the compound's toxicity to parasites in *in vivo* animal studies (Fidock *et al.*, 2004). Malonganenone A also represents an intriguing and novel class of compounds which has limited toxicity in human cells, and has antimalarial activity possibly due to Hsp70 modulation. This study thus warrants not only further investigation of the prenylated alkaloid class of compounds as antimalarials (Section 6.3), but also further investigation into Hsp70 as a novel antimalarial drug target. In this study malonganenone A was found to inhibit malarial Hsp70s with some degree of specificity (HsHsp70 was not affected), and was also found to have antimalarial activity. Despite these findings, it cannot be deduced from the present work that the observed antimalarial activity is due to PfHsp70-1 and/or PfHsp70-x modulation, and that the malarial Hsp70s are the target for the compound's biological activity. Malonganenone A may well be acting via a different mechanism on a different target and further experiments (Section 6.3) have to be conducted to clarify the mechanism of action of the compounds.

It must be noted as a possible limitation of this study that the human Hsp70 (HSPA1A), being a heat-inducible rather than constitutively expressed Hsp70, was perhaps not an ideal human Hsp70 to use as a control protein. Inhibition of a heat-inducible Hsp70 such as HSPA1A, which is generally not expressed by cells under normal growth conditions, may not have any effect on cell growth. This is in contrast to PfHsp70-1 which, though being heat-inducible, is highly expressed at all stages of the erythrocytic lifecycle of the parasite. Whether or not PfHsp70-x is heat-inducible has not been investigated as yet. The use of a constitutively expressed Hsp70, such as Hsc70, would perhaps have been a better choice. Inhibition of this protein could potentially have led to induction of the heat shock response, allowing Hsc70 inhibition to be observed and monitored as an *in vivo* output of Hsc70 inhibition. The human Hsp70 used, however, did successfully serve to illustrate that highly homologous Hsp70s can be differentially modulated by small molecules.

Though the compound set included in this study is very small, the fact that the set of test compounds included two groups of molecules each containing structurally related members allows for tentative

inference of possible structure-activity relationships (SAR) based on findings of distinct effects of structurally similar compounds. In the case of the malonganenones, for example, it is interesting to note that malonganenones B and C had very similar effects on the modulation of Hsp70 ATPase activities, both having significant modulatory effects only on the Hsj1a-stimulated ATPase activity of PfHsp70-x and not on any other Hsp70s of Hsp70-Hsp40 systems they were tested on. Similarly, both malonganenone B and C inhibited the aggregation suppression activity of PfHsp70-1 but not of PfHsp70-x. Malonganenone A, on the other hand, inhibited the aggregation suppression activity of both PfHsp70s and modulated the ATPase activities of several Hsp70 or Hsp70-Hsp40 systems. Structural differences or similarities between the compounds can be seen in Table 3.1, in which compounds have been drawn in configurations highlighting the similarities. In malonganenones A-C, the hydrophobic hydrocarbon chain portions of the three compounds is identical, and structural differences lie in the nitrogen-containing portions of the compounds on the left extremes of the molecules as they are depicted in Table 3.1. Malonganenone A contains a purine constituent (a six-membered heterocyclic ring containing two nitrogen atoms fused to an imidazole ring – a five-membered heterocyclic ring also containing two nitrogen atoms) whereas malonganenone B contains only the furan portion of the fused ring, and malonganenone C contains no ring structures at all. These observations suggest that the binding of malonganenones A-C to Hsp70s is perhaps determined by the hydrocarbon chain portion of the compounds or alternatively by the overall shape, size, and hydrophobicity of the compound. The observed effect of modulation upon such binding, however, is likely to be incurred by the purine portion in malonganenone A, or in the case of malonganenones B and C, the corresponding portions of the compounds. As discussed in Chapter 3 (Section 3.4), the hydrophobic malonganenone compounds may be binding in the hydrophobic substrate binding pocket of Hsp70s. The proposed binding of the malonganenone compounds to Hsp70s via the hydrocarbon chain portion of the compounds is further supported by the fact that the compound PGKC4\_4I, which is identical to the ring portion of malonganenone B but lacks the hydrocarbon chain, had no effect on the aggregation suppression activity of PfHsp70-1, whereas malonganenone B had a significant effect.

A potentially problematic structural feature of the compounds tested in this study is the presence of  $\alpha,\beta$ -unsaturated ketones. These functional groups are highly susceptible to nucleophilic attack, and thus it is possible that the compounds that were found to modulate Hsp70 function are doing so in an irreversible, covalent manner, as was recently described for methylene blue: the compound was found to inhibit human Hsp70 (HSPA1A), and after dialysis to facilitate the removal of compound, the Hsp70

did not regain full activity, an observation indicative of a covalent, non-reversible mechanism of inhibition (Miyata *et al.*, 2012). Irreversible inhibitors of protein targets have a number of favourable properties including high biochemical efficiency and longer duration of action compared to non-covalent drugs, however, irreversible inhibitors are generally avoided in drug discovery or design due to the associated toxic effects attributed to factors such as lack of specificity and immunogenicity toward target-compound adducts (Johnson *et al.*, 2010).

From the various findings of the assessments of small molecules as malarial Hsp70 modulators and as potential antimalarial compounds discussed above, comparisons can be made between the small molecules in this study and those reported on in literature, in terms of Hsp70 modulation and whole cell toxicities. Malonganenone A exhibited *in vitro* toxicity to *P. falciparum* in the same range as MAL3-39 and related compounds reported on in the study by Brodsky research group, where MAL3-39 was found to have an  $IC_{50}$  of 0.8  $\mu$ M toward *P. falciparum* (Chiang *et al.*, 2009) – the same toxicity determined for malonganenone A in this study. The degree of modulation of the basal steady-state ATPase activity of PfHsp70-1 by malonganenone A is also similar to that by MAL3-39 (both compounds at 300  $\mu$ M): 28 % inhibition of activity by MAL3-39 vs. 15 % stimulation by malonganenone A (Chiang *et al.*, 2009). In the case of both compounds, the basal ATPase activity of HsHsp70 was less affected (or in the case of malonganenone A, unaffected) by the small molecules than PfHsp70-1.

PfHsp70-x, a previously uncharacterised protein in terms of chaperone activity, was significantly modulated by small molecules in this study. Compared to PfHsp70-1 (in this study as well as previous studies: Chiang *et al.*, 2009; Botha *et al.*, 2011), the basal ATPase activity (steady-state) of PfHsp70-x was modulated to a much higher degree, in particular by the 1,4 naphthoquinone compounds: lapachol and bromo- $\beta$ -lapachona inhibited PfHsp70-1 activity by  $\sim$  60 % and  $\sim$  80 % respectively – a significantly higher degree of modulation than reported for any small molecules tested on PfHsp70-1 activity. Much lower levels of modulation on both PfHsp70-1 and HsHsp70 by these small molecules suggest a degree of specificity of the compounds for PfHsp70-x.

The spergualin compound DSG has been extensively characterised as an Hsp70 modulator, and various characteristics of the molecule as a modulator can be compared to the small molecules of interest to this study. DSG has been found to modulate the steady-state ATPase activities of several Hsp70s and/or Hsc70s, stimulating the activity of mammalian Hsc70 by  $\sim$  40 % (Nadeau *et al.*, 1994; Brodsky, 1999).

DSG has been found to bind to Hsc70 with an affinity ( $K_D$ ) of  $4 \times 10^{-6}$  M (Nadeau *et al.*, 1994), with the C-terminal EEVD domain of Hsp70 being the proposed binding site for the compound (Nadeau *et al.*, 1994; Nadler *et al.*, 1998; Ramya *et al.*, 2006). In addition to modulating the ATPase activity of Hsp70, DSG has been shown to modulate the ATP-stimulated aggregation suppression activity of PfHsp70-1 (Ramya *et al.*, 2006). Affinities of some of the small molecules in this study for Hsp70s are comparable to the affinity of DSG for Hsp70: a number of Hsp70-small molecule interactions were quantified as having  $K_D$  in the micromolar range (for example lapachol and Hsp70s:  $\sim 1-2 \times 10^{-6}$  M). Similar levels of binding of lapachol were observed between the malarial Hsp70s and HsHsp70 in this study (using SPR), and thus it is unlikely that the binding site for lapachol is the EEVD motif, since the HsHsp70 produced for use in this study lacks the EEVD motif. In the case of malonganenone A, however, it is feasible to consider the EEVD motif as a possible binding site; based on the finding that malonganenone A had higher affinities for the malarial Hsp70s than for HsHsp70, which lacked the EEVD motif. Malonganenone A and DSG also share similar *in vitro* parasite toxicities, with  $IC_{50}$ s of 0.8 and 0.81  $\mu$ M respectively (Ramya *et al.*, 2007). It must be re-iterated here, however, that the binding affinities reported in this study are considered preliminary, and need to be validated by further experiments as described in Section 4.4.

Findings reported on in Chapter 3 (discussed in Section 3.4) suggest that malonganenone A was physically disrupting the interaction between PfHsp70-x and Hsj1a, a hypothesis further supported by the binding studies shown in Chapter 4, showing diminished binding of Hsj1a to Hsp70s in the presence of malonganenone A. As reviewed in Chapter 1 (Section 1.1.4.1), a small molecule (115-7c) has been identified by the Gestwicki research group as regulating Hsp70 activity by binding at the Hsp70-Hsp40 interface. The compound was found, using ITC, to have a higher affinity for the Hsp70-Hsp40 complex ( $K_D = 113 \times 10^{-6}$  M) than for Hsp70 alone ( $K_D = 220 \times 10^{-6}$  M) or Hsp40 alone ( $K_D > 1000 \mu$ M). Malonganenone A was found to bind to PfHsp70-x with a higher affinity than 115-7c did to Hsp70 (DnaK) in the Gestwicki study; however, it is possible that malonganenone A is binding to PfHsp70-x in a similar way. The binding of malonganenone A could be further investigated using ITC to assess the relative affinities of the compound for PfHsp70-x in the presence and absence of Hsj1a, and for Hsj1a alone. Such an investigation could potentially help determine the binding site of the compound. The possible binding sites for the malonganenone compounds as well as the naphthoquinones were also discussed in Chapter 3 (Section 3.4).

In the work carried out in Chapters 3 and 4, Hsj1a was used simply to demonstrate Hsp70-Hsp40 interactions to allow for the assessment of the effects of compounds on such interactions. In reality, however, it is unlikely that either PfHsp70-1 or PfHsp70-x would ever encounter Hsj1a in the biological system. PfHsp70-1 is a parasite resident protein, and thus would not come into contact with any human Hsp40s, and though PfHsp70-x is exported into the human erythrocyte, and thus may encounter and interact with human Hsp40s, Hsj1a (DNAJB2) has not been reported to be expressed in the erythrocyte. In fact, to our knowledge, proteomic studies have only identified four human Hsp40s in the erythrocyte: DNAJC13 (Rme8, Gm1124), DNAJB4 (Hsc40), DNAJB1 (Hsp40, Hdj1) (van Gestel *et al.*, 2010, Kampinga *et al.*, 2009) and DNAJC5 (Csp) (Pasini *et al.*, 2006; Kampinga *et al.*, 2009). Of these four human Hsp40s, which could potentially act as co-chaperones to the exported PfHsp70-x, only one (DNAJB4) has a putative homolog in *P. falciparum* (PFB0595w, Njunge *et al.*, 2013). Though DNAJB1 (Hdj1) and DNAJB2 (Hsj1a) are not closely related Hsp40s (Hageman and Kampinga, 2009), both are type II Hsp40s, and they have been suggested to interact with and stimulate the ATPase activity of Hsp70 in a similar manner (Gao *et al.*, 2012). For this reason, the use of Hsj1a as a model co-chaperone partner to PfHsp70-x in this study is justified.

Not only does malonganenone A represent an interesting new class of antimalarials, but the compound, and indeed all five compounds of interest in this study, are a useful tool for further investigating Hsp70s and Hsp70-Hsp40 systems and the mechanisms involved in their interactions and modulation. The varied and diverse range of effects of compounds on the different and yet highly conserved Hsp70s as well as on the highly conserved Hsp70-Hsp40 interactions further supports previous work (Chiang *et al.*, 2009; Botha *et al.*, 2011) showing not only that, despite high sequence identity, different Hsp70s can be differentially modulated by small molecules, but also that the ways in which Hsp70s interact with different Hsp40s are distinct enough from each other to allow for Hsp70-Hsp40 systems to be specifically modulated, as illustrated in this study by the opposing modulatory effects that lapachol, bromo- $\beta$ -lapachona and malonganenone A had on the ATPase activity of PfHsp70-1-PfHsp40 compared to PfHsp70-1-Hsj1a. It must be noted, however, the PfHsp70-1-Hsj1a interaction is a biologically irrelevant one, since PfHsp70-1 is a parasite resident Hsp70 and Hsj1a is a human Hsp40, whereas PfHsp40 is thought to be the endogenous, cytosolic co-chaperone partner to PfHsp70-1. This difference may account in part for the distinct modulatory effects observed between the two Hsp70-Hsp40 systems.



The use of MDH aggregation suppression assays for the assessment of small molecules as potential modulators of chaperone activity of Hsp70s has not been previously reported, and thus represents a novel tool for screening for Hsp70 modulators. Limitations of the methods include the fact that the assay is not conducive to high throughput screening, and requires large amounts of proteins. In addition, as described in Section 3.3.1, the assay is not suitable for use with some compounds, as the compounds themselves affected the degree of MDH aggregation in the absence of chaperone. The assay is also not suitable for use with all proteins, as was the case for the HsHsp70 purified for use in this study. The chaperone itself was found to be thermolabile, aggregating at 48 °C. In contrast, the malarial Hsp70s used were found to be highly thermostable and thus suitable for assessment by the MDH aggregation suppression assay. Alternative methods of assessing the aggregation suppression activity of chaperones include the use of different substrates, such as citrate synthase (Yano *et al.*, 2004), glutamate dehydrogenase, alcohol dehydrogenase and lactalbumin (Ramya *et al.*, 2006); as well as the inclusion of ATP, which has been found to enhance the aggregation suppression activity of chaperones (Ramya *et al.*, 2006). Compared to the ATP-free MDH aggregation suppression assay carried out in this study, a similar assay including ATP could be considered a more physiologically accurate system. Related to the aggregation suppression activity of chaperones is the refolding activity, commonly exploited as a means of assessing chaperone activity *in vitro*. Refolding assays generally involve the thermal or chemical denaturation of a substrate, and subsequent refolding of the substrate by dilution of the denatured substrate into chaperone-containing refolding buffer. A commonly used substrate in such assays is luciferase, where the assessment of the degree of refolding is achieved by monitoring the luciferase activity by luminescence detection (Minami *et al.*, 1996; Gassler *et al.*, 1998; Wisén and Gestwicki, 2008).

Cell death mechanisms in *P. falciparum* have been researched to some extent; however, as reviewed in a recent publication, findings in literature on the matter are somewhat contradictory and inconclusive. Various studies have been carried out, with conflicting conclusions, where *P. falciparum* cell death induced by stimuli including drugs and heat have been reported by some groups to occur via programmed cell death, while others report necrotic cell death. The review discusses these discrepancies and possible reasons for them, but also illustrates how little is known about exact cell death mechanisms and pathways in *P. falciparum* (Engelbrecht *et al.*, 2012). For this reason, it is difficult to speculate about the exact pathways or mechanisms by which Hsp70 inhibition could potentially cause death in malaria parasites at a molecular level, however, in a broader sense a number of scenarios are

conceivable. As reviewed in Chapter 1 (Section 1.1.3.1), PfHsp70-1 is considered the major cytosolic Hsp70 in *P. falciparum* and has been found to be upregulated upon heat treatment of parasites, and thus is assumed to play a major role in preventing the heat-induced cell death of parasites. Inhibition of this protein, therefore, may result in diminished parasite survival, particularly during the high temperature fevers associated with the malaria disease in humans. Considering PfHsp70-x is the only exported Hsp70 in *P. falciparum*, the exported Hsp70 may be a more promising drug target. PfHsp70-x, as reviewed in Section 1.1.3.1, is thought to play a role in trafficking of PfEMP1 to the erythrocyte membrane. Inhibition of this protein, therefore, could potentially result in abrogated trafficking of PfEMP1 and other exported proteins in the erythrocyte, which could result in a loss in the parasites ability to remodel the host cells. This loss of cell remodelling, and in particular the inability of the parasite to facilitate knob formation, could have a number of detrimental implications for the parasite. Not only would the severe effects of the malaria disease attributed to infected erythrocyte sequestration be avoided, but the parasite would no longer be able to avoid splenic clearance via sequestration, and infected erythrocytes would possibly be destroyed by the immune system.

The hypothesis of this study stated that “the basal and/or Hsp40-stimulated *in vitro* chaperone activity of PfHsp70-1 and/or PfHsp70-x can be selectively modulated by small molecules which inhibit the growth of *P. falciparum* parasites in culture”, and was shown to be supported by the findings of the research conducted. The data provides a platform for further studies into drug design and optimisation and towards gaining a deeper understanding of Hsp70 and Hsp70-Hsp40 mechanisms as well as the mechanisms by which modulators of these chaperones function. Such future studies are outlined in Section 6.3.

### 6.3. FUTURE WORK

---

Further work based on the findings in the present study could include the following:

#### 6.3.1. *Validation of biophysical findings*

---

As described and discussed in Chapter 4, the surface plasmon work carried out in this study had a number of limitations, and therefore the results were considered preliminary. For this reason, additional experiments would need to be carried out to validate the results. These experiments could include:

- Additional and more rigorous SPR analyses of the potential Hsp70-compound interactions including more extensive concentration ranges for to allow for more accurate quantification of affinities, as well as more replicates under various conditions (levels of protein immobilisation, association times).
- Alternative biophysical techniques could be employed to further validate the interactions and affinities of these, such as ITC or NMR.

#### 6.3.2. *Elucidating mechanisms of Hsp70(-Hsp40) modulation by small molecules*

---

- The inclusion of a non-hydrolysable ATP analogue such as AMP-PNP in MDH aggregation suppression assays could contribute to the understanding of mechanisms of Hsp70 modulation by the compounds. Compounds whose inhibitory effects on Hsp70 aggregation suppression activity are reduced in the presence of AMP-PNP are likely to bind in the ATPase domain of the Hsp70, whereas those whose effect is unchanged are likely to bind elsewhere, being able to exert their effect despite the ATPase domain being occupied.
- The use of truncated forms of Hsp70s of interest in ATPase assays, in particular Hsp70s possessing only ATPase domains and no SBDs, would allow for the discrimination between compounds which modulate ATPase activity directly (competitive binding in the ATPase domain) and those which have an indirect effect on ATPase activity (binding in for example the SBD, affecting ATPase activity by inducing a conformational change in the ATPase domain).

- Following on from the previous point, truncated forms of Hsp70s, possessing either only the ATPase domain or only the SBD, could be used in binding studies to determine the binding sites of small molecule modulators. SPR, for example, could be used to determine whether compounds preferentially bind to the ATPase domain or the SBD of an Hsp70.
- Bioinformatic assessments, such as *in silico* docking studies of compounds of interest with 3D models of PfHsp70-1 and PfHsp70-x would help elucidate mechanisms of modulation of Hsp70s by small molecules.
- Methods such as NMR and X-ray crystallography could be used to further investigate and confirm the specific binding sites of compounds on Hsp70s.

### **6.3.3. Development of novel antimalarials targeting PfHsp70s based on malonganenone A**

---

- For a broader profile of the antimalarial effect of malonganenone A, as well as the toxicity of the compound to mammalian cells, the molecule should be tested in a wide range of *P. falciparum* strains, including drug resistant strains, as well as in a wide range of mammalian cells including human cells from a wide range of tissues.
- As a means of further assessing the antimalarial properties of malonganenone A, *in vivo* toxicity assays should be conducted, using, for example, *Plasmodium* infected mice.
- Using malonganenone A as a starting point, chemical analogues of the compound could be synthesized and assessed for their modulatory effects on Hsp70s, as well as toxicity to parasites and mammalian cells. This process could contribute to the identification of more potent antimalarials targeting PfHsp70s, and would allow for structure-activity relationships to be determined for the chemical series.
- Freely available databases containing information on compounds and their reported biological activities could be used to identify small molecules with antimalarial activity which could be

tested as Hsp70 modulators, or alternatively, to identify more known Hsp70 modulators which could then be tested for antimalarial activity. One such repository is PubChem ([www.pubchem.ncbi.nlm.nih.gov](http://www.pubchem.ncbi.nlm.nih.gov)), in which the compounds described by the Brodsky group (Chiang *et al.*, 2009) along with their Hsp70 modulating effects are deposited. The PubChem database contains the chemical structures and biological properties of small molecules, along with descriptions of assays they have been tested in and the results of such testing (Wang *et al.*, 2010). A similar resource, ChemSpider ([www.chemspider.com](http://www.chemspider.com)), also freely available, is a project by the Royal Society of Chemistry. The ChemSpider database centralises and combines published compound data, allowing searches to be carried out by name or by chemical structure of small molecules, and yielding properties of the molecules, as well links to any original research articles in which the molecules are included. A further database is a set of over 13, 000 compounds which, in a screen of ~ 2 million compounds in GlaxoSmithKline's library, were found to inhibit *P. falciparum* growth by at least 80 % at 2  $\mu$ M, and over 8000 of these compounds were potent inhibitors of growth of a multidrug resistant *P. falciparum* strain (Gamo *et al.*, 2010). This set of compounds, including details of the screening results, is freely available ([https://www.ebi.ac.uk/chemblntd/download/#tcams\\_dataset](https://www.ebi.ac.uk/chemblntd/download/#tcams_dataset)). According to a structure similarity search conducted ([https://www.ebi.ac.uk/chemblntd/compound/structure\\_home](https://www.ebi.ac.uk/chemblntd/compound/structure_home)) the five compounds of interest from this study are not included in the GSK compound set.

#### **6.3.4. Identification of PfHsp70s as targets**

---

A number of experiments could be conducted toward identifying PfHsp70-1 and/or PfHsp70-x as the target for the observed antimalarial activity of compounds, and particularly of malonganenone A. These could include:

- Pull-down studies using immobilised compound(s), and subsequent identification of target proteins using mass spectroscopy.
- Genetic experiments: PfHsp70-1 and PfHsp70-x (separately) could be under- and over-expressed in *P. falciparum*, and then treated with compound(s). Changes in susceptibility ( $IC_{50}$ ) to

compound treatment of the strain under- or over-expressing Hsp70 compared to the wild type strain would suggest that the malarial Hsp70 concerned is indeed the target whose modulation has led to compromised parasite survival.

- The identification of client proteins of PfHsp70 which would potentially be affected in parasite death mediated by PfHsp70 modulation would be beneficial in additional target validation experiments. Such client proteins could be used as *in vivo* biomarkers for PfHsp70 modulation.

## REFERENCES

---

- Achan, J., Talisuna, A.O., Erhart, A., Yeka, A., Tibenderana, J.K., Baliraine, F.N., Rosenthal, P.J. and D'Alessandro, U. (2011). **Quinine, an old anti-malarial drug in a modern world: role in the treatment of malaria.** *Malaria Journal*, 10, 144-155.
- Acharya, P., Chaubey, S., Grover, M. and Tatu, U. (2012). **Pathogenesis-related knobs in *Plasmodium falciparum* infected erythrocytes.** *PLoS One*, 7, e44605.
- Acharya, P., Kumar, R. and Tatu, U. (2007). **Chaperoning a cellular upheaval in malaria: Heat shock proteins in *Plasmodium falciparum*.** *Molecular & Biochemical Parasitology*, 153, 85–94.
- Adams, S., Brown, H. and Turner, G. (2002). **Breaking down the blood-brain barrier: signalling a path to cerebral malaria?** *Trends in Parasitology*, 18, 360-366.
- Ahmad, A., Bhattacharya, A., McDonald, R.A., Cordes, M., Ellington, B., Bertelsen, E.B. and Zuiderweg, R.P. (2011). **Heat shock protein 70 kDa Chaperone/DnaJ cochaperone complex employs an unusual dynamic interface.** *Proceedings of the National Academy of Sciences of the United States of America*, 108, 18966-18971.
- Angov, E. (2011a). **Codon usage: Nature's roadmap to expression and folding of proteins.** *Biotechnology Journal*, 6, 650-659.
- Angov, E., Hillier, C.J., Kincaid, R.L. and Lyon, J.A. (2008). **Heterologous protein expression is enhanced by harmonizing the codon usage frequencies of the target gene with those of the expression host.** *PLoS One*, 3, e2189.
- Angov, E., Legler, P.M. and Mease, R.M. (2011b). **Adjustment of Codon Usage Frequencies by Codon Harmonization Improves Protein Expression and Folding.** In Evans T.C. Jr. and Xu., M.-Q. (Eds.), *Heterologous Gene Expression in E. coli* (pp. 1-13). New York: Humana Press.
- Ansorge, I., Benting, J., Bhakdi, S. and Lingelbach, K. (1996). **Protein sorting in *Plasmodium falciparum*-infected red blood cells permeabilized with the pore-forming protein streptolysin O.** *Biochemistry Journal*, 315, 307-315.
- Aurrecochea, C., Brestelli, J., Brunk, B.P., Dommer, J., Fischer, S., Gajria, B., Gao, X., Gingle, A., Grant, G., Harb, O.S., Heiges, M., Innamorato, F., Iodice, J., Kissinger, J.C., Kraemer, E., Li, W., Miller, J.A., Nayak, V., Pennington, C., Pinney, D.F., Roos, D.S., Ross, C., Stoeckert, C.J. Jr., Treatman, C. and Wang, H. (2009). **PlasmoDB: a functional genomic database for malaria parasites.** *Nucleic Acids Research*, 37, D539–D543.

- Baca, A.M. and Hol, W.G.J. (2000). **Overcoming codon bias: a method for high-level overexpression of *Plasmodium* and other AT-rich parasite genes in *Escherichia coli*.** *International Journal for Parasitology*, 30, 113-118.
- Baggish, A.L. and Hill, D.R., (2002). **Antiparasitic agent atovaquone.** *Antimicrobial Agents and Chemotherapy*, 46, 1163–1173.
- Banerjee, T., Singh, R.R., Gupta, S., Surolia, A. and Surolia, N. (2012). **15-Deoxyspergualin Hinders Physical Interaction Between Basic Residues of Transit Peptide in *PfENR* and Hsp70-1.** *IUBMB Life*, 64, 99-107.
- Bannister, L.H. (2001). **Looking for the exit: How do malaria parasites escape from red blood cells?** *Proceedings of the National Academy of Sciences of the United States of America*, 98, 383-384.
- Barnwell, J.W., Ash, A.A., Nachman, R.L., Yamaya, M., Aikawa, M and Igravallo, P. (1989). **A human 88-kD membrane glycoprotein (CD36) functions *in vitro* as a receptor for a cytoadherence ligand on *Plasmodium falciparum*-infected erythrocytes.** *Journal of Clinical Investigations*, 84, 765-772.
- Baruch, D.I., Ma, X.C., Singh, H.B., Bi, X., Pasloske, B.L. and Howard, R.J. (1997). **Identification of a region of PfEMP1 that mediates adherence of *Plasmodium falciparum* infected erythrocytes to CD36: conserved function with variant sequence.** *Blood*, 90, 3766-3775.
- Baruch, D.I., Pasloske, B.L., Singh, H.B., Bi, X., Ma, X.C., Feldman, M., Taraschi, T.F. and Howard, R.J. (2005). **Cloning the *P. falciparum* gene encoding PfEMP1, a malarial variant antigen and adherence receptor on the surface of parasitized human erythrocytes.** *Cell*, 92, 77-97.
- Basco, L.K., Marquet, F., Makler, M.M. and Le Bras, J. (1995). ***Plasmodium falciparum* and *Plasmodium vivax*: lactate dehydrogenase activity and its application for *in vitro* drug susceptibility assay.** *Experimental Parasitology*, 80, 260-271.
- Bell, S., L., Chiang, A.N. and Brodsky, J.L. (2011). **Expression of a Malarial Hsp70 Improves Defects in chaperone-dependent activities in *ssa1* mutant yeast.** *PLoS One*, 6, e20047.
- Bennett, T.N., Patel, J., Ferdig, M.T. and Roepe, P.D. (2007). ***Plasmodium falciparum* Na<sup>+</sup>/H<sup>+</sup> exchanger activity and quinine resistance.** *Molecular and Biochemical Parasitology*, 153, 48–58.
- Bhal, S.K., Kassam, K., Peirson, I.G. and Pearl, G.M. (2007). **The Rule of Five Revisited: Applying Log D in Place of Log P in Drug-Likeness Filters.** *Molecular pharmaceuticals*, 4, 556-560.



- Bhattacharya, A., Kurochkin, A.V., Yip, G.N.B., Zhang, Y., Bertelsen, E. and Zuiderweg, E.R.P. (2009). **Allostery in Hsp70 chaperones is transduced by subdomain rotations.** *Journal of Molecular Biology*, 388, 475–490.
- Birkholtz, L.-M., Blatch, G., Coetzer, T.L., Hoppe, H.C., Human, E., Morris, E.J., Ngcete, Z., Oldfield, L., Roth, R., Shonhai, A., Stephens, L. and Louw, A.I. (2008). **Heterologous expression of plasmodial proteins for structural studies and functional annotation.** *Malaria Journal*, 7, 197-216.
- Blatch G.L. and Lässle, M. (1999). **The tetratricopeptide repeat: a structural motif mediating protein-protein interactions.** *Bioessays*, 11, 932-939.
- Bloland, P.B. (2001). **Drug resistance in malaria.** World Health Organisation: <http://www.who.int/csr/resources/publications/drugresist/malaria.pdf>.
- Blond-Elguindi, S., Cwirla, S.E., Dower, W.J., Lipshutz, R.J., Sprang, S.R., Sambrook, J.F. and Gething, M.-J.H. (1993). **Affinity panning of a library of peptides displayed on bacteriophages reveals the binding specificity of BiP.** *Cell*, 75, 717-728.
- Boddey, J.A., Hodder, A.N., Günther, S., Gilson, P.R., Patsiouras, H., Kapp, E.A., Pearce, J.A., de Koning-Ward, T.F., Simpson, R.J., Crabb, B.S. and Cowman, A.F. (2010). **An aspartyl protease directs malaria effector proteins to the host cell.** *Nature*, 463, 627-631.
- Bonifazi, E.L., Ríos-Luci, C., León, L.G., Burton, G., Padro'n, J.M., and Misico, R.I. (2010). **Antiproliferative activity of synthetic naphthoquinones related to lapachol. First synthesis of 5-hydroxylapachol.** *Bioorganic and Medicinal Chemistry*, 18, 2621–2630.
- Bork, P., Sander, C. and Valencia, A. (1992). **An ATPase domain common to prokaryotic cell cycle proteins, sugar kinases, actin, and hsp70 heat shock proteins.** *Proceedings of the National Academy of Sciences of the United States of America*, 89, 7290-7294.
- Boshoff, A., Stephens, L.L. and Blatch, G.L. (2008). **The *Agrobacterium tumefaciens* DnaK: ATPase cycle, oligomeric state and chaperone properties.** *The International Journal of Biochemistry and Cell Biology*, 40, 804–812.
- Botha, M., Chiang, A.N., Needham, P.G., Stephens, L.L., Hoppe, H.C., Külzer, S., Przyborski, J.M., Lingelbach, K., Wipf, P., Brodsky, J.L., Shonhai, A. and Blatch, G.L. (2011). ***Plasmodium falciparum* encodes a single cytosolic type I Hsp40 that functionally interacts with Hsp70 and is upregulated by heat shock.** *Cell Stress and Chaperones*, 16, 389-401.

- Botha, M., Pesce, E.-R. and Blatch, G.L. (2007). **The Hsp40 proteins of *Plasmodium falciparum* and other apicomplexa: Regulating chaperone power in the parasite and the host.** *The International Journal of Biochemistry and Cell Biology*, 39, 1781–1803.
- Brodsky, J. (1999). **Selectivity of the molecular chaperone-specific immunosuppressive agent 15-deoxyspergualin: modulation of Hsc70 ATPase activity without compromising DnaJ chaperone interactions.** *Biochemical Pharmacology*, 57, 877-880.
- Brodsky, J.L. and Chiosis, G. (2006). **Hsp70 molecular chaperones: emerging roles in human disease and identification of small molecule modulators.** *Current Topics in Medicinal Chemistry*, 6, 1215-1225.
- Buffet, P.A., Safeukui, I., Deplaine, G., Brousse, V., Prendki, V., Thellier, M., Turner, G.D. and Mercereau-Puijalon, O. (2011). **The pathogenesis of *Plasmodium falciparum* malaria in humans: insights from splenic physiology.** *Blood*, 117, 381-392.
- Butler, A.R., Khan, S. and Ferguson, E. (2010). **A brief history of malaria chemotherapy.** *Journal of the Royal College of Physicians of Edinburgh*, 40, 172-177.
- Caplan, A. J. (1999). **Hsp90's secrets unfold. New insights from structural and functional studies.** *Trends in Cellular Biology*, 9, 262-268.
- Castelli, F., Odolini, S., Autino, B, Foca E. and Russo, R. (2010). **Malaria prophylaxis: a comprehensive review.** *Pharmaceuticals*, 3, 3212-3239.
- Cheetham, M.E. and Caplan, A.J. (1998). **Structure, function and evolution of DnaJ: conservation and adaptation of chaperone function.** *Cell Stress and Chaperones*, 3, 28-36.
- Cheetham, M.E., Brion, J.-P. and Anderton, B.H. (1992). **Human homologues of the bacterial heat-shock protein DnaJ are preferentially expressed in neurons.** *Biochemistry Journal*, 284, 469-476.
- Cheetham, M.E., Jackson, A.P. and Anderton, B.H. (1994). **Regulation of 70-kDa heat-shock-protein ATPase activity and substrate binding by human DnaJ-like proteins, HSJ1a and HSJ1b.** *European Journal of Biochemistry*, 226, 99–107.
- Chiang, A.N., Valderramos, J.-C., Balachandran, R., Chovatiya, R.J., Mead, B.P., Schneider, C., Bell, S.L., Klein, M.G., Hury, D.M., Chen, X.S., Day, B.W., Fidock, D.A., Wipf, P., Brodsky, J.L. (2009). **Select pyrimidinones inhibit the propagation of the malarial parasite, *Plasmodium falciparum*.** *Bioorganic and Medicinal Chemistry*, 17, 1527-1533.

- Chowdhury, D.R., Angov, E., Kariuki, T. and Kumar, N. (2009). **A potent malaria transmission blocking vaccine based on codon harmonized full length Pfs48/45 expressed in *Escherichia coli*.** *PLoS One*, 4, e6352.
- Clark, I.A., Chaudhri, G. and Cowden, W.B. (1989). **Some roles of Free Radicals in Malaria.** *Free Radical Biology and Medicine*, 6, 315-321.
- Cockburn, I.L., Pesce, E.-R., Przyborski, J.M., Davies-Coleman, M.T., Clark, P.G.K., Keyzers, R.A., Stephens, L.L. and Blatch, G.L. (2011). **Screening for small molecule modulators of Hsp70 chaperone activity using protein aggregation suppression assays: inhibition of the plasmodial chaperone PfHsp70-1.** *Biological Chemistry*, 392, 431-438.
- Cowman, A.F. and Crabb, B.S. (2006). **Invasion of red blood cells by malaria parasites.** *Cell*, 124, 755-766.
- Craig, A. and Scherf, A. (2001). **Molecules on the surface of the *Plasmodium falciparum* infected erythrocyte and their role in malaria pathogenesis and immune invasion.** *Molecular and Biochemical Parasitology*, 115, 129-143.
- Crampton, A. and Vanniasinkam, T. (2007). **Parasite vaccines: The new generation.** *Infection, Genetics and Evolution*, 7, 664-673.
- Culvenor, J.G., Langford, C.J., Crewther P.E., Saint, R.B., Coppel, R.L., Kemp, D.J., Anders, R.F. and Brown, G.V. (1987). ***Plasmodium falciparum*: identification and localization of a knob protein antigen expressed by a cDNA clone.** *Experimental Parasitology*, 63, 58-67.
- Cyrklaff, M., Sanchez, C.P., Frischknecht, F. and Lanzer, M. (2012). **Host actin remodeling and protection from malaria by hemoglobinopathies.** *Trends in Parasitology*, 28, 479-485.
- Daniel, S., Bradley, G., Longshaw, V.M., Söti, C., Csermely, P and Blatch, G.L. (2008). **Nuclear translocation of the phosphoprotein Hop (Hsp70/Hsp90 organizing protein) occurs under heat shock, and its proposed nuclear localization signal is involved in Hsp90 binding.** *Biochimica et Biophysica Acta*, 1783, 1003–1014.
- Davis, J., Voisine, C. and Craig, E. (1999). **Intragenic suppressors of Hsp70 mutants: Interplay between the ATPase- and peptide-binding domains.** *Proceedings of the National Academy of Sciences of the United States of America*, 96, 9269–9276.
- De Crescenzo, G., Boucher, C., Durocher, Y. and Jolicouer, M. (2008). **Kinetic characterization by surface plasmon resonance-based biosensors: principle and emerging trends.** *Cellular and Molecular Bioengineering*, 1, 204-215.

- de Konig-Ward, T.F., Gilson, P.R., Boddey, J.A., Rug, M., Smith, B.J., Papenfuss, A.T., Sanders, P.R., Lundie, R.J., Maier, A.G., Cowman, A.F., Crabb, B.S. (2009). **A newly discovered protein export machine in malaria parasites.** *Nature*, 459, 945-949.
- de Marco, A. and de Marco, V. (2004). **Bacteria co-transformed with recombinant proteins and chaperones cloned in independent plasmids are suitable for expression tuning.** *Journal of Biotechnology*, 109, 45–52.
- Demain, A.L. and Vaishnav, P. (2009). **Production of recombinant proteins by microbes and higher organisms.** *Biotechnology Advances*, 27, 297–306.
- Edkins, A.L. and Blatch, G.L. (2012). **Targeting Conserved Pathways as a Strategy for Novel Drug Development.** In Chibale, K., Davies-Coleman, M. and Masimirembwa, C. (Eds.), *Drug Discovery in Africa: Impacts of Genomics, Insights into Medicinal Chemistry, and Technology Platforms in Pursuit of New Anti-Parasitic Drugs* (1<sup>st</sup> ed., pp. 85-100). Heidelberg: Springer.
- Eksi, S. and Williamson, K.C. (2011). **Protein targeting to the parasitophorous vacuole membrane of *Plasmodium falciparum*.** *Eukaryotic Cell*, 10, 744–752.
- Ellis, R.J. (1987). **Proteins as molecular chaperones.** *Nature*, 328, 378-379.
- Engelbrecht, D., Durand, P.M. and Coetzer, T.L. (2012). **On programmed cell death in *Plasmodium falciparum*: Status Quo.** *Journal of Tropical Medicine*, 2012, 646534.
- Evans, C.G., Chang, L. and Gestwicki, J.E. (2010). **Heat shock protein 70 (Hsp70) as an emerging drug target.** *Journal of Medicinal Chemistry*, 53, 4585–4602.
- Fewell, S.W., Smith, C.M., Lyon, M.A., Dumitrescu, T.P., Wipf, P., Day, B.W. and Brodsky, J.L. (2004). **Small molecule modulators of endogenous and co-chaperone-stimulated Hsp70 ATPase activity.** *The Journal of Biological Chemistry*, 279, 51131-51140.
- Fidock, D.A. (2010). **Priming the antimalarial pipeline.** *Nature*, 465, 297-298.
- Fidock, D.A., Rosenthal, P.J., Croft, S.L., Brun, L. and Nwaka, S. (2004). **Antimalarial drug discovery: efficacy models for compound screening.** *Nature Reviews*, 3, 509-520.
- Flaherty, K.M., Deluca-Flaherty, C. and McKay, D.B. (1990). **Three-dimensional structure of the ATPase fragment of a 70K heat-shock cognate protein.** *Nature*, 346, 623 – 628.
- Flick, K. and Chen, Q. (2004). **var genes, PfEMP1 and the human host.** *Molecular and Biochemical Parasitology*, 134, 3–9.
- Freeman, B.C., Myers, M.P., Schumacher, R. and Morimoto, R.I. (1995). **Identification of a regulatory motif in Hsp70 that affects ATPase activity, substrate binding and interaction with HDJ-1.** *The EMBO Journal*, 14, 2281-2292.

- Fujioka, H. and Aikawa, M. (2002). **Structure and life cycle.** *Chemical Immunology*, 80, 1-26.
- Gamain, B., Smith, J.D., Viebig, N.K., Gysin, J. and Scherf, A. (2007). **Pregnancy-associated malaria: Parasite binding, natural immunity and vaccine development.** *International Journal for Parasitology*, 37, 273–283.
- Gamer, J., Multhaup, G., Tomoyasu, T., McCarty, J.S., Rüdiger, S., Schönfeld, H.-J., Schirra, C., Bujard, H. and Bukau, B. (1996). **A cycle of binding and release of the DnaK, DnaJ and GrpE chaperones regulates activity of the *Escherichia coli* heat shock transcription factor  $\sigma^{32}$ .** *The EMBO Journal*, 15, 607-617.
- Gamo, F.-J., Sanz, L.M., Vidal, J., de Cozar, C., Alvarez, E., Lavandera, J.-L., Vanderwall, D.E., Green, D.V.S., Kumar, V., Hasan, S., Brown, J.R., Peishoff, C.E., Cardon, L.R. and Garcia-Bustos, J.F. (2010). **Thousands of chemical starting points for antimalarial lead identification.** *Nature*, 465, 305-312.
- Ganesan, A. (2008). **The impact of natural products upon modern drug discovery.** *Current Opinion in Chemical Biology*, 12, 306–317.
- Gao, X.-C., Zhou, C.-J., Zhou, Z.-R., Wu, M., Cao, C.-Y. and Hu, H.-Y. (2012). **The C-terminal helices of heat shock protein 70 are essential for J-domain binding and ATPase activation.** *The Journal of Biological Chemistry*, 287, 6044–6052.
- Gardner, M.J., Hall, N., Fung, E., White, O., Berriman, M., Hyman, R.W., Carlton, J.M., Pain, A., Nelson, K., Bowman, S., Paulsen, I.T., James, K., Eisen, J.A., Rutherford, K., Salzberg, S.L., Craig, A., Kyes, S., Chan, M.-S., Nene, V., Shallom, S.J., Suh, B., Peterson, J., Angiuoli, S., Pertea, M., Allen, J., Selengut, J., Haft, D., Mather, M.W., Vaidya, A., Martin, D.M.A., Fairlamb, A.H., Fraunholz, M.J., Roos, D.S., Ralph, S.A., McFadden, G.I., Cummings, L.M., Subramanian, G.M., Mungall, C., Venter, J.C., Carucci, D.J, Hoffman, S.L., Newbold, C., Davis, R.W., Fraser, C.M. and Barrell, B. (2002). **Genome sequence of the human malaria parasite *Plasmodium falciparum*.** *Nature*, 419, 498-511.
- Gässler, S. C., Buchberger, A., Laufen, T., Mayer, M. P., Schröder, H., Valencia, A., and Bukau, B. (1998). **Mutations in the DnaK chaperone affecting interaction with the DnaJ co-chaperone.** *Biochemistry*, 95, 15229- 15234.
- Gässler, C.S., Wiederkehr, T., Brehmer, D., Bukau, B. and Mayer, M.P. (2001). **Bag-1M accelerates nucleotide release for human Hsc70 and Hsp70 and can act concentration-dependent as positive and negative cofactor.** *The Journal of Biological Chemistry*, 276, 32538-32544.

- Genentech press release 1978:  
[www.gene.com/gene/news/press-releases/display.do?method=detail&id=4160](http://www.gene.com/gene/news/press-releases/display.do?method=detail&id=4160)
- Gillies, A.T., Taylor, R. and Gestwicki, J.E. (2012). **Synthetic lethal interactions in yeast reveal functional roles of J protein co-chaperones.** *Molecular BioSystems*, 8, 2901–2908.
- Ginsburg, H. and Deharo, E. (2011). **A call for using natural compounds in the development of new antimalarial treatments—an introduction.** *Malaria Journal*, 10, S1.
- Gitau, G.W., Mandal, P., Blatch, G.L., Przyborski, J. and Shonhai, A. (2012). **Characterisation of the *Plasmodium falciparum* Hsp70–Hsp90 organising protein (PfHop).** *Cell Stress and Chaperones*, 17, 191–202.
- Glover, J.R. and Lindquist, S. (1998). **Hsp104, Hsp70 and Hsp40: A Novel Chaperone System that Rescues Previously Aggregated Proteins.** *Cell*, 94, 73-82.
- Goble, J.L., Johnson, H., de Ridder, J., Stephens, L.L., Louw, A., Blatch, G.L. and Boshoff, A. (2012). **The druggable antimalarial target PfDXR: overproduction strategies and kinetic characterization.** *Protein and Peptide Letters*, Article in Press.
- Guo, F., Rocha, K., Bali, P., Pranpat, M., Fiskus, W., Boyapalle, S., Kumaraswamy, S., Balasis, M., Greedy, B., Armitage, E.S., Lawrence, N. and Bhalla, K. (2005). **Abrogation of heat shock protein 70 induction as a strategy to increase antileukemia activity of heat shock protein 90 inhibitor 17-allylamino-demethoxy geldanamycin.** *Cancer Research*, 65, 10536-10544.
- Gustafsson, C., Govindarajan, S. and Minshull, J. (2004). **Codon Bias and heterologous protein expression.** *Trends in Biotechnology*, 22,346-53.
- Haldar, K. and Mohandas, N. (2007). **Erythrocyte remodeling by malaria parasites.** *Current Opinions in Hematology*, 14, 203–209.
- Hageman, J. and Kampinga, H.H. (2009). **Computational analysis of the human HSPH / HSPA / DNAJ family and cloning of a human HSPH / HSPA / DNAJ expression library.** *Cell Stress and Chaperones*, 14, 1-21.
- Hageman, J., van Waarde, M.A.W.H., Zylicz, A., Walerych, D. and Kampinga, H.H. (2011). **The diverse members of the mammalian HSP70 machine show distinct chaperone-like activities.** *Biochemistry Journal*, 435, 127–142.
- Hamada, H., Arakawa, T. and Shiraki, K. (2009). **Effect of additives on protein aggregation.** *Current Pharmaceutical Biotechnology*, 10, 400-407.
- Haris, P.I. and Severcan, F. (1999). **FTIR spectroscopic characterization of protein structure in aqueous and non-aqueous media.** *Journal of Molecular Catalysis B: Enzymatic*, 7, 207–221.

- Hendrick, J.P. and Hartl, F.U. (1993). **Molecular chaperone functions of heat-shock proteins.** *Annual Review of Biochemistry*, 62, 349-384.
- Hennessy, F., Nicoll, W.S., Zimmerman, R., Cheetham, M.E. and Blatch, G.L. (2005). **Not all J domains are created equal: implications for the specificity of Hsp40-Hsp70 interactions.** *Protein Science*, 14, 1697- 1709.
- Hill, A.V.S. (2011). **Vaccines against malaria.** *Philosophical Transactions of the Royal Society B*, 366, 2806-2814.
- Hill, D.A., Pillai, A.D., Nawaz, F., Hayton, K., Doan, L., Lisk, G. and Desai, S.A. (2006). **A blasticidin S-resistant *Plasmodium falciparum* mutant with a defective plasmodial surface anion channel.** *Proceedings of the National Academy of Sciences*, 104, 1063–1068.
- Hiller, N.L., Bhattacharjee, S., van Ooij, C., Liolios, K., Harrison, T., Lopez-Estraño, C. and Haldar, K. (2004). **A host-targeting signal in virulence proteins reveals a secretome in malarial infection.** *Science*, 306, 1934-1937.
- Hobbs, C. and Duffy, P. (2011). **Drugs for malaria: something old, something new, something borrowed.** *F1000 Biology Reports*, 3, 24-32.
- Hooker, S. C. (1896). **Constitution of Lapachol and Its Derivatives: The Structure of the Anylene Chain.** *Journal of the Chemical Society, Transactions*, 69, 1355-1381.
- Huber, W. and Mueller, F. (2006). **Biomolecular interaction analysis in drug discovery using surface Plasmon resonance technology.** *Current Pharmaceutical Design*, 12, 3999-4021.
- Hyde, J.E. (2005). **Exploring the folate pathway in *Plasmodium falciparum*.** *Acta Tropica*, 94, 191-206.
- Ingolia, T. and Craig, E.A. (1982). ***Drosophila* gene related to the major heat shock-induced gene is transcribed at normal temperatures and not induced by heat shock.** *Proceedings of the National Academy of Sciences of the United States of America*, 79, 525-529.
- Itakura, K., Hirose, T., Crea, R., Riggs, A.D., Heyneker, H.L., Bolivar, F. and Boyer, H.W. (1977). **Expression in *Escherichia coli* of a chemically synthesized gene for the hormone somatostatin.** *Science, New Series*, 198, 1056-1063.
- Jecklin, M.C., Schauer, S., Dumelin, C.E. and Zenobi, R. (2009). **Label-free determination of protein–ligand binding constants using mass spectrometry and validation using surface plasmon resonance and isothermal titration calorimetry.** *Journal of Molecular Recognition*, 22, 319–329.

- Jegou, G., Hazooumé, A., Seigneuric R. and Garrido, C. (2010). **Targeting heat shock proteins in cancer.** *Cancer Letters, Article in Press*, DOI:10.1016/j.canlet.2010.10.014.
- Jiang, J., Maes, E.G., Taylor, A.B., Wang, L., Hinck, A.P., Lafer, E.M. and Sousa, R. (2007). **Structural basis of J cochaperone binding and regulation of Hsp70.** *Molecular Cell*, 28, 422–433.
- Jiang, J., Prasad, K., Lafer, E.M. and Sousa, R. (2005). **Structural basis of interdomain communication in the Hsc70 chaperone.** *Molecular Cell*, 20, 513–524.
- Jinwal, U.K., Akoury, E., Abisambra, J.F., O’Leary, J.C.<sup>3rd</sup>, Thompson, A.D., Blair, L.J., Jin, Y., Bacon, J., Nordhues, B.A., Cockman, M., Zhang, J., Li, P., Zhang, B., Borysov, S., Uversky, V.N., Biernat, J., Mandelkow, E., Gestwicki, J.E., Zweckstetter, M. and Dickey, C.A. (2012). **Imbalance of Hsp70 family variants fosters tau accumulation.** *Federation of American Societies for Experimental Biology Journal, Article in Press*, DOI: 10.1096/fj.12-220889fj.
- Jinwal, U.K., Miyata, Y., Koren, J., Jones, J.R., Trotter, J.H., Chang, L., O’Leary, J., Morgan, D., Lee, D.C., Shults, C.L., Rousaki, A., Weeber, E.J., Zuiderweg, E.R.P. Gestwicki, J.E. and Dickey, C.A. (2009). **Chemical manipulation of Hsp70 ATPase activity regulates tau stability.** *The Journal of Neuroscience*, 29, 12079–12088.
- Johnson, D.S., Weerapana, E. and Cravatt, B.F. (2010). **Strategies for discovering and derisking covalent, irreversible enzyme inhibitors.** *Future Medicinal Chemistry*, 2, 949-964.
- Jönsson, U., Fägerstam, L., Ivarsson, B., Johnsson, B., Karlsson, R., Lundh, K., Löfas, S., Persson, B., Roos, H., Rönnberg, I., Sjölander, S., Stenberg, E., Stahlberg, R., Urbaniczky, S., Östlin, H., Malmqvist, M. (1991). **Real-time biospecific interaction analysis using surface plasmon resonance and a sensor chip technology.** *Biotechniques*, 11, 620–627.
- Kampinga, H.H. and Craig, E.A. (2010). **The HSP70 chaperone machinery: J proteins as drivers of functional specificity.** *Nature Reviews Molecular Cell Biology*, 11, 579–592.
- Kanchanaphum, P. and Krungkrai, J. (2010). **Co-expression of human malaria parasite *Plasmodium falciparum* orotate phosphoribosyltransferase and orotidine 5’-monophosphate decarboxylase as enzyme complex in *Escherichia coli*: a novel strategy for drug development.** *Asian Biomedicine*, 4, 297-306.
- Kane, J.F. and Hartley, D.L. (1988). **Formation of recombinant protein inclusion bodies in *Escherichia coli*.** *Trends in Biotechnology*, 6, 95-101.
- Karl, S., Wong, R.P.M., St. Pierre, T.G. and Davis, T.M.E. (2009). **A comparative study of a flow-cytometry-based assessment of *in vitro Plasmodium falciparum* drug sensitivity.** *Malaria Journal*, 8, 294-304.



- Karlsson, R. and Fält, A. (1997). **Experimental design for kinetic analysis of protein-protein interactions with surface plasmon resonance biosensors.** *Journal of Immunological Methods*, 200, 121-133.
- Karlsson, R., Håkan, R., Bruno, J. and Stolz, L. (1997). **Practical aspects concerning direct detection of low molecular weight analytes using BIACORE® 2000.** *BIA Journal, Special Issue*, 18-21.
- Keller, T.H., Pichota, A. and Yin, Z. (2006). **A practical view of 'druggability'.** *Current Opinion in Chemical Biology*, 10, 357–361.
- Keyzers, R.A., Gray, C.A., Schleyer, M.H., Whibley, C.E., Hendricks D.T., and Davies-Coleman, M.T. (2006). **Malonganenones A–C, novel tetraprenylated alkaloids from the Mozambique gorgonian *Leptogorgia gilchristi*.** *Tetrahedron*, 62, 2200–2206.
- Keyzers, R.A., Gray, C.A., Schleyer, M.H., Whibley, C.E., Hendricks D.T., and Davies-Coleman, M.T. (2006). **Malonganenones A–C, novel tetraprenylated alkaloids from the Mozambique gorgonian *Leptogorgia gilchristi*.** *Tetrahedron*, 62, 2200–2206.
- Kilejian, A. (1979). **Characterization of a protein correlated with the production of knob-like protrusions on membranes of erythrocytes infected with *Plasmodium falciparum*.** *Proceedings of the National Academy of Sciences of the United States of America*, 76, 4650–4653.
- Kilejian, A., Rashid, M.A., Aikawa, M., Aji, T. and Yang Y.-F. (1991). **Selective association of a fragment of the knob protein with spectrin, actin and the red cell membrane.** *Molecular and Biochemical Parasitology*, 44, 175-182.
- Kinyanjui, S.M., Mberu. E.K., Winstanley, P.A., Jacobus, D.P. and Watkins, W.M. (1999). **The Antimalarial triazine WR99210 and the prodrug Ps-15: Folate reversal of *in vitro* activity against *Plasmodium falciparum* and a non-antifolate mode of action of the prodrug.** *American Journal of Tropical Medicine and Hygiene*, 60, 943–947.
- Kirk, K. (2004). **Channels and transporters as drug targets in the *Plasmodium*-infected erythrocyte.** *Acta Tropica*, 89, 285-298.
- Kityk, R., Kopp, J., Sinning, I. and Mayer, M.P. (2012). **Structure and dynamics of the ATP-bound open conformation of Hsp70 chaperones.** *Molecular Cell*, Article in press, DOI: 10.1016/j.molcel.2012.09.023.
- Kota, P., Summers, D.W., Ren, H.-Y., Cyr, .M. and Dokholyan, N.V. (2009). **Identification of a consensus motif in substrates bound by a Type I Hsp40.** *Proceedings of the National academy of Sciences of the United States of America*, 106, 11073–11078.

- Külzer, S., Charnaud, S., Dagan, T., Riedel, J., Mandal, P., Pesce, E.-R., Blatch, G.L., Crabb, B.S., Gilson, P.R. and Przyborski, J.M. (2012). ***Plasmodium falciparum*-encoded exported hsp70/hsp40 chaperone/co-chaperone complexes within the host erythrocyte.** *Cellular Microbiology, Article in Press*, DOI: 10.1111/j.1462-5822.2012.01840.x.
- Külzer, S., Rug, M., Brinkmann, K., Cannon, P., Cowman, A., Lingelbach, K., Blatch, G.L., Maier, A.G. and Przyborski, J.M. (2010). **Parasite-encoded Hsp40 proteins define novel mobile structures in the cytosol of the *P. falciparum*-infected erythrocyte.** *Cellular Microbiology* 12, 1398-1420.
- Kumar, N., Koski, G., Masakadu, H., Masamichi, A., Hong, Z. (1991). **Induction and localization of *Plasmodium falciparum* stress proteins related to the heat shock protein 70 family.** *Molecular and Biochemical Parasitology*, 48, 47-58.
- Kumar, R., Musiyenko, A. and Barik, S. (2003). **The heat shock protein 90 of *Plasmodium falciparum* and antimalarial activity of its inhibitor, geldanamycin.** *Malaria Journal*, 2, 30.
- Laemmli, U.K. (1970). **Cleavage of structural proteins during the assembly of the head of bacteriophage T4.** *Nature*, 227, 680-685.
- Lambros, C., and Vanderberg, J.P. (1979). **Synchronization of *Plasmodium falciparum* erythrocytic stages in culture.** *Journal of Parasitology*, 65, 418–420.
- Landry, S.J. (2003). **Structure and energetics of an allele-specific genetic interaction between dnaJ and dnaK: correlation of nuclear magnetic resonance chemical shift perturbations in the J domain of Hsp40/DnaJ with binding affinity for the ATPase domain of Hsp70/DnaK.** *Biochemistry*, 42, 4926–4936.
- Lanzer, M., Wickert, H., Krohne, G., Vincensini, L. and Braun-Breton, C. (2006). **Maurer’s clefts: A novel multi-functional organelle in the cytoplasm of *Plasmodium falciparum*-infected erythrocytes.** *International Journal for Parasitology*, 36, 23-36.
- Laufen, T., Mayer, M. P., Beisel, C., Klostermeier, D., Reinstein, J. and Bukau, B. (1999). **Mechanism of regulation of Hsp70 chaperones by DnaJ co-chaperones.** *Proceedings of the National Academy of Sciences of the United States of America*, 96, 5452–5457.
- Levine, N.D. (1971). **Uniform terminology for the protozoan subphylum Apicomplexa.** *Journal of Eukaryotic Microbiology*, 18, 352-355.
- Liberek, K., Marszalek, J., Ang, D., Georgopoulos, C., and Zylicz, M. (1991). ***Escherichia coli* DnaJ and GrpE heat shock proteins jointly stimulate ATPase activity of DnaK.** *Proceedings of the National Academy of Sciences of the United States of America*, 88, 2874–2878.

- Lim, L. and McFadden, I.G. (2010). **The evolution, metabolism and functions of the apicoplast.** *Philosophical Transactions of the Royal Society B*, 365, 749–763.
- Lipinski, C.A., Lombardo, F., Dominy, B.W. and Feeney, P.J. (2001). **Experimental and computational approaches to estimate solubility and permeability in drug discovery and development settings.** *Advanced Drug Delivery Reviews*, 46, 3-26.
- Looareesuwan, S., Chulay, J.D., Canfield, C.J. and Hutchinson, D.B.A. (1999). **Malarone™ (Atovaquone and proguanil hydrochloride): a review of its clinical development for treatment of malaria.** *American Journal of Tropical Medicine and Hygiene*, 60, 533-541.
- Luke, T.C. and Hoffman, S.L. (2003). **Rationale and plans for developing a non-replicating, metabolically active, radiation-attenuated Plasmodium falciparum sporozoite vaccine.** *The Journal of Experimental Biology*, 206, 3803-3808.
- Maier, A.G., Rug, M., O'Neill, M.T., Brown, M., Chakravorty, S., Szeszak, T., Chesson, J., Wu, Y., Hughes, K., Coppel, R.L., Newbold, C., Beeson, J.G., Craig, A., Crabb, B.S. and Cowman, A.F. (2008). **Exported proteins required for virulence and rigidity of Plasmodium falciparum-infected human erythrocytes.** *Cell*, 134, 48–61.
- Makler, M.T., Ries, J.M., Williams, J.A., Bancroft, J.E., Piper, R.C., Gibbins, B.L., and Hinrichs, D.J. (1993). **Parasite lactate dehydrogenase as an assay for Plasmodium falciparum drug sensitivity.** *American Journal of Tropical Medicine and Hygiene*, 48, 739–741.
- Makrides, S.C. (1996). **Strategies for achieving high-level expression of genes in Escherichia coli.** *Microbiological Reviews*, 60, 512–538.
- Marti, M., Good, R.T., Rug, M., Knuepfer, E. and Cowman, A.F. (2004). **Targeting malaria virulence and remodelling proteins to the host erythrocyte.** *Science*, 306, 1930-1933.
- Massey, A.J. (2010). **ATPases as drug targets: insights from heat shock proteins 70 and 90.** *Journal of Medicinal Chemistry*, 53, 7280–7286.
- Matambo, T.S., Odunuga, O.O., Boshoff, A. and Blatch, G.L. (2004). **Overproduction, purification, and characterization of the Plasmodium falciparum heat shock protein 70.** *Protein Expression and Purification*, 33, 214-222.
- Mayer, M., Laufen, T., Paal, K., McCarty, J and Bukau, B. (1999). **Investigation of the Interaction between DnaK and DnaJ by Surface Plasmon Resonance Spectroscopy.** *Journal of Molecular Biology*, 289, 1131-1144.
- Mayer, M.P. and Bukau, B. (2005). **Hsp70 chaperones: Cellular functions and molecular mechanisms.** *Cellular and Molecular Life Sciences*, 62, 670-684.

- McNamara, C. (2006). **Characterisation of human Hsj1a: an Hsp40 molecular chaperone similar to malarial Pfj4**. MSc Thesis, Rhodes University, Grahamstown, South Africa.
- Mehlin, C., Boni, E., Buckner, F.S., Engel, L., Feist, T., Gelb, M.H., Haji, L., Kim, D., Liu, C., Mueller, N., Myler, P.J., Reddy, J.T., Sampson, J.N., Subramanian, E., Van Voorhis, W.C., Worthey, E., Zucker, F. and Hol, W.G.J. (2006). **Heterologous expression of proteins from *Plasmodium falciparum*: Results from 1000 genes**. *Molecular and Biochemical Parasitology*, 148, 144–160.
- Meñendez, J.A., del Mar Barbacid, M., Montero, S., Sevilla, E., Escrich, E., Solanas, M., Cortés-Funes, H. and Colomer, R. (2001). **Effects of gamma-linolenic acid and oleic acid on paclitaxel cytotoxicity in human breast cancer cells**. *European Journal of Cancer*, 37, 402-413.
- Meyn, R.E., Stephens, L.C., Hunter, N.R. and Milas, L. (1995). **Apoptosis in murine tumors treated with chemotherapy agents**. *Anti-Cancer Drugs* 1995, 6, 443-450.
- Midorikawa, Y. and Haque, Q.M. (1997). **15-Deoxyspergualin, an immunosuppressive agent, used in organ transplantation showed suppressive effects on malarial parasites**. *Chemotherapy*, 43, 31-35.
- Midorikawa, Y., Haque, Q.M., Nakazawa, S. (1998). **Inhibition of malaria-infected erythrocytes by deoxyspergualin: effect on in vitro growth of malarial cultures**. *Chemotherapy*, 44, 409-413.
- Milas, L., Hunter, N.R., Kurdoglu, B., Mason, K.A., Meyn, R.E., Stephens, L.C. and Peters, L.J. (1995). **Kinetics of mitotic arrest and apoptosis in murine mammary and ovarian tumors treated with taxol**. *Cancer Chemotherapy and Pharmacology*, 4, 297-303.
- Minami, Y., Höhfeld, J., Ohtsuka, K. and Hartl, F.-U. (1996). **Regulation of the heat-shock protein 70 reaction cycle by the mammalian DnaJ homolog, Hsp40**. *The Journal of Biological Chemistry*, 271, 19617–19624.
- Misra, G. and Ramachandran, R. (2009). **Hsp70-1 from *Plasmodium falciparum*: protein stability, domain analysis and chaperone activity**. *Biophysical Chemistry*, 142, 55-64.
- Misselwitz, B., Staeck, O. and Rapoport, T.A. (1998). **J Proteins catalytically activate Hsp70 molecules to trap a wide range of peptide sequences**. *Molecular Cell*, 2, 593–603.
- Miyata, Y., Rauch, J.N., Jinwal, U.K., Thompson, A.D., Srinivasan, S., Dickey, C.A. and Gestwicki, J.E. (2012). **Cysteine reactivity distinguishes redox sensing by the heat-inducible and constitutive forms of heat shock protein 70**. *Chemistry & Biology*, 19, 1391-1399.
- Moriguchi, I., Hirono, S., Liu, Q., Nakagome, Y. and Matsushita, Y. (1992). **Simple method of calculating octanol /water partition coefficient**. *Chemical and Pharmaceutical Bulletin*, 40, 127–130.

- Moriguchi, I., Hirono, S., Nakagome, I. and Hirano, H. (1994). **Comparison of log P values for drugs calculated by several methods.** *Chemical and Pharmaceutical Bulletin*, 42, 976–978.
- Muralidharan, V., Oksman, A., Pal, P., Lindquist, S. and Goldberg, D.E. (2012). ***Plasmodium falciparum* heat shock protein 110 stabilizes the asparagine repeat-rich parasite proteome during malarial fevers.** *Nature Communications*, 3, 1310.
- Musto, H., Romero, H., Zavala, A., Jabbari, K. and Bernardi, G. (1999). **Synonymous codon choices in the extremely GC-poor genome of *Plasmodium falciparum*: compositional constraints and translational selection.** *Journal of Molecular Evolution*, 49, 27-35.
- Myszka, D.G. (1997). **Kinetic analysis of macromolecular interactions using surface plasmon resonance biosensors.** *Current Opinion in Biotechnology*, 8, 50-57.
- Myszka, D.G. (2000). **Kinetic, equilibrium, and thermodynamic analysis of macromolecular interactions with Biacore.** *Methods Enzymology*, 323, 325–340.
- Myszka, D.G. (2004). **Analysis of small-molecule interactions using Biacore S51 technology.** *Analytical Biochemistry*, 329, 316–323.
- Myszka, D.G. and Rich, R.L. (2000). **Implementing surface plasmon resonance biosensors in drug discovery.** *PSTT*, 3, 310-317.
- Nadeau, K., Nadler, S.G., Saulnier, M., Tepper, M.A. and Walsh, C.T. (1994). **Quantitation of the interaction of the immunosuppressant deoxyspergualin and analogs with Hsc70 and Hsp90.** *Biochemistry*, 33, 2561–2567.
- Nadler, S.G., Dischino, D.D., Malacko, A.R., Cleaveland, J.S., Fujihara, S.M. and Marquardt, H. (1998). **Identification of a binding site on Hsc70 for the immunosuppressant 15-deoxyspergualin.** *Biochemical and Biophysical Research Communications*, 253, 176-180.
- Nakayama, S., Torikoshi, Y., Takahashi, T., Yoshida, T., Sudo, T., Matsushima, T., Kawasaki, Y., Katayama, A., Gohda, K., Hortobagyi, G.N., Noguchi, S., Sakai, T., Ishihara, H. and Ueno, N.T. (2009). **Prediction of paclitaxel sensitivity by CDK1 and CDK2 activity in human breast cancer cells.** *Breast Cancer Research*, 11, R12.
- Neckers, L. and Tatu, U. (2008). **Molecular chaperones in pathogen virulence: emerging new targets for therapy.** *Cell Host and Microbe*, 4, 519-527.
- Nemoto, T., Ohara-Nemoto, Y., Ota, M., Takagi, T. and Yokoyama, K. (1995). **Mechanism of dimer formation of the 90-kDa heat-shock protein.** *European Journal of Biochemistry*, 233, 18.
- Nguyen, B., Tanius, F.A. and Wilson, W.D. (2007). **Biosensor-surface plasmon resonance: Quantitative analysis of small molecule–nucleic acid interactions.** *Methods*, 42, 150–161.

- Nicoll, W. S., Boshoff, A., Ludewig, M. H., Hennessy, F., Jung, M., and Blatch, G. L. (2006). **Approaches to the isolation and characterization of molecular chaperones.** *Protein Expression and Purification*, 46, 1-15.
- Nicoll, W.S., Botha, M., McNamara, C., Schlange, M., Pesce, E.-R., Boshoff, A., Ludewig, M.H., Zimmerman, R., Cheetham, M.E., Chapple, J.P. and Blatch, G.L. (2007). **Cytosolic and ER J-domains of mammalian and parasitic origin can functionally interact with DnaK.** *The International Journal of Biochemistry and Cell Biology*, 39, 736–751.
- Njunge, J.M., Ludewig, M.H., Boshoff, A., Pesce, E.-R. and Blatch, G.L. (2013). **Hsp70s and J proteins of *Plasmodium* Parasites infecting rodents and primates: structure, function, clinical relevance, and drug targets.** *Current Pharmaceutical Design*, 19, Article in Press.
- Noedl, H., Wongsrichanalai, C. and Wernsdorfer, W.H. (2003). **Malaria drug-sensitivity testing: new assays, new perspectives.** *Trends in Parasitology*, 19, 175-181.
- Nonaka, G., Blankschien, M., Herman, C., Gross, C.A. and Rhodius, V.A. (2006). **Regulon and promoter analysis of the *E. coli* heat-shock factor,  $\sigma^{32}$ , reveals a multifaceted cellular response to heat stress.** *Genes & Development*, 20, 1776-1789.
- Nyalwidhe, J. and Lingelbach, K. (2006). **Proteases and chaperones are the most abundant proteins in the parasitophorous vacuole of *Plasmodium falciparum*-infected erythrocytes.** *Proteomics*, 6, 1563-1573.
- Oakley, M.S.M., Kumar, S., Anantharaman, V., Zheng, H., Mahajan, B., Haynes, J.D., Moch, J.K., Fairhurst, R., McCutchan, T.F. and Aravind, L. (2007). **Molecular factors and biochemical pathways induced by febrile temperature in intraerythrocytic *Plasmodium falciparum* parasites.** *Infection and Immunity*, 75, 2012-2025.
- Odunuga, O.O., Longshaw, V.M. and Blatch, G.L. (2004). **Hop: more than an Hsp70/Hsp90 adaptor protein.** *BioEssays*, 26, 1058-1068.
- O’Shannessy, D.J., Brigham-Burke, M., Soneson, K.K., Hensley, P. and Brook, S.I. (1993). **Determination of rate and equilibrium binding constants for macromolecular interactions using surface plasmon resonance: use of nonlinear least of squares analysis methods.** *Analytical Biochemistry*, 212, 457-468.
- Orthwein, A., Zahn, A., Methot, S.P., Godin, D., Conticello, S.G., Terada, K. and Di Noia, J.M. (2011). **Optimal functional levels of activation-induced deaminase specifically require the Hsp40 DnaJa1.** *The EMBO Journal*, 31, 679-691.

- Pallavi, R., Roy, N., Nageshan, R.K., Talukdar, P., Pavithra, S.R., Reddy, R., Venketesh, S., Kumar, R., Gupta, A.K., Singh, R.K., Yadav, S.C. and Tatu, U. **Heat Shock Protein 90 as a drug target against protozoan infections.** *The Journal of Biological Chemistry*, 285, 37964–37975.
- Pasini, E.M., Kirkegaard, M., Mortensen, P., Lutz, H.U., Thomas, A.W. and Mann, M. (2006). **In-depth analysis of the membrane and cytosolic proteome of red blood cells.** *Blood*, 108, 791-801.
- Paternó, E. (1882). **Ricerche Sull'Acido Lapico.** *Gazzetta Chimica Italiana*, 12, 337-392.
- Patury, S., Miyata, Y. and Gestwicki, J.E. (2009). **Pharmacological targeting of the Hsp70 chaperone.** *Current Topics in Medicinal Chemistry*, 9, 1337-1351.
- Pavithra, S.R., Banumathy, G., Joy, O., Singh, V. and Tatu, U. (2004). **Recurrent fever promotes *Plasmodium falciparum* development in human erythrocytes.** *The Journal of Biological Chemistry*, 279, 46692-46699.
- Pavithra, S.R., Kumar, R. and Tatu, U. (2007). **Systems analysis of chaperone networks in the malarial parasite *Plasmodium falciparum*.** *PLoS Computational Biology*, 3, e168.
- Pérez-Sacau, E., Estevez-Braun, A., Ravelo, A.G., Yapu, D.G., and Turba, A.G. (2005). **Antiplasmodial activity of naphthoquinones related to Lapachol and  $\beta$ -Lapachone.** *Chemical Biodiversity*, 2, 264–274.
- Pesce, E.-R., Acharya, P., Tatu, U., Nicoll, W.S., Shonhai, A., Hoppe, H.C. and Blatch, G.L. (2008). **The *Plasmodium falciparum* heat shock protein 40, Pfj4, associates with heat shock protein 70 and shows similar heat induction and localisation patterns.** *The International Journal of Biochemistry and Cell Biology*, 40, 2914–2926.
- Pesce, E.-R., Cockburn, I.L., Goble, J.L., Stephens, L.L and Blatch, G.L. (2010). **Malaria heat shock proteins: drug targets that chaperone other drug targets.** *Infectious Disorders - Drug Targets*, 10, 147-157.
- Plassmeyer, M.L., Reiter, K., Shimp, R.L. Jr., Kotova, S., Smith, P.D., Hurt, D.E., House, B., Zou, X., Zhang, Y., Hickman, M., Uchime, O., Herrera, R., Nguyen, V., Glen, J., Lebowitz, J., Jin, A.J., Miller, L.H., MacDonald, N.J., Wu, Y. and Narum, D.L. (2009). **Structure of the *Plasmodium falciparum* circumsporozoite protein, a leading malaria vaccine candidate.** *The Journal of Biological Chemistry*, 284, 26951–26963.
- Pologe, L.G., Pavlovec, A., Shio, H. and Ravetch, J.V. (1987). **Primary structure and subcellular localization of the knob-associated histidine-rich protein of *Plasmodium falciparum*.**

*Proceedings of the National Academy of Sciences of the United States of America*, 84, 7139-7143.

- Porath, J., Carlsson, J., Olsson, I., and Belfrage, G. (1975). **Metal chelate affinity chromatography, a new approach to protein fractionation.** *Nature*, 258, 598–599.
- Prinsloo, E., Kramer, A.H., Edkins, A.L. and Blatch, G.L. (2012). **STAT3 interacts directly with Hsp90.** *IUBMB Life*, 64, 266-273.
- Qi, Y., Fu, X., Xiong, Z., Zhang, H., Hill, S.M., Rowan, B.G. and Dong, Y. (2012). **Methylseleninic acid enhances paclitaxel efficacy for the treatment of triple-negative breast cancer.** *PLoS One*, 7, e31539.
- Qiu, X.-B., Shao, Y.-M., Miao, S. and Wang, L. (2006). **The diversity of the DnaJ/Hsp40 family, the crucial partners for Hsp70 chaperones.** *Cellular and Molecular Life Sciences*, 63, 2560-2570.
- Ramya T., Surolia, N. and Surolia, A. (2006). **15-Deoxyspergualin modulates *Plasmodium falciparum* heat shock protein function.** *Biochemical and Biophysical Research Communications*, 348, 585-592.
- Ramya, T.N.C., Karmodiya, K., Surolia, A. and Surolia, N. (2007). **15-Deoxyspergualin primarily targets the trafficking of apicoplast proteins in *Plasmodium falciparum*.** *The Journal of Biological Chemistry*, 282, 6388–6397.
- Reuben, R. (1993). **Women and malaria – special risks and appropriate control strategy.** *Social Science and Medicine*, 37, 473-480.
- Rial, D.V. and Ceccarelli, E.A. (2002). **Removal of DnaK contamination during fusion protein purifications.** *Protein Expression and Purification*, 25, 503-507.
- Rich, R. and Myszka, D.G. (2004). **Why you should be using more SPR biosensor technology.** *Drug Discovery Today: Technologies*, 1, 301-308.
- Rich, R.L. and Myszka, D.G. (2000). **Advances in surface plasmon resonance biosensor analysis.** *Current Opinion in Biotechnology*, 11, 54–61.
- Rüdiger, S., Germeroth, L., Schneider-Mergener, J. and Bukau, B. (1997). **Substrate specificity of the DnaK chaperone determined by screening cellulose peptide libraries.** *The EMBO Journal*, 16, 1501-1507.
- Russo, I., Babbit, S., Muralidharan, V., Butler, T., Oksman, A. and Goldberg, D.E. (2010). **Plasmeprin V licenses Plasmodium proteins for export into the host erythrocyte.** *Nature*, 463, 632-636.



- Sá, J.M., Chong, J.L. and Wellem, T.E. (2011). **Malaria drug resistance: new observations and developments.** *Essays in Biochemistry*, 51, 137–160.
- Sargeant, T.J., Marti, M., Caler, E., Carlton, J.M., Simpson, K., Speed, T.P. and Cowman, A.F. (2006). **Lineage-specific expansion of proteins exported to erythrocytes in malaria parasites.** *Genome Biology*, 7, R12.1-R12.22.
- Scheufler, C., Brinker, A., Bourenkov, G., Pegoraro, S., Moroder, L., Bartunik, H. Hartl, F.U. and Moarefi, I. (2000). **Structure of TPR domain-peptide complexes: critical elements in the assembly of the Hsp70-Hsp90 multichaperone machine.** *Cell*, 101, 199-210.
- Schirmer, R.H., Adler, H., Pickhardt, M. and Manelkow, E. (2011). **“Lest we forget you — methylene blue...”.** *Neurobiology of Aging*, 32, 2325: e7-16.
- Schlieker, C., Tews, I., Bukau, B. and Mogk, A. (2004). **Solubilization of aggregated proteins by ClpB/DnaK relies on the continuous extraction of unfolded polypeptides.** *FEBS Letters*, 578, 351-356.
- Schnedier-Poetsch, T., Ju, J., Eyler, D.E., Dang, Yongjun, D., Bhat, S., Merrick, W., Green, R., Shen, B. and Lui, J.O. (2010). **Inhibition of eukaryotic translation elongation by cycloheximide and lactimidomycin.** *Nature Chemical Biology*, 6, 209–217.
- Schröder, H., Langer, T., Hartl, F.-U. and Bukau, B. (1993). **DanK, DnaJ and GrpE form a cellular chaperone machinery capable of repairing heat-induced protein damage.** *The EMBO Journal*, 12, 4137-4144.
- Sharma, Y.D. (1992). **Structure and possible function of heat-shock proteins in *Plasmodium falciparum* malaria.** *Comparative Biochemistry and Physiology*, 102, 437-444.
- Shonhai, A. (2010). **Plasmodial heat shock proteins: targets for chemotherapy.** *FEMS Immunology and Medical Microbiology*. 58, 61-74.
- Shonhai, A., Boshoff, A. and Blatch, G.L. (2005). ***Plasmodium falciparum* heat shock protein 70 is able to suppress the thermosensitivity of an *Escherichia coli* DnaK mutant strain.** *Molecular Genetics and Genomics*, 274, 70-78.
- Shonhai, A., Boshoff, A. and Blatch, G.L. (2007). **The structural and functional diversity of Hsp70 proteins from *Plasmodium falciparum*.** *Protein Science*, 16, 1803-1818.
- Shonhai, A., Botha, M., De Beer, T.J., Boshoff, A. and Blatch, G.L. (2008). **Structure-function study of a *Plasmodium falciparum* Hsp70 using three dimensional modelling and *in vitro* analyses.** *Protein and Peptide Letters*, 15, 1117-1125.

- Sinnis, P. and Sim, B.K.L. (1997) **Cell invasion by the vertebrate stages of *Plasmodium***. *Trends in Microbiology*, 5, 52-58.
- Šlapeta, J. and Keithly, J.S. (2004). ***Cryptosporidium parvum* mitochondrial-type Hsp70 targets homologous and heterologous mitochondria**. *Eukaryotic Cell*, 3, 483-494.
- Smith, J.D., Chitnis, C.E., Craig, A.G., Roberts, D.J., Hudson-Taylor, D.E., Peterson, D.S., Pinches, R., Newbold, C. and Miller, L.H. (1995). **Switches in expression of *Plasmodium falciparum* var genes correlate with changes in antigenic and cytoadherent phenotypes of infected erythrocytes**. *Cell*, 82, 101-110.
- Southworth, D.R. and Agard, D.A. (2011). **Client-loading conformation of the Hsp90 molecular chaperone revealed in the Cryo-EM structure of the human Hsp90:Hop complex**. *Molecular Cell*, 42, 771–781.
- Stephens, L.L., Shonhai, A. and Blatch, G.L. (2011). **Co-expression of the *Plasmodium falciparum* molecular chaperone, PfHsp70, improves the heterologous production of the antimalarial drug target GTP cyclohydrolase I, PfGCHI**. *Protein Expression and Purification* 77, 159–165.
- Structural Genomics Consortium, China Structural Genomics Consortium, Northeast Structural Genomics Consortium, Gräslund, S., Nordlund, P., Weigelt, J., Hallberg, B.M., Bray, J., Gileadi, O., Knapp, S., Oppermann, U., Arrowsmith, C., Hui, R., Ming, J., dhe-Paganon, S., Park, H.W., Savchenko, A., Yee, A., Edwards, A., Vincentelli, R., Cambillau, C., Kim, R., Kim, S.H., Rao, Z., Shi, Y., Terwilliger, T.C., Kim, C.Y., Hung, L.W., Waldo, G.S., Peleg, Y., Albeck, S., Unger, T., Dym, O., Prilusky, J., Sussman, J.L., Stevens, R.C., Lesley, S.A., Wilson, I.A., Joachimiak, A., Collart, F., Dementieva, I., Donnelly, M.I., Eschenfeldt, W.H., Kim, Y., Stols, L., Wu, R., Zhou, M., Burley, S.K., Emtage, J.S., Sauder, J.M., Thompson, D., Bain, K., Luz, J., Gheyi, T., Zhang, F., Atwell, S., Almo, S.C., Bonanno, J.B., Fiser, A., Swaminathan, S., Studier, F.W., Chance, M.R., Sali, A., Acton, T.B., Xiao, R., Zhao, L., Ma, L.C., Hunt, J.F., Tong, L., Cunningham, K., Inouye, M., Anderson, S., Janjua, H., Shastry, R., Ho, C.K., Wang, D., Wang, H., Jiang, M., Montelione, G.T., Stuart, D.I., Owens, R.J., Daenke, S., Schütz, A., Heinemann, U., Yokoyama, S., Büssov, K. and Gunsalus, K.C. (2008). **Protein production and purification**. *Nature Methods*, 5, 135–146.
- Su, X.Z. and Wellems, T.E. (1994). **Sequence, transcript characterization and polymorphisms of a *Plasmodium falciparum* gene belonging to the heat-shock protein (HSP) 90 family**. *Gene*, 151, 225–230.

- Suh, W. C., Burkholder, W. F., Lu, C. Z., Zhao, X., Gottesman, M. E., and Gross, C. A. (1998). **Interaction of the Hsp70 molecular chaperone, DnaK, with its cochaperone DnaJ.** *Proceedings of the National Academy of Sciences of the United States of America*, *95*, 15223-15228.
- Sulkowski, E. (1985). **Purification of proteins by IMAC.** *Trends in Biotechnology*, *3*, 1-7.
- Swain, J.F., Dinler, G., Sivendran, R., Montgomery, D.L., Stotz, M. and Gierasch, L.M. (2007). **Hsp70 chaperone ligands control domain association via an allosteric mechanism mediated by the interdomain linker.** *Molecular Cell*, *26*, 27–39.
- Szabo, A., Langer, T., Schrodgers, H., Flanagan, J., Bukau, B. and Hartl, F.U. (1994). **The ATP hydrolysis-dependent reaction cycle of the *Escherichia coli* Hsp70 system- DnaK, DnaJ, and GrpE.** *Proceedings of the National Academy of Sciences of the United States of America*, *91*, 10345-10349.
- Szabo, A., Stolz, L and Granzow, R. (1995). **Surface Plasmon resonance and its use in biomolecular interaction analysis (BIA).** *Current Opinion in Structural Biology*, *5*, 699-705.
- Tassone, P., Tagliaferri, P., Perricelli, A., Blotta, S., Quaresima, B., Martelli M.L., Goel, A., Barbieri, V, Constanzo, F., Boland, C.R. and Venuta, S. (2003). **BRCA1 expression modulates chemosensitivity of BRCA1-defective HCC1937 human breast cancer cells.** *British Journal of Cancer*, *88*, 1285-1291.
- Terada, K. and Oike, Y. (2010). **Multiple molecules of Hsc70 and a dimer of DjA1 independently bind to an unfolded protein.** *The Journal of Biological Chemistry*, *285*, 16789–16797.
- Terasawa, K., Minami, M., and Minami, Y. (2005). **Constantly updated knowledge of Hsp90.** *Journal of Biochemistry*, *137*, 443–447.
- The RTS,S Clinical Trials Partnership (2012). **A phase 3 trial of RTS,S/As01 Malaria Vaccine in African Infants.** *The New England Journal of Medicine*, *Article in Press*, DOI: 10.1056/NEJMoa1208394.
- Thera, M.A. and Plowe, C.T. (2012). **Vaccines for malaria: how close are we?** *Annual Review of Medicine*, *63*, 345–357.
- Tolia, N.H. and Joshua-Tor, L. (2006). **Strategies for protein coexpression in *Escherichia coli*.** *Nature Methods*, *3*, 55-64.
- Towbin, H., Staehelin, T and Gordon, J. (1979). **Electrophoretic transfer of proteins from polyacrylamide gels to nitrocellulose sheets: procedure and some applications.** *Proceedings of the National Academy of Sciences of the United States of America*, *76*, 4350-4354.

- Trabbic-Carlson, K., Liu, L., Kim, B. and Chilkoti, A. (2004). **Expression and purification of recombinant proteins from *Escherichia coli*: comparison of an elastin-like polypeptide fusion with an oligohistidine fusion.** *Protein Science*, 13, 3274-3284.
- Trager, W. and Jensen, J.B. (1976). **Human malaria parasites in continuous culture.** *Science*, 193, 673–675.
- Trésaugues, L., Collinet, B., Minard, P., Henckes, G., Aufrère, R., Blondeau, K., Liger, D., Zhou, C.-Z., Janin, J., van Tilbeurgh, H. and Quevillon-Cheruel, S. (2004). **Refolding strategies from inclusion bodies in a structural genomics project.** *Journal of Structural and Functional Genomics*, 5, 195–204.
- Tsai, J. and Douglas, M.G. (1996). **A conserved HPD sequence of the J-domain is necessary for YDJ1 stimulation of Hsp70 ATPase activity at a site distinct from substrate Binding.** *The Journal of Biological Chemistry*, 271, 9347–9354.
- Tsutsumi, S., Mollapour, M., Prodromou, C., Lee, C.-T., Panaretou, B., Yoshida, S., Mayer, M.P. and Neckers, L.-M. (2012). **Charged linker sequence modulates eukaryotic heat shock protein 90 (Hsp90) chaperone activity.** *Proceedings of the National Academy of Sciences of the United States of America*, 109, 2937-2942.
- Tuteja, R. (2007). **Malaria – an overview.** *FEBS Journal*, 274, 4670–4679.
- Ungewickell, E., Ungewickell, H., Holstein, S.E., Linder, R., Kondury, P., Barouch, W., Martini, B., Greene, L.E., and Eisenberg, E. (1995). **Role of auxilin in uncoating clathrin-coated vesicles.** *Nature*, 378, 632–635.
- van Gestel, R.A., van Soilingec, W.W., vander Toorna, H.W.P., Rijksenc, G., Hecka, A.J.R., van Wijck, R. and Slijper, M. (2010). **Quantitative erythrocyte membrane proteome analysis with Blue-Native/SDS PAGE.** *Journal of Proteomics*, 73, 456-465.
- Vistica, D.T., Skehan, P., Scudiero, D., Monks, A., Pittman, A. and Boyd, M.R. (1991). **Tetrazolium-based assays for cellular viability: a critical examination of selected parameters affecting formazan production.** *Cancer research*, 51, 2515-2520.
- Vythilingam, I., Tan, C.H., Asmad, M., Chan, S.T., Lee, K.S. and Singh, B. (2006). **Natural transmission of *Plasmodium knowlesi* to humans by *Anopheles latens* in Sarawak, Malaysia.** *Transactions of the Royal Society of Tropical Medicine and Hygiene*, 100, 1087–1088.
- Walsh, P., Bursac, D, Law, Y.C., Cyr, D. and Lithgow, T. (2004). **The J-protein family: modulating protein assembly, disassembly and translocation.** *EMBO Reports*, 5, 567-571.

- Wang, Y., Bolton, E., Dracheva, S., Karapetyan, K., Shoemaker, B.A., Suzek, T.O., Wang, J., Xiao, J., Zhang, J. and Bryant, S.H. (2010). **An overview of the PubChem BioAssay resource.** *Nucleic Acids Research*, 38 (Databases issue), D255-D266.
- Watanabe, J. (1997). **Cloning and characterization of heat shock protein DnaJ homologues from *Plasmodium falciparum* and comparison with ring infected erythrocyte surface antigen.** *Molecular and Biochemical Parasitology*, 88, 253-258.
- Wayne, N. and Bolon, D.N. (2007). **Dimerization of Hsp90 is required for *in vivo* function. Design and analysis of monomers and dimers.** *The Journal of Biological Chemistry*, 282, 35386-35395.
- Wells, T.N.C. (2011). **Natural products as starting points for future anti-malarial therapies: going back to our roots?** *Malaria Journal*, 10, S3.
- Westhoff, B., Chapple, P., van der Spuy, J., Höhfeld, J. and Cheetham, M.E. (2005). **HSJ1 Is a neuronal shuttling factor for the sorting of chaperone clients to the proteasome.** *Current Biology*, 15, 1058–1064.
- Weyermann, J., Lochmann, D and Zimmer, A. (2005). **A practical note on the use of cytotoxicity assays.** *International Journal of Pharmaceutics* 288, 369–376.
- WHO 2008: World Malaria Report: [www.who.int/malaria/wmr2008](http://www.who.int/malaria/wmr2008)
- WHO 2011: World Malaria Report: [www.who.int/malaria/world\\_malaria\\_report\\_2011](http://www.who.int/malaria/world_malaria_report_2011)
- Willander, M. and Al-Hilli, S. (2009). **Analysis of biomolecules using surface plasmons.** *Methods in Molecular Biology*, 544, 201-229.
- Williamson, D.S., Borgognoni, J., Clay, A., Daniels, Z., Dokurno, P., Drysdale, M.J., Foloppe, N., Francis, G.L., Graham, C.J., Howes, R., Macias, A.T., Murray, J.B., Parsons, R., Shaw, T., Surgenor, A.E., Terry, L., Wang, Y., Wood, M., and Massey, A.J. (2009). **Novel adenosine-derived inhibitors of 70 kDa heat shock protein, discovered through structure-based design.** *Journal of Medicinal Chemistry*, 52, 1510–1513.
- Wirth, D.F. (2002). **The parasite genome: biological revelations.** *Nature*, 419, 495-496.
- Wisén, S. and Gestwicki, J.E. (2008). **Identification of small molecules that modify the protein folding activity of heat shock protein 70.** *Analytical Biochemistry*, 374, 371–377.
- Wisén, S., Bertelsen, E.B., Thompson, A.D., Patury, S., Ung, P., Chang, L., Evans, C.G., Walter, G.M., Wipf, P., Carlson, H.A., Brodsky, J.L., Zuiderweg, E.R. and Gestwicki, J. (2010). **Binding of a small molecule at a protein-protein interface regulates the chaperone activity of Hsp70-Hsp40.** *ACS Chemical Biology*, 5, 611–622.

- Wisniewska, M., Karlberg, T., Lehtiö, L., Johansson, I., Kotenyova, T., Moche, M and Schüler, H. (2010). **Crystal structures of the ATPase domains of four human Hsp70 isoforms: HSPA1L/Hsp70-hom, HSPA2/Hsp70-2, HSPA6/Hsp70B', and HSPA5/BiP/GRP78.** *PLoS One*, *5*, e8625.
- Witkowski, B., Lelièvre, J., Barragán, M.J.L., Laurent, V., Su, X.-Z., Berry, A and Benoit-Vical, F. (2010). **Increased Tolerance to artemisinin in *Plasmodium falciparum* is mediated by a quiescence mechanism.** *Antimicrobial Agents and Chemotherapy*, *54*, 1872–1877.
- Wright, C.M., Chovatiya, R.J., Jameson, N.E., Turner, D.M., Zhu, G., Werner, S., Huryn, D.M., Pipas, J.M., Day, B.W., Wipf, P. and Brodsky, J.L. (2008). **Pyrimidinone-peptoid hybrid molecules with distinct effects on molecular chaperone function and cell proliferation.** *Bioorganic and Medicinal Chemistry*, *16*, 3291-3301.
- Yamaguchi, H., Yamamoto, C. and Tanaka, N. (1965). **Inhibition of protein synthesis by Blastidicin S.** *The Journal of Biochemistry*, *57*, 667-677.
- Yamamoto, S., Nakano, S., Owari, K., Fuziwara, K., Ogawa, N., Otaka, M., Tamaki, K., Watanabe, S., Komatsuda, A., Wakui, H., Sawada, K., Kubota, H. and Itoh, H. (2010). **Gentamicin inhibits HSP70-assisted protein folding by interfering with substrate recognition.** *FEBS Letters*, *584*, 645–651.
- Yano, M., Terada, K. and Mori, M. (2004). **Mitochondrial import receptors Tom20 and Tom22 have chaperone-like activity.** *The Journal of Biological Chemistry*, *279*, 10808-10813.
- Zhang, H., Xu, L.-Q. and Perret, S. (2011). **Studying the effects of chaperones on amyloid fibril formation.** *Methods*, *53*, 285-294.
- Zhou, V., Han, S., Brinker, A., Klock, H., Caldwell, J and Gu, X. (2004). **A time-resolved Fluorescence resonance energy transfer-based HTS assay and a surface plasmon resonance-based binding assay for heat shock protein 90 inhibitors.** *Analytical Biochemistry*, *331*, 349–357.
- Zhu, X., Zhao, X., Burkholder, W.F., Gragerov, A., Ogata, C.M., Gottesman, M.E., and Hendrickson, W.A. (1996). **Structural analysis of substrate binding by the molecular chaperone DnaK.** *Science*, *272*, 1606–1614.
- Zhuravleva, A., and Gierasch, L.M. (2011). **Allosteric signal transmission in the nucleotide binding domain of 70-kDa heat shock protein (Hsp70) molecular chaperones.** *Proceedings of the National Academy of Sciences of the United States of America*, *108*, 6987-6992.

- Zuiderweg, E.R.P., Bertelsen, E.B., Rousaki, A., Mayer, M.P., Gestwicki, J.E. and Ahmad, A. (2012). **Allostery in the Hsp70 chaperone proteins.** *Topics in Current Chemistry, Article in Press*, DOI: 10.1007/128\_2012\_323.

## APPENDIX

---

### 7.1. APPENDIX A: GENERAL BIOCHEMICAL AND MOLECULAR BIOLOGY TECHNIQUES

---

#### 7.1.1. *Competent cell production*

---

5 ml 2 x YT broth was inoculated with a single colony of cells of the *E. coli* strain of interest, and incubated, shaking at 200 rpm, overnight at 37 °C. The overnight starter culture was split into two flasks each containing 100 ml 2 x YT broth, and grown further at 37 °C until mid-log phase ( $A_{600} \sim 0.6 - 0.8$ ). Cultures were pooled, and cells were harvested (in sterile centrifuge tubes) for 10 minutes at 2700 *g* (4 °C). The cell pellet was resuspended in ~ 8 ml buffer RF 1 (15 % glycerol [v/v], 100 mM KCl, 50 mM MnCl<sub>2</sub>, 30 mM CH<sub>3</sub>COOK, 10 mM CaCl<sub>2</sub>, pH 5.8), and incubated on ice for 20 minutes. Cells were harvested again (as above), and then resuspended in ~ 2 ml buffer RF 2 (15 % glycerol (v/v), 10 mM Mops, 10 mM KCl, 75 mM CaCl<sub>2</sub>, pH 6.8). Resuspended cells were aliquoted (~ 200 ul / aliquot) and stored at -80 °C until needed for bacterial transformation.

#### 7.1.2. *Bacterial transformation*

---

50 µl competent *E. coli* cells were incubated with 2 µl DNA on ice for 20 minutes. The incubation mixture was then subjected to heat shock at 42 °C for 45 seconds, followed by cold shock on ice for 2 minutes. The cells were then diluted into 1 ml 2 x YT broth (pre-warmed to 37 °C), and incubated, shaking, at 37 °C for 1 hour. After the incubation period, the bacterial culture was centrifuged at 13 000 rpm for 1 minute. 900 µl of the supernatant (broth) were removed, and the cell pellet was resuspended in the remaining 100 µl broth. The resuspended cells were spread-plated onto an agar plate (containing appropriate antibiotic if necessary), and grown overnight at 37 °C. A negative control transformation was carried out with each plasmid transformation. In the negative control, plasmid DNA was replaced with deionised water.



### **7.1.3. Sodium-dodecyl sulphate polyacrylamide gel electrophoresis (SDS-PAGE)**

---

SDS-PAGE analyses were carried using protocols based on previously described methods (Laemmli, 1970). 5 x SDS-PAGE loading buffer (10 % glycerol [v/v], 2 % SDS, 5 %  $\beta$ -mercaptoethanol, 0.05 % [w/v] bromophenol blue, 0.0625 M Tris, pH 6.8) was added to protein samples, which were subsequently boiled at  $\sim 95$  °C for 5 minutes, centrifuged at 16 000 g for 1 minute, and then kept on ice until needed. An SDS-PAGE gel was prepared as follows: a 12 % resolving gel (12 % [w/v] acrylamide / bis-acrylamide, 0.1 % [w/v] SDS, 0.05 % [w/v] ammonium persulphate, 0.005 % [v/v] N, N, N', N'-tetramethylethylenediamine (TEMED), 0.375 M Tris, pH 8.8) was poured between glass plates and was allowed to set. A 4 % stacking gel (4 % [w/v] acrylamide / bis-acrylamide, 0.1 % [w/v] SDS, 0.05 % [w/v] ammonium persulphate, 0.005 % [v/v] TEMED, 0.125 M Tris, pH 6.8) was then poured, a comb inserted, and was allowed to set. Protein samples were loaded into prepared gels, then run at 100 – 160 V until the dye front reached the end of the gel. Gels were set and run using a Mini ProteanR II system (Bio-Rad Laboratories, Inc., U.S.A.). Gels were either used for Western blotting (Section 7.1.4), or were stained. Gels were stained in Coomassie stain (0.25 % Coomassie Blue R-250, 40 % [v/v] methanol, 7 % [v/v] acetic acid) for at least an hour (or overnight), then destained in destain solution (40 % [v/v] methanol, 7 % [v/v] acetic acid) until protein bands were easily visible on the destained gel, after which the gel was visualized using a an HP scanner.

### **7.1.4. Western Blotting**

---

For the detection of proteins using Western Blotting analysis, protocols adapted from previously described methods (Towbin *et al.*, 1979) were used. A 12 % SDS-PAGE gel (Section 7.1.3) of the protein samples was run. Proteins were transferred onto nitrocellulose membrane (Section 2.2.1), sandwiched between filter paper and fibre pads, using transfer buffer (20 % [v/v] methanol, 192 mM Glycine, 25 mM Tris) under a voltage of 100 V for 2 hours, in a Mini Protean R II Western trans-blot system (Bio-Rad Laboratories, Inc., U.S.A.). Staining of the nitrocellulose membrane in Ponceau-S stain (0.5 % [w/v] Ponceau-S, 1 % [v/v] glacial acetic acid) for 2 minutes allowed for the assessment of the success of the transfer. Ponceau-S stain was partially rinsed off the membrane with distilled water, allowing for the protein marker bands as well as lanes to be marked on the membrane. The Ponceau-S stain was

completely rinsed off the membrane with Tris-buffered saline (TBS: 50 mM Tris, 150 mM NaCl, pH 7.5). The nitrocellulose membrane was incubated in blocking solution (5 % [w/v] fat-free milk powder in TBS) for 1 hour at room temperature, and then incubated in primary antibody (diluted in blocking solution at dilutions specified in Chapter 2) overnight at 4 °C with gentle agitation (on a rocker or in a falcon tube on a roller). After incubation with primary antibody, the nitrocellulose membrane was washed twice for 20 minutes with TBS containing 0.1 % [v/v] Tween 20 (TBS-T), before incubating in secondary horse-radish peroxidase (HRP) – conjugated antibody (diluted in blocking solution, at dilutions specified in Chapter 2) for 45 minutes at room temperature. The membrane was finally washed four times, 15 minutes each, with TBS-T. Proteins were detected on Western blotting membranes using Chemiluminescence, and visualised using a VersaDoc™ (4000 Model) imaging system (Bio-Rad Laboratories Inc., U.S.A.), using Quantity One® (v. 4.4.1) software (Bio-Rad Laboratories Inc., U.S.A.).

#### ***7.1.5. Charging of Sepharose beads with nickel sulphate***

---

Chelating Sepharose beads were charged with nickel sulphate for use in nickel affinity chromatography. A volume of beads as supplied by the manufacturers (~ 75 % slurry in 20 % ethanol) was sedimented by centrifugation at 1500 *g* for 2 minutes. The supernatant was removed and discarded. Five bead volumes of distilled water was added to the beads, which were shaken until fully resuspended, and agitated gently for 5 minutes. Beads were sedimented as above. The supernatant was again removed and disposed of. One bead volume of NiSO<sub>4</sub> solution (0.1 M) was added to the beads, which were shaken until fully resuspended, and then gently agitated for 15 minutes. Beads were again sedimented as above, and the supernatant was removed and disposed of. The beads were washed by the addition of five bead volumes of distilled water and gentle agitation for 5 minutes. Beads were sedimented as above, and the supernatant was removed and disposed of. This wash step was repeated twice more, and charged beads were resuspended in one bead volume of native lysis buffer (Section 2.2.2.2), resulting in a 50 % slurry of nickel-charged sepharose beads.

### 7.1.6. Buffer exchange

---

After purification, recombinant proteins were subjected to buffer exchange to facilitate the removal of imidazole (used in the elution of proteins off nickel-charged sepharose beads) from the protein solution prior to use in *in vitro* work.

#### 7.1.6.1. Buffer exchange by dialysis

---

Eluted recombinant proteins were suspended in assay buffer (50 mM Tris, pH 7.4, 100 mM NaCl) in dialysis tubes made by tying both ends of a section of dialysis tubing (Section 2.2.1) with string. An air pocket of ~ 50 % of the volume of the eluted protein was left at one end of the tube to allow for the volume of the solution to increase as buffer exchange took place. The tubes containing the eluted protein were suspended in 1 l assay buffer, and dialysis was carried out, stirring, overnight (~ 16 hours) at 4 °C. The following day the protein was further dialysed for 6 hours in a fresh volume (1 l) of assay buffer. After dialysis, the integrity of the protein was assessed by SDS-PAGE.

#### 7.1.6.2. Buffer exchange using Amicon Spin Column filters

---

Amicon spin column filters (Section 2.2.1) were conditioned using the appropriate buffer: either assay buffer (50 mM Tris, pH 7.4, 100 mM NaCl) or Hepes buffer (Hepes) depending on whether proteins were to be used in *in vitro* assays (Chapter 3) or in SPR spectroscopy (Chapter 4), respectively. Conditioning was carried out by passing 15 ml of the appropriate buffer through the column by centrifugation at 2000 *g* for 5 minutes at a time until all but ~ 0.5 – 1.5 ml of the buffer had passed through the filter membrane. The eluted protein (no more than ~ 8 ml), along with assay buffer (enough to completely fill the tube) were added into the filter column, and centrifuged (2000 *g*, 5 minutes at a time) until ~ 2 ml remained in the top of the filter. The filter column was topped up (completely full) with the appropriate buffer three more times, and centrifuged each time until ~ 2 ml remained. After this buffer exchange procedure the protein solution was diluted with the appropriate buffer to the required volume to yield the desired concentration. To assess the integrity of the protein, SDS-PAGE was carried out after buffer exchange.

### **7.1.7. Protein quantification**

---

#### *7.1.7.1. Protein quantification by NanoDrop*

---

Protein quantification was carried out using a NanoDrop 2000 spectrophotometer (Thermo Scientific), controlled by NanoDrop 2000/2000c software (v.1.4.2, Thermo Fisher Scientific Inc., U.S.A.) Measurements based on the absorbance of the protein solutions at 280 nm were carried out by blanking the instrument with the buffer that the protein was buffer exchanged into, and then taking triplicate measurements of the protein concentration, to allow for an average protein concentration to be determined.

#### *7.1.7.2. Protein quantification by Bradford's method*

---

Protein quantification by the Bradford's assay was carried out by a method based on that described by Bradford and colleagues (1976). In a 96-well plate, 200  $\mu$ l Bradford's reagent (Section 2.2.1) was added to 10  $\mu$ l protein samples to be quantified. Along with the samples of unknown protein concentration, a set of bovine serum albumin (BSA) standards of known concentrations were assayed. The samples were allowed to incubate at room temperature for 10 minutes, after which the absorbance of the samples at 595 nm was read using a Powerwave 96-well plate reader (BioTek Instruments Inc., U.S.A.). The absorbance of the BSA standards against BSA concentrations was plotted in a standard curve to allow for the determination of the concentrations of the recombinant proteins. Any recombinant proteins determined have a higher concentration than the highest BSA concentration (200 g/ml) was diluted ten and one hundred fold and assayed again for accurate concentration determination.

## 7.2. APPENDIX B: SUPPLEMENTARY DATA

---

### 7.2.1. Chapter 2: Protein expression and purification

---

#### 7.2.1.1. Information on expression plasmids

---

The plasmids used in the expression of the target proteins in this study were either purchased, or constructed (as part of previous projects) by other researchers. The pQE30-PfHsp70-1 (wild type) plasmid encoding the wild type sequence of the *P. falciparum* cytosolic Hsp70 isoform 1, PfHsp70-1 (PlasmoDB ID: PF08\_0054), in frame with an N-terminal hexa-histidine tag, was constructed and contributed by Dr. T.S. Matambo (Matambo *et al.*, 2004). The pQE30-PfHsp70-1 (optimised) plasmid encoding the codon optimised form of the *P. falciparum* cytosolic Hsp70 isoform 1 in frame with an N-terminal hexa-histidine tag was synthesised by and purchased from GenScript (U.S.A.). The wild type and optimised forms of the hexa-histidine tagged PfHsp70-1 protein encoded by the plasmids described above will henceforth be referred to as PfHsp70-1(wt) and PfHsp70-1(opt) respectively. The optimised coding region for the amino acid sequence of the *P. falciparum* Hsp70, PfHsp70-x (PlasmoDB ID: MAL-7P1.228), downstream of the predicted ER signal (amino acids 25-679) contained in a pUC57 vector, was purchased from GenScript (U.S.A.), and was ligated into a pQE30 plasmid in-frame with the coding region for the N-terminal hexa-histidine tag, by Mr. R. Hatherley (Hatherley, 2010). The hexa-histidine tagged protein encoded by this plasmid will be referred to as PfHsp70-x. The pQE30-PfHsp40 plasmid encoding the codon harmonised sequence of the only canonical, cytosolic type I Hsp40 protein in *P. falciparum*, termed PfHsp40 (PlasmoDB ID: PF14\_0359), in frame with an N-terminal hexa-histidine tag, was constructed by Dr. M. Botha (Botha *et al.*, 2011). The codon harmonisation of the PfHsp40 coding region toward improved heterologous expression was carried out by Dr. Evelina Angov (Walter Reed Army Institute of Research, MA, U.S.A; Botha *et al.*, 2011). The hexa-histidine protein encoded by this plasmid will be referred to as PfHsp40. The pQE30-Hsj1a plasmid encoding the wild type sequence of a human type II Hsp40, Hsj1a (GenBank ID: DNAJB2) in frame with an N-terminal hexa-histidine tag, was constructed by Ms. C. McNamara (McNamara, 2006). The hexa-histidine tagged protein encoded by this plasmid will be referred to as Hsj1a. The pMSHsp70 plasmid encoding human Hsp70 (GenBank ID: HSPA1A), with a C-terminal hexa-histidine tag replacing the last six residues of the human Hsp70 amino acid sequence, was received as a kind gift from Professor J. Brodsky, University of Pittsburgh, U.S.A. (Chiang *et al.*, 2009). The hexa-histidine tagged protein encoded by this plasmid will be referred to as

HsHsp70. Table 7.1 summarises the plasmids used, the *E. coli* strains used for target protein expression, and the antibiotics used in the expression.

**Table 7.1: Plasmids used in the expression of target proteins.** The proteins encoded by the plasmids, as well as the *E. coli* strains used in the protein expression and the antibiotic used are given.

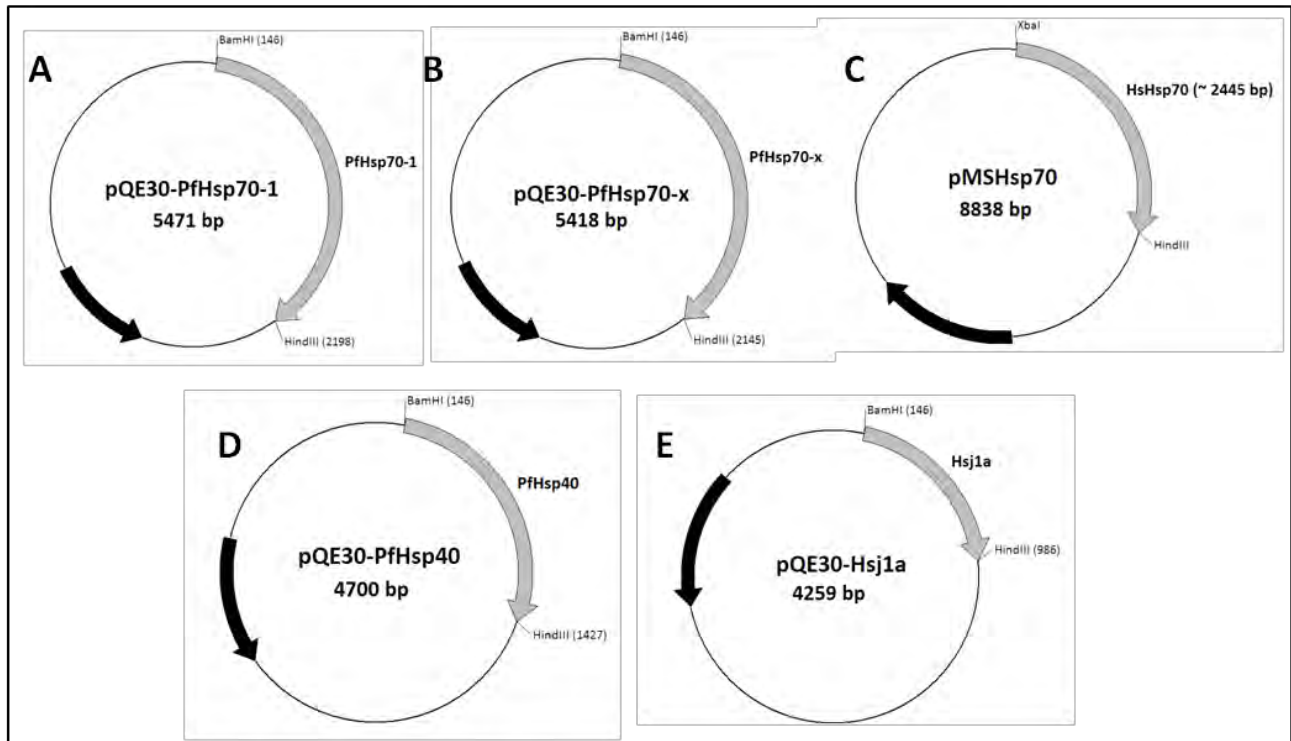
Plasmid	Encoded protein	<i>E. coli</i> strain	Antibiotic (concentration)
pQE30-PfHsp70-1 wild type coding region	PfHsp70-1 (PF08_0054)	XL1 Blue	Ampicillin (100 µg/ml)
pQE30-PfHsp70-1 optimised coding region	PfHsp70-1 (PF08_0054)	XL1 Blue	Ampicillin (100 µg/ml)
pQE30-PfHsp70-x	PfHsp70-x (MAL-7P1.228)	M15[pRep4]	Ampicillin (100 µg/ml), Kanamycin (50 µg/ml)
pMSHsp70	HsHsp70 (HSPA1A)	BL21	Ampicillin, 100 µg/ml
pQE30-Hsj1a	Hsj1a (DNAJB2)	XL1 Blue	Ampicillin, 100 µg/ml
pQE30-PfHsp40	PfHsp40 (PF14_0359)	M15[pRep4]	Ampicillin (100 µg/ml), Kanamycin (50 µg/ml)

#### 7.2.1.2. Diagnostic restriction digestion for plasmid identification

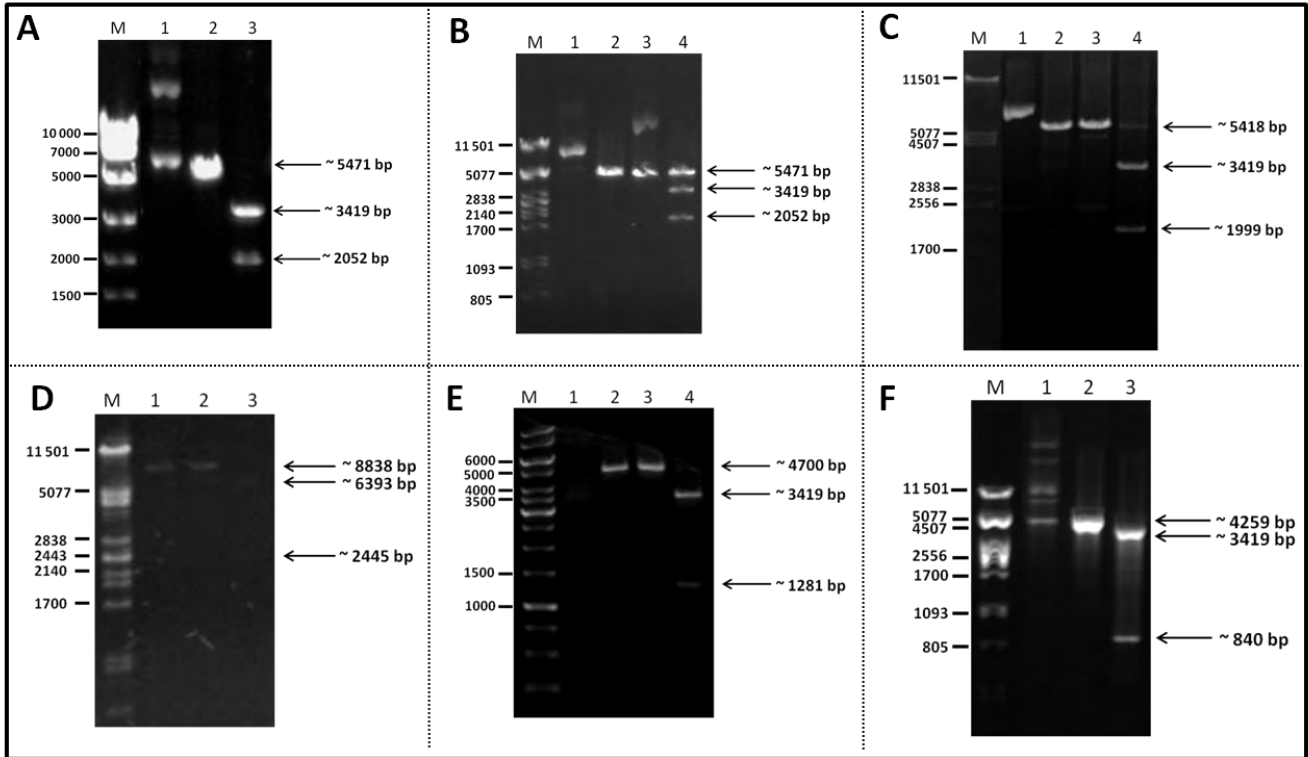
The expression vectors used for the heterologous production of proteins of interest in various *E. coli* strains were subjected to diagnostic restriction digests as a way of confirming their identities based on the predicted fragment patterns and sizes for each plasmid. Digest reactions (20 µl reaction volume) consisted of 50 – 200 ng DNA, 1 - 2 U restriction enzyme 1, 1 - 2 U restriction enzyme 2 (where applicable) and 2 µl 10 x reaction buffer. Restriction digest reactions were carried out at 37 °C, for 4 hours or overnight and were terminated by the addition of 6 x DNA loading dye (30 % v/v glycerol, 0.25 % (w/v) bromophenol blue). The resulting samples were analysed by agarose gel electrophoresis using 0.8 % (w/v) agarose gel prepared in 0.5 x TBE buffer (40 mM Tris-borate, 1 mM EDTA) containing 0.5 µg/ml ethidium bromide, and visualised under UV light.

Figure 7.1 shows plasmid maps of each expression vector used in this study, and the results of the diagnostic restriction digests confirming the identities of each of the expression plasmids are shown in Figure 7.2. For all six plasmids, the double digest reactions with *Bam*HI and *Hind*III, or *Bam*HI and *Xba*I in the case of pMSHsp70, resulted in fragments of the expected sizes on the agarose gel: the pQE30-PfHsp70-1(wt) (Figure 7.2A) and pQE30-PfHsp70(opt) (Figure 7.2B) plasmids resulted in two fragments of 3419 and 2052 bp each; the pQE30-PfHsp70-x plasmid (Figure 7.2C) resulted in fragments of 3419 and

1999 bp; the pMSHsp70 plasmid (Figure 7.2D) resulted in fragments of 6393 and 2445 bp; the pQE30-PfHsp40 plasmid (Figure 7.2E) resulted in fragments of 3419 and 1281 bp; and the pQE30-Hsj1a plasmid (Figure 7.2F) resulted in fragments of 3419 and 840 bp. Comparing these fragment sizes to the expected sizes of the plasmid inserts encoding the six target proteins shown in Figure 7.1 confirms the identities of the six expression vectors.



**Figure 7.1: Plasmid maps of each expression vector used to express and purify proteins of interest in this study.** (A): pQE30-PfHsp70-1 (represents both the wild type and optimised versions of the PfHsp70-1 cDNA), (B): pQE30-PfHsp70-x, (C): pMSHsp70, (D) pQE30-PfHsp40 and (E) pQE30-Hsj1a. Black arrows on each map represent the gene encoding ampicillin resistance. Plasmid maps were generated using BioEdit Sequence Alignment Editor (v. 7.1.3.0; Hall, 1999).



**Figure 7.2: Confirmation of the identities of expression plasmids by diagnostic restriction enzyme digests and 0.8 % agarose gel electrophoresis.** (A) pQE30-PfHsp70-1(wild type). M: Fermentas DNA Ladder; 1: Uncut plasmid; 2: Plasmid linearised with *Bam*HI (single fragment of 5471 bp expected); 3: Plasmid digested with *Bam*HI and *Hind*III (two fragments of 3419 bp and 2052 bp expected). (B) pQE30-PfHsp70-1(optimised). M: *Pst*I digested  $\lambda$  DNA marker; 1: Uncut plasmid; 2: Plasmid linearised with *Bam*HI (single fragment of 5471 bp expected); Plasmid linearised with *Hind*III (single fragment of 5471 bp expected); 4: Plasmid digested with *Bam*HI and *Hind*III (two fragments of 3419 bp and 2052 bp expected). (C) pQE30-PfHsp70-x. M: *Pst*I digested  $\lambda$  DNA marker; 1: Uncut plasmid; 2: Plasmid linearised with *Bam*HI (single fragment of 5418 bp expected); Plasmid linearised with *Hind*III (single fragment of 5418 bp expected); 4: Plasmid digested with *Bam*HI and *Hind*III (two fragments of 3419 bp and 1999 bp expected). (D) pMSHsp70. M: *Pst*I digested  $\lambda$  DNA marker; 1: Uncut plasmid; 2: Plasmid linearised with *Hind*III (single fragment of 8838 bp expected); 4: Plasmid digested with *Xba*I and *Hind*III (two fragments of 6393 bp and 2445 bp expected). (E) pQE30-PfHsp40. M: *Pst*I digested  $\lambda$  DNA marker; 1: Uncut plasmid; 2: Plasmid linearised with *Hind*III (single fragment of 4700 bp expected); 4: Plasmid digested with *Bam*HI and *Hind*III (two fragments of 3419 bp and 1281 bp expected). (F) pQE30-Hsj1a. M: *Pst*I digested  $\lambda$  DNA marker; 1: Uncut plasmid; 2: Plasmid linearised with *Hind*III (single fragment of 4259 bp expected); 3: Plasmid digested with *Bam*HI and *Hind*III (two fragments of 3419 bp and 840 bp expected). Agarose gels contained 0.5  $\mu$ g/ml ethidium bromide and were visualised under UV light. Marker sizes (in bp) are indicated to the left of each figure.



## 7.2.2. Chapter 3: In vitro chaperone assays

### 7.2.2.1. ATPase assays

The effect of DMSO on the basal and Hsp40-stimulated ATPase activities was assessed, and was, in all cases, found to have no significant effect on ATPase activity, as shown in Figure 7.3 below. For this reason, all ATPase activities tested in the presence of small molecules were expressed relative to a no-compound control.

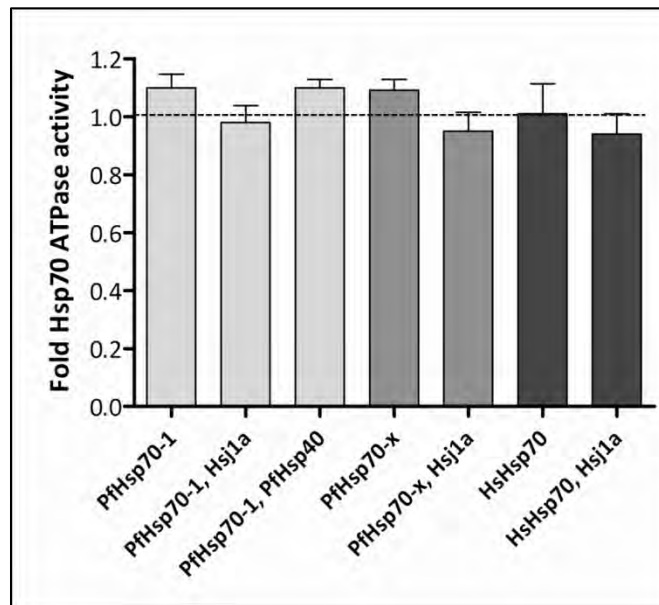


**Figure 7.3: Effect of DMSO on the basal and Hsp40-stimulated ATPase activities of Hsp70s.** The effects of DMSO, expressed as fold change in activity relative to an untreated control for each protein, are shown for PfHsp70-1, PfHsp70-x and HsHsp70. Error bars represent standard deviation ( $n = 9$ ), and the dotted line indicates the position of “1 fold”: no change in activity.

### 7.2.2.2. MDH aggregation suppression assays

As described in Section 3.3.1, several compounds (nor- $\beta$ -lapachona, hydroxy- $\beta$ -lapachona, c-alil-laurosona and PGKC4\_7C and PGKC4\_4I) were found to act as chemical chaperones to MDH, preventing, themselves, the thermal aggregation of MDH in the absence of Hsp70s. Examples of these effects by compounds are shown in Figure 7.4 below. To avoid the confounding effects these compounds would have on the assessments of compounds as modulators of *in vitro* Hsp70 activity, they were excluded from further assessments.

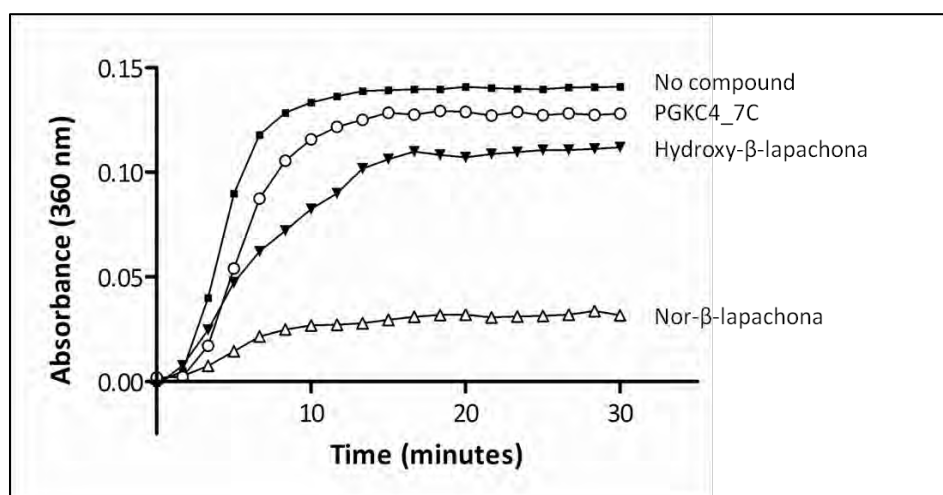
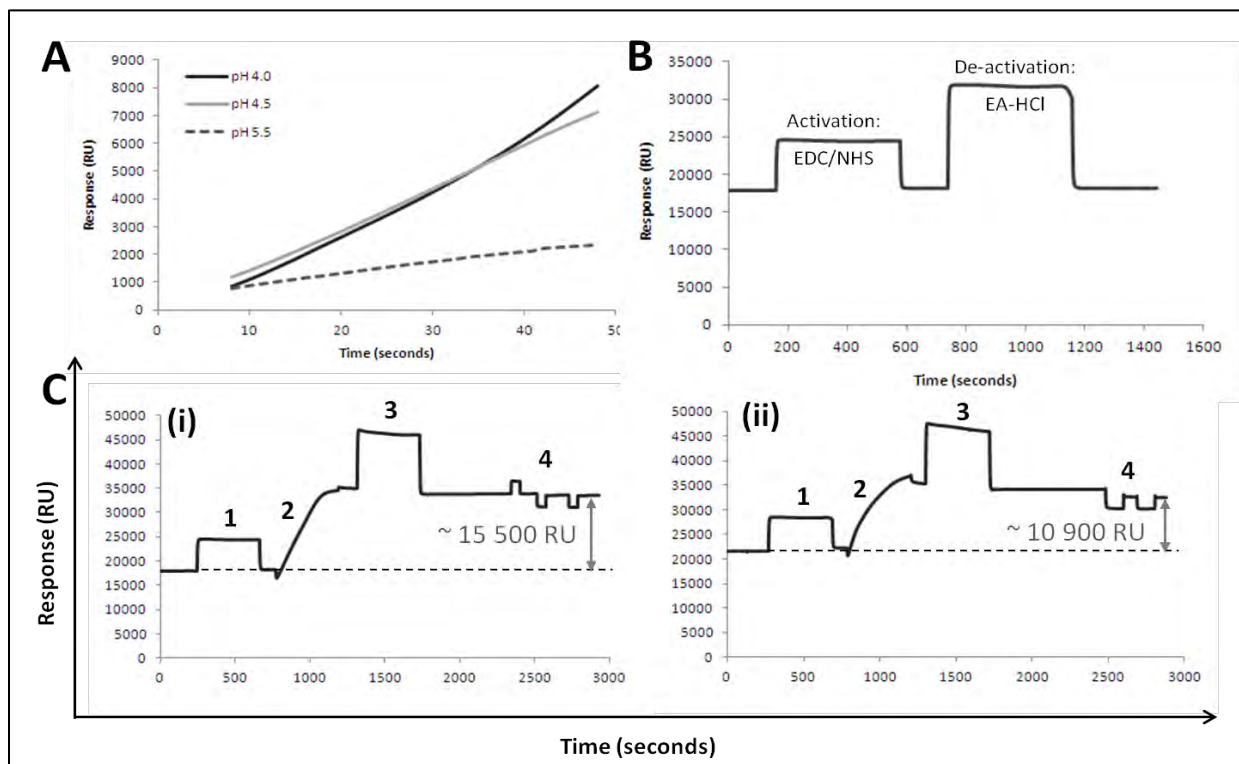


**Figure 7.4: The effect of selected compounds on the aggregation of MDH.** The aggregation of MDH (closed squares) at 48 °C, monitored spectrophotometrically at 360 nm, is reduced in the presence of PGKC4\_7C (open circles), hydroxy- $\beta$ -lapachona (closed downward triangles) and nor- $\beta$ -lapachona (closed triangles).

### 7.2.3. Chapter 4: Surface Plasmon resonance spectroscopy

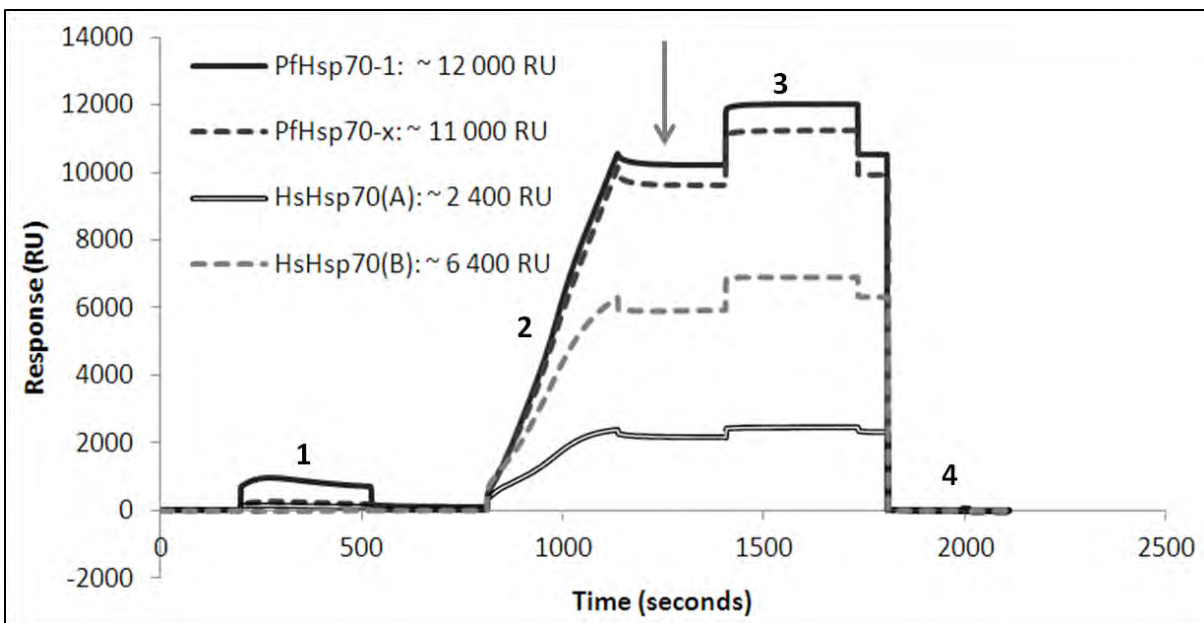
#### 7.2.3.1. Protein immobilisations

Figure 7.5 shows the sensorgrams of the pre-concentration and immobilisation procedures carried out on CM5 chips for BIAcore®X experiments as described in Sections 4.2.2.3 and 4.2.2.4. Figure 7.5A shows the pre-concentration procedure for PfHsp70-1, and Figure 7.3B shows the de-activation of the reference flow cell of a CM5 chip. The immobilisation sensorgrams for PfHsp70-1 and PfHsp70-x are shown in Figures 7.5C(i) and 7.5C(ii) respectively. In Figure 7.5A, the gradient of the slope of increasing response units with time at pH 5.5 is much lower than that at pH 4.5 and pH 5.0. A pH of 4.5 was used in the immobilisation of both PfHsp70-1 and PfHsp70-x. Figure 7.5C shows that both PfHsp70-1 and PfHsp70-x were successfully immobilised onto CM5 chips to high levels of immobilisation (> 10 000 RU).



**Figure 7.5: Pre-concentration and immobilisation procedures carried out toward the immobilisation of recombinant proteins on CM5 sensor chips.** Pre-concentration procedure of PfHsp70-1 used to determine the optimal immobilisation pH of PfHsp70-1 (A). The de-activation of the reference flow cell by injection of activator (EDC/NHS) and de-activator (EA-HCl) (B). PfHsp70-1 and PfHsp70-x were immobilised by 1: activation of amine sites by EDC/NHS; 2: injection of recombinant proteins; 3: de-activation of amine sites; 4: regeneration of the sensor surface (C), resulting in 15 500 and 10 900 RU due to immobilised PfHsp70-1 and PfHsp70-x respectively. The level of immobilisation is indicated by the grey arrows.

Figure 7.6 below shows the sensorgrams of the procedure carried out to immobilise recombinant proteins onto a GLH sensor chip for use in the ProteOn™ XPR36 instrument, as described in Section 4.2.3.3. All recombinant proteins were successfully immobilised to levels indicated in the figure.



**Figure 7.6: Sensorgram of the procedure carried out toward the immobilisation of recombinant proteins onto a GLH sensor chip.** Immobilisation of recombinant proteins onto the GLH sensor ship was achieved by 1: activation by EDC/NHS; 2: injection of recombinant protein; 3: de-activation of amine sites by ethanolamine-HCl, and 4: regeneration with glycine. The sensorgram shows the immobilisation carried out on five of the channels on the GLH chip, corrected for the sixth (reference) channel. The resulting levels of immobilisation are indicated by the grey arrow. HsHsp70 was immobilised in two channels at two different concentrations: 10 µg/ml (A) and 25 µg/ml (B). The level of immobilisation for each protein is indicated in the legend inset in the figure.

Table 7.2 below shows the levels of immobilisation resulting from the immobilisation procedures shown in Figures 7.5 and 7.6.

**Table 7.2: Levels of immobilisation of recombinant proteins on SPR sensor chips.** Immobilisation levels (RU) are shown for CM5 and GLH chips.

Levels of immobilisation on sensor chips (RU)		
	CM5 chips (BIAcore®X instrument)	GLH chip (ProteOn™ XPR36 instrument)
PfHsp70-1(opt)	15 500	12 000
PfHsp70-x	10 900	11 000
HsHsp70	-	2 400 (10 µg/ml) and 6 400 (25 µg/ml)

### 7.2.3.2. SPR data: Hsp70-small molecule interactions: BIAcore®X data

The results of the Hsp70-small molecule SPR assessments using the BIAcore®X system are shown in Figures 7.7-7.11 below.

Lapachol was found to have no interaction with PfHsp70-x. In addition to showing a lack of dose-dependency in the observed responses, the dissociation phase of the sensorgrams (Figure 7.7A, ~ 75 – 145 seconds) shows an increase in response with time, contrary to dissociation phases associated with typical SPR sensorgrams (shown in Figure 4.1). The observed effect was attributed to non-specific binding, where the compounds have dissociated off the reference flow cell at a slower rate than off the active flow cell, thus resulting in positive slopes in the dissociation phase when subtracting the reference cell response from the active cell response.

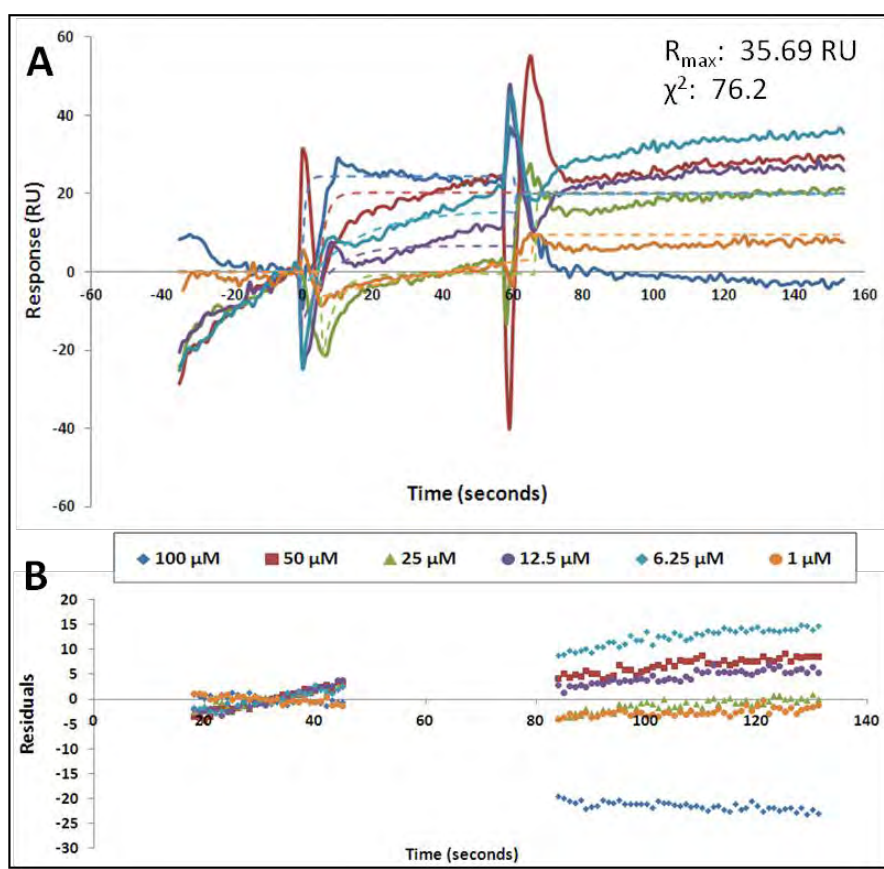


**Figure 7.7: SPR analysis of the potential interaction between lapachol and PfHsp70-x.** SPR sensorgram of a range of concentrations of lapachol passed over immobilised PfHsp70-x (solid lines) at 5  $\mu$ l/min, with the Langmuir model (dashed lines, corresponding colours) fitted to the data, including the resulting theoretical  $R_{max}$  and  $\chi^2$  values (A). The residual plot shows deviation from the Langmuir model (B).

For bromo- $\beta$ -lapachona, no interaction was observed with either PfHsp70-1 (Figure 7.8) or PfHsp70-x (Figure 7.9), and significant non-specific binding to the reference flow cell was observed (data not shown), resulting, as shown in Figures 7.8 and 7.9, in negative responses in the association phase of the sensorgram. As described in Section 4.2.2.5, the data shown has been corrected by subtraction of the effect of compound injection on the reference flow cell. A resulting negative sensorgram trace thus indicates that the response on the reference flow cell was greater than that in the active flow cell, and thus that the analyte bound non-specifically on the reference flow cell.

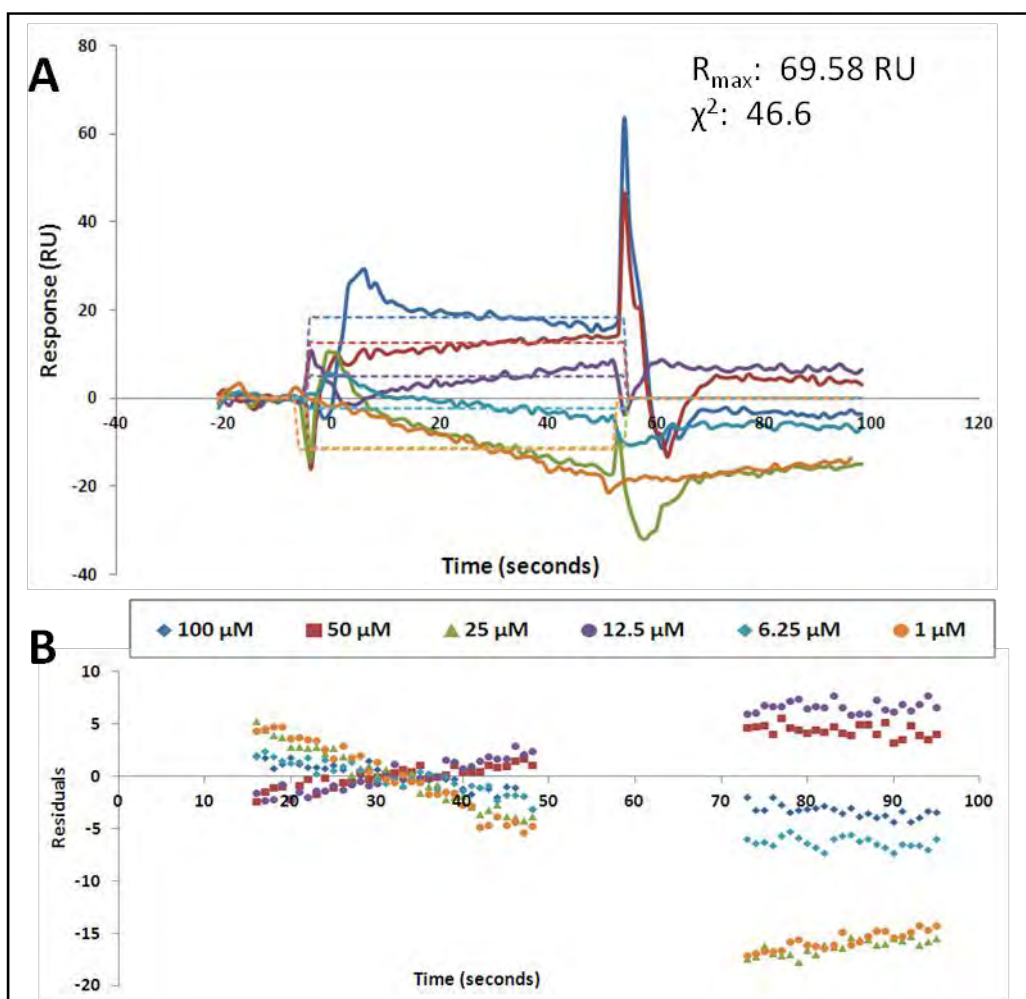


**Figure 7.8: SPR analysis of the potential interaction between bromo- $\beta$ -lapachona and PfHsp70-1.** SPR sensorgram of a range of concentrations of bromo- $\beta$ -lapachona passed over immobilised PfHsp70-1 (solid lines) at 5  $\mu$ l/min, with the Langmuir model (dashed lines, corresponding colours) fitted to the data, including the resulting theoretical  $R_{\max}$  and  $\chi^2$  values (A). The residual plot shows deviation from the Langmuir model (B).

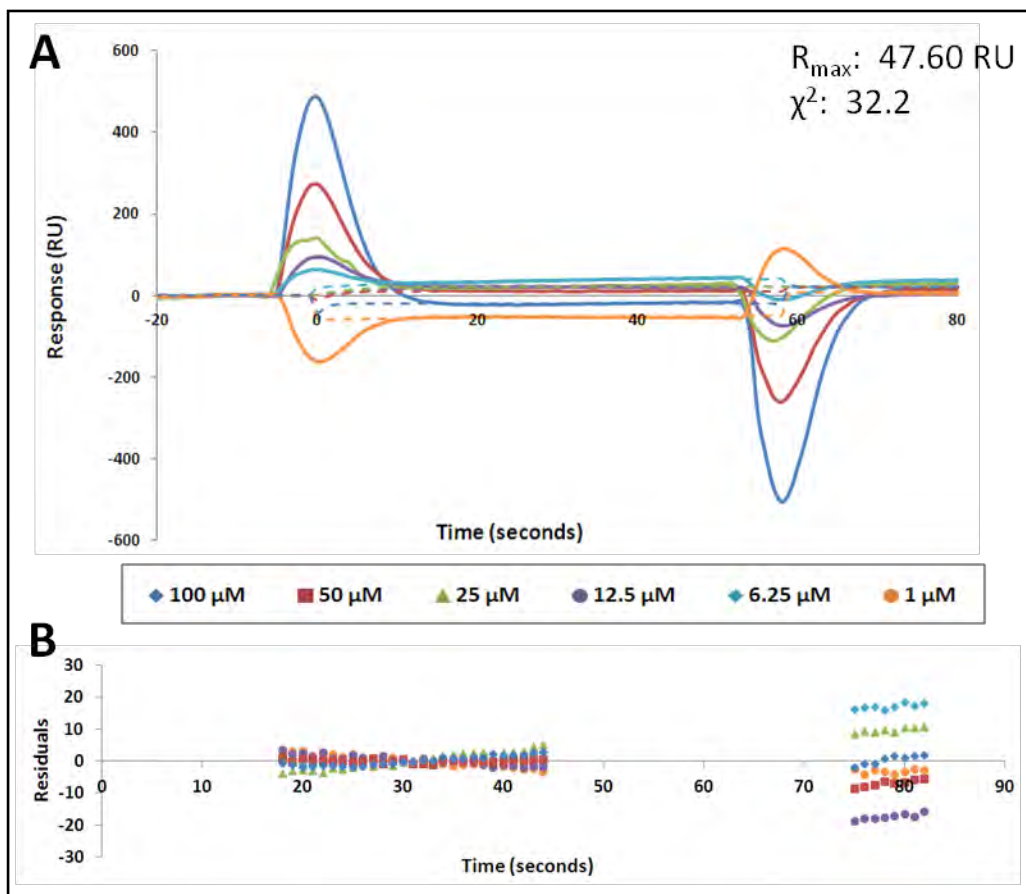


**Figure 7.9: SPR analysis of the potential interaction between bromo- $\beta$ -lapachona and PfHsp70-x.** SPR sensorgram (main figure: scaled-up view of the steady-state portion of the interaction; inset: entire sensorgram) of a range of concentrations of bromo- $\beta$ -lapachona passed over immobilised PfHsp70-x (solid lines) at 5  $\mu$ l/min, with the Langmuir model (dashed lines, corresponding colours) fitted to the data, including the resulting theoretical  $R_{\max}$  and  $\chi^2$  values (A). The residual plot shows deviation from the Langmuir model (B).

Malonganenone B (only assessed with immobilised PfHsp70-1 and not PfHsp70-x) was found to have no interaction with PfHsp70-1 based on the observed responses (Figures 7.10A) showing no concentration-dependent increase with compound concentration. Furthermore, the resulting sensorgram of the experiment (Figure 7.10A) shows a dose-dependent decrease in steady-state response with increasing compound concentration, indicative of significant non-specific binding in a dose-dependent manner to the reference flow cell and little to no binding on the active channel, such that, after correction for the reference flow cell, observed responses decreased with increasing concentrations, resulting also in negative responses at higher compound concentrations. As expected due to the reversed dose-response effect, the residual plots showed significant deviation of the data from the Langmuir model in clear trends at each compound concentration, and the  $\chi^2$  value was well out of the acceptable range (222).

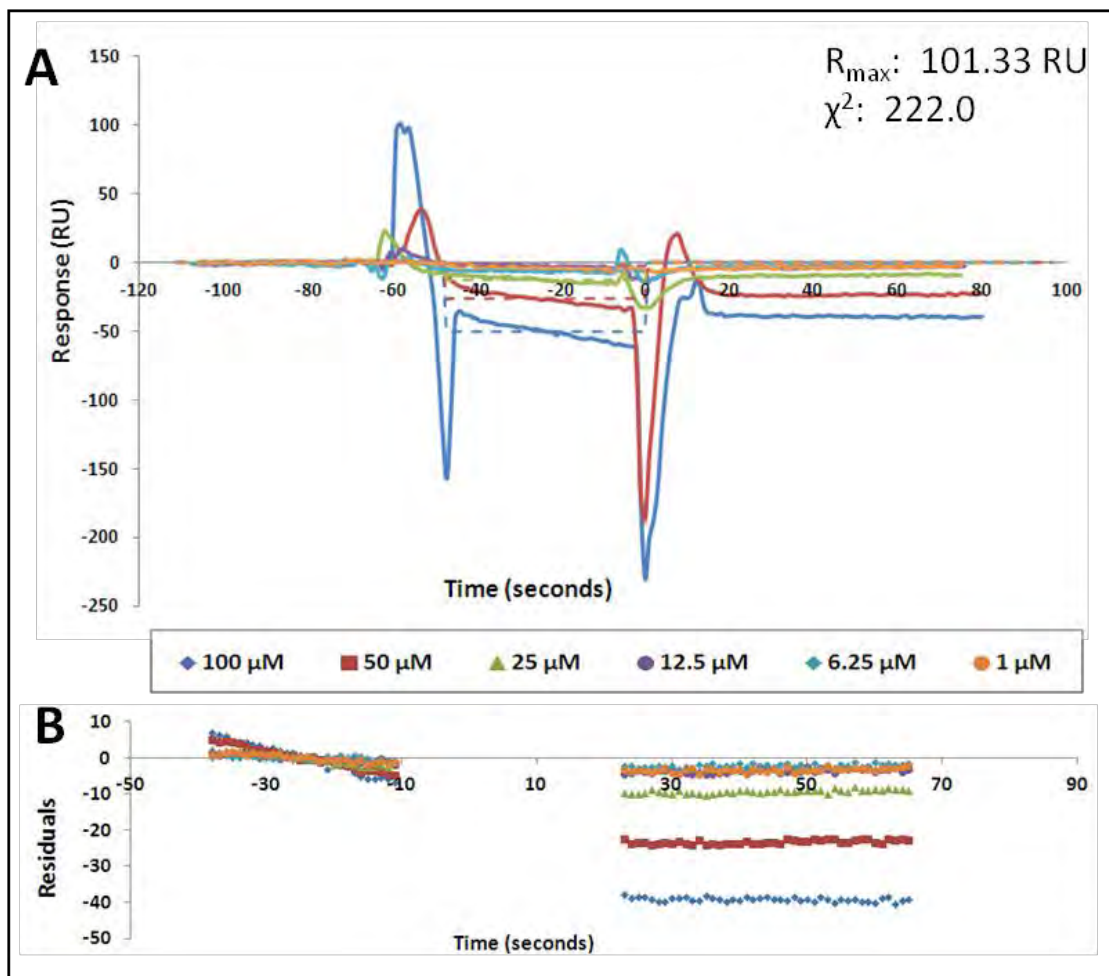


**Figure 7.10: SPR analysis of the potential interaction between malonganenone B and PfHsp70-1.** SPR sensorgram of a range of concentrations of malonganenone B passed over immobilised PfHsp70-1 (solid lines) at 5  $\mu\text{l}/\text{min}$ , with the Langmuir model (dashed lines, corresponding colours) fitted to the data, including the resulting theoretical  $R_{\text{max}}$  and  $\chi^2$  values (A). The residual plot shows deviation from the Langmuir model (B).



For malonganenone C, sensorgram traces showed a lack of concentration-dependency in the responses (Figure 7.11A). This observation, as well as the high  $\chi^2$  value (16) and residuals showing strong deviating from the Langmuir model fit (Figure 7.11B), indicated that no interaction was observed between PfHsp70-1 and malonganenone C.

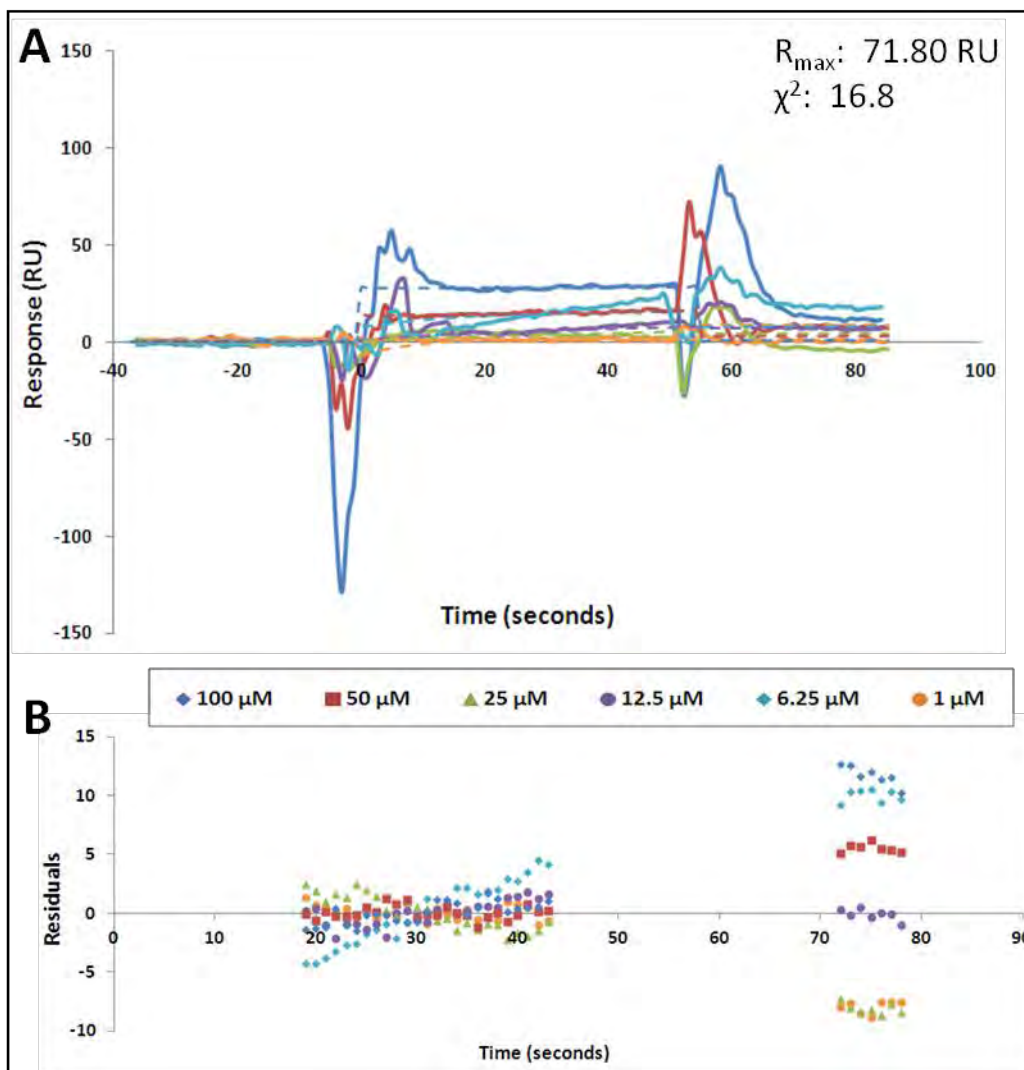


**Figure 7.11: SPR analysis of the potential interaction between malonganenone C and PfHsp70-1.** SPR sensorgram of a range of concentrations of malonganenone C passed over immobilised PfHsp70-1 (solid lines) at 5  $\mu\text{l}/\text{min}$ , with the Langmuir model (dashed lines, corresponding colours) fitted to the data, including the resulting theoretical  $R_{max}$  and  $\chi^2$  values (A). The residual plot shows deviation from the Langmuir model (B).

### 7.2.3.3. SPR data: Hsp70-small molecule interactions: BiacoreX® data

---

The results of the Hsp70-small molecule SPR assessments using the ProteOn™ XPR36 system are shown in Figures 7.12-7.16 below.

In the case of lapachol, similar responses (in terms of sensorgram shape) due to binding were observed for all three Hsp70s (Figure 7.12). The highest responses were observed for PfHsp70-1, and the lowest for HsHsp70, which can be attributed to the relative levels of immobilisation in the respective ligand channels (Table 7.2), with PfHsp70-1 having the highest level of immobilisation and thus resulting in the highest responses upon ligand injections.

For PfHsp70-1 (Figure 7.12, left panel), the response due to lapachol binding is dose-dependent in the association phase; however, in the dissociation phase (time ~ 100 – 400 seconds), the 100 µM injection dissociates at a lower rate and to a lesser extent than the 200 µM injection, and does not follow the otherwise dose-dependent trend in the dissociation phases of the sensorgram traces. This deviation is reflected in the residual plot of the fitted data (Figure 7.12, left, below sensorgram), where the data points for all other concentrations are randomly distributed about the x-axis, but for the 100 µM injection, the residual points are clearly almost exclusively above the x-axis. The observed effect could possibly be attributed to mass transport, despite the high flow rate (100 µl/min) used in the experiment. Mass transport in the dissociation phase can result in re-binding of an analyte to ligand in close proximity to the point of dissociation, which results in an apparent dissociation rate that is significantly lower than the actual dissociation rate. The very steep increase in response units upon injection of lapachol, particularly at 200 µM and 100 µM is also indicative of mass transport. At the lower concentrations (up to 50 µM), the association and dissociation rates seem unaffected by mass transport, and conform well to the Langmuir model. The apparent mass transport effect observed for lapachol injected over immobilised PfHsp70-1 was not observed for PfHsp70-x (Figure 7.12, middle) and HsHsp70 (Figure 7.12, right). In these experiments, observed responses are dose-dependent in both the association and dissociation phases of the sensorgrams, and both data sets fit closely to the Langmuir model based on the very even and random distribution of points in the residual plots (Figure 7.12, below sensorgrams). Based on the fact that the residual plots for lapachol binding to PfHsp70-x and HsHsp70 show good fits of the data sets to the Langmuir model, the measured affinities of lapachol for these two

Hsp70s was considered accurate; supported by the  $\chi^2$  values reported for these two interactions being less or in the case of HsHsp70 only just exceeding 10 % of the reported  $R_{\max}$  values. However, due to the fact that the affinities determined (lapachol and PfHsp70x:  $K_D = 0.79 \times 10^{-6}$ ; lapachol and HsHsp70:  $K_D = 1.7 \times 10^{-6}$ ) are below the experimental concentration range ( $12.5 \times 10^{-6}$  M to  $200 \times 10^{-6}$  M), these apparent interactions would have to be further validated by expanding the concentration range to include the affinity concentrations, and should thus be considered preliminary.

Figure 7.13 shows the results of the injection of bromo- $\beta$ -lapachona over immobilised PfHsp70-1, PfHsp70-x and HsHsp70. In all three cases, the compounds seemed to have significant mass transport effects, despite the high flow rate used in the experiments. The mass transport effect can be seen in the very steep, almost vertical, increases in response upon compound injection (time = 0 seconds), especially apparent in the injections of 200  $\mu$ M compound for all three Hsp70s, and in the case of PfHsp70-1 (left panel), also in the injection of 100  $\mu$ M of compound. In the case of all three Hsp70s, the mass transport effect is very apparent in the dissociation phase of the 50  $\mu$ M injection of compound, which dissociates at a much slower rate and to a much lesser extent than both the 100  $\mu$ M and 200  $\mu$ M injections, and thus deviates from the otherwise dose-dependent dissociation rates. This pronounced deviation of the 50  $\mu$ M injections of bromo- $\beta$ -lapachona over all three Hsp70s from the dose-dependent responses is again reflected in the residual plots for each interaction shown below the sensorgrams for each protein in Figure 7.13: the data points for the 50  $\mu$ M injections of compound are all well above the x-axis in a defined and clear trend. This significant mass transport effect has a confounding effect on the quantification of the affinity between ligand and analyte, particularly in the dissociation rate of the interaction, and thus, though there does seem to be an interaction between bromo- $\beta$ -lapachona and each of the three Hsp70s, this interaction could not be quantified from this data. The unsuitability of the data for fitting to the Langmuir model for quantification is also supported by the  $\chi^2$  values, which in the case of all three Hsp70s, significantly exceeds 10 % of the reported  $R_{\max}$  values.

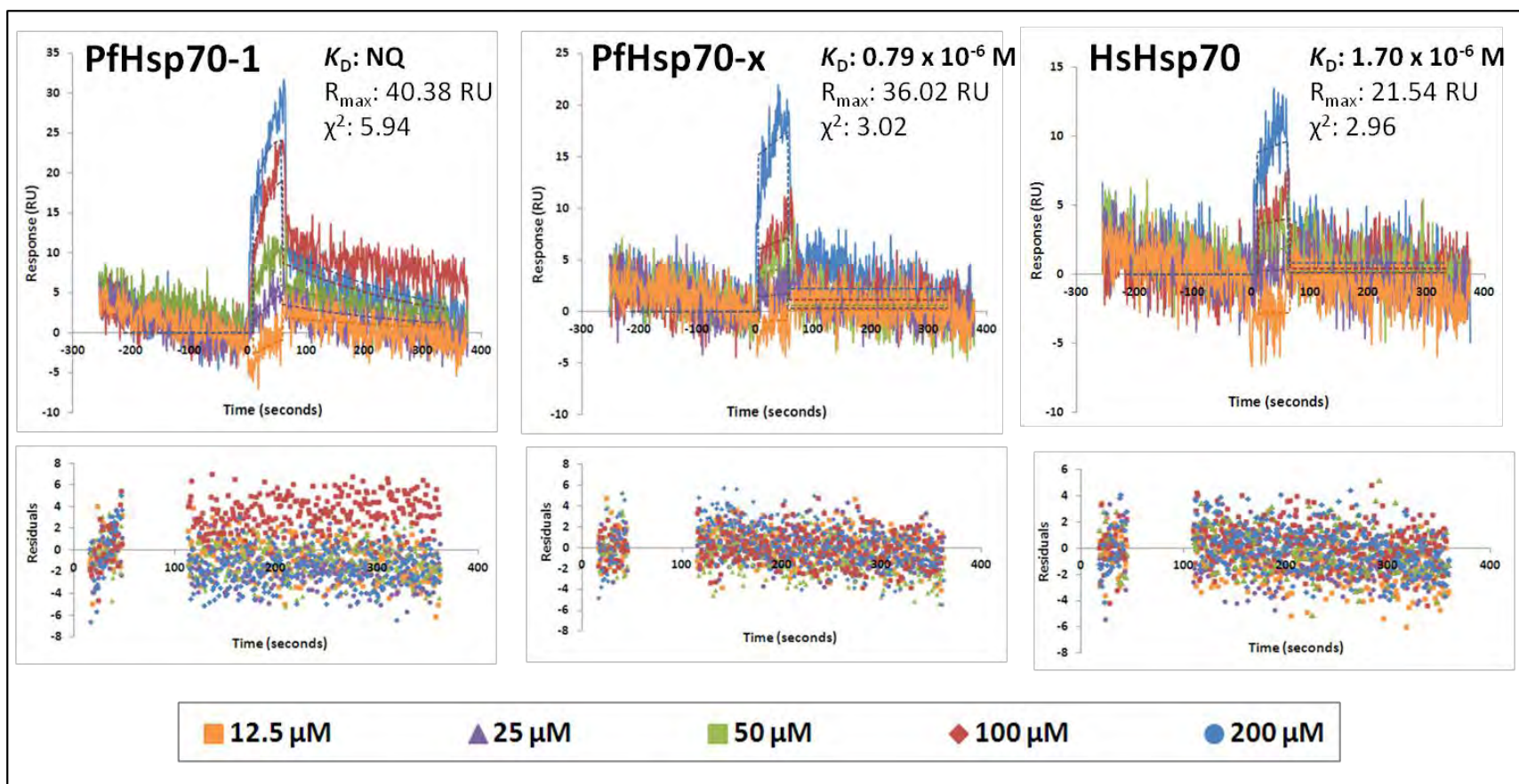


**Figure 7.12: SPR analysis of the interactions between lapachol and Hsp70s.** SPR sensorgrams (top panel; solid lines) of a range of concentrations of lapachol injected over immobilised PfHsp70-1 (left), PfHsp70-x (middle) and HsHsp70 (right) at 100  $\mu$ l/min. The Langmuir model (top panel, dashed lines) fitted to the data is overlaid. The affinity ( $K_D$ ; NQ = not quantifiable), the resulting theoretical  $R_{max}$  and  $\chi^2$  values are shown. The residual plots (lower panel) show deviations from the Langmuir model.

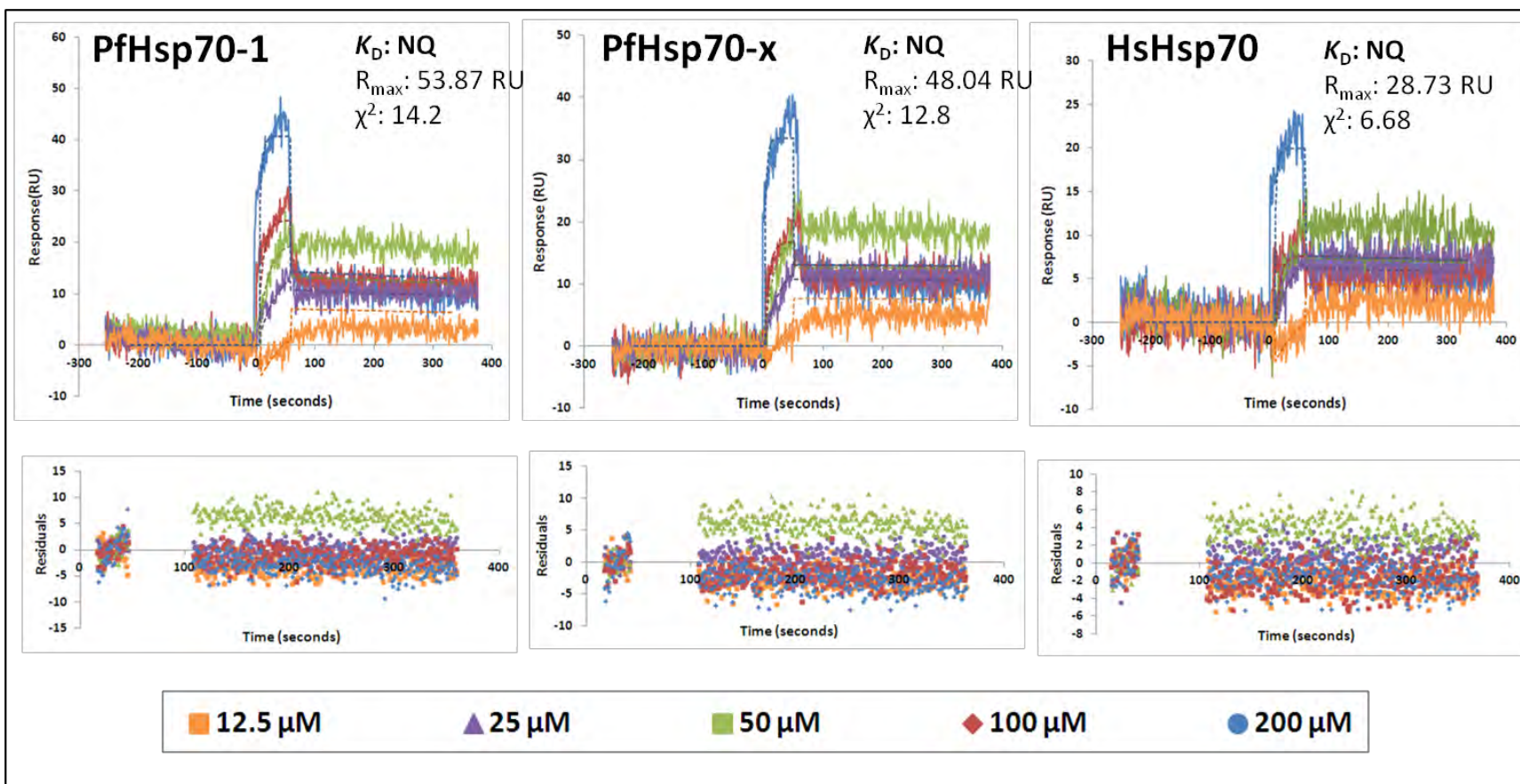


**Figure 7.13: SPR analysis of the interactions between bromo- $\beta$ -lapachona and Hsp70s.** SPR sensorgrams (top panel; solid lines) of a range of concentrations of bromo- $\beta$ -lapachona injected over immobilised PfHsp70-1 (left), PfHsp70-x (middle) and HsHsp70 (right) at 100  $\mu$ l/min. The Langmuir model (top panel, dashed lines) fitted to the data is overlaid. The resulting theoretical  $R_{max}$  and  $\chi^2$  values are shown. NQ: Non-quantifiable. The residual plots (lower panel) show deviations from the Langmuir model.

The results of the assessment of the potential interactions between malonganenone A and Hsp70s are shown in Figure 7.14. These interactions were assessed in triplicate, and in Figure 7.14, the resulting affinity ( $K_D$ ) of the replicate of the data shown is given (bold type), as well as (in bold type, underlined,  $\pm$  standard deviation) the average affinity from the three replicates of the experiment. Comparing the responses due to lapachol and bromo- $\beta$ -lapachona injections over the immobilised Hsp70s with those due to malonganenone A injections (as well as malonganenones B and C, Figures 7.15 – 7.16), the responses are significantly higher due to the malonganenones, and this can be attributed to the higher molecular masses of the malonganenone compounds compared to the naphthoquinones (440 g/mol compared to 240 and 320 g/mol).

Malonganenone A was found to result in binding responses which increased with increasing compound concentrations, with the exception of malonganenone A injected over PfHsp70-x (Figure 7.14, middle panel), where the sensorgram traces for 100  $\mu$ M and 125  $\mu$ M were found to overlap to a large extent, especially in the association phase of the interaction. This effect was seen in all three replicates of the data (additional replicates not shown), and could not be attributed to errors in dilution of the compounds, since on the ProteOn™ XPR36 instrument a single tube of each compound dilution is made up, and is injected over all ligand channels, and thus, if an error had been made in either the 100  $\mu$ M or the 125  $\mu$ M compound dilution, the effect would have been observed in the other ligand channels too. A similar but less pronounced effect was observed in the HsHsp70 channel too (Figure 7.14, right panel), in which there was little difference between the responses for 100  $\mu$ M and 125  $\mu$ M malonganenone A, however, the two traces are still distinguishable from each other, with the 125  $\mu$ M injection, as expected, showing a slightly greater response in the association phase of the interaction than the 100  $\mu$ M injection. Based on the clear dose-dependent binding response, the low  $\chi^2$  value (well below 10 %  $R_{max}$ ) and the evenly distributed residual values obtained for binding of malonganenone A to PfHsp70-1, the affinity determined for the interaction [ $K_D = (10.2 \pm 10.1) \times 10^{-6}$ ] was considered accurate. Despite the suitably fitted Langmuir model; however, the measured affinity fell just out of the experimental compound concentration range used in this experiment ( $25 \times 10^{-6}$  M to  $150 \times 10^{-6}$  M), and thus would have to be further validated using an expanded concentration range. For PfHsp70-x and HsHsp70, because the  $\chi^2$  values are not within the acceptable range, and because of the slight deviation from dose-dependency of the malonganenone A concentrations, resulting in residuals with clear trends (Figures 7.14, middle and right panels, below sensorgrams), quantification of affinities for these interactions are considered inaccurate, and thus they should be considered preliminary.

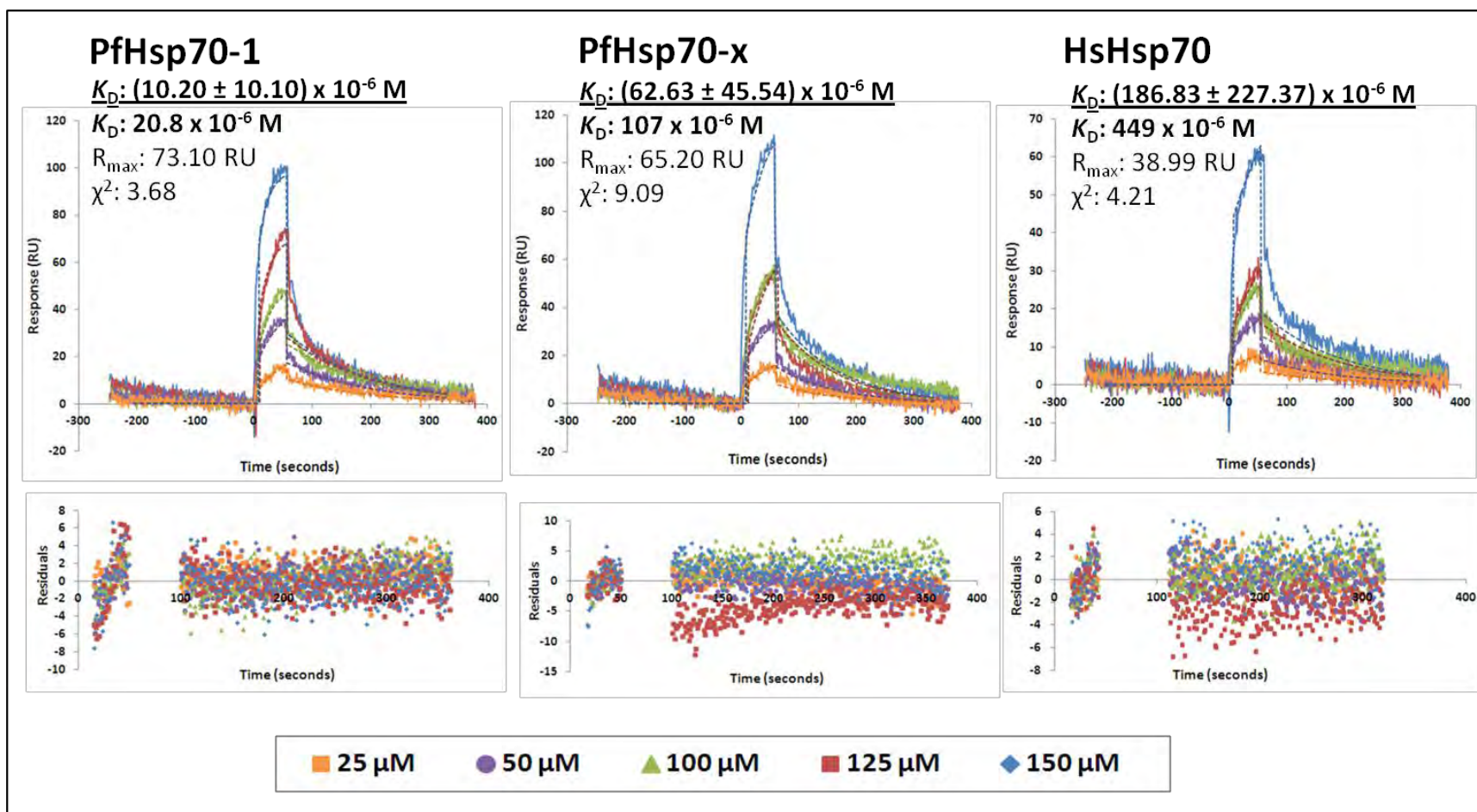


**Figure 7.14: SPR analysis of the interactions between malonganenone A and Hsp70s.** SPR sensorgrams (top panel; solid lines) of a range of concentrations of malonganenone A injected over immobilised PfHsp70-1 (left), PfHsp70-x (middle) and HsHsp70 (right) at 100  $\mu\text{l}/\text{min}$ . The Langmuir model (top panel, dashed lines) fitted to the data is overlaid. The affinity ( $K_D$ ), the resulting theoretical  $R_{\max}$  and  $\chi^2$  values are shown. The residual plots (lower panel) show deviations from the Langmuir model.

The results of the experiments assessing the potential interactions between malonganenone B and Hsp70s are shown in Figure 7.15. Very similar binding responses were observed for malonganenone B across the three Hsp70s. Though a concentration-dependent response was observed in the association phases of the three interactions, suggesting specific interactions between malonganenone B and the Hsp70, significant mass transport effects were apparent in the sensorgrams, particularly in the traces for the 200  $\mu\text{M}$  injections of compound. In these traces, a very steep and large increase in response occurred upon compound injection. The mass transport effect was also apparent in the dissociation phase of the interactions, in which there are deviations from the otherwise concentration-dependent dissociations by the 100  $\mu\text{M}$  injections, particularly pronounced in the interactions with PfHsp70-x (Figure 7.14, middle) and HsHsp70 (Figure 7.14, right). In both these cases, the compound at 100  $\mu\text{M}$  seemed to dissociate at a much lower rate and to a lesser extent than at other concentrations, possibly due to re-binding of dissociated compound as a result of mass transport, as described for the interaction between lapachol and PfHsp70-1. Again, this pronounced mass transport has a confounding effect on the data analysis, and thus the measured affinities cannot be considered accurate. For the interaction between malonganenone B and PfHsp70-1 (Figure 7.14, left), the  $\chi^2$  value of the Langmuir model fitted to the data is in the acceptable range, however, the residual plot (Figure 7.14, bottom left) shows distinct trends for all concentrations of compounds, indicative of an unsuitable fit of the model to the data. The same trends in residuals were also observed for the interactions of malonganenone B with PfHsp70-x (Figure 7.14, middle) and HsHsp70 (Figure 7.14, right). These unevenly distributed residuals, along with  $\chi^2$  values exceeding the acceptable range and the fact that the reported affinities are out of the assessed concentration range of  $12.5 \times 10^{-6}$  M to  $200 \times 10^{-6}$  M deem the measured affinities inaccurate.



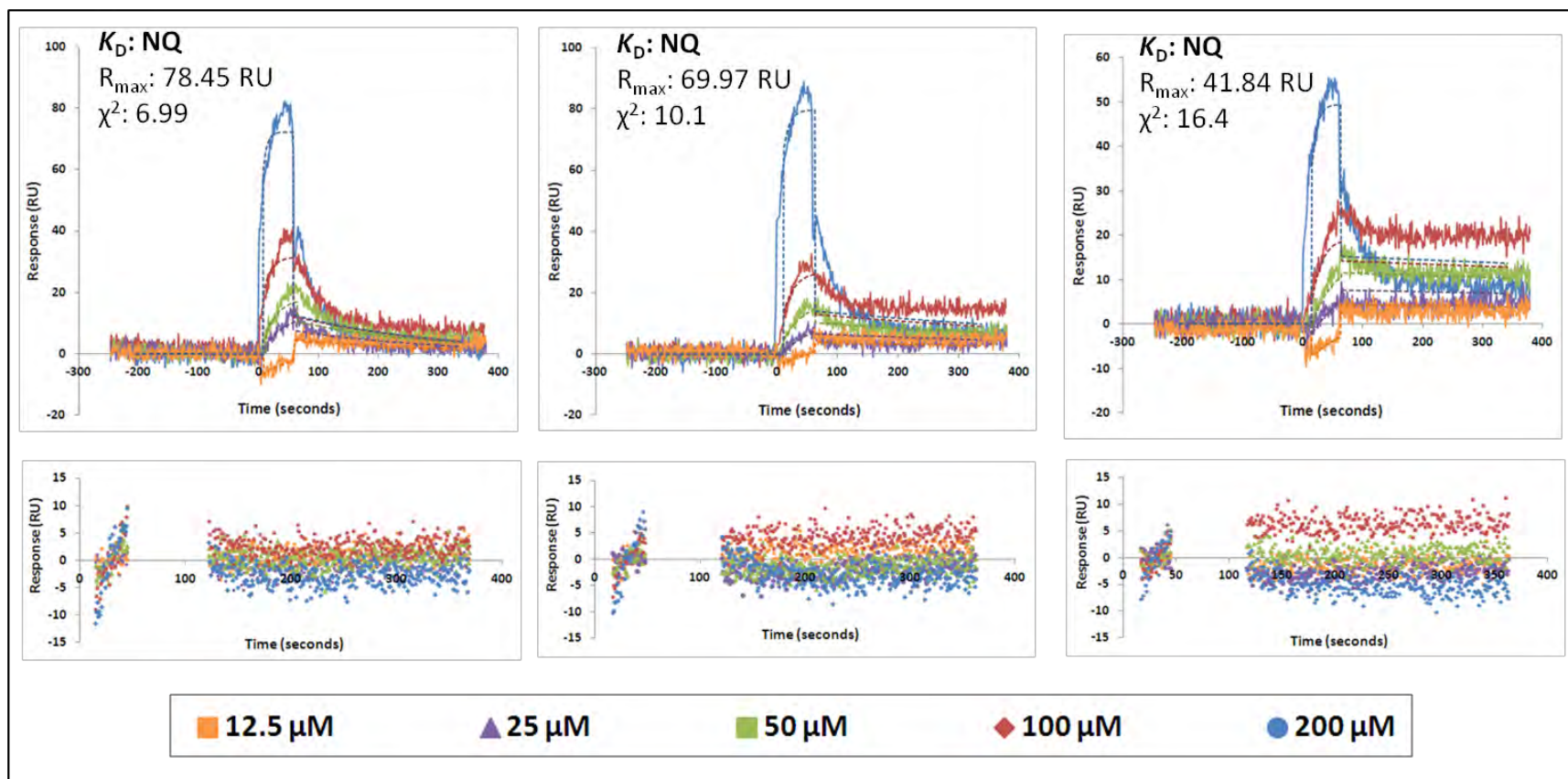


**Figure 7.15: SPR analysis of the interactions between malonganenone B and Hsp70s.** SPR sensorgrams (top panel; solid lines) of a range of concentrations of malonganenone B injected over immobilised PfHsp70-1 (left), PfHsp70-x (middle) and HsHsp70 (right) at 100  $\mu\text{l}/\text{min}$ . The Langmuir model (top panel, dashed lines) fitted to the data is overlaid. The resulting theoretical  $R_{\text{max}}$  and  $\chi^2$  values are shown. NQ: Non-quantifiable. The residual plots (lower panel) show deviations from the Langmuir model.

The results showing the potential interactions between Malonganenone C and Hsp70s are shown in Figure 7.16. In the case of all three Hsp70s, the concentration-dependence in both the association and dissociation phases of the sensorgrams is indicative of a specific interaction between malonganenone C and each of PfHsp70-1, PfHsp70-x and HsHsp70. Though a possible mass transport effect is suggested by the very steep, almost vertical increase in response upon injection of 200  $\mu\text{M}$  malonganenone B over each of the immobilised Hsp70s, there is no apparent effect on the dissociation phase of the interaction, which retain their concentration-dependency. The possible effect is also not reflected in the residual plots (Figure 4.12, below sensorgrams) of the fitted data, which show residual points very evenly dispersed about the x-axis. The  $\chi^2$  values were all well within the acceptable range (all < 10 % of corresponding  $R_{\text{max}}$  values), further confirming that the Langmuir model fits each of the data sets well. Based on the data fit to the Langmuir model, the measured affinities can be considered accurate; however, they would have to be further validated in terms of reproducibility by replication of the experiments, as well as expansion of the concentration range of malonganenone C to include the measured affinities, and are thus considered preliminary.

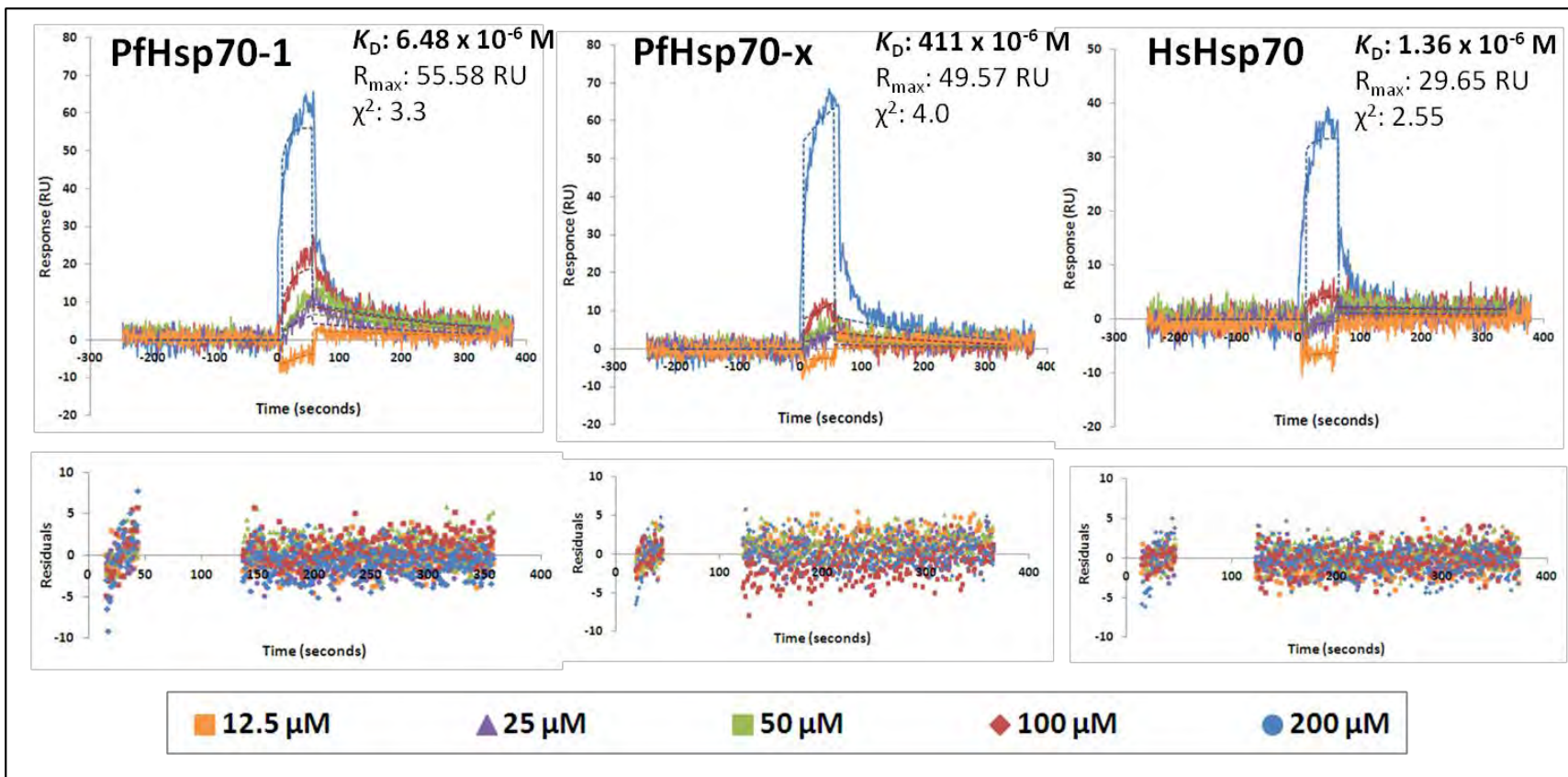


**Figure 7.16: SPR analysis of the interactions between malonganenone C and Hsp70s.** SPR sensorgrams (top panel; solid lines) of a range of concentrations of malonganenone C injected over immobilised PfHsp70-1 (left), PfHsp70-x (middle) and HsHsp70 (right) at 100  $\mu\text{l}/\text{min}$ . The Langmuir model (top panel, dashed lines) fitted to the data is overlaid. The affinity ( $K_D$ ), the resulting theoretical  $R_{\max}$  and  $\chi^2$  values are shown. The residual plots (lower panel) show deviations from the Langmuir model.